The Endogenous and Exogenous Substrate Spectrum of the Human Organic Cation Transporter OCT1 — a Comprehensive Characterization

Dissertation

for the award of the degree

"Doctor rerum naturalium"

of the Georg-August-Universität Göttingen

within the doctoral program Molecular Medicine

of the Georg-August University School of Science (GAUSS)

submitted by

Ole Jensen

from Langenhagen

Göttingen 2021

Thesis Committee

Prof. Dr. Jürgen Brockmöller
Institute of Clinical Pharmacology
University Medical Center Göttingen

Prof. Dr. Silvio Rizzoli
Department of Neuro- and Sensory Physiology
University Medical Center Göttingen

Prof. Dr. Rüdiger Behr
Platform Degenerative Diseases
German Primate Center, Göttingen

Further members of the Examination Board

Prof. Dr. Christian Griesinger
NMR-based Structural Biology
Max Planck Institute for Biophysical Chemistry, Göttingen

Prof. Dr. mult. Thomas Meyer
Department of Psychosomatic Medicine and Psychotherapy
University Medical Center Göttingen

Prof. Dr. Michael Zeisberg
Department of Nephrology and Rheumatology
University Medical Center Göttingen

Date of oral examination: 12.07.2021

Table of Content

Figure index

Abbreviations

5-HT	Serotonin (5-hydroxytryptamine)
ASP^+	4-(4-(dimethylamino)styryl)-N-methylpyridinium
cDNA	Complementary deoxyribonucleic acid
Cl_{int}	Intrinsic clearance
CNS	Central nervous system
DAT	Dopamine transporter
Flp	Flippase (a genetic recombinase)
FRET	Förster resonance energy transfer
K_m	Michaelis-Menten constant
MAT	Monoamine transporter
MPP^+	1-Methyl-4-phenylpyridinium
NET	Norepinephrine transporter
OCT	Organic cation transporter
OCTN	Organic cation transporter novel
qPCR	Quantitative polymerase chain reaction
SERT	Serotonin reuptake transporter
SLC	Solute carrier
TEA^+	Tetraethylammonium
TMD	Transmembrane domain
v_{max}	Maximum velocity

The abbreviations used in the presented publications are provided with the articles.

1 Summary

The organic cation transporter 1 (OCT1) is most extensively expressed in the human liver. OCT1 is involved in the hepatic uptake of several drugs and endogenous compounds, which then undergo bioactivation, recycling, metabolism, or elimination.

The aim of this work was to extend the knowledge about OCT1 substrates and non-substrates of endogenous and exogenous origin. Establishing an *in vitro* model for studying uptake and subsequent metabolism was an additional goal, as well as finding an endogenous biomarker for OCT1 activity. These studies should contribute to our basic understanding of the biological role of this transporter and to the understanding of the role of OCT1 in pharmacology and toxicology.

Influx transport of 18 psychostimulant or hallucinogenic compounds, which all meet the conventional physicochemical criteria of OCT1 substrates, was investigated for OCT1 and related transporters. Mescaline was newly identified as a substrate of OCT1. To more systematically and comprehensively search for additional substrates, a machine learning-based model was used. This approach exploited existing knowledge about OCT1 substrates. Machine learning-aided prediction of new substrates was highly reliable as subsequent *in vitro* validation showed. The *in silico* prediction, which was based on two-dimensional structures, did not include three-dimensional information, which is important for enantiomers. Therefore, stereoselectivity of OCT1 transport was investigated *in vitro*. It revealed a surprisingly stereoselective cell uptake for some substrates, e.g. fenoterol, but not all, e.g. salbutamol.

For the purpose of *in vitro*-to-*in vivo* translation in more complex biological systems, a cell model was developed, which allowed the chromosomal integration of two genes of interest in a targeted manner, to investigate uptake and metabolism in a more holistic fashion. Both genes can be transfected simultaneously and are expressed with equal strength. As a first proof of the value, the sequential uptake of proguanil and subsequent CYP-dependent activation to cycloguanil resembled indeed the uptake and metabolism in primary hepatocytes. Several European and American investigators have already expressed their interest to adopt the system for their research.

Thiamine (Vitamin B1) had been proposed as a biomarker for *in vivo* OCT1 activity. Although thiamine was a substrate of OCT1 *in vitro,* thiamine was rejected as a suitable biomarker for OCT1 activity through a human clinical trial. After the intake of a large thiamine dose, neither thiamine trough concentrations nor maximum concentrations showed any correlation with individual OCT1 activity according to genotype. Results suggested that other transporters play the central role in thiamine uptake into the liver and other organs.

In total, I could add more than 20 previously unknown substrates to the list of well characterized OCT1 substrates. I could show that OCT1 transport can be quite different depending on subtle structural differences between enantiomers. Moreover, the developed cell model may serve as an interesting tool to mimic the complex interplay between hepatic uptake and metabolism, and human pharmacokinetics of thiamine is not dependent on OCT1 - at least not in a quantitatively

relevant fashion. Together, these findings may contribute to a gradually improving understanding of OCT1 functionality and biomedical relevance.

2 Introduction

Compartmentation is a prerequisite for life. Without biological barriers, separation of functional compartments would not exist and development of life as we know would not have been possible. This separation, however, has some disadvantages. At least, vital nutrients and harmful metabolites need to pass these barriers for an organism to survive. In single cells as well as higher developed living beings, transport proteins realize the task of taking up compounds, which are not able to cross lipid bilayers. In humans, this is essential when it comes to nutrient uptake, reuptake of neurotransmitters, translocation of a variety of compounds across cellular but also intracellular barriers, renal or biliary elimination of metabolites, and many more.

Three quarters of the top 200 prescribed drugs in the United States require uptake into the liver for metabolism or direct biliary excretion, and only about 30 % are cleared unchanged via urine (Morrissey et al. 2013; Williams et al. 2004). Numerous of those drugs are organic cations, meaning weak bases, which are positively charged at physiologic pH. Their elimination requires protein-mediated transport across cell membranes. In the liver, this is achieved, amongst others, by transport proteins of the SLC22 family, primarily by the organic cation transporter 1 (OCT1).

2.1 OCT1 – A member of the SLC22 family

The organic cation transporter 1 (OCT1) is a transport protein encoded by the *SLC22A1* gene. OCT1 has been studied since its discovery in the late 1990s, when it was successfully cloned and characterized (Gorboulev et al. 1997; Zhang Lei et al. 1998). The SLC22 family further comprises the organic cation transporters OCT2 (*SLC22A2*), OCT3 (*SLC22A3*), OCTN1 (*SLC22A4*), and OCTN2 (*SLC22A5*) (Figure 1).

	OCT1	OCT2	OCT3	OCTN1	OCTN2	MATE1	MATE2-K
OCT1	100.0						
OCT2	70.0	100.0					
OCT3	49.5	50.2	100.0				
OCTN1	31.8	33.3	30.2	100.0			
OCTN2	33.6	33.1	31.7	76.2	100.0		
MATE1	14.6	14.7	13.8	15.2	14.4	100.0	
MATE2-K	13.3	14.7	13.4	13.8	14.9	48.9	100.0

Figure 1: Amino acid sequence comparison of selected organic cation transporters. The identity matrix of the organic cation transporters from the SLC22 family (OCT1, OCT2, OCT3, OCTN1, OCTN2) and two multidrug and toxin extrusion proteins MATE1 (*SLC47A1*) and MATE2-K (*SLC47A2*) shows the amino acid sequence identity from pairwise comparisons in percent (left). The phylogenetic tree indicates evolutionary distances of these transporters (right). Amino acid sequences were analyzed by "Multiple Sequence Comparison by Log-Expectation" (*MUSCLE*) provided by the European Bioinformatics Institute, Hinxton (https://www.ebi.ac.uk/), and the phylogenetic tree was created from resulting data via the "Interactive Tree Of Life" (iTOL) online tool version 6 (https://itol.embl.de/).

Together with many other transporters, OCT1 is expressed in the human liver (Figure 2). More specifically, it is expressed in the sinusoidal membrane facing the space of Disse and the bloodstream in the liver (Meyer-Wentrup et al. 1998; Zamek-Gliszczynski et al. 2018). It serves for the hepatic uptake allowing for subsequent hepatobiliary elimination of a variety of exogenous drugs and toxins as well as endogenous amines (Meijer et al. 1990; Oude Elferink et al. 1995).
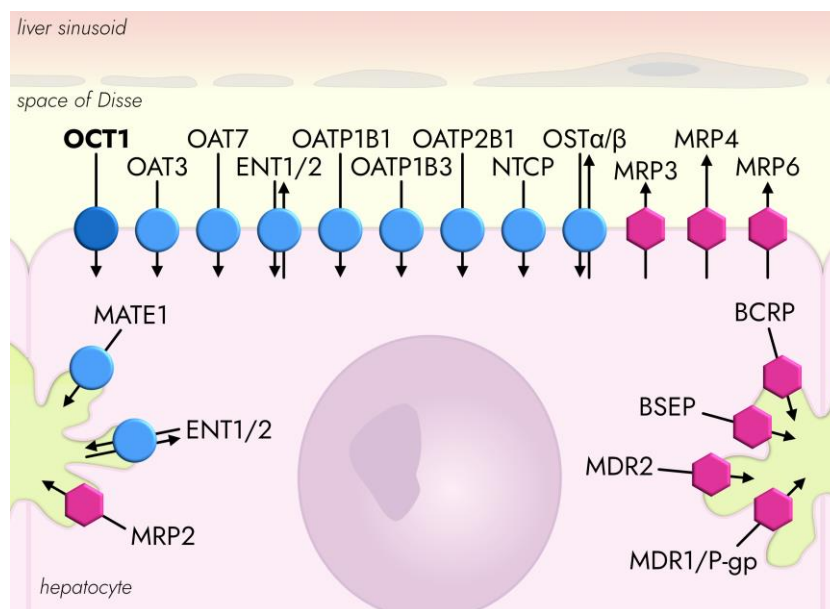

Figure 2: Transport proteins relevant for hepatic uptake and elimination. Both, SLC (blue circles) and ABC (pink hexagons) transporters are involved in uptake and elimination in the liver. Figure inspired by Figure 1 in the 2018 White Paper of the International Transporter Consortium (Zamek-Gliszczynski et al. 2018). BSEP, bile salt export pump; BRCP, breast cancer resistance protein; ENT, equilibrative nucleoside transporter; MATE, multidrug and toxin extrusion protein; MDR, multidrug resistance protein; MRP, multidrug resistance-associated protein; NTCP, sodium taurocholate cotransporting peptide; OAT, organic anion transporter; OATP, organic anion transporting polypeptide; OCT, organic cation transporter; OST, organic solute transporter.

The other SLC22 family members (OCT2, OCT3, OCTN1, and OCTN2) are known for the uptake of organic cations and/or zwitterionic substances like carnitine (Tamai et al. 1997; Tamai et al. 1998; Yabuuchi et al. 1999). The transporters OCTN1 and OCTN2 stand out because they do not mediate electrogenic transport of cations like the other three transporters OCT1, OCT2, and OCT3. OCTN1 and OCTN2 translocate organic cations or (together with Na^+) carnitine in exchange with protons.

In contrast to the predominantly hepatic expression of OCT1, OCT2 is expressed in the basolateral membrane of renal tubular epithelial cells, where it mediates the uptake of organic cations prior to luminal excretion (Motohashi et al. 2002; Nies et al. 2009; Tzvetkov et al. 2009; Zhang L. et al. 1997). OCT3 is expressed more broadly and was detected in brain, heart, liver, lung, kidney, placenta, and skeletal muscle (Gründemann et al. 1998; Verhaagh et al. 1999; Wu et al. 2000).

OCTN1 and OCTN2 are expressed in several tissues, such as heart, kidney, placenta, prostate, and skeletal muscle (Koepsell et al. 2003; Wu et al. 1998). Amino acid identities among the SLC22 family members with OCT1 range from 32 % for OCTN1 to 70 % for OCT2 (Koepsell et al. 2003). One commonality among the SLC22 family members is the structural arrangement of twelve transmembrane domains (TMD), including one large extracellular loop (connecting TMD 1 and 2) and a large intracellular loop (connecting TMD 6 and 7, Figure 3). These 12 transmembrane domains are thought to form the central binding pocket (Bednarczyk et al. 2003).
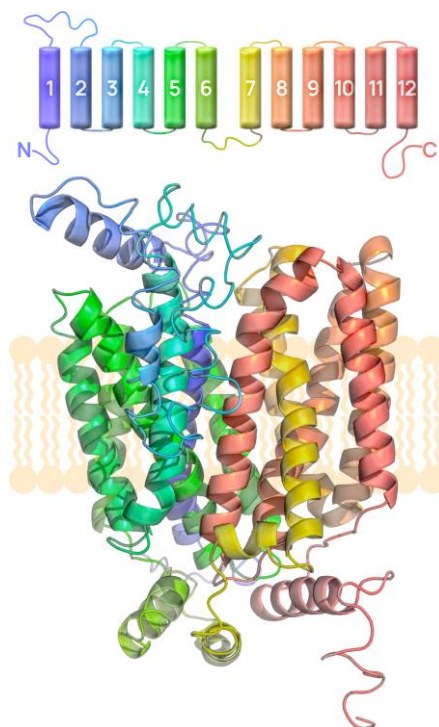
Figure 3: Three-dimensional homology model of OCT1. The OCT1 homology model by Dakal *et al.* shows the arrangement of the 12 TMD and the formation of a central binding cleft (Dakal et al. 2017).

The substrate translocation by OCT1 has been described with the alternating access model (Koepsell 2011; Volk et al. 2009). The substrate binds to the transporter in its outward-open conformation and induces subsequent changes in protein conformation (Figure 4). In a non-ATP-dependent manner ('facilitated diffusion'), the protein changes to the outward-occluded and inward-occluded state, in which the substrate is trapped inside the transporter, before it gets released from the transport protein in its inward-open state (Abramson et al. 2003; Koepsell 2015; Koepsell und Keller 2016). This process of facilitative diffusion depends on substrate concentration and membrane potential (Egenberger et al. 2012). In contrast to antiporters, such as OCTN1 and OCTN2, transport by OCT1 is electrogenic, meaning charged molecules (cations) are transported across the cell membrane without compensation (Busch et al. 1996). It was shown that OCT1 and other OCTs as well are able to facilitate not only uptake but also efflux of cations (Busch et al. 1996; Jensen et al. 2021b; Kim et al. 2017; Nagel et al. 1997). Besides transport,

previous work also focused on inhibition (Ahlin et al. 2008; Chen EC et al. 2017), as translocation of substrates can be restricted by inhibitors on the one hand and genetic variants on the other.
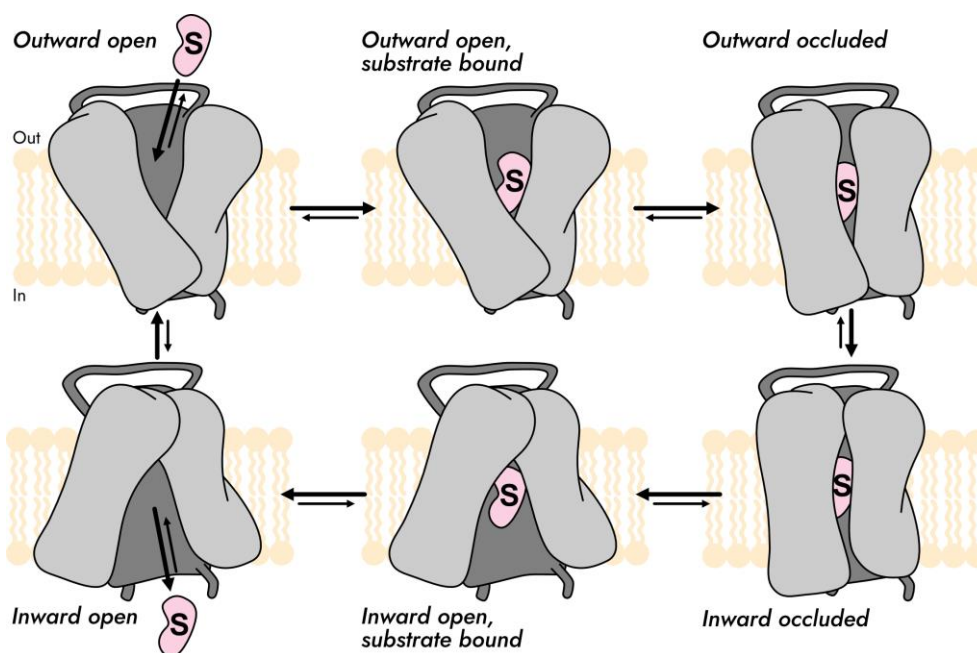
Figure 4: Substrate translocation by OCT1 described with the alternating access model. The substrate binds to the transport protein in the outward open conformation. Subsequent conformational changes lead to formation of the inward- and outward-occluded states and the release of the substrate from the inward-open conformation. This model is based on findings, which differentiate OCT1 from an ion channel (Koepsell et al. 2003).

2.2   Genetic variability of *OCT1*

The *OCT1* gene is highly polymorphic, particularly in its coding region. Among all genes of organic cation transporters of the SLC22 and SLC47 family, *OCT1* showed the highest variability, especially for non-synonymous polymorphisms (Leabman et al. 2003; Tzvetkov et al. 2016). Until today, 16 different *OCT1* haplotypes and additional sub-haplotypes have been described and functionally characterized (Seitz et al. 2015; Shu et al. 2007; Shu et al. 2003).

Besides the most prevalent reference (wild-type) allele, five distinct haplotypes are present in the European population (Table 1). This includes the alleles OCT1*2 to *6, which are defined by a deletion of Met420 and/or amino acid substitutions. All these haplotypes can also be found in North Africa and the Middle East, as well as the two haplotypes OCT1*7 and *8. The latter ones have also been identified in populations of sub-Saharan Africa, where they exist next to the reference and the *2 allele. Even more diverse in the genetic landscape of OCT1 are Central Asia, East Asia and Oceania, where variants OCT1*9 to *16 can be found. A special exception in the worldwide distribution of OCT1 alleles is South America, where the reference allele and the *2 allele coexist with almost the same frequency.

Table 1: OCT1 haplotypes and their prevalences

Haplotype	S14F	S29L	R61C	C88R	P117L	S189L	R206C	G220V	T245M	E284K	G401S	M420del	I449T	G465R	R488M	AM	EU	NA	SA	OC	CA
OCT1*1	S	S	R	C	P	S	R	G	T	E	G	M	I	G	R	50.3	74.4	78.2	84.6	97.8	78.7
OCT1*2	S	S	R	C	P	S	R	G	T	E	G	del	I	G	R	49.7	15.5	13.3	5.1	0.7	14.8
OCT1*3	S	S	C	C	P	S	R	G	T	E	G	M	I	G	R	-	5.1	4.7	-	-	3.8
OCT1*4	S	S	R	C	P	S	R	G	T	E	S	M	I	G	R	-	2.5	0.4	-	-	-
OCT1*5	S	S	R	C	P	S	R	G	T	E	G	del	I	R	R	-	1.8	0.8	-	-	1.0
OCT1*6	S	S	R	R	P	S	R	G	T	E	G	del	I	G	R	-	0.3	1.0	-	-	0.2
OCT1*7	F	S	R	C	P	S	R	G	T	E	G	M	I	G	R	-	-	1.5	3.8	-	0.4
OCT1*8	S	S	R	C	P	S	R	G	T	E	G	M	I	G	M	-	-	0.3	6.6	-	0.4
OCT1*9	S	S	R	C	L	S	R	G	T	E	G	M	I	G	R	-	-	-	-	0.3	0.4
OCT1*10	S	S	R	C	P	L	R	G	T	E	G	M	I	G	R	-	0.3	-	-	-	-
OCT1*11	S	S	R	C	P	S	R	G	T	E	G	M	T	G	R	-	-	-	-	0.3	-
OCT1*12	S	L	R	C	P	S	R	G	T	E	G	M	I	G	R	-	-	-	-	0.5	-
OCT1*13	S	S	R	C	P	S	R	G	M	E	G	M	I	G	R	-	-	-	-	-	0.4
OCT1*14	S	S	R	C	P	S	C	G	T	E	G	del	I	G	R	-	-	-	-	-	0.2
OCT1*15	S	S	R	C	P	S	R	G	T	K	G	M	I	G	R	-	-	-	-	0.2	-
OCT1*16	S	S	R	C	P	S	R	V	T	E	G	M	I	G	R	-	-	-	-	0.2	-

Polymorphisms defining haplotypes according to Seitz *et al.* (Seitz et al. 2015) are indicated and highlighted with red circles. Prevalences ≥ 0.05 % of haplotypes in major populations are indicated in percentages. AM – Central and Southern America; EU – Europe; NA – North Africa and Middle East; SA – Southern Africa; OC – East Asia and Oceania; CA – Central Asia

Distribution differences have consequences as OCT1 variants lead to functional impairments (Jensen et al. 2020a; Jensen et al. 2020b; Matthaei et al. 2019; Matthaei et al. 2016; Seitz et al. 2015; Shu et al. 2003; Tzvetkov et al. 2012; Tzvetkov et al. 2018). The most common variant OCT1*2 is associated with a substrate-specific loss-of-function. Depending on the substrate, transport activity ranges from a complete loss of function to activity above reference OCT1 (Kerb et al. 2002; Saadatmand et al. 2012; Shu et al. 2007; Tzvetkov et al. 2013). The haplotypes OCT1*3 and *4 show a strong reduction (70 and 80 %, respectively) of transport activity in the vast majority of substrates (Seitz et al. 2015; Tzvetkov et al. 2016). However, it is to note that measurements at single concentrations do not reveal the complete picture. For example, uptake of fenoterol by OCT1*4 is reduced (compared to reference OCT1) at low concentrations, but v_{max} by OCT1*4 is increased. The haplotypes OCT1*5 and *6 both consist of a SNP and the Met420 deletion. Both haplotypes are characterized by impaired localization into the plasma membrane (Seitz et al. 2015). The haplotype OCT1*7, which is present in African, Middle Eastern and Central Asian populations, is often associated with reference OCT1-like transport. For some substrates, however, a strong reduction has been observed. OCT1*8 is the only variant, which has consistently been described with transport activity at the same level as the reference allele or even

7

above (Seitz et al. 2015). The less common variants *9 to *16 have only rarely been studied and summary statements about these are not possible at this point in time.

2.3 Substrate spectrum and polyspecificity of OCT1

While many known transport proteins serve a distinct function and facilitate the uptake of a specific substrate, there is no specific or prototypic substrate for OCT1. Instead, it is a so-called polyspecific transporter, which means that OCT1 translocates a number of heterogeneous molecules. This polyspecificity is common amongst the SLC22 family. For OCT1, major criteria for substrates are compound size, charge, and lipophilicity. A certain size should not be exceeded in order to ensure the fit of the molecule into the transporter. Positive charge is somehow essential and the most prominent commonality between known substrates (even though there are exceptions). Low lipophilicity is associated with the need of transport across the lipid bilayer. Lipophilic compounds will diffuse through cell membranes. The logD value (octanol-water-partition coefficient) is an indicator to determine the lipophilicity of ionizable compounds, and thus a predictor for the possibility of substances being taken up into cells via diffusion. While previous studies showed that OCT1 transports a large number of cationic compounds, it was also shown that not all cationic substances are substrates for OCT1 (Figure 5).

It was shown that molecular volume is one major descriptor of OCT1 uptake and that compounds with a volume > 500 Å^3 were unlikely to be transported (Hendrickx et al. 2013). However, Hendrickx *et al.* did not find correlation between OCT1 uptake of compounds and their logD or polar surface area (PSA). A striking commonality of OCT1 substrates is the positive charge. The pK$_a$ values of ionizable moieties provide information about the (total) charge of a molecule at a certain pH. Positively charged bases and compounds with quaternary amine groups (positively charged independent of the surrounding pH) belong to the favorable OCT1 substrates (Hendrickx et al. 2013) (Figure 5). Quaternary amines have been identified as good molecular fingerprint to identify OCT1 substrates (Baidya et al. 2020). Other favorable molecular fingerprints included the presence of two aromatic cycles at one bond distance or the presence of sulfur.
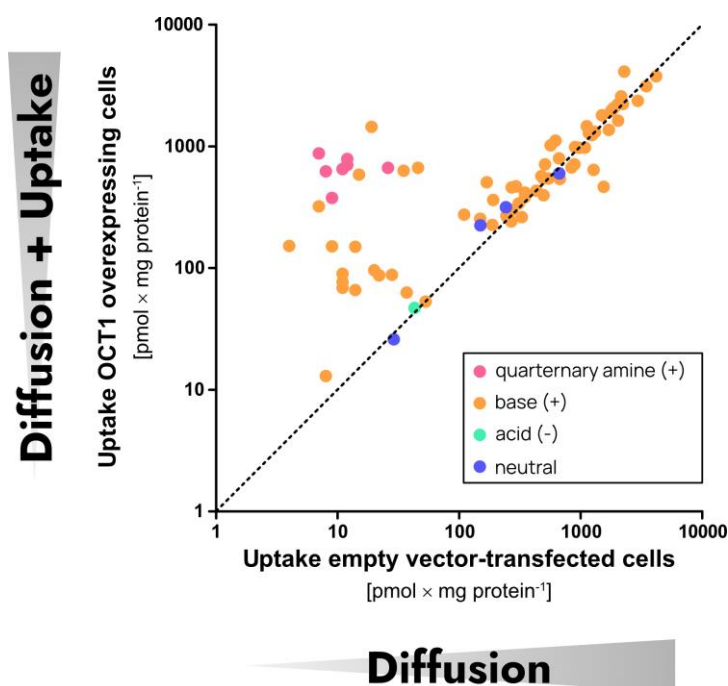
Figure 5: The OCT1 protein facilitates the uptake of many substrates. Dashed line (function x = y) indicates case, in which uptake is only influenced by diffusion and not by additional transport. Data by Hendrickx (Hendrickx et al. 2013), reduced to non-experimental molecules.

Previous descriptions of OCT1 substrates include hydrogen bond donors (e.g. by an hydroxyl group), ion pair interaction sites (e.g. via a positively charged nitrogen), and hydrophobic interaction sites (e.g. via aromatic structures) (Moaddel et al. 2005). These descriptors, however, are by no means part of all OCT1 substrates, nor do they sufficiently explain the different transport rates of different substrates.

Probe substrates commonly used for OCT1 studies include MPP^+ (Shu et al. 2003; Zhang L. et al. 1997), TEA^+ (Sakata et al. 2004), and ASP^+ (Ahlin et al. 2008). These substrates are not among the substrates with the highest affinities or transport rates, but their use is historically justified. The range of OCT1 substrates overall is highly diverse and includes dozens of substrates from different drug classes (Koepsell 2020) (Figure 6). Small substrates, such as TEA^+ with a mass of 130.3 g × mol^{-1} and amifampridine, which is a K^+/Na^+ channel blocker with a mass of 109.1 g × mol^{-1}, are considered OCT1 substrates. On the other hand, also large compounds, such as the anticholinergic butylscopolamine (440.4 g × mol^{-1}) and the most bitter chemical compound known, denatonium (446.6 g × mol^{-1}), are OCT1 substrates. However, not just sizes and molecular masses of substrates differ significantly, also structural components do. Known substrates vary in their composition. The number of phenyls, for example, ranges from zero to three, and the number of hydroxyl groups range from zero to four. The most common denominator of all OCT1 substrates is the presence of at least one nitrogen atom.
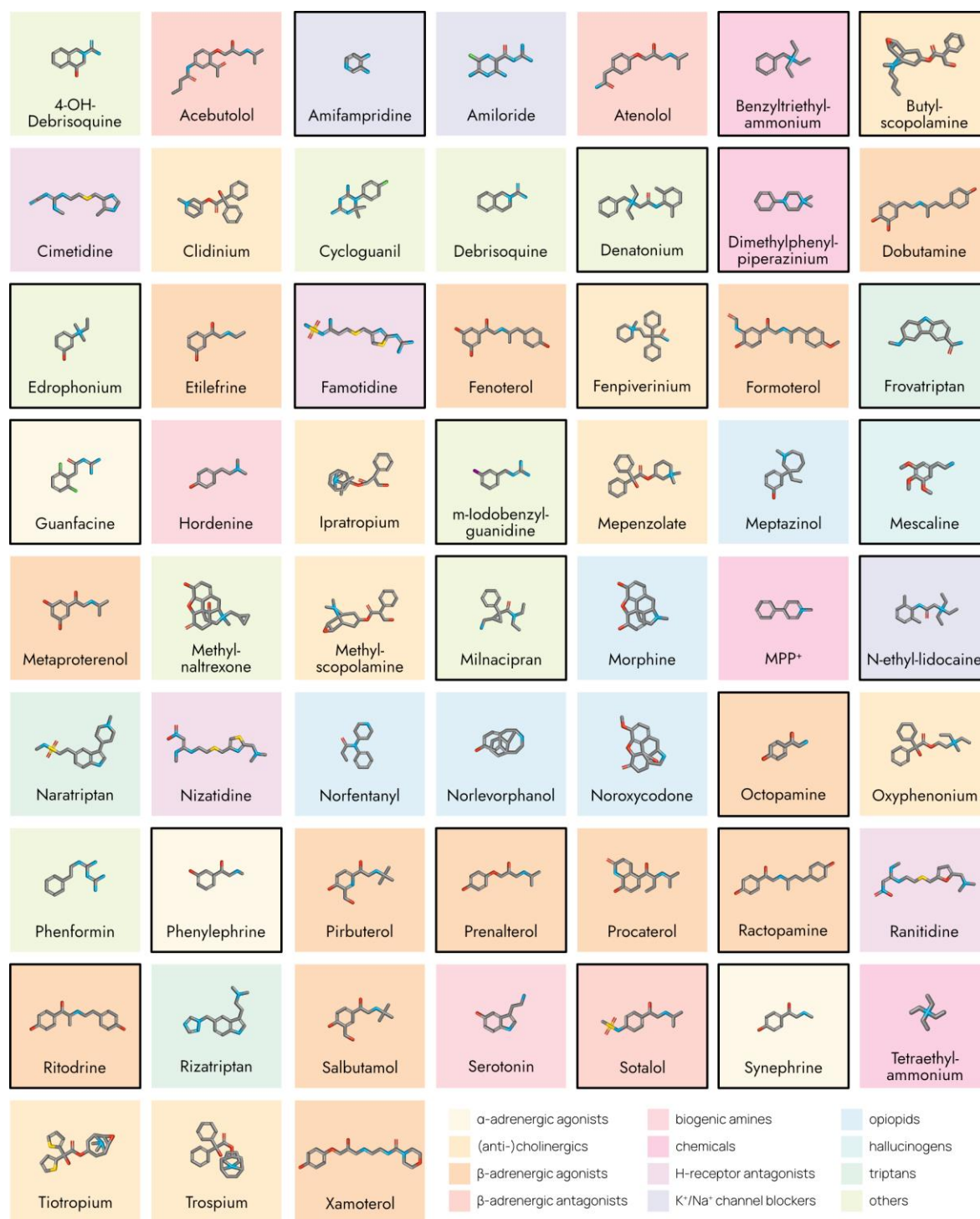
Figure 6: Selection of OCT1 substrates illustrates marked polyspecificity. Molecule structures of substrates with uptake ratio ≥ 3 (uptake into cells overexpressing OCT1/uptake into empty vector-transfected cells) and $Cl_{int} ≥ 5$ are shown in alphabetical order and grouped into drug classes by background colors.

The polyspecific nature of OCT1, might be caused by different binding sites within the binding pocket of the transporter. These binding sites could separately or in combination facilitate substrate recognition (Gorboulev et al. 2005; Gorboulev et al. 1999; Popp et al. 2005; Volk et al. 2009). Several studies indicate that the different binding sites differ in their affinities to the

investigated substrates (Gorbunov et al. 2008; Keller et al. 2019; Minuesa et al. 2009). By targeted mutageneses, it was shown, that the loss of specific amino acids can alter substrate affinity or transport velocity (Koepsell 2019). Targeted mutageneses suggested a role for the amino acids Phe159, Trp217, and Asp474 for binding (Figure 7). The exchange by other amino acids decreased (D475E for TEA$^+$; W217Y for MPP$^+$) or increased K$_m$ (F159A/Y for MPP$^+$; W217F for TEA$^+$) or the IC50 (for different model substrates) in a substrate-dependent manner (Gorboulev et al. 2018; Popp et al. 2005).
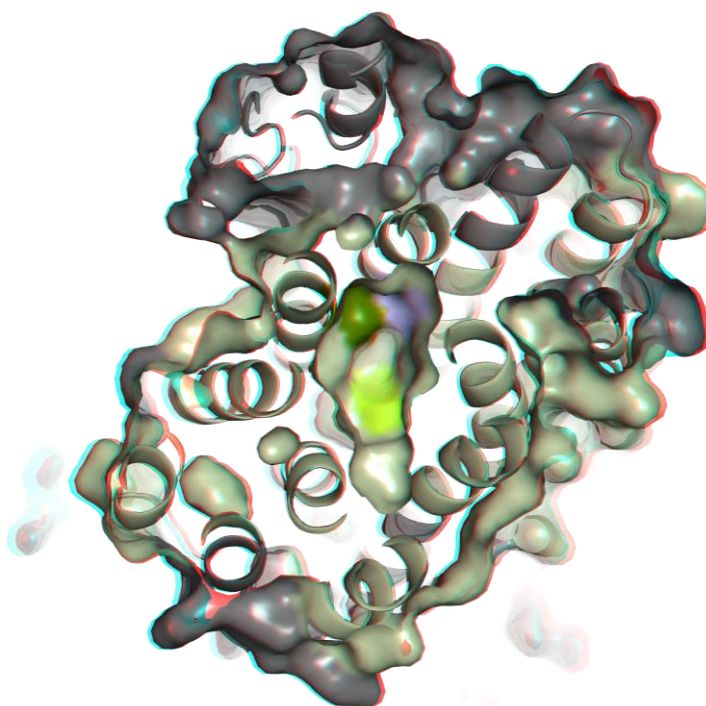
Figure 7: View from the extracellular side into the binding cleft of OCT1 in the outward-open conformation. Transmembrane helices are colored in 'wheat' and the amino acids F159, W217, and D474 are highlighted in purple, yellow, and olive green, respectively. For optimal experience use anaglyph 3D glasses, such as the ones enclosed with the printed version. Structure Model by Dakal et al. (Dakal et al. 2017), generation of the anaglyphic rendering with The PyMOL Molecular Graphics System, Version 2.2.0 Schrödinger, LLC.

At the current time, there is no crystal structure data of human OCT1 available and homology models used as a substitute rely on sequence identity of as low as 20 % to the closest crystallized protein (Dakal et al. 2017). The protein structure-based approach, analyzing the effects of mutageneses, is a proper way to study the structure-to-function relationship of OCT1 (Meyer 2020; Popp et al. 2005). In addition, ligand-based approaches are a way to circumvent the lack of a crystal structure by putting known substrates in the foreground of the analyses (Baidya et al. 2020). Still, these analyses are often based on two-dimensional representations. Therefore, ligand-based approaches often do not account for enantiomeric differences.

2.4 Pharmacological relevance of OCT1

The possible pharmacological relevance of OCT1 was shown in several *in vitro* studies for different substrates. Main distinction needs to be made between drugs, which act in the liver (e.g. metformin) or require hepatic uptake for metabolism into the active compound (type IB prodrugs, e.g. proguanil), and drugs, which are taken up into hepatocytes and subsequently eliminated via the bile. Loss-of-function variants of OCT1 will lead to reduced uptake and efficacy in the first and increased blood concentration leading potentially to increased side effects in the second case. With OCT1, genetic effects on pharmacokinetics and -dynamics have to be considered in addition to drug-drug interactions that have to be considered for all transporters. In addition to a large number of *in vitro* studies, also clinical studies were carried out to investigate the influence of OCT1 on the pharmacokinetics of numerous drugs in the real context of a living human organism.

One of the best-known OCT1 substrates is the antidiabetic biguanide metformin (Christensen et al. 2011; Pernicova und Korbonits 2014; Wang et al. 2002; Zolk 2009). It was shown *in vitro* that the effect of metformin correlated with the activity of OCT1 variants (Shu et al. 2007). Furthermore, in healthy human volunteers and patients treated with metformin, OCT1 variants lead to reduced response, indicated by higher glucose and HbA_{1c} levels (Becker et al. 2009; Shikata et al. 2007; Shu et al. 2008). However, this data was not unequivocally confirmed by other studies. Concerning systemic exposure, the extrarenal clearance of metformin was not significantly altered by OCT1 variants, as 99.9 % of intravenously administered metformin is eliminated via the kidneys (Pentikäinen et al. 1979; Tzvetkov et al. 2009). Interestingly enough, recent experiments could even demonstrate a possible metformin efflux activity of OCT1 (Jensen et al. 2021b).

Many beta-adrenergic agonists, such as fenoterol, salbutamol, and terbutaline were shown to be transported by OCT1 *in vitro* (Hendrickx et al. 2013). In addition, for fenoterol, it was shown *in vivo* that loss-of-function OCT1 variants lead to increased fenoterol plasma concentrations and even to measurably increased plasma glucose and heart rates (Tzvetkov et al. 2018).

The impact of loss-of function OCT1 variants on transport activity was also shown by *in vitro* studies for the antihistaminic ranitidine as well as the 5-HT receptor antagonists ondansetron and tropisetron (Meyer et al. 2017; Tzvetkov et al. 2012). The same holds true for the active metabolite of the pain medication tramadol, O-desmethyltramadol (Tzvetkov et al. 2011), for which *in vivo* increased plasma concentrations were shown in OCT1-deficient individuals even after reduced tramadol consumption (Stamer et al. 2016).

In healthy volunteers, hepatic uptake of the opiate morphine by OCT1 was shown to be affected by common polymorphisms after codeine intake (Tzvetkov et al. 2013). Genetic variants also influence morphine clearance in children (Fukuda et al. 2013). However, the association of OCT1 variants and morphine pharmacokinetics and pharmacodynamics was not found in all studies (Nielsen et al. 2017).

Another commonly prescribed OCT1 substrate is sumatriptan, an anti-migraine drug. Sumatriptan is eliminated after inactivating metabolism by MAO-A in the liver (Dixon et al. 1994; Fowler et al. 1991). Loss-of function OCT1 variants were shown to affect sumatriptan pharmacokinetics, and results of *in vitro* uptake experiments pointed towards potential interaction with other triptans as well (Matthaei et al. 2016).

Pharmacokinetics – and even more pharmacodynamics – are difficult to predict, because reliable *in vitro* models are rare or imprecise, and large interspecies differences in transporter expression and activity profiles complicate the exploration. In the end, only studies in humans can elucidate the role of transporters for pharmacokinetics, including the impact of loss-of-function variants.

Apart from therapeutic drugs, OCT1 also mediates the uptake of several toxic agents, such as aflatoxin B1 or ethidium (Tachampa et al. 2008). The lack of endogenous substrates, for which OCT1 could be considered as the only hepatic transporter, allows only speculation about the reasons for evolutionary conservation of *OCT1*. The general hepatic detoxification of all kinds of differently shaped organic cations could be a reason for its preservation (Zhang L. et al. 2006).

2.5 Physiological relevance of OCT1

Compared to pharmaceuticals, there is little information available about the OCT1-mediated uptake of endogenous substances. In the last few years, the knowledge on thiamine as a possible substrate for OCT1 has improved. It was shown that OCT1 is a high-capacity thiamine (vitamin B1) transporter (Chen L et al. 2014). In Oct1-deficient mice, hepatic steatosis was observed, probably due to thiamine deficiency (Chen L et al. 2014; Liang X et al. 2018). However, much of this data was supported by murine Oct1 only and there is a substantial difference between rodent and human OCT1 concerning substrate specificity and tissue expression.

Serotonin transport was first only discovered for rodent Oct1, but later for human OCT1 as well (Amphoux et al. 2006; Jensen 2017). Other monoamines, such as adrenaline, dopamine, noradrenaline, and tyramine were reported as OCT1 substrates and inhibitors of OCT1 transport as well (Amphoux et al. 2006; Bednarczyk et al. 2003; Breidert et al. 1998). However, these studies were performed with the rat orthologue of OCT1 (rOct1) or reported IC_{50} values beyond physiologic concentrations.

2.6 Aims of this study

The goals listed below encompass the central aspects of this work and will be addressed in the next chapter by published articles.

1. The expansion of the known OCT1 substrate spectrum should contribute to a better understanding of the possible biological roles of OCT1 and can be carried out by further exploration of the chemical space on substances which are even not highly structurally related to previously known substrates. Many psychostimulants and hallucinogens are organic cations and reasonably hydrophilic. These water-soluble compounds most likely require transporter-mediated uptake into the brain to exert their effects. Influx transporters like OCT1 might be involved in the uptake of these psychostimulants. Therefore, psychostimulant and hallucinogenic compounds, such as, amphetamine, cocaine, and mescaline were investigated for their potential of transport by OCT1. This should contribute to our toxicological understanding of the impact of OCT1 on potentially dangerous psychostimulant and hallucinogenic substances.

2. The list of already known OCT1 substrates is long, and this knowledge can be exploited to find additional substrates. The traditional approach to find new substrates would utilize all the chemical knowledge and ingenuity of the chemist, but nowadays a significant part of this can be performed using computational assistance. Large databases can be screened more systematically and less error-prone. Our traditional approach considered substances with a molecular weight below 600 Da, a $pK_a > 7.4$ and a $logD < 1$ as likely candidates of OCT1 substrates. However, as shown in the psychostimulant project many substances fulfilling these criteria were nevertheless no (good) substrates of OCT1. Therefore, apparently additional criteria are needed to describe OCT1 substrates and a machine learning-guided approach was used to predict additional OCT1 substrates. Still, the gold-standard to identify a substrate of an enzyme or transporter is the experimental proof. Therefore, validation of newly suggested compounds was performed by *in vitro* transport.

3. As machine learning approaches are often restricted to two-dimensional representations of molecules, predictions of enantiomeric effects are limited. About one third of all drugs are still marketed as racemic mixtures, containing both enantiomers. Little is currently known about whether enantiomers are transported equally well or with certain stereoselectivity. In comparison to many enzymes, which are highly substrate- and enantiospecific, the broad specificity of OCT1 might be accompanied by reduced stereoselectivity. Therefore, potential stereoselective transport by OCT1 was tested *in vitro* to investigate how specific the interaction between the transporter and enantiomeric substrates is.

4. Modern systems biology tries to comprehensively understand the complex interactions of processes in the human body. Understanding the entire interplay between thousands of enzymes and transporters may start with more simple models including only two or three partners. Loss of OCT1 expression in most hepatocyte-derived cell lines makes it difficult to predict *in vivo* uptake and subsequent metabolism from *in vitro* experiments if not primary hepatocytes are used. Therefore, a cell model for the uptake and subsequent metabolism was developed. Overexpression of multiple genes in one cell is not an entirely new technique, but the technique developed here has particular advantages: Successfully double-transfected cells can be selected with one antibiotic, the cell line generation is relatively quick, and it results in equally strong overexpression of two proteins and can almost universally be applied.

5. The final validation of *in vitro* findings can only be achieved by *in vivo* studies. This is especially true for potential endogenous biomarkers, which are thought to reflect the phenotype of metabolizing enzymes or transport proteins. For OCT1, thiamine had been suggested as a biomarker on the basis of previous *in vitro* and animal experiments. Therefore, the role of OCT1 in the uptake of thiamine was studied *in vitro* and its relevance as a biomarker for OCT1 activity *in vivo* in healthy male and female volunteers.
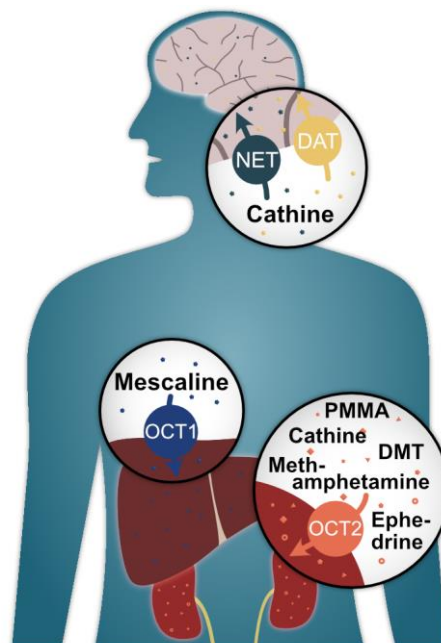
3 Publications

3.1 Publication 1

Cellular Uptake of Psychostimulants — Are High- and Low-Affinity Organic Cation Transporters Drug Traffickers?

Ole Jensen, Muhammad Rafehi, Lukas Gebauer, and Jürgen Brockmöller

Institute of Clinical Pharmacology, University Medical Center Göttingen, Göttingen, Germany

Cellular Uptake of Psychostimulants – Are High- and Low-Affinity Organic Cation Transporters Drug Traffickers?

Ole Jensen*, Muhammad Rafehi*, Lukas Gebauer and Jürgen Brockmöller

Institute of Clinical Pharmacology, University Medical Center Göttingen, Göttingen, Germany

Psychostimulants are used therapeutically and for illegal recreational purposes. Many of these are inhibitors of the presynaptic noradrenaline, dopamine, and serotonin transporters (NET, DAT, and SERT). According to their physicochemical properties, some might also be substrates of polyspecific organic cation transporters (OCTs) that mediate uptake in liver and kidneys for metabolism and excretion. OCT1 is genetically highly polymorphic, with strong effects on transporter activity and expression. To study potential interindividual differences in their pharmacokinetics, 18 psychostimulants and hallucinogens were assessed *in vitro* for transport by different OCTs as well as by the high-affinity monoamine transporters NET, DAT, and SERT. The hallucinogenic natural compound mescaline was found to be strongly transported by wild-type OCT1 with a K_m of 24.3 μM and a v_{max} of 642 pmol × mg protein^{-1} × min^{-1}. Transport was modestly reduced in variants *2 and *7, more strongly reduced in *3 and *4, and lowest in *5 and *6, while *8 showed a moderately increased transport capacity. The other phenylethylamine derivatives methamphetamine, *para*-methoxymethamphetamine, (-)-ephedrine, and cathine ((+)-norpseudoephedrine), as well as dimethyltryptamine, were substrates of OCT2 with K_m values in the range of 7.9–46.0 μM and v_{max} values between 70.7 and 570 pmol × mg protein^{-1} × min^{-1}. Affinities were similar or modestly reduced and the transport capacities were reduced down to half in the naturally occurring variant A270S. Cathine was found to be a substrate for NET and DAT, with the K_m being 21-fold and the v_{max} 10-fold higher for DAT but still significantly lower compared to OCT2. This study has shown that several psychostimulants and hallucinogens are substrates for OCTs. Given the extensive cellular uptake of mescaline by the genetically highly polymorphic OCT1, strong interindividual variation in the pharmacokinetics of mescaline might be possible, which could be a reason for highly variable adverse reactions. The involvement of the polymorphic OCT2 in the renal excretion of several psychostimulants could be one reason for individual differences in toxicity.

Keywords: membrane transport, monoamine transporter, OCT1, organic cation transporter, psychostimulant, SLC22A1, solute carrier, hallucinogen

Abbreviations: CYP, cytochrome P450; DAT, dopamine transporter; DET, diethyltryptamine; DMT, dimethyltryptamine; DOI, 2,5-dimethoxy-4-iodoamphetamine; MATE2-K, multidrug and toxin extrusion protein 2 kidney-specific; MBDB, *N*-methyl-1,3-benzodioxolylbutanamine; MDAI, 5,6-methylenedioxy-2-aminoindane; MDEA, 3,4-methylenedioxy-*N*-ethyl-amphetamine; MDMA, 3,4-methylenedioxymethamphetamine; MPP$^+$, 1-methyl-4-phenylpyridinium; NET, noradrenaline (norepinephrine) transporter; OCT, organic cation transporter; PCR, polymerase chain reaction; PMA, *para*-methox-yamphetamine; PMMA, *para*-methoxymethamphetamine; SERT, serotonin transporter; SLC, solute carrier; WT, wild-type.

FIGURE 1 | Psychostimulant and hallucinogenic drugs assessed for cell uptake by OCTs and high-affinity monoamine transporters.
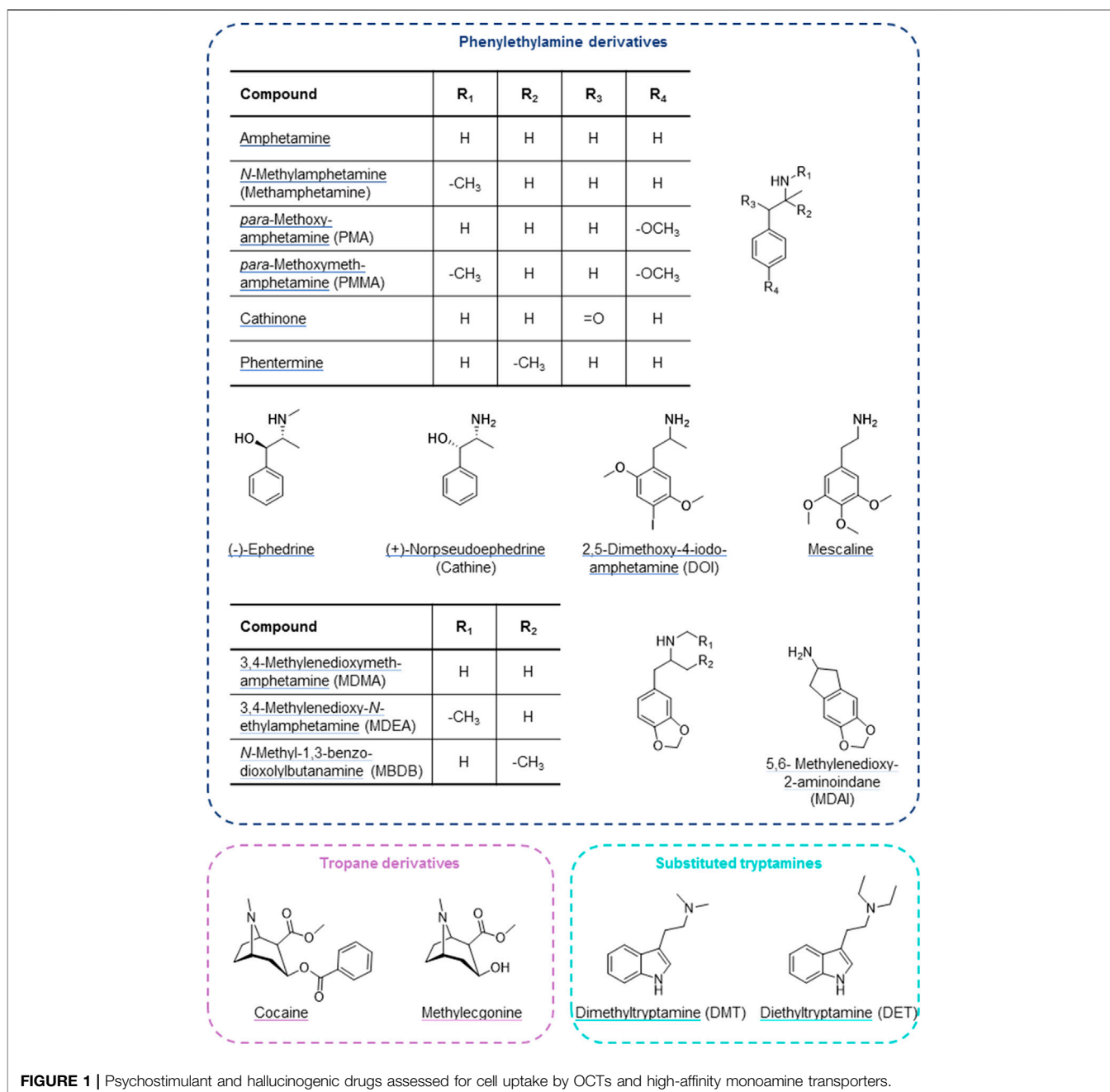
INTRODUCTION

Psychostimulants modulate wakefulness and mental performance. They function as indirect sympathomimetics by raising synaptic concentrations of monoamine neurotransmitters through stimulating their release from presynaptic vesicles and/or inhibiting reuptake. Psychostimulants can also interfere with monoaminergic neurotransmitter metabolism and interact with monoaminergic receptors and other targets (Luethi and Liechti, 2020; Reith and Gnegy, 2020). Amphetamine and other phenylethylamine derivatives (**Figure 1** top) form a large group of such indirect sympathomimetics. They are used in the treatment of attention deficit hyperactivity disorder and narcolepsy but are also frequently found in illicit drugs (e.g., "speed", "ecstasy", "crystal meth") (Sharma and Couture, 2014; Luethi and Liechti, 2020). Another indirect sympathomimetic is cocaine (**Figure 1** bottom left), a tropa-alkaloid and, historically, the first local anesthetic. Its (widely illegal) use as a psychostimulant nowadays far exceeds its therapeutic application in local anesthesia. Psychostimulants are among the most popular drugs of abuse. A related and partially overlapping class of psychoactive substances are the hallucinogens (psychedelics), which alter perception, cognition, and mood. These include tryptamine derivatives, such as the alkaloid dimethyltryptamine (DMT). It

TABLE 1 | Physicochemical properties of investigated psychoactive compounds (predicted using MarvinSketch, version 19.8, ChemAxon, Budapest, Hungary).

Test compound	LogD$_{pH\ 7.4}$	pK$_a$	% Positively charged at pH 7.4
Amphetamine	−0.67	10.01	99.76
Methylamphetamine	−0.44	10.21	99.85
PMA	−0.85	10.04	99.77
PMMA	−0.52	10.03	99.76
Cathinone	0.79	7.55	58.59
Phentermine	−0.55	10.25	99.78
(-)-Ephedrine	−0.78	9.53	99.26
Cathine	−1.05	9.37	98.94
DOI	0.02	9.90	99.69
Mescaline	−1.37	9.77	99.58
MDMA	−0.76	10.14	99.82
MDEA	−0.46	10.22	99.85
MBDB	−0.34	10.28	99.87
MDAI	−1.33	9.96	99.73
Cocaine	0.82	8.85	96.54
Methylecgonine	−1.86	9.04	97.76
DMT	0.17	9.55	99.29
DET	0.39	10.08	99.79

is a main constituent of ayahuasca, the plant brew used traditionally by indigenous inhabitants of the Amazon region for spiritual and religious ceremonies. DMT and its diethyl analogue (**Figure 1** bottom right) show structural resemblance to the neurotransmitter serotonin and thereby function as agonists at 5-HT$_{2A}$ and related receptors (Nichols, 2016; Luethi and Liechti, 2020). Another traditional hallucinogen is mescaline, a phenethylamine alkaloid found in cacti (Ogunbodede et al., 2010; Nichols, 2016; Luethi and Liechti, 2020). It is a partial agonist at 5-HT$_{2A}$ and 5-HT$_{2B}$ receptors and a full agonist at the 5-HT$_{2C}$ receptor (Dinis-Oliveira et al., 2019).

Many psychoactive substances are substrates or inhibitors of the noradrenaline (norepinephrine) transporter (NET), the dopamine transporter (DAT), and/or the serotonin transporter (SERT) (Luethi and Liechti, 2020). These high-affinity transport proteins are expressed at presynaptic neurons, where they mediate the reuptake of monoamine neurotransmitters from the synaptic cleft to terminate synaptic signal transmission and for recycling (Torres et al., 2003). They are members of the large Solute Carrier (SLC) superfamily and coded for by the genes *SLC6A2* (NET), *SLC6A3* (DAT), and *SLC6A4* (SERT).

Organic cation transporters (OCTs) are also SLCs with a broad, partially overlapping substrate spectrum that is predominantly comprised of hydrophilic, organic cationic substances (including monoamine neurotransmitters as well as many drugs) (Busch et al., 1998; Gründemann et al., 1998; Wu et al., 1998; Koepsell et al., 2007). OCT1 (*SLC22A1*) and, to a lesser extent, OCT3 (*SLC22A3*) are expressed on the sinusoidal membrane of hepatocytes, where they mediate cellular uptake for hepatic metabolism (Nishimura and Naito, 2005; Nies et al., 2009). A high degree of genetic variation exists for *SLC22A1*, and several of these variants strongly impact transporter expression and function (Koepsell et al., 2007; Seitz et al., 2015). This may affect the pharmacokinetics of compounds

that are substrates of OCT1, as has been shown, for example, for the opioid analgesics morphine and *O*-desmethyltramadol (Tzvetkov et al., 2011; Tzvetkov et al., 2013; Venkatasubramanian et al., 2014; Stamer et al., 2016), the antimalarial prodrug proguanil (Matthaei et al., 2019), the anti-asthma drug fenoterol (Tzvetkov et al., 2018), sumatriptan that is used for the treatment of migraine (Matthaei et al., 2016), and, to a minor extent, for the antidiabetic drug metformin (Tzvetkov et al., 2009; Yee et al., 2018). The psychoactive substances studied here (**Figure 1**) were selected based on physicochemical properties (organic cations with pK$_a$ > 8.4 and relatively hydrophilic substances with a logD$_{pH\ 7.4}$ < 2; **Table 1**) that make them potential substrates for OCTs. Consequently, their pharmacokinetics could potentially be affected by OCT polymorphism as well. OCT2 (*SLC22A2*) is mainly found on the basolateral membrane of kidney epithelial cells (Motohashi et al., 2002; Motohashi et al., 2013). Together with multidrug and toxin extrusion protein 2 kidney-specific (MATE2-K, *SLC47A2*), an efflux transporter expressed on the brush-border membrane of the proximal tubule, it mediates transport across the epithelium for renal excretion (Motohashi et al., 2013). *SLC22A2* variants are less frequent compared to the gene coding for OCT1, and only a few affect OCT2 expression or function. The most frequent of these is Ala270Ser, which causes a moderate decrease in OCT2 activity (Zolk et al., 2009). As many psychoactive substances are structurally related to the neurotransmitters and OCT substrates noradrenaline, dopamine, and serotonin and have physicochemical properties in line with typical OCT substrates, their pharmacokinetics may be determined by OCTs and influenced by OCT1 (and possibly OCT2) polymorphism.

Although mainly expressed in peripheral tissues, OCT2 and OCT3 are also found on postsynaptic neurons (and OCT3 in astrocytes) predominantly in aminergic regions of the central nervous system. There, they may be involved in reuptake of monoamine neurotransmitters in brain areas lacking the high-affinity transporters, at distance from the aminergic nerve endings, or as an alternative when the high-affinity transporters are saturated or inhibited (Wu et al., 1998; Vialou et al., 2008; Bacq et al., 2012; Couroussé and Gautron, 2015). OCT2 appears to be involved in the uptake of noradrenaline and serotonin in particular, while OCT3 was found to be more strongly responsible for dopamine clearance (Vialou et al., 2008; Bacq et al., 2012). Interestingly, it has also been shown that amphetamines can induce neurotransmitter release through OCT3, which is capable of bi-directional transport (Mayer et al., 2018; Mayer et al., 2019). Thus, OCTs may not only determine the pharmacokinetics of psychoactive drugs but appear to be also involved in their actions.

Given the potential dual role of OCTs with respect to psychoactive drugs and the current lack of understanding of the pharmacokinetics and pharmacogenetics for these compounds, we characterised the transmembrane transport by polyspecific OCTs as well as high-affinity monoamine reuptake transporters. Of particular interest are those psychostimulants that are stereoisomers of one another (ephedrine, norephedrine, their enantiomers and diastereomers), because the impact of

stereospecificity on membrane transport is as yet not well understood but previous results suggest partially strong enantiopreferences (Jensen et al., 2020).

MATERIALS AND METHODS

Test Compounds

The psychoactive compounds studied here were selected based on their physicochemical properties that would make them likely substrates for OCTs. Selection criteria included hydrophilicity (logD at pH 7.4 of less than 2), at least 90% positively charged at physiological pH ($pK_a > 8.4$), and molecular mass not higher than 500 Da. The reasons for these were that lipophilic compounds permeate membranes mostly by diffusion, while membrane transport is mostly relevant for more hydrophilic compounds, as well as the observation that typical OCT1 substrates are usually positively charged and of low to moderate size. Cathinone (pK_a of 7.55) did not meet our selection criteria but was nonetheless included due to a low renal elimination (2–7% unchanged in urine) and, consequently, high rate of metabolism which, if taking place in the liver, might depend on hepatic uptake via OCT1 (Kalix and Braenden, 1985; Toennes and Kauert, 2002). Ranitidine-d6 was purchased from Toronto Research Chemicals (Toronto, Canada) and Tulobuterol from Santa Cruz Biotechnology (Darmstadt, Germany); all other test compounds and internal standards were bought from Sigma-Aldrich (Taufkirchen, Germany).

Generation of Transporter-Overexpressing Cell Lines

Transport experiments were done using HEK293 cells stably transfected to overexpress OCT1*1 (wild-type), OCT1*2 (M420del), OCT1*3 (R61C), OCT1*4 (G401S), OCT1*5 (M420del, G465R), OCT1*6 (C88R, M420del), OCT1*7 (S14F), OCT1*8 (R488M), as well as wild-type OCT2, OCT3, NET, DAT, SERT, or MATE2-K. All cell lines were generated using the Flp-In system (Thermo Fisher Scientific, Darmstadt, Germany) as previously described (Saadatmand et al., 2012; Seitz et al., 2015; Chen et al., 2017), except for the OCT3-overexpressing HEK293 cells that were a kind gift from Drs. Koepsell and Gorbulev (University of Würzburg, Germany). The cells were kept in culture for no more than 30 passages.

The high-affinity monoamine transporters were also stably transfected into HEK293 cells by use of the Flp-In system (Thermo Fisher Scientific, Darmstadt, Germany). Coding sequences of *SLC6A2* (NET), *SLC6A3* (DAT), and *SLC6A4* (SERT) were obtained from Source BioScience (Nottingham, United Kingdom; pBluescriptR:SLC6A2) or Addgene (Watertown, MA, United States; pcDNA3.1-hDAT was a gift from Susan Amara, Addgene plasmid # 32810, http://n2t.net/addgene:32810, RRID:Addgene_32810 and hSERT pcDNA3 was a gift from Randy Blakely, Addgene plasmid # 15483, http://n2t.net/addgene:15483, RRID:Addgene_15483 (Ramamoorthy et al., 1993)). After sequence correction and cloning into the pcDNA5 vector, generation and characterization of the cell lines were carried out as described before for the above-mentioned cell lines

(Saadatmand et al., 2012; Seitz et al., 2015). Genomic integration was validated for two independent cell clones by three polymerase chain reactions (PCR; **Figure 2**) to verify proper integration (integration PCR) and exclude multiple integration (multiple integration PCR). The presence of the gene of interest was verified by Sanger sequencing of the product of the third PCR (gene-of-interest PCR) after gel extraction (**Figure 2**). Overexpression of monoamine transporters was compared between cell clones by TaqMan® gene expression assays (Thermo Fisher Scientific, Darmstadt, Germany; **Figure 2**). Functional validation of newly generated cell clones was performed using noradrenaline and serotonin as probe drugs and one clone for each transporter was chosen for further transport studies.

In vitro Cellular Uptake Experiments

The HEK293 cells were cultered in DMEM medium supplemented with 10% (v/v) fetal bovine serum as well as penicillin (100 U/ml) and streptomycin (100 μg/ml) obtained from Thermo Fisher Scientific (Darmstadt, Germany). Cells were seeded on 12-well plates coated with poly-D-lysine (Sigma-Aldrich, Taufkirchen, Germany) 48 h before the transport experiments and incubated at 37°C, 95% relative humidity, and 5% CO_2. Cell lines overexpressing MATE2-K were incubated with 30 mM NH_4Cl in HBSS+ (10 mM HEPES in HBSS, pH 7.4; Thermo Fisher Scientific, Darmstadt, Germany) for 30 min prior to the assay to invert the direction of transport. All cell lines were washed with 37°C HBSS+ and subsequently incubated with the pre-warmed substrate in HBSS+ at 37°C. The time points for measuring substrate uptake were 1 min for MATE2-K and 2 min for the other SLCs. The uptake rate was experimentally determined to be linear for at least 10 min for OCT1*1. It was assumed to be linear for the other transporters as well, based on previous experience with these expression systems. The reaction was stopped by adding ice-cold HBSS+, and the cells were washed twice with ice-cold HBSS+ before lysis with 80% acetonitrile (LGC Standards, Wesel, Germany) including an internal standard. Subsequently, the intracellular substrate accumulation was determined using LC-MS/MS.

Concentration Analyses

Intracellular accumulation was measured by HPLC-MS/MS using a Shimadzu Nexera HPLC system with a LC-30AD pump, a SIL-30AC autosampler, a CTO-20AC column oven, and a CBM-20A controller (Shimadzu, Kyoto, Japan). Separation was done on a Brownlee SPP RP-Amide column (4.6 × 100 mm inner dimension with 2.7 μm particle size) with a C18 pre-column. The aqueous mobile phase contained 0.1% (v/v) formic acid and either 3% (v/v) organic additive (acetonitrile:methanol 6:1 (v/v)) for methylecgonine, 8% for amphetamine, methylamphetamine, cathinone, cathine, (-)-ephedrine, mescaline, MDAI, and DMT, or 20% for PMA, PMMA, DOI, phentermine, MDMA, MDEA, MBDB, cocaine, and DET. Chromatography was done at a flow rate of 0.3 ml/min. For detection, an API 4000 tandem mass spectrometer (AB SCIEX, Darmstadt, Germany) was used in MRM mode. The analytes, corresponding internal standards, and detection parameters are listed in the **Supplementary Table S1**. Peak integration and quantification of the analytes was done using the Analyst software
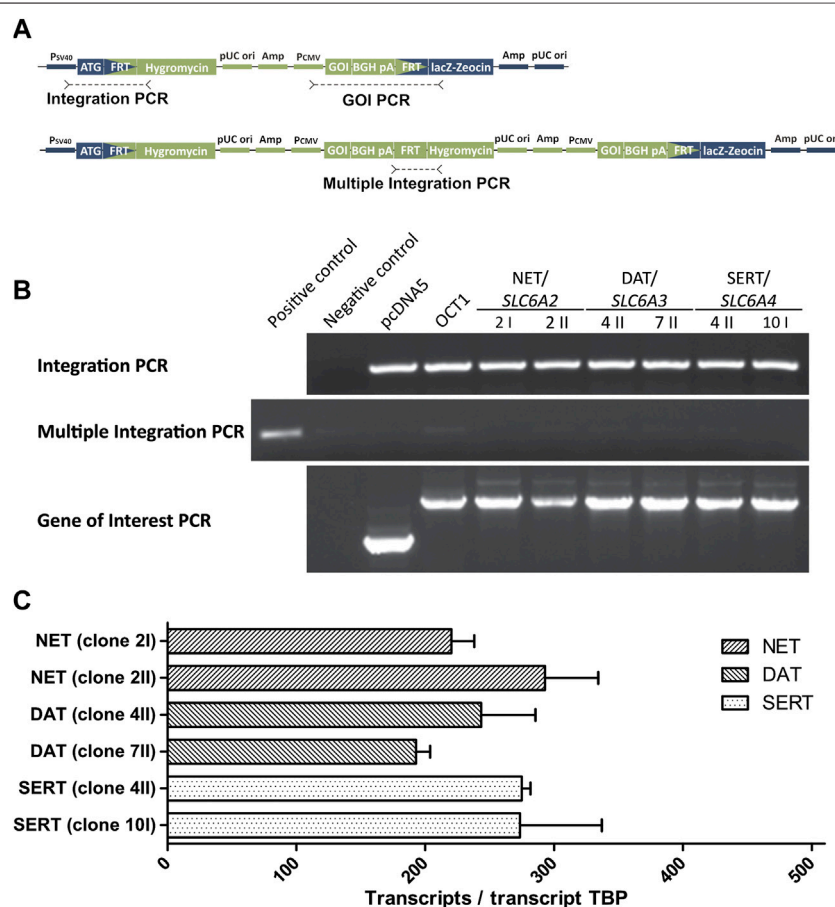
FIGURE 2 | Validation of HEK293 cell clones overexpressing monoamine neurotransmitter transporters **(A)** Schematic representation of the expression plasmid pcDNA5 (green) and the host cell line genome (blue) at the FRT site showing the target positions of the three conducted PCRs **(B)** Results of the three validation PCRs that show a successful integration (Integration PCR) for all newly created cell clones that overexpress the high-affinity monoamine transporters. The absence of amplicons in the Multiple Integration PCR indicate a single integration of the pcDNA5 plasmid. The correctness of amplified genes in the Gene of Interest (GOI) PCR was validated by Sanger sequencing **(C)** Quantitative real-time PCR results to confirm comparable overexpression of monoamine transporters, shown as transcripts per transcript of the TATA-binding protein. Only one cell clone was selected per transporter for experiments.

(Version 1.6.2, AB SCIEX, Darmstadt, Germany) and determined by simultaneous measurement of standard curves with known concentrations.

Calculations

For the screenings, cellular uptake measured in cell lines overexpressing the respective transporter was divided by the uptake measured in an empty vector control cell line to calculate normalised ratios to enable comparisons between test compounds. For studying transport kinetics, the net transport mediated by the overexpressed transporters was calculated by subtracting the cellular uptake measured in an empty vector control cell line from the uptake in cell lines overexpressing the respective transporter. The parameters K_m and v_{max} were estimated by regression analysis using the Michaelis-Menten equation (GraphPad Prism version 5.01 for Windows, GraphPad Software, La Jolla, CA, United States). Means and standard errors were calculated from individual K_m and v_{max}

values of at least three independent experiments. The kinetic parameters v_{max} and K_m were tested for statistical significance over empty vector control cells using Student's t-test with an alpha value of 0.05.

RESULTS

Screening of Transport Activity at OCTs, Monoamine Transporters, and MATE2-K

Eighteen psychostimulants and hallucinogens were initially screened for their potential to be substrates for different polyspecific OCTs and high-affinity monoamine neurotransmitter transporters (**Figure 3**), as well as for the efflux transporter MATE2-K (**Supplementary Figure S1**). The compounds were assessed at a concentration of 1 μM, because it is unlikely that low-affinity transport at higher concentrations may have any medical relevance and the relative contribution of
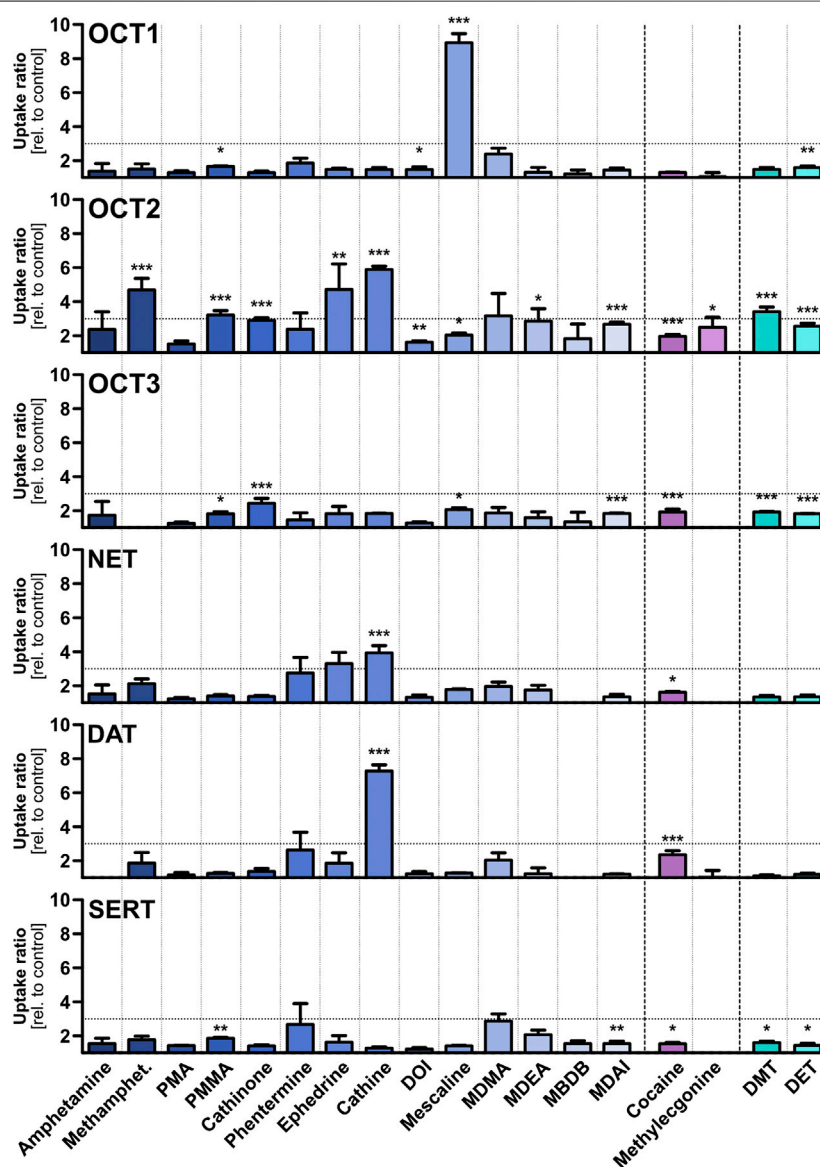
FIGURE 3 | Transport of different psychostimulant and hallucinogenic substances at a concentration of 1 µM by OCTs and high-affinity monoamine transporters, shown as the ratios of uptake after 2 min in transporter-transfected cells over empty vector control cells. Shown are the mean values of ≥3 independent experiments +SEM. The horizontal dotted line indicates an uptake ratio of 3, which was set as the minimum threshold for more detailed characterisation. Statistical significance over empty vector control cells was determined using Student's t-test with $*p < 0.05$, $**p < 0.01$, and $***p < 0.001$.

carrier-mediated transport over passive diffusion is significantly greater at lower compared to higher substrate concentrations, as was previously shown for morphine (Tzvetkov et al., 2013). Although the test compounds were selected based on physicochemical properties that are in accordance with those of typical OCT substrates, OCT1 showed high transport activity at this concentration only for mescaline. A cellular uptake in transporter-transfected cells of at least 3-fold higher than in non-overexpressing control cells was selected as the threshold for further studies, as this ratio is suitable to distinguish substrates from non-substrates. Cellular uptake of mescaline was more than 8-fold higher in OCT1-overexpressing cells, which was the

highest transport activity that was observed altogether in this study. Interestingly, mescaline was not transported much at 1 µM by any of the other transporters. In contrast to the substrate-specific but very strong transport activity exhibited by OCT1, moderate (4- to 6-fold) cellular uptake by OCT2 was seen for methamphetamine, (-)-ephedrine, and cathine ((+)-norpseudoephedrine) and approximately 3-fold for *para*-methoxymethamphetamine (PMMA) and DMT. OCT3 and MATE2-K (**Supplementary Figure S1**) showed little or no transport activity with any of the 18 psychoactive compounds studied here at 1 µM. Our observation, that amphetamine does not appear to be a substrate of OCT3, is in accordance with previous reports (Zhu et al., 2010).

FIGURE 4 | (A) Transport of mescaline at different concentrations by OCT1*1 (wild-type) and genetic variants, shown as the cellular uptake in transporter-overexpressing cells with substracted uptake in non-overexpressing control cells. Shown are the mean values of ≥3 independent experiments ±SEM. K_m and v_{max} values are given in **Table 2**. **(B)** Time-dependent uptake of 1 µM mescaline in OCT1*1-overexpressing (blue) and non-overexpressing control (pcDNA5, gray) cells, shown as the mean values of 3 independent experiments ±SEM **(C)** Mescaline transport by OCT1 could be completely inhibited by 1 mM MPP$^+$ to values not significantly different from the unspecific cellular uptake observed in empty vector-transfected cells (control).

TABLE 2 | Kinetic parameters for the transport of mescaline by different OCT1 genetic variants.

Variant	K_m [µM]	v_{max} [pmol × mg protein^{-1} × min^{-1}]
OCT1*1 (WT)	24.3 (±6.3)	641.7 (±57.1)
OCT1*2 (M420del)	34.7 (±7.4)	500.7 (±42.1)
OCT1*3 (R61C)	93.6 (±110.8)	390.7 (±265.8)
OCT1*4 (G401S)	98.2 (±46.7)	329.4 (±91.6)
OCT1*5 (M420del, G465R)	Not determinable	Not determinable
OCT1*6 (M420del, C88R)	Not determinable	Not determinable
OCT1*7 (S14F)	20.2 (±7.9)	514.6 (±63.8)
OCT1*8 (R488M)	18.6 (±3.7)	837.2 (±51.5)

The OCTs are known as low-affinity, high-capacity solute carriers with a very broad substrate spectrum that comprises structurally diverse compounds. In contrast, the monoamine neurotransmitter reuptake transporters NET, DAT, and SERT show high affinities to their respective endogenous substrates and a more narrow substrate profile than the OCTs. Cathine was transported modestly (4-fold) by NET and higher (7-fold) by DAT. No notable transport activity was observed for the other compounds, and none by SERT altogether. Cathine and (-)-ephedrine (as well as their stereoisomers) have been described previously as substrates for NET and DAT in *vitro* experiments with very different setup (Rothman et al., 2003). The slightly higher (albeit still low) uptake of PMA and PMMA by SERT compared to DAT is in line with literature reports that substitution in *para*-position of the phenyl ring of amphetamine derivatives shifts substrate preference toward SERT (Simmler et al., 2014).
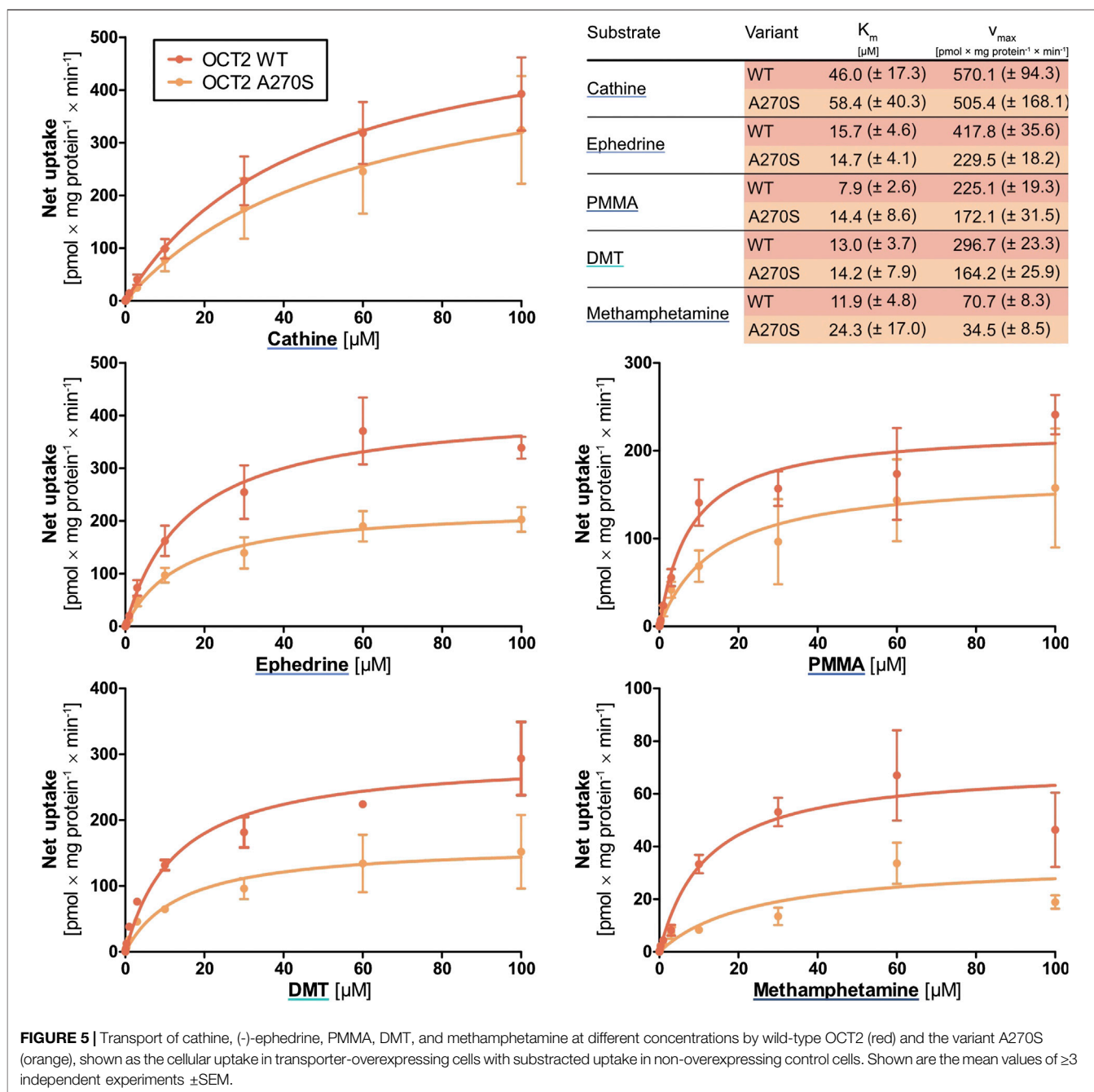
Concentration-dependent Transport of Mescaline by OCT1 Genetic Variants

Mescaline was found in our substrate screenings to be strongly transported by OCT1 and, therefore, it was studied in more detail. Given the high degree of genetic polymorphism and the large differences in transporter activity and expression for some variants,

cellular uptake of mescaline was not only characterised for wild-type (OCT1*1) but for OCT1 variants *2 to *8 as well. OCT1*1 transported mescaline with a K_m of 24.3 ± 6.3 µM and a v_{max} of 642 ± 57 pmol × mg protein^{-1} × min^{-1} (**Figure 4A**, **Table 2**). Time-dependent uptake of 1 µM mescaline showed a faster uptake rate within the first minute of incubation and a constant, linear uptake rate for 2 to at least 10 min (**Figure 4B**). The apparently more rapid initial uptake rate is likely a result of high-affinity binding to OCT1, but a short-lived more rapid transport might also be possible. The constant transport rate after 2 min of incubation might be the more relevant transport rate for pharmacokinetics because the exposure of the liver and other organs to drugs and other substances usually occurs for several hours. Mescaline uptake could be completely inhibited by the competitive OCT1 inhibitor 1-methyl-4-phenylpyridinium (MPP$^+$; **Figure 4C**). The K_m was slightly higher and the v_{max} slightly lower for *2, which is analogous to literature data on reduced transport activity for *2 (Seitz et al., 2015; Koepsell, 2020). This was even more pronounced (K_m of 93.6 ± 110.8 and 98.2 ± 46.7 µM; v_{max} of 391 ± 266 and 329 ± 92 pmol × mg protein^{-1} × min^{-1}) for *3 and *4, which are known to have strongly reduced transport activity (Seitz et al., 2015; Koepsell, 2020). For the variants *5 and *6 that result in impaired translocation to the plasma membrane (Seitz et al., 2015), very low transport activity was observed. Consequently, K_m and v_{max} values could not be reliably calculated. OCT1*7 exhibited a similar K_m and a modestly reduced v_{max} than OCT1*1. OCT1*8, on the other hand, showed a higher v_{max} than the wild-type, which has been reported previously for a number of substrates as well (Seitz et al., 2015; Koepsell, 2020). To summarise, transport activity of mescaline was slightly lower than wild-type OCT1 in variants *2 and *7, more drastically reduced in *3 and *4, and lowest in *5 and *6, while *8 showed a moderately higher v_{max} than wild-type OCT1.

Concentration-dependent Transport of Methamphetamine, PMMA, (-)-Ephedrine, Cathine, and DMT by OCT2 Wild-type and A270S Variant

Whereas only mescaline appeared to be a substrate for OCT1, transport *via* OCT2 was seen for methamphetamine, PMMA,
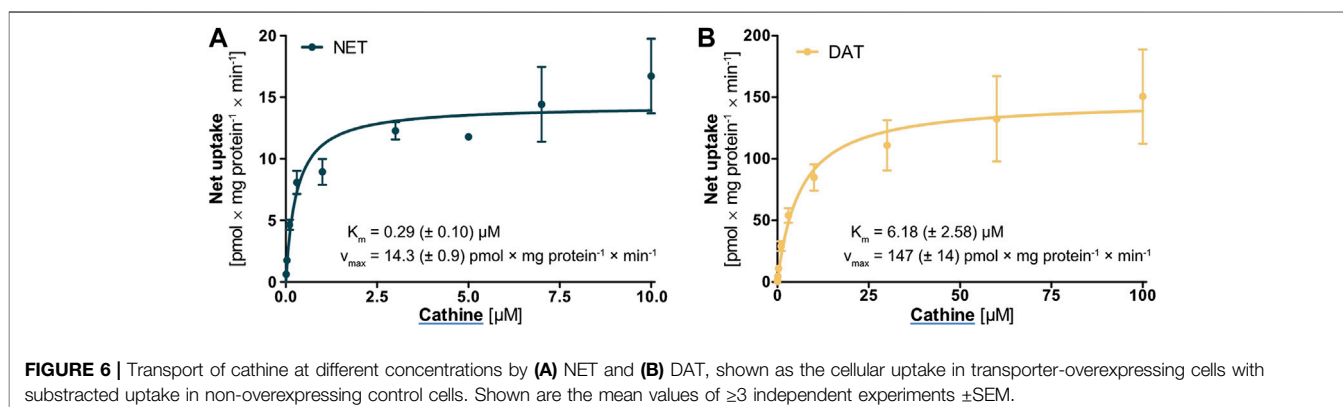
Substrate	Variant	K_m [μM]	v_{max} [pmol × mg protein^{-1} × min^{-1}]
Cathine	WT	46.0 (± 17.3)	570.1 (± 94.3)
	A270S	58.4 (± 40.3)	505.4 (± 168.1)
Ephedrine	WT	15.7 (± 4.6)	417.8 (± 35.6)
	A270S	14.7 (± 4.1)	229.5 (± 18.2)
PMMA	WT	7.9 (± 2.6)	225.1 (± 19.3)
	A270S	14.4 (± 8.6)	172.1 (± 31.5)
DMT	WT	13.0 (± 3.7)	296.7 (± 23.3)
	A270S	14.2 (± 7.9)	164.2 (± 25.9)
Methamphetamine	WT	11.9 (± 4.8)	70.7 (± 8.3)
	A270S	24.3 (± 17.0)	34.5 (± 8.5)

FIGURE 5 | Transport of cathine, (-)-ephedrine, PMMA, DMT, and methamphetamine at different concentrations by wild-type OCT2 (red) and the variant A270S (orange), shown as the cellular uptake in transporter-overexpressing cells with substracted uptake in non-overexpressing control cells. Shown are the mean values of ≥3 independent experiments ±SEM.

(-)-ephedrine, cathine, and DMT. These compounds were subsequently assessed in greater detail (**Figure 5**). For methamphetamine, the v_{max} for wild-type OCT2 was only 70.7 ± 8.3 pmol × mg protein^{-1} × min^{-1}, whereas it was between 225 and 570 pmol × mg protein^{-1} × min^{-1} for the other four compounds. The K_m values were around 10 μM except for cathine (46.0 ± 17.3 μM). For the A270S variant, the v_{max} values were slightly to moderately lower (except for PMMA) and the K_m values either similar ((-)-ephedrine and DMT) or up to 4-fold higher (methamphetamine, PMMA, cathine) compared to wild-type OCT2, in agreement with

literature reports that the A270S exchange can lead to a moderate decrease in OCT2 activity (Zolk et al., 2009).

Concentration-dependent Transport of Cathine by NET and DAT

Cathine was the only compound for which notable cellular uptake was observed by the high-affinity monoamine transporters NET and DAT. Further characterisation and a comparison between NET and DAT revealed that the K_m was 21-fold and the v_{max} 10-fold higher for DAT (**Figure 6**). Yet, both K_m and v_{max} were still

FIGURE 6 | Transport of cathine at different concentrations by **(A)** NET and **(B)** DAT, shown as the cellular uptake in transporter-overexpressing cells with substracted uptake in non-overexpressing control cells. Shown are the mean values of ≥3 independent experiments ±SEM.
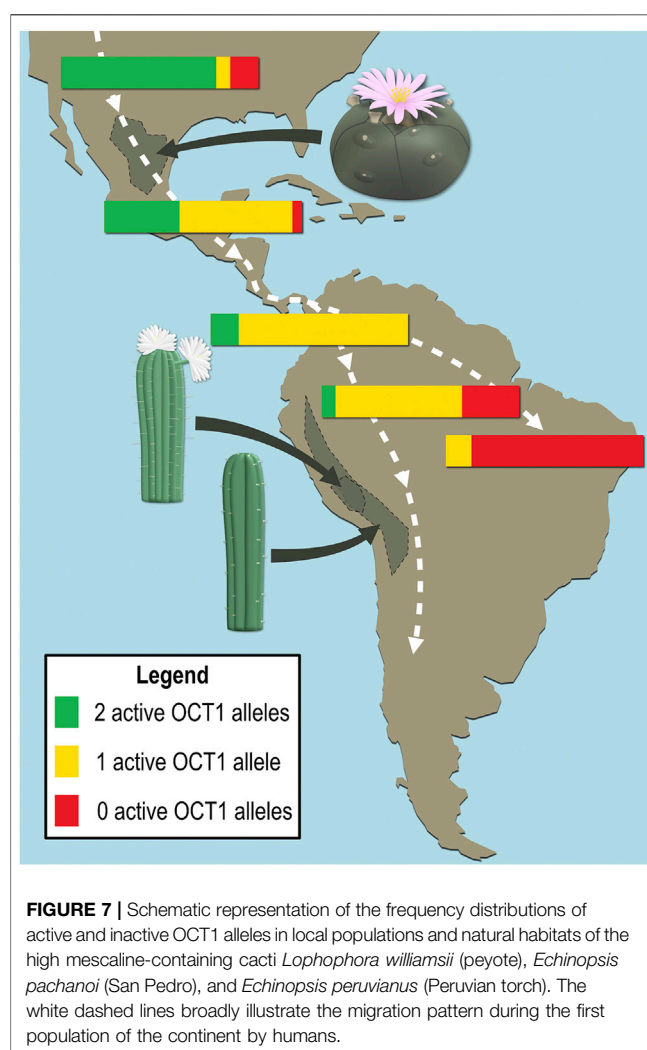
significantly lower compared to OCT2, in line with the general description of NET and DAT as high-affinity and low-capacity transporters.

DISCUSSION

In this study, three groups of psychostimulants and hallucinogens (14 phenylethylamine derivatives, the tropanes cocaine and methylecgonine, and the substituted tryptamines dimethyl- and diethyltryptamine) were assessed for their substrate properties for OCTs as well as for high-affinity monoamine transporters. OCTs are known to have a very broad substrate profile that comprises many different structural classes. It is therefore surprising that only relatively few of the 18 psychoactive compounds studied here were moderate or good OCT substrates, especially because these were selected based on physicochemical properties that were in accordance with those of typical OCT substrates. Other transporters, such as OCTN1 and OCTN2, the proposed H^+-organic cation antiporter, or ATP-binding cassette efflux transporters might potentially be more relevant for some of the tested psychoactive compounds.

Only mescaline was transported significantly at 1 μM by OCT1, and that this was the highest transport activity observed here altogether. With a pK_a of 9.77, a $logD_{pH\ 7.4}$ of -1.37, and a molecular mass of 211.3 g/mol, its physicochemical properties are not significantly different from those of the other compounds (**Table 1**). It is thus reasonable to wonder what properties make mescaline the only substrate at this concentration compared to the 17 other compounds studied here. Possible explanations are not evident from its chemical structure, as it is an amphetamine derivative structurally relatively similar to many of the other phenylethylamines.

Mescaline is an alkaloid biosynthesised from tyrosine in different cacti, where it is found at concentrations of 0.05–4.7% by dry weight (Ogunbodede et al., 2010). *Lophophora williamsii* (peyote cactus) and several *Echinopsis* species (e.g., *Echinopsis pachanoi* and *Echinopsis peruvianus*, also known as the San Pedro and the Peruvian torch cacti) have a long-standing use in religious ceremonies and traditional medicine of South American indigenous populations. The hallucinogenic effects of these cacti were

FIGURE 7 | Schematic representation of the frequency distributions of active and inactive OCT1 alleles in local populations and natural habitats of the high mescaline-containing cacti *Lophophora williamsii* (peyote), *Echinopsis pachanoi* (San Pedro), and *Echinopsis peruvianus* (Peruvian torch). The white dashed lines broadly illustrate the migration pattern during the first population of the continent by humans.

attributed to their relatively high mescaline contents (Ogunbodede et al., 2010; Dinis-Oliveira et al., 2019; da Silveira Agostini-Costa, 2020). Interestingly, OCT1 deficiency or reduced activity is more frequently found in Central and South American populations than in most other parts of the

world and the prevalence of inactive alleles generally increases further south on the American continent (**Figure 7**) (Seitz et al., 2015). It is likely that OCT1 deficiency was somehow advantageous, e.g., in connection with dietary ingredients that are OCT1 substrates (or perhaps mescaline?), and inactive alleles thus dominated as the first human inhabitants of the continent migrated south.

Typical mescaline dosages are in the range of 170–400 mg, which induce a psychedelic state that may involve visual hallucinations, altered perception, synesthaesia, and euphoria. The lifetime prevalence of mescaline use over the past 3 decades was estimated to be between 3–4% in the United States (Dinis-Oliveira et al., 2019; Johnson et al., 2019). Being a high-affinity partial agonist for the 5-HT$_{2A}$ receptor, potential therapeutic uses for mescaline were proposed for disorders associated with serotonin deficiency, such as addiction, anxiety, and depression (Kyzar et al., 2017; Johnson et al., 2019). Based on the key finding of this study, that mescaline is a strong substrate of the genetically highly polymorphic OCT1, large interindividual variations in mescaline pharmacokinetics might be possible. This could lead to intoxication and other adverse effects due to decreased elimination in carriers of alleles with reduced or absent OCT1 activity (e.g., OCT1 variants *2 to *6, which are particularly common in European populations, or OCT1*7 that is frequently found in Africans and Afro-Americans (Seitz et al., 2015)). However, a substance being identified as OCT1 substrate in vitro may not necessarily be affected by OCT1 genetic polymorphism in vivo, as illustrated by the example of the indirect sympathomimetic compound tyramine (Rafehi et al., 2019). Thus, the effects of OCT1 genotype on mescaline should be studied in vivo and its clinical implications taken into consideration when developing therapeutic interventions involving mescaline.

Another key result of this study was that methamphetamine, PMMA, (-)-ephedrine, cathine, and DMT were substrates of OCT2 and that their transport was moderately reduced in the A270S variant. OCT2 is strongly expressed in the kidneys, where it contributes to transepithelial transport of usually hydrophilic substances and thereby renal elimination. Cathine was excreted unchanged in urine to 46–65% in four healthy volunteers and the renal elimination was reported to be 70% for (-)-ephedrine and 30–54% for methamphetamine (Toennes and Kauert, 2002; www.dosing.de and www.drugbank.ca, both accessed on September 16, 2020). The reduced transport by the A270S variant of OCT2 might thus possibly result in a decreased elimination of these compounds. Besides variation due to inherited polymorphisms, variation in renal elimination of these psychostimulants may additionally arise from drug-drug interactions or conditions associated with increased blood concentrations of endogenous organic cations. DMT, on the other hand, is extensively metabolised and excreted unchanged in urine only to a very low extent (e.g., 0.16% following intramuscular administration) (Sitaram et al., 1987; Barker, 2018). OCT2 polymorphism is thus unlikely to have any significant effects on DMT pharmacokinetics but might still influence local concentrations of DMT as well as of methamphetamine, PMMA, (-)-ephedrine, and cathine in the central nervous system due to OCT2 expression in postsynaptic neurons.
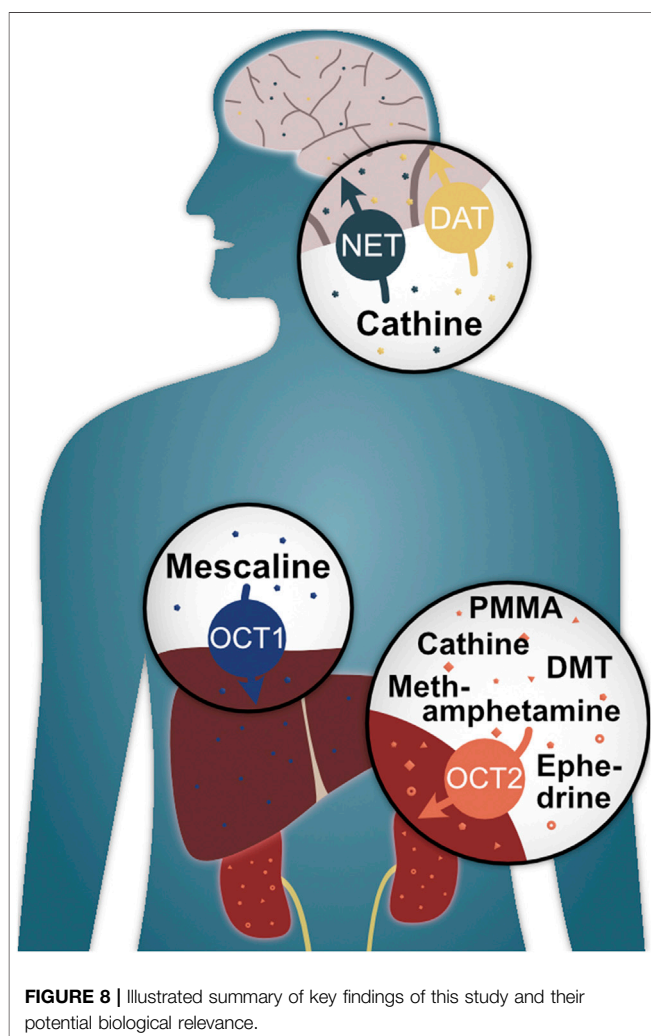
OCT1 and OCT2 polymorphism is not the only form of genetic variation that may affect the above-mentioned compounds. Metabolising enzymes and target receptors may also be polymorphic. A few examples regarding the pharmacogenetics of these compounds are given in **Table 3**. A good example for discussing the general importance of genetic polymorphism is MDMA, as this psychostimulant has been studied in greater detail. MDMA is widely used as the recreational drug "ecstasy" but therapeutic use for the treatment of posttraumatic stress disorder has also been proposed (Mithoefer et al., 2011; Mithoefer et al., 2013; Amoroso and Workman, 2016; Mithoefer et al., 2016). It is a substrate of the polymorphic enzymes cytochrome P450 (CYP) 2C19, 2B6, and 1A2, which catalyze the conversion to 3,4-methylenedioxyamphetamine. Carriers of genetic variants that result in increased activity of these enzymes showed higher metabolism and CYP2C19 poor metabolisers had greater cardiovascular effects in response to MDMA consumption (Schindler et al., 2014; Vizeli et al., 2017). Poor metabolisers for the highly polymorphic CYP2D6 also showed higher cardiovascular responses, but only to a minor extent due to the inhibition of CYP2D6 (Schmid et al., 2016). Based on in vitro data, the effect of CYP2D6 polymorphism was previously predicted to be higher (La Torre et al., 2012). MDMA has a basic secondary amine group that is protonated to 99.8% at physiological pH (**Table 1**). It would thus require a transport mechanism for efficient passage across cell membranes and into hepatocytes for metabolism. Our results suggest that OCTs only contribute to a minor extent. Although MDMA is not a good OCT substrate, its metabolites might possibly be (as we had previously shown analogously for different opioids, where their more hydrophilic metabolites were better OCT substrates (Meyer et al., 2019)). For example, the main metabolites 3,4-dihydroxyamphetamine and 3,4-dihydroxymethamphetamine are more hydrophilic than MDMA and might thus potentially be better OCT substrates, as they would likely rely more strongly on transport mechanisms to traverse cell membranes. However, the present study has shown that substrate specificity cannot always be predicted based on physicochemical properties alone. Although a number of contributors to the serotonergic system are polymorphic, significant variation in MDMA effects were not seen in healthy humans (Vizeli et al., 2019). NET polymorphism also showed only minor effects on the cardiovascular response to MDMA in clinical studies (Vizeli et al., 2018). To summarise this, genetic polymorphism significantly determines the pharmacokinetics but not so much the pharmacodynamics of MDMA (and possibly of other psychostimulants as well).

A concept that has so far not received much attention is stereoselectivity in membrane transport. Recent results from our laboratory have shown that transmembrane transport of adrenergic drugs by OCTs can show strong enantiospecificity (Jensen et al., 2020). The phenylethylamine derivatives cathine (also referred to as (+)-norpseudoephedrine) and (-)-ephedrine that were assessed in this study are chiral compounds and structurally very closely related. If it were not for the methyl substitution at the amino group (**Figure 1**), both compounds would be stereoisomers of one another. With this in mind, it

TABLE 3 | Pharmacogenetics of methamphetamine, PMMA, (-)-ephedrine, cathine, mescaline, and DMT (this list is not exhaustive).

Test compound	Substrate of			Polymorphic targets[a]	References
	OCT1	OCT2	Polymorphic enzymes[a]		
Methamphetamine	–	++	CYP2D6, FMO3	TAAR1, VMAT2, MAO	Cashman et al. (1999), Eiden and Weihe (2011), Miller 2011, Smith et al. (2012), and Matsusue et al. (2018)
PMMA	–	+	CYP2D6	TAAR1, 5-HT$_{2A}$	Simmler et al. (2014), and Vevelstad et al. (2017)
(-)-Ephedrine	–	++		β_2-adrenoceptor	Rao et al. (2019)
Cathine	–	+++		β_1- and a_{2A}-adrenoceptors	Adeoya-Osiguwa and Fraser (2007)
Mescaline	+++	–	Possibly MAO	5-HT$_{2A}$,5-HT$_{2C}$,TAAR1	Spector (1961), Lerer et al. (2001), Mulder et al. (2007), Kling et al. (2008), Hoekstra et al. (2010), Rickli et al. (2015), and Dinis-Oliveira et al. (2019)
DMT	–	+	MAO-A	5-HT$_{2A}$,5-HT$_{2C}$,TAAR1	Keiser et al. (2009), Rickli et al. (2016), and Barker (2018)

[a]Abbreviations: 5-HT, 5-hydroxytryptamine; CYP2D6, cytochrome P450 subtype 2D6; FMO3, Flavin-containing monooxygenase 3; MAO, monoamine oxidase; TAAR1, trace amine-associated receptor 1, VMAT2, vesicular monoamine transporter 2

FIGURE 8 | Illustrated summary of key findings of this study and their potential biological relevance.

appears astonishing that cathine was found to be a good substrate of DAT whereas (-)-ephedrine was not, despite their close structural resemblance. Whether this difference in transport was due to the opposite steric orientation of the hydroxyl group or due to the methyl substitution at the amino group cannot be deduced from this study.

To summarise, this study has shown that the classic hallucinogen mescaline is a strong substrate of the genetically highly polymorphic OCT1 (**Figure 8**) and that genetic variants show altered cell uptake, which may have clinical implications. It was also found that the psychoactive compounds methamphetamine, PMMA, (-)-ephedrine, cathine, and DMT are substrates of OCT2 with partially moderate reductions in cell uptake in the A270S variant. Cathine was also discovered to be a substrate of NET and DAT. As to the question of whether OCT1 is a drug trafficker or not, we would argue that it is one indeed. However, it is a very selective one with a clear preference for the hallucinogenic compound mescaline, which is rather unusual for OCT1 given its generally broad substrate profile.

DATA AVAILABILITY STATEMENT

The raw data supporting the conclusions of this article will be made available by the authors, without undue reservation.

AUTHOR CONTRIBUTIONS

Conceptualisation: OJ, MR, and JB; Funding acquisition: MR and JB; Investigation: OJ and LG; Methodology: OJ and JB; Project administration: OJ, MR, and JB; Supervision: JB; Visualisation: OJ and MR; Writing – original draft: OJ and MR; Writing – review and editing: MR and JB.

FUNDING

ACKNOWLEDGMENTS

REFERENCES

Adeoya-Osiguwa, S. A., and Fraser, L. R. (2007). Cathine, an amphetamine-related compound, acts on mammalian spermatozoa via beta1- and alpha2A-adrenergic receptors in a capacitation state-dependent manner. *Hum. Reprod.* 22, 756–765. doi:10.1093/humrep/del454

Amoroso, T., and Workman, M. (2016). Treating posttraumatic stress disorder with MDMA-assisted psychotherapy: a preliminary meta-analysis and comparison to prolonged exposure therapy. *J. Psychopharmacol.* 30, 595–600. doi:10.1177/0269881116642542

Bacq, A., Balasse, L., Biala, G., Guiard, B., Gardier, A. M., Schinkel, A., et al. (2012). Organic cation transporter 2 controls brain norepinephrine and serotonin clearance and antidepressant response. *Mol. Psychiatr.* 17, 926–939. doi:10.1038/mp.2011.87

Barker, S. A. (2018). N, N-dimethyltryptamine (DMT), an endogenous hallucinogen: past, present, and future research to determine its role and function. *Front. Neurosci.* 12, 536. doi:10.3389/fnins.2018.00536

Busch, A. E., Karbach, U., Miska, D., Gorboulev, V., Akhoundova, A., Volk, C., et al. (1998). Human neurons express the polyspecific cation transporter hOCT2, which translocates monoamine neurotransmitters, amantadine, and memantine. *Mol. Pharmacol.* 54, 342–352. doi:10.1124/mol.54.2.342

Cashman, J. R., Xiong, Y. N., Xu, L., and Janowsky, A. (1999). N-oxygenation of amphetamine and methamphetamine by the human flavin-containing monooxygenase (form 3): role in bioactivation and detoxication. *J. Pharmacol. Exp. Therapeut.* 288, 1251–1260.

Chen, J., Brockmöller, J., Seitz, T., König, J., Tzvetkov, M. V., and Chen, X. (2017). Erratum to: tropane alkaloids as substrates and inhibitors of human organic cation transporters of the SLC22 (OCT) and the SLC47 (MATE) families. *Biol. Chem.* 398, 813–249. doi:10.1515/hsz-2016-0236

Couroussé, T., and Gautron, S. (2015). Role of organic cation transporters (OCTs) in the brain. *Pharmacol. Therapeut.* 146, 94–103. doi:10.1016/j.pharmthera.2014.09.008

da Silveira Agostini-Costa, T. (2020). Bioactive compounds and health benefits of Pereskioideae and Cactoideae: a review. *Food Chem.* 327, 126961. doi:10.1016/j.foodchem.2020.126961

Dinis-Oliveira, R. J., Pereira, C. L., and da Silva, D. D. (2019). Pharmacokinetic and pharmacodynamic aspects of peyote and mescaline: clinical and forensic repercussions. *Curr. Mol. Pharmacol.* 12, 184–194. doi:10.2174/1874467211666181010154139

Eiden, L. E., and Weihe, E. (2011). VMAT2: a dynamic regulator of brain monoaminergic neuronal function interacting with drugs of abuse. *Ann. N. Y. Acad. Sci.* 1216, 86–98. doi:10.1111/j.1749-6632.2010.05906.x

Gründemann, D., Köster, S., Kiefer, N., Breidert, T., Engelhardt, M., Spitzenberger, F., et al. (1998). Transport of monoamine transmitters by the organic cation transporter type 2, OCT2. *J. Biol. Chem.* 273, 30915–30920. doi:10.1074/jbc.273.47.30915

Hoekstra, P. J., Troost, P. W., Lahuis, B. E., Mulder, H., Mulder, E. J., Franke, B., et al. (2010). Risperidone-induced weight gain in referred children with autism spectrum disorders is associated with a common polymorphism in the 5-hydroxytryptamine 2C receptor gene. *J. Child Adolesc. Psychopharmacol.* 20, 473–477. doi:10.1089/cap.2009.0071

Jensen, O., Rafehi, M., Tzvetkov, M. V., and Brockmöller, J. (2020). Stereoselective cell uptake of adrenergic agonists and antagonists by organic cation transporters. *Biochem. Pharmacol.* 171, 113731. doi:10.1016/j.bcp.2019.113731

Johnson, M. W., Hendricks, P. S., Barrett, F. S., and Griffiths, R. R. (2019). Classic psychedelics: an integrative review of epidemiology, therapeutics, mystical experience, and brain network function. *Pharmacol. Therapeut.* 197, 83–102. doi:10.1016/j.pharmthera.2018.11.010
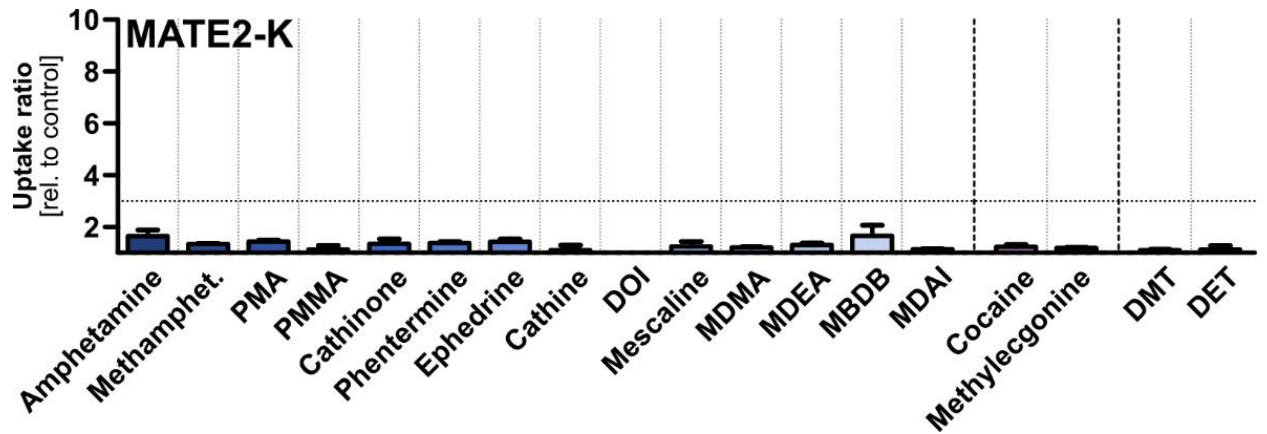
SUPPLEMENTARY MATERIAL

Kalix, P., and Braenden, O. (1985). Pharmacological aspects of the chewing of khat leaves. *Pharmacol. Rev.* 37, 149–164.

Keiser, M. J., Setola, V., Irwin, J. J., Laggner, C., Abbas, A. I., Hufeisen, S. J., et al. (2009). Predicting new molecular targets for known drugs. *Nature.* 462, 175–181. doi:10.1038/nature08506

Kling, A., Seddighzadeh, M., Arlestig, L., Alfredsson, L., Rantapää-Dahlqvist, S., and Padyukov, L. (2008). Genetic variations in the serotonin 5-HT2A receptor gene (HTR2A) are associated with rheumatoid arthritis. *Ann. Rheum. Dis.* 67, 1111–1115. doi:10.1136/ard.2007.074948

Koepsell, H. (2020). Organic cation transporters in health and disease. *Pharmacol. Rev.* 72, 253–319. doi:10.1124/pr.118.015578

Koepsell, H., Lips, K., and Volk, C. (2007). Polyspecific organic cation transporters: structure, function, physiological roles, and biopharmaceutical implications. *Pharm. Res.* 24, 1227–1251. doi:10.1007/s11095-007-9254-z

Kyzar, E. J., Nichols, C. D., Gainetdinov, R. R., Nichols, D. E., and Kalueff, A. V. (2017). Psychedelic drugs in biomedicine. *Trends Pharmacol. Sci.* 38, 992–1005. doi:10.1016/j.tips.2017.08.003

La Torre, R. de., Yubero-Lahoz, S., Pardo-Lozano, R., and Farré, M. (2012). MDMA, methamphetamine, and CYP2D6 pharmacogenetics: what is clinically relevant? *Front. Genet.* 3, 235. doi:10.3389/fgene.2012.00235

Lerer, B., Macciardi, F., Segman, R. H., Adolfsson, R., Blackwood, D., Blairy, S., et al. (2001). Variability of 5-HT2C receptor cys23ser polymorphism among European populations and vulnerability to affective disorder. *Mol. Psychiatr.* 6, 579–585. doi:10.1038/sj.mp.4000883

Luethi, D., and Liechti, M. E. (2020). Designer drugs: mechanism of action and adverse effects. *Arch. Toxicol.* 94, 1085–1133. doi:10.1007/s00204-020-02693-7

Matsusue, A., Ikeda, T., Tani, N., Waters, B., Hara, K., Kashiwagi, M., et al. (2018). Association between cytochrome P450 2D6 polymorphisms and body fluid methamphetamine concentrations in Japanese forensic autopsy cases. *Forensic Sci. Int.* 289, 33–39. doi:10.1016/j.forsciint.2018.05.018

Matthaei, J., Kuron, D., Faltraco, F., Knoch, T., Dos Santos Pereira, J. N., Abu Abed, M., et al. (2016). OCT1 mediates hepatic uptake of sumatriptan and loss-of-function OCT1 polymorphisms affect sumatriptan pharmacokinetics. *Clin. Pharmacol. Ther.* 99, 633–641. doi:10.1002/cpt.317

Matthaei, J., Seitz, T., Jensen, O., Tann, A., Prukop, T., Tadjerpisheh, S., et al. (2019). OCT1 deficiency affects hepatocellular concentrations and pharmacokinetics of cycloguanil, the active metabolite of the antimalarial drug proguanil. *Clin. Pharmacol. Ther.* 105, 190–200. doi:10.1002/cpt.1128

Mayer, F. P., Schmid, D., Holy, M., Daws, L. C., and Sitte, H. H. (2019). "Polytox" synthetic cathinone abuse: a potential role for organic cation transporter 3 in combined cathinone-induced efflux. *Neurochem. Int.* 123, 7–12. doi:10.1016/j.neuint.2018.09.008

Mayer, F. P., Schmid, D., Owens, W. A., Gould, G. G., Apuschkin, M., Kudlacek, O., et al. (2018). An unsuspected role for organic cation transporter 3 in the actions of amphetamine, *Neuropsychopharmacology.* 43, 2408–2417. doi:10.1038/s41386-018-0053-5

Meyer, M. J., Neumann, V. E., Friesacher, H. R., Zdrazil, B., Brockmöller, J., and Tzvetkov, M. V. (2019). Opioids as substrates and inhibitors of the genetically highly variable organic cation transporter OCT1. *J. Med. Chem.* 62, 9890–9905. doi:10.1021/acs.jmedchem.9b01301

Miller, G. M. (2011). The emerging role of trace amine-associated receptor 1 in the functional regulation of monoamine transporters and dopaminergic activity. *J. Neurochem.* 116, 164–176. doi:10.1111/j.1471-4159.2010.07109.x

Mithoefer, M. C., Grob, C. S., and Brewerton, T. D. (2016). Novel psychopharmacological therapies for psychiatric disorders: psilocybin and MDMA. *Lancet Psychiatry.* 3 (5), 481–488. doi:10.1016/S2215-0366(15)00576-3

Mithoefer, M. C., Wagner, M. T., Mithoefer, A. T., Jerome, L., and Doblin, R. (2011). The safety and efficacy of {+/-}3,4-methylenedioxymethamphetamine-assisted psychotherapy in subjects with chronic, treatment-resistant

posttraumatic stress disorder: the first randomized controlled pilot study. *J. Psychopharmacol.* 25, 439–452. doi:10.1177/0269881110378371

Mithoefer, M. C., Wagner, M. T., Mithoefer, A. T., Jerome, L., Martin, S. F., Yazar-Klosinski, B., et al. (2013). Durability of improvement in post-traumatic stress disorder symptoms and absence of harmful effects or drug dependency after 3,4-methylenedioxymethamphetamine-assisted psychotherapy: a prospective long-term follow-up study. *J. Psychopharmacol.* 27, 28–39. doi:10.1177/0269881112456611

Motohashi, H., Nakao, Y., Masuda, S., Katsura, T., Kamba, T., Ogawa, O., et al. (2013). Precise comparison of protein localization among OCT, OAT, and MATE in human kidney. *J. Pharmacol. Sci.* 102, 3302–3308. doi:10.1002/jps.23567

Motohashi, H., Sakurai, Y., Saito, H., Masuda, S., Urakami, Y., Goto, M., et al. (2002). Gene expression levels and immunolocalization of organic ion transporters in the human kidney. *J. Am. Soc. Nephrol.* 13, 866–874.

Mulder, H., Franke, B., van der-Beek van der, A. A., Arends, J., Wilmink, F. W., Scheffer, H., et al. (2007). The association between HTR2C gene polymorphisms and the metabolic syndrome in patients with schizophrenia. *J. Clin. Psychopharmacol.* 27, 338–343. doi:10.1097/JCP.0b013e3180a76dc0

Nichols, D. E. (2016). Psychedelics. *Pharmacol. Rev.* 68, 264–355. doi:10.1124/pr.115.011478

Nies, A. T., Koepsell, H., Winter, S., Burk, O., Klein, K., Kerb, R., et al. (2009). Expression of organic cation transporters OCT1 (SLC22A1) and OCT3 (SLC22A3) is affected by genetic factors and cholestasis in human liver. *Hepatology.* 50, 1227–1240. doi:10.1002/hep.23103

Nishimura, M., and Naito, S. (2005). Tissue-specific mRNA expression profiles of human ATP-binding cassette and solute carrier transporter superfamilies. *Drug Metabol. Pharmacokinet.* 20, 452–477. doi:10.2133/dmpk.20.452

Ogunbodede, O., McCombs, D., Trout, K., Daley, P., and Terry, M. (2010). New mescaline concentrations from 14 taxa/cultivars of Echinopsis spp. (Cactaceae) ("San Pedro") and their relevance to shamanic practice. *J. Ethnopharmacol.* 131, 356–362. doi:10.1016/j.jep.2010.07.021

Rafehi, M., Faltraco, F., Matthaei, J., Prukop, T., Jensen, O., Grytzmann, A., et al. (2019). Highly variable pharmacokinetics of tyramine in humans and polymorphisms in OCT1, CYP2D6, and MAO-A. *Front. Pharmacol.* 10, 1297. doi:10.3389/fphar.2019.01297

Ramamoorthy, S., Bauman, A. L., Moore, K. R., Han, H., Yang-Feng, T., Chang, A. S., et al. (1993). Antidepressant- and cocaine-sensitive human serotonin transporter: molecular cloning, expression, and chromosomal localization. *Proc. Natl. Acad. Sci. U.S.A.* 90, 2542–2546. doi:10.1073/pnas.90.6.2542

Rao, T., Tan, Z., Peng, J., Guo, Y., Chen, Y., Zhou, H., et al. (2019). The pharmacogenetics of natural products: a pharmacokinetic and pharmacodynamic perspective. *Pharmacol. Res.* 146, 104283. doi:10.1016/j.phrs.2019.104283

Reith, M. E. A., and Gnegy, M. E. (2020). Molecular mechanisms of amphetamines. *Handb. Exp. Pharmacol.* 258, 265–297. doi:10.1007/164_2019_251

Rickli, A., Luethi, D., Reinisch, J., Buchy, D., Hoener, M. C., and Liechti, M. E. (2015). Receptor interaction profiles of novel N-2-methoxybenzyl (NBOMe) derivatives of 2,5-dimethoxy-substituted phenethylamines (2C drugs). *Neuropharmacology.* 99, 546–553. doi:10.1016/j.neuropharm.2015.08.034

Rickli, A., Moning, O. D., Hoener, M. C., and Liechti, M. E. (2016). Receptor interaction profiles of novel psychoactive tryptamines compared with classic hallucinogens. *Eur. Neuropsychopharmacol.* 26, 1327–1337. doi:10.1016/j.euroneuro.2016.05.001

Rothman, R. B., Vu, N., Partilla, J. S., Roth, B. L., Hufeisen, S. J., Compton-Toth, B. A., et al. (2003). In vitro characterization of ephedrine-related stereoisomers at biogenic amine transporters and the receptorome reveals selective actions as norepinephrine transporter substrates. *J. Pharmacol. Exp. Therapeut.* 307, 138–145. doi:10.1124/jpet.103.053975

Saadatmand, A. R., Tadjerpisheh, S., Brockmöller, J., and Tzvetkov, M. V. (2012). The prototypic pharmacogenetic drug debrisoquine is a substrate of the genetically polymorphic organic cation transporter OCT1. *Biochem. Pharmacol.* 83, 1427–1434. doi:10.1016/j.bcp.2012.01.032

Schindler, C. W., Thorndike, E. B., Blough, B. E., Tella, S. R., Goldberg, S. R., and Baumann, M. H. (2014). Effects of 3,4-methylenedioxymethamphetamine (MDMA) and its main metabolites on cardiovascular function in conscious rats. *Br. J. Pharmacol.* 171, 83–91. doi:10.1111/bph.12423

Schmid, Y., Vizeli, P., Hysek, C. M., Prestin, K., Meyer Zu Schwabedissen, H. E., and Liechti, M. E. (2016). CYP2D6 function moderates the pharmacokinetics and pharmacodynamics of 3,4-methylene-dioxymethamphetamine in a controlled study in healthy individuals. *Pharmacogenetics Genom.* 26, 397–401. doi:10.1097/FPC.0000000000000231

Seitz, T., Stalmann, R., Dalila, N., Chen, J., Pojar, S., Dos Santos Pereira, J. N., et al. (2015). Global genetic analyses reveal strong inter-ethnic variability in the loss of activity of the organic cation transporter OCT1. *Genome Med.* 7, 56. doi:10.1186/s13073-015-0172-0

Sharma, A., and Couture, J. (2014). A review of the pathophysiology, etiology, and treatment of attention-deficit hyperactivity disorder (ADHD). *Ann. Pharmacother.* 48, 209–225. doi:10.1177/1060028013510699

Simmler, L. D., Rickli, A., Hoener, M. C., and Liechti, M. E. (2014). Monoamine transporter and receptor interaction profiles of a new series of designer cathinones. *Neuropharmacology.* 79, 152–160. doi:10.1016/j.neuropharm.2013.11.008

Sitaram, B. R., Lockett, L., Blackman, G. L., and McLeod, W. R. (1987). Urinary excretion of 5-methoxy-N,N-dimethyltryptamine, N,N-dimethyltryptamine and their N-oxides in the rat. *Biochem. Pharmacol.* 36, 2235–2237. doi:10.1016/0006-2952(87)90159-6

Smith, S. B., Maixner, D. W., Fillingim, R. B., Slade, G., Gracely, R. H., Ambrose, K., et al. (2012). Large candidate gene association study reveals genetic risk factors and therapeutic targets for fibromyalgia. *Arthritis Rheum.* 64, 584–593. doi:10.1002/art.33338

Spector, E. (1961). Identification of 3,4,5-trimethoxyphenylacetic acid as the major metabolite of mescaline in the dog. *Nature.* 189, 751–752. doi:10.1038/189751b0

Stamer, U. M., Musshoff, F., Stüber, F., Brockmöller, J., Steffens, M., and Tzvetkov, M. V. (2016). Loss-of-function polymorphisms in the organic cation transporter OCT1 are associated with reduced postoperative tramadol consumption. *Pain.* 157, 2467–2475. doi:10.1097/j.pain.0000000000000662

Toennes, S. W., and Kauert, G. F. (2002). Excretion and detection of cathinone, cathine, and phenylpropanolamine in urine after kath chewing. *Clin. Chem.* 48, 1715–1719. doi:10.1093/clinchem/48.10.1715

Torres, G. E., Gainetdinov, R. R., and Caron, M. G. (2003). Plasma membrane monoamine transporters: structure, regulation and function. *Nat. Rev. Neurosci.* 4, 13–25. doi:10.1038/nrn1008

Tzvetkov, M. V., Dos Santos Pereira, J. N., Meineke, I., Saadatmand, A. R., Stingl, J. C., and Brockmöller, J. (2013). Morphine is a substrate of the organic cation transporter OCT1 and polymorphisms in OCT1 gene affect morphine pharmacokinetics after codeine administration. *Biochem. Pharmacol.* 86, 666–678. doi:10.1016/j.bcp.2013.06.019

Tzvetkov, M. V., Matthaei, J., Pojar, S., Faltraco, F., Vogler, S., Prukop, T., et al. (2018). Increased systemic exposure and stronger cardiovascular and metabolic adverse reactions to fenoterol in individuals with heritable OCT1 deficiency. *Clin. Pharmacol. Ther.* 103, 868. doi:10.1002/cpt.812

Tzvetkov, M. V., Saadatmand, A. R., Lötsch, J., Tegeder, I., Stingl, J. C., and Brockmöller, J. (2011). Genetically polymorphic OCT1: another piece in the puzzle of the variable pharmacokinetics and pharmacodynamics of the opioidergic drug tramadol. *Clin. Pharmacol. Ther.* 90, 143–150. doi:10.1038/clpt.2011.56

Tzvetkov, M. V., Vormfelde, S. V., Balen, D., Meineke, I., Schmidt, T., Sehrt, D., et al. (2009). The effects of genetic polymorphisms in the organic cation transporters OCT1, OCT2, and OCT3 on the renal clearance of metformin. *Clin. Pharmacol. Ther.* 86, 299–306. doi:10.1038/clpt.2009.92

Venkatasubramanian, R., Fukuda, T., Niu, J., Mizuno, T., Chidambaran, V., Vinks, A. A., et al. (2014). ABCC3 and OCT1 genotypes influence pharmacokinetics of morphine in children. *Pharmacogenomics.* 15, 1297–1309. doi:10.2217/pgs.14.99

Vevelstad, M., Øiestad, E. L., Nerem, E., Arnestad, M., and Bogen, I. L. (2017). Studies on para-methoxymethamphetamine (PMMA) metabolite pattern and influence of CYP2D6 genetics in human liver microsomes and authentic samples from fatal PMMA intoxications. *Drug Metab. Dispos.* 45, 1326–1335. doi:10.1124/dmd.117.077263

Vialou, V., Balasse, L., Callebert, J., Launay, J. M., Giros, B., and Gautron, S. (2008). Altered aminergic neurotransmission in the brain of organic cation transporter

3-deficient mice. *J. Neurochem*. 106, 1471–1482. doi:10.1111/j.1471-4159.2008.05506.x

Vizeli, P., Meyer Zu Schwabedissen, H. E., and Liechti, M. E. (2018). No major role of norepinephrine transporter gene variations in the cardiostimulant effects of MDMA. *Eur. J. Clin. Pharmacol*. 74, 275–283. doi:10.1007/s00228-017-2392-2

Vizeli, P., Meyer Zu Schwabedissen, H. E., and Liechti, M. E. (2019). Role of serotonin transporter and receptor gene variations in the acute effects of MDMA in healthy subjects. *ACS Chem. Neurosci*. 10, 3120–3131. doi:10.1021/acschemneuro.8b00590

Vizeli, P., Schmid, Y., Prestin, K., Meyer Zu Schwabedissen, H. E., and Liechti, M. E. (2017). Pharmacogenetics of ecstasy: CYP1A2, CYP2C19, and CYP2B6 polymorphisms moderate pharmacokinetics of MDMA in healthy subjects. *Eur. Neuropsychopharmacol*. 27, 232–238. doi:10.1016/j.euroneuro.2017.01.008

Wu, X., Kekuda, R., Huang, W., Fei, Y. J., Leibach, F. H., Chen, J., et al. (1998). Identity of the organic cation transporter OCT3 as the extraneuronal monoamine transporter (uptake2) and evidence for the expression of the transporter in the brain. *J. Biol. Chem*. 273, 32776–32786. doi:10.1074/jbc.273.49.32776

Yee, S. W., Brackman, D. J., Ennis, E. A., Sugiyama, Y., Kamdem, L. K., Blanchard, R., et al. (2018). Influence of transporter polymorphisms on drug disposition and response: a perspective from the international transporter consortium. *Clin. Pharmacol. Ther*. 104, 803–817. doi:10.1002/cpt.1098

Zhu, H. J., Appel, D. I., Gründemann, D., and Markowitz, J. S. (2010). Interaction of organic cation transporter 3 (SLC22A3) and amphetamine. *J. Neurochem*. 114, 142–149. doi:10.1111/j.1471-4159.2010.06738.x

Zolk, O., Solbach, T. F., König, J., and Fromm, M. F. (2009). Functional characterization of the human organic cation transporter 2 variant p.270Ala>Ser. *Drug Metab. Dispos*. 37, 1312–1318. doi:10.1124/dmd.108.023762

Figure S1 Transport of different psychostimulant and hallucinogenic substances at a concentration of 1 µM by MATE2-K, shown as the ratios of uptake after 1 min in transporter-transfected cells over empty vector control cells. Shown are the mean values of ≥ 3 independent experiments + SEM. The horizontal dotted line indicates an uptake ratio of 3, which was set as the minimum threshold for more detailed characterisation. The uptake in OCT1-overexpressing cells was not found to be significantly different to control cells, according to Student's t-test.

Table S1 Mass spectrometry detection parameters of analytes and internal standards

Test compound	RT[a] (min)	Mass Q1 (Da)	Mass Q3 (Da)	DP[a] (V)	CE[a] (V)	CXP[a] (V)	Internal standard
Amphetamine	5.8	136.0	91.0 (119.0)	41	21 (13)	16 (14)	ranitidine-d6
Methylamphetamine	6.8	150.2	91.0 (119.0)	31	23 (15)	16 (8)	sumatriptan
PMA	3.5	166.1	149.1 (121.1)	36	13 (25)	10 (15)	nadolol
PMMA	3.6	180.1	149.0 (121.0)	46	17 (28)	9 (22)	nadolol
Cathinone	4.4	321.2	176.0 (130.1)	65	25 (35)	15 (15)	ranitidine-d6
Phentermine	3.6	150.2	133.0 (91.1)	31	9 (23)	8 (16)	nadolol
(-)-Ephedrine	4.6	166.0	148.1 (133.0)	41	17 (27)	9 (8)	ranitidine-d6
Cathine	4.3	152.1	117.0 (91.0)	39	23 (39)	22 (16)	ranitidine-d6
DOI	9.7	322.0	277.0 (302.0)	51	27 (17)	18 (20)	guanfacine
Mescaline	6.6	211.9	165.0 (195.0)	46	31 (15)	10 (12)	ranitidine-d6
MDMA	3.5	193.9	163.0 (104.9)	41	17 (33)	10 (6)	nadolol
MDEA	3.7	208.0	163.0 (105.0)	51	19 (35)	10 (20)	nadolol
MBDB	4.0	208.0	135.0 (177.1)	51	24 (15)	8 (11)	nadolol
MDAI	5.4	178.0	161.0 (131.0)	43	17 (27)	10 (16)	ranitidine-d6

	RT			DP	CE	CXP	
Cocaine	5.2	304.3	182.0 (77.0)	41	27 (77)	12 (14)	caffeine
Methylecgonine	2.9	200.2	182.1 (82.0)	46	25 (35)	12 (6)	metformin
DMT	8.0	189.2	58.1 (143.9)	46	25 (21)	10 (8)	fenoterol
DET	4.6	217.3	86.0 (143.9)	51	19 (27)	16 (10)	tulobuterol
Caffeine	4.5	195.2	138.1 (110.0)	70	27 (32)	8 (8)	-
Fenoterol	8.9	304.1	107.1 (135.2)	80	44 (24)	12 (12)	-
Guanfacine	6.1	246.2	59.9 229.2	36	32 (9)	10 (6)	-
Metformin	2.7	130.0	71.0 (60)	46	35 (19)	10 (10)	-
Nadolol	3.5	310.1	254.1 201.0	66	23 (31)	16 (16)	-
Ranitidin-d6	4.1	321.0	176.0 (130.1)	65	25 (35)	15 (15)	-
Sumatriptan	6.3	296.2	58.2 (251.2)	50	30 (24)	12 (12)	-
Tulobuterol	4.7	228.1	153.9 (119.1)	60	23 (41)	10 (8)	-

[a]Abbreviations: RT, retention time; DP, declustering potential; CE, collision energy; CXP, collision cell exit potential

3.2 Publication 2

Identification of Novel High-Affinity Substrates of OCT1 Using

Machine Learning-Guided Virtual Screening and Experimental Validation

Ole Jensen, Jürgen Brockmöller, Christof Dücker

Institute of Clinical Pharmacology, University Medical Center Göttingen, Georg-August University, Robert-Koch-Str. 40, 37075 Göttingen, Germany
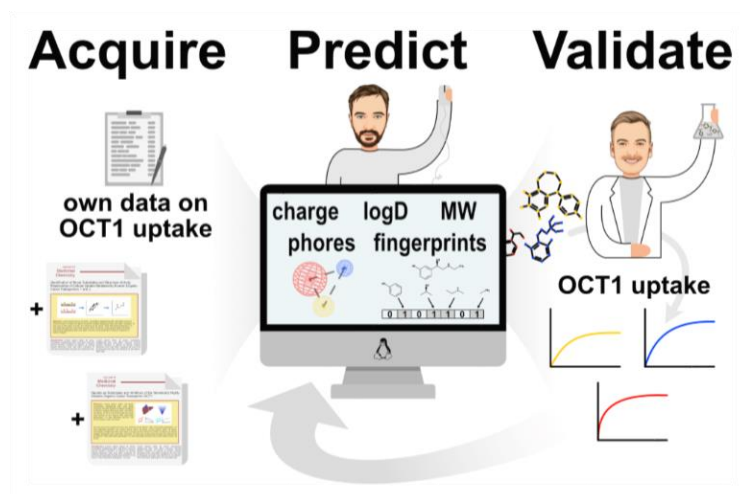
The *Supplementary Tables S2, S3, S4*, and the *Electronic Supplement S1* are available in the online version of this article (http://doi.org/10.1021/acs.jmedchem.0c02047).

Identification of Novel High-Affinity Substrates of OCT1 Using Machine Learning-Guided Virtual Screening and Experimental Validation

Ole Jensen, Jürgen Brockmöller, and Christof Dücker*

Cite This: https://dx.doi.org/10.1021/acs.jmedchem.0c02047

Read Online

ACCESS | Metrics & More | Article Recommendations | Supporting Information

ABSTRACT: OCT1 is the most highly expressed cation transporter in the liver and affects pharmacokinetics and pharmacodynamics. Newly marketed drugs have previously been screened as potential OCT1 substrates and verified by virtual docking. Here, we used machine learning with transport experiment data to predict OCT1 substrates based on classic molecular descriptors, pharmacophore features, and extended-connectivity fingerprints and confirmed them by *in vitro* uptake experiments. We virtually screened a database of more than 1000 substances. Nineteen predicted substances were chosen for *in vitro* testing. Sixteen of the 19 newly tested substances (85%) were confirmed as, mostly strong, substrates, including edrophonium, fenpiverinium, ritodrine, and ractopamine. Even without a crystal structure of OCT1, machine learning algorithms predict substrates accurately and may contribute not only to a more focused screening in drug development but also to a better molecular understanding of OCT1 in general.
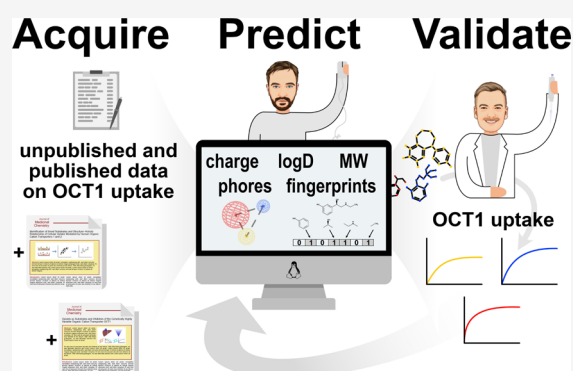
INTRODUCTION

OCT1 is the most strongly expressed organic cation transporter in the sinusoidal membrane of the human liver[1,2] and has numerous effects on endogenous substrate concentrations and pharmacokinetics of many drugs.[3−9] These effects of the highly polymorphic OCT1 on pharmacokinetics may translate into highly variable drug effects or adverse drug reactions.[10−12]

Known OCT1 substrates are highly polymorphic in their molecular structures.[3,13] Nevertheless, although numerous drugs are transported by OCT1, so far they mainly belong to a limited number of drug classes. These drug classes include H$_2$-receptor antagonists, anticholinergic drugs, serotonin receptor agonists and antagonists, sympathomimetic drugs, and a few opioids.

The physicochemical and structural features of OCT1 substrates have been studied extensively.[13,14] Typical substrates of OCT1 are smaller than 500 Å in volume.[13] Structural characteristics of major importance for the OCT1 substrate include a positively charged nitrogen either as a basic group or as a quaternary amine, an aromatic group, and moieties which increase hydrophilicity. The need for carrier-mediated transport across the lipid bilayer increases for any cell uptake (required for absorption, pharmacologic action, and/or elimination) with positively charged and hydrophilic groups. Based on these findings, screening for new substrates by a traditional approach relies on molecular weight, log $D_{7.4}$, pK_a, the percentage of charged substrate molecules at pH 7.4, and

the presence of structural features commonly found in known substrates.

Since there are no X-ray crystallography data from OCT1 available yet, *in silico* screening for substrates of OCT1 can primarily be achieved using ligand-based approaches or homology modeling and virtual docking. The latter has been successfully performed by several groups,[15−17] but one limitation is the relatively small protein sequence homology between OCT1 and those transporters (approximately 20%[15]), for which crystal structural data do exist and which were used as the basis of OCT1 homology modeling.

Ligand-based machine learning approaches have been applied for the identification of OCT1 substrates and for the analysis of the molecular interactions between the transporter and its substrates.[18,19] Extensive research has been performed on other transporters as well, such as OAT1, OAT3, and URAT1.[20−23] Two-dimensional virtual screening using extended-connectivity fingerprints and molecular descriptors is a standard approach with widely appreciated capabilities and has been shown to lead to good model performance in general as
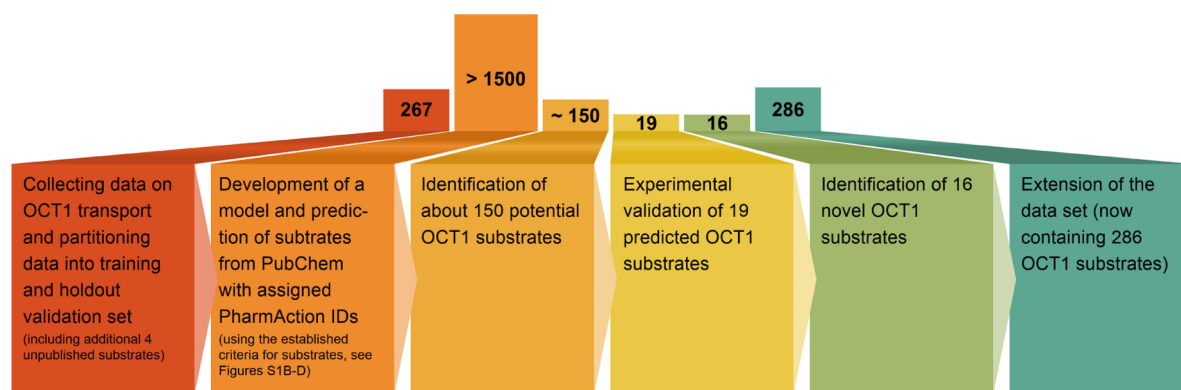
Figure 1. Flowchart illustrating the course of the study with the number of substances within the respective step shown in the upper part.

well as specifically in the case of OCT1.[8] In a recent publication, two-dimensional virtual screening was performed and newly predicted substrates were successfully tested via virtual docking.[19] This approach, however, includes the uncertainties of a potentially not valid transporter model derived from homology modeling with proteins having low sequence homology to OCT1. Therefore, testing of substrates in actual transport experiments with cells overexpressing OCT1 can still be considered the gold standard for validation in this specific situation. While we use the ligand-based approach here, the combination of different approaches, which complement each other, is highly valuable and may ultimately lead to the best possible results, as is also discussed in the recent literature.[24]

For OCT1, as for many other transporters, there are much data from screening substances for inhibition of transport of model substrates.[15,25] As screening for substrates of influx or efflux transporters is laborious, there are significantly less experimental data on transport. For OCT1, nonetheless, there is a large enough high-quality data pool of active transport in HEK293 to allow for virtual screening. Therefore, when interested in novel substrates of OCT1, it is apparently more promising to perform a virtual screening on this set of substrates for which OCT1-mediated influx transport has been truly experimentally verified instead of screening based on inhibition data. The usefulness of inhibition data to identify substrates is limited by the fact that inhibitory properties of a substance do not imply at all that the substance is also transported.[14,15,21] This problem is well known and a subject of current discussions. For prediction of transporter activity, substrate activity assays, implying the direct measurement of substrate uptake, are essential.[26]

In this study, we combined published data from OCT1-mediated transport with unpublished data from our laboratory to create a comprehensive database of molecular structures, physicochemical descriptors, and experimentally determined transport-kinetics data of more than 250 molecules. We trained a machine learning classifier based on physicochemical descriptors as well as pharmacophore features (descriptors of spatial relation of molecular features) and chemical fingerprints (descriptors of spatial relation of chemical structures); screened a database of more than 1000 substances for possible new substrates of OCT1; tested 19 randomly chosen drugs predicted as substrates in a concentration-dependent manner providing v_{max}, K_m, and intrinsic clearance data; and analyzed the new substrates' structural relationship with known substrates of OCT1.

RESULTS

First, we define a substrate/non-substrate cutoff for the ratio (of cell uptake with over without OCT1 overexpression) and intrinsic clearance (v_{max}/K_m) data as a basis for screening for potential new substrates (leading to around 44% substrates and 56% non-substrates in the overall data set). Second, we present the validation of our final model based on a holdout validation set. Third, we present the experimental *in vitro* validation of our final model. Fourth, we describe the final model as well as commonalities and differences of the newly found substrates. Fifth, we characterize the set of OCT1 substrates now, also including the newly found substrates. This process is depicted in Figure 1. The complete set of experimentally verified OCT1 substrates and non-substrates is provided in Table S2 (.pdf), Table S3 (.csv), and an sd-file in the Supporting Information, S1, allowing for structure-based analyses.

Common Cutoff between OCT1 Substrates and Non-substrates. Although the Food and Drug Administration (FDA) guidance for drug–drug interactions advises on further in vivo investigation if in vitro studies show ratios ≥2 (uptake in OCT1 overexpressing cells divided by uptake in mock-transfected cells),[27] the intrinsic clearance (Cl_{int}) is more robust as it is based on more measurements and integrative parameter estimation. Therefore, we decided to use Cl_{int} data wherever available and needed a common cutoff (substrate–non-substrate) for Cl_{int} and the ratio.

We set an intrinsic clearance of 5 mL × g protein^{-1} × min^{-1} as a cutoff between substrates and non-substrates. The decision not to choose a cutoff at any Cl_{int} slightly but significantly above 0 was made based on the expected medical relevance. An OCT1-mediated drug clearance slightly above 0 is medically of minor interest as it will most probably not translate into clinical effects.

The ratio cutoff was based on the subset of drugs where both ratios and clearances were available. Plotting clearances against ratios (Figure S1A), with a cutoff at a clearance of 5 mL × g protein^{-1} × min^{-1} and a cutoff at a ratio of 3, leads to overly congruent classification into substrates and non-substrates (Figure S1B,C). In cases where there was a discrepancy between ratio- and clearance-based classification into substrates and non-substrates, we relied on the Cl_{int} data (because it is usually based on much more measurements).

Model Performance in Cross-Validation and the Holdout Set. The model was reduced to the 33 most important predictive features based on their importance in the trainings set. Hyperparameters were also established based on the trainings set (estimators = 1000, learning rate = 0.01,

subsample = 0.7, maximum depth = 1, feature sample per tree = 0.5; all other hyperparameters were set to default). The hyperparameters were chosen as to achieve high areas under the curve (AUCs) for the validation sets in repeated 5-fold cross-validation, while avoiding overfitting for the training sets in repeated 5-fold cross-validation.

The final model achieved an AUC of 0.88 for the holdout validation set (Figure S1D) and an AUC of 0.96 for the training set, which was in line with the performance of another published OCT1 model based only on the data published by Hendrickx et al.[13] (AUC validation: 0.81, AUC training: 0.93[19]). We set the cutoff for the predicted substrate versus the predicted non-substrate so that with a share of 40% substrates in the screening set (in line with the percentage of substrates among single-charged cations with log $D_{7.4}$ below 1 among the substances in our database so far), the positive predictive value was >0.8. As substrates of OCT1 are mostly single-charged cations (pK_a > 7.4) and a log $D_{7.4}$ above 1 lowers the probability of the need for active transport due to increased membrane permeability, we *in vitro* tested only single-charged cations with log $D_{7.4} \leq 1.0$. The complete list with predicted substances beyond our scope of log $D_{7.4} < 1$ and charge = 1 is provided in Table S4. A summary of model parameters, performances, and predictors is illustrated in Figure S1E,F.

***In Vitro* Validation of Predicted Substrates.** Nineteen randomly selected substances from the set of predicted substrates were tested [an additional selection of predicted substrates is provided in Table S4 as well as the complete list, including those substances previously considered as unlikely OCT1 substrates (log $D_{7.4} > 1$ and no positive charge)]. The transport kinetic constants and concentration ratios measured with overexpressing over empty vector-transfected cell lines at a concentration of 2.5 μM are provided in Table 1. Additional four substrates of OCT1 were tested in our lab prior to modeling as these results have not been shown so far, and the data are also included in Table 1. Of these additional four substrates, milnacipran, a noradrenaline−serotonin reuptake inhibitor; dobutamine, a β_1-receptor agonist; and amifampridine, a potassium channel inhibitor to our knowledge have not been reported as OCT1 substrates earlier. Dobutamine has been reported as an OCT1 inhibitor earlier.[15]

Overall, 19 substances predicted by the final model were tested. Structures of these compounds, grouped by their pharmacological actions, are shown in Figure 2. For all substances showing OCT1-mediated influx transport, data from concentration-dependent experiments are presented in Figure 3 [additionally also for mepenzolate, K_m = 29.5 μM (±11.6), v_{max} = 2194 pmol mg protein^{-1} min^{-1} (±180), Cl$_{int}$ = 74.4, ratio = 30.7, which is a known substrate,[13] but kinetic data have not been published to our knowledge].

All but three substances, namely, labetalol, norphenylephrine, and sematilide, proved to be OCT1 substrates according to our strict criteria (a clearance of $\geq$ 5 mL × g protein^{-1} × min^{-1} or a ratio $\geq$ 3). While labetalol was not actively transported at all, sematilide and norphenylephrine were actively transported but at a very low rate (3.3 mL × g protein^{-1} × min^{-1} and ratio 3.5, and 4.6 mL × g protein^{-1} × min^{-1} and ratio 2.1, respectively), and with a more liberal definition, they can be called substrates. With this, the prediction of OCT1 substrates was correct even with 95% of the tested substances.

Famotidine, mepenzolate, and *meta*-iodobenzyl-guanidine (*m*IBG) had already been reported as OCT1 substrates.[3,38]

However, the direct measurement of uptake kinetics of famotidine and mepenzolate by OCT1 has not been reported before to our knowledge.[34] *m*IBG uptake has previously been described without empty-vector control.[47] This has been accepted as sufficient evidence elsewhere.[48] *m*IBG data on OCT1 transport were published, while our experiments presented here were already completed.[38] Therefore, *m*IBG serves as a validation of our final model, even though this is not the first study presenting it as a substrate. Intrinsic clearances and OCT1/vector-transfected ratios for the overall data set, the non-substrates, and substrates according to our criteria (including the newly tested substances) are shown in Figure 4A.

Model Predictors and Characteristics of Validated and Predicted Substrates. Among the 33 features with the best predictive value (Figure S1F), 19 were structural features and all but 1 of them were pharmacophores (the remaining one was a Morgan fingerprint), and the rest were general descriptors including strongest acidic pK_a, log $D_{7.4}$, heavy atom count, and strongest basic pK_a. The top six features were all pharmacophores, followed by strongest acidic pK_a. The top five pharmacophore features are shown in Figure 4B, together with their frequencies among OCT1 non-substrates and substrates (according to our criteria) in the overall data set.

The newly validated drugs with high and very high OCT1-mediated intrinsic clearance were from various therapeutic classes. Interestingly, the algorithm has identified OCT1 substrates with—on average—higher intrinsic clearance compared with the thus far known OCT1 substrates (Figure 5). Including newly validated as well as known substrates, among the classes with the highest median ratios and clearances were anticholinergics, H$_2$-antagonists, triptans, and β_2-agonists. Interestingly, the category "others" also performed quite well, showing that OCT1, while being important for specific drug classes, is also important for a wide range of substances from other classes. As four of the newly identified substrates fall within the "others" category, one can conclude that the algorithm used here is well able to identify OCT1 substrates beyond structural analogues in already known drug classes. The ranking of our newly identified substrates among the already known substrates shows that an enrichment of substrates with high clearances and ratios could be achieved [for the newly identified substrates, the mean K_m, v_{max}, Cl$_{int}$, and ratio were 127 μM (±50), 2358 pmol × mg protein^{-1} × min^{-1} (±473), 70 mL × g protein^{-1} × min^{-1} (±15), and 20 (±4), respectively].

In addition to the screening database, another database with drugs including information on the drug class they belong to was built. Class names and assignment to classes identical to the PharmAction category in the PubChem advanced search were used. Classes with members already known to be substrates of OCT1, for example, were included, and additional common drug classes were added. Duplicates within classes were removed, and duplicates between classes were kept as categories, which were not mutually exclusive. Drugs already known to be OCT1 substrates were not removed.

For predicted substances with regard to drug classes, especially high percentages can be found within cholinergic agents (including agonists and antagonists), adrenergic agonists, and the related classes of sympathomimetics and vasoconstrictor agents (Figure 6). This is mainly in line with the classes already known substrates come from. Interestingly, a relevant number of predicted substrates were also found

Table 1. Characterization of Investigated Substances[a]

| substance	K_m (±SEM) [μM]	v_{max} (±SEM) [pmol × mg protein⁻¹ × min⁻¹]	Cl_{int} [mL × g protein⁻¹ × min⁻¹]	ratio (HEK293-OCT1/ HEK293-EV)	target	usage[28]	previously considered as an OCT1 substrate?	set
amifampridine	508.1 (±247.3)	9569 (±2127)	18.8	6.8	inhibitor of voltage-gated potassium channels increasing acetylcholine release[29]	treatment of the Lambert–Eaton syndrome		tested prior to modeling
benzyltriethyl-ammonium	38.6 (±9.9)	2424 (±151)	62.8	67.5	transfer catalyst			predicted by the model
denatonium	12.6 (±1.0)	901.6 (±14.5)	71.4	21.6	bitter taste receptor (TAS22) agonist[30]	extremely bitter substance used as a deterrent for example in Nintendo cartridges to prevent ingestion		predicted by the model
dimethylphenyl-piperazinium	62.0 (±23.3)	2928 (±251)	47.2	38.9	ganglionic nicotinergic acetylcholine-receptor agonist[31]	investigational drug[31]		predicted by the model
dobutamine	28.4 (±16.8)	147.4 (±26.3)	5.2	14.7	$β_1$-receptor agonist[32]	treatment of shock and diagnostically in stress echocardiogram	inhibitor of OCT1[15]	tested prior to modeling
edrophonium	26.4 (±9.1)	2628 (±227)	99.5	42.6	cholinesterase inhibitor	diagnostics of myasthenia gravis[33]		predicted by the model
famotidine	35.7 (±7.3)	3121 (±154)	87.4	34.2	histamine-2-receptor antagonist	treatment of peptic ulcer		predicted by the model
fenpiverinium	8.6 (±3.2)	971.4 (±87.0)	113.5	30.9	muscarinergic acetylcholine-receptor antagonist	used experimentally and used as a spasmolytic[35]	inhibits uptake and trans-stimulates MPP⁺ efflux from OCT1-overexpressing oocytes[34]	predicted by the model
frovatriptan	61.9 (±10.3)	3113 (±147)	50.3	33.1	5-HT-receptor agonist	treatment of migraine		predicted by the model
guanfacine	8.6 (±6.1)	1183 (±191)	137.6	4.3	selective $α_2$-adreno receptor agonist[36]	treatment of attention deficit/hyperactivity disorder[36]		tested prior to modeling
labetalol				1.3	$α$- and $β$-receptor antagonist	treatment for acute hypertensive crisis[37]		predicted by the model
meta-iodobenzyl-guanidine (m-IBG)	15.9 (±5.3)	5033 (±380)	316.5	10.1	substrate of catecholamine transporters	scintigraphy and treatment of neuroendocrine tumors	meanwhile shown as the OCT1 substrate elsewhere[38]	predicted by the model
methylscopolamine	23.4 (±4.0)	1208 (±43)	51.6	39.2	muscarinic acetylcholine receptor agonist	formerly used in peptic ulcer		predicted by the model
milnacipran	2.26 (±1.43)	340.3 (±42.2)	150.6	6.3	norepinephrine serotonin reuptake inhibitor[39]	treatment of depression		tested prior to modeling
N-ethyl-lidocaine	51.4 (±15.4)	2725 (±189)	53.0	48.4	sodium-channel blocker	experimental local anesthetic[40]		predicted by the model
norphenylephrine	994.1 (±316.5)	4553 (±851)	4.6	2.1	$α$-receptor agonist[41]			predicted by the model
octopamine	388.6 (±246.4)	3543 (±922)	9.1	b	$α$- and $β$-adrenoreceptor agonist[42]	endogenous metabolite, exposure primarily via food[42]		predicted by the model

D

Table 1. continued

substance	K_m (±SEM) [μM]	v_{max} (±SEM) [pmol × mg protein^{-1} × min^{-1}]	Cl_{int} [mL × g protein^{-1} × min^{-1}]	ratio (HEK293-OCT1/ HEK293-EV)	target	usage[28]	previously considered as an OCT1 substrate?	set
phenylephrine	221.2 (±60.3)	3821 (±343.5)	17.3	10.6	α_1-receptor agonist	treatment of hypotension		predicted by the model
prenalterol	13.3 (±3.4)	165.0 (±10.3)	12.4	5.3	β_1-receptor agonist	treatment of cardiogenic shock, an antidote for intoxication with β-antagonists		predicted by the model
ractopamine	2.10 (±0.76)	233.5 (±17.2)	111.2	7.1	agonist at the trace-amine-associated receptor 1, possibly a β-adrenoreceptor agonist[28]	livestock food additive		predicted by the model
ritodrine	1.67 (±0.21)	172.9 (±4.8)	103.5	7.6	β_2-receptor agonist	tocolytic drug[43]		predicted by the model
sematilide	102.0 (±24.6)	338.5 (±31.1)	3.3	3.5	voltage-gated potassium-channel blocker	experimental class III antiarrhythmic drug[44]		predicted by the model
sotalol	195.9 (±72.1)	2764 (±390)	14.1	6.5	β-adrenergic receptor antagonist and a voltage-gated potassium-channel blocker	treatment of tachycardia[45]	no[46] or weak[25] OCT1 inhibition	predicted by the model

^{a}The ratio was calculated as "uptake HEK293-OCT1"/"uptake HEK293-EV" at a 2.5 μM substrate concentration. ^{b}The ratio could not be determined due to intrinsic octopamine concentrations, which affected the calculation at a 2.5 μM substrate concentration.

among antiarrhythmics, which are also in line with our results on sotalol and amifampridine (a potassium-channel blocker even though not prescribed as an antiarrhythmic) as well as sematilide (which was no substrate according to our strict criteria but showed active transport).

For four classes that contain especially strong OCT1 substrates, namely, triptans, β_2-sympathomimetics, H$_2$-antagonists, and anticholinergics, an overview on how our newly tested substance is structurally related to previously tested substances from the same classes is provided in Figure 7.

Frovatriptan differs from already tested triptans in that the positively charged nitrogen is closer to the indoline group (although there is high flexibility in the tested triptans, except for naratriptan). In addition, it is apparent that compared with all other triptans tested so far, frovatriptan is more rigid due to its ring closure. Frovatriptan is an above-average triptan-class substrate of OCT1, second only to naratriptan. In the class of β_2-agonists, ritodrine and ractopamine contain adrenaline almost entirely as a substructure just as most β_2-agonists do. They do not show close resemblance to any of the already known substrates differing at several positions. Interestingly, ritodrine and ractopamine turned out to have an at least 2-fold increased Cl_{int} compared to the other β_2-agonists (except fenoterol). The H$_2$-antagonists are structurally diverse. The newly reported famotidine is the best OCT1 substrate among them. Famotidine shows some resemblance to the non-substrate nizatidine, but nizatidine has no positively charged nitrogen at pH 7.4, which is the obvious explanation. Several anticholinergic drugs rank among the best OCT1 substrates. With the exception of scopolamine (not positively charged at pH 7.4), atropine, and tolterodine (as well as methoctramine, which is structurally far different), all the anticholinergics fare far above average. The newly tested fenpiverinium differs from all other antimuscarinic substrates of OCT1 by the missing ether and relatively short linker between charged nitrogen and the rings. Only tolterodine as an anticholinergic non-substrate does not have an ether group and does have a short linker region either. In addition to the ether, a hydroxy group at the c-atom combining the rings is considered relevant for binding to the mACh receptor. For fenpiverinium, missing both does obviously prevent neither binding to the mACh receptor nor being a substrate of OCT1. Methylscopolamine (clearance 51.6 mL × g protein^{-1} × min^{-1}), when compared to butylscopolamine (clearance 31.8 mL × g protein^{-1} × min^{-1}), shows that while a bulky configuration around the charged nitrogen is not impedimental for being a substrate (see also trospium, ipratropium), the butyl chain might be compared to a methyl group. As others of the novel substrates are much more different from substrates known so far, we do not discuss them here structurally. To classify them within the body of OCT1-tested substrates nonetheless, we provide a similarity clustering on a wallpaper (Figure S2). There, m-IBG appears in a cluster with other guanidines, namely, phenformin, proguanil, cycloguanil, and guanfacine. Amifampridine clusters relatively late with a group including the aforementioned guanidines as well as amiloride as another guanidine. With a molecular mass of 109 g × mol^{-1}, amifampridine is among the smallest substrates of OCT1, and as compared with other low-molecular-weight substances, it is a distinctly good substrate [a clearance of 18.8 mL × g protein^{-1} × min^{-1}, for comparison: tetraethylammonium (TEA), molecular weight 130 × g mol^{-1}, clearance 5.46 mL × g protein^{-1} × min^{-1}]. Famotidine is clustered together with the other H$_2$-antagonists. Dobutamine,
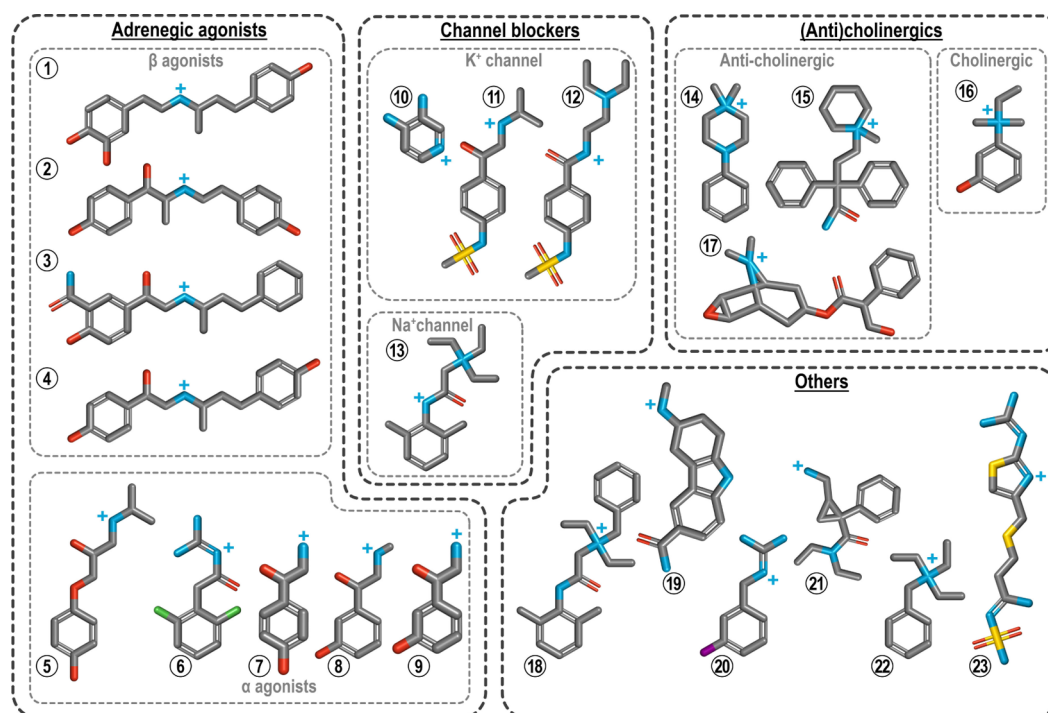
Figure 2. Molecules investigated in this study grouped by drug classes. (1) Dobutamine, (2) ritodrine, (3) labetalol, (4) ractopamine, (5) prenalterol, (6) guanfacine, (7) octopamine, (8) phenylephrine, (9) norphenylephrine, (10) amifampridine, (11) sotalol, (12) sematilide, (13) N-ethyl-lidocaine, (14) dimethylphenylpiperazinium, (15) fenpiverinium, (16) edrophonium, (17) methylscopolamine, (18) denatonium, (19) frovatriptan, (20) m-iodobenzylguanidine, (21) milnacipran, (22) benzyltriethylammonium, and (23) famotidine.

edrophonium, octopamine, norphenylephrine, phenylephrine, ritodrine, ractopamine, and prenalterol cluster together mainly with β-agonists, whereas sotalol, sematilide, and frovatriptan join this cluster later. Octopamine, phenylephrine, and norphenylephrine are structurally highly similar and therefore cluster closely together (norphenylephrine is not shown in Figure S2 as only substrates with a clearance ≥ 5 mL × g protein^{-1} × min^{-1} or a ratio ≥ 3 according to our criteria are included). Interestingly, while octopamine and phenylephrine are good substrates (clearance 9.1 and 17.3 mL × g protein^{-1} × min^{-1}), norphenylephrine had only a clearance of 4.6 mL × g protein^{-1} × min^{-1}.

Milnacipran first clustered with norfentanyl abide relatively late, clustering with the anticholinergics afterward. Interestingly, norfentanyl clusters with milnacipran earlier than with other opioid substrates. The structures for milnacipran, norfentanyl, and noroxycodone from the larger opioid cluster are shown together in Figure 7.

Finally, N-ethyl-lidocaine and denatonium cluster together early as they share a large common substructure (Figure 2), subsequently clustering with the newly tested benzyltriethylammonium (which is a substructure of denatonium, see Figure 2) as well as with the model substrate TEA.

Characteristics of the Overall Database after Addition of New Substrates and Non-substrates. The database here with its reliance purely on directly measured transport is a useful addition to larger data sets with more lenient consideration of data.[3] Therefore, a short summary of the basic characteristics of the overall data set including 286 substances (after addition of the novel substrates and non-substrates, see Table 2) appears appropriate.

The median molecular weight of substrates and non-substrates in the data set does not differ substantially, as

seen in Table 2. The maximum weight of non-substrates was much higher than that of substrates. The median number of hydrogen donors was higher in substrates than in non-substrates. The median number of hydrogen acceptors was the same in substrates and non-substrates. While the ring count in substrates was on the median one lower than in non-substrates, the median number of aromatic rings was the same.

With regard to the position of the positive charge, substrates had a guanidinium group in 9% of cases and non-substrates in 2%. Regarding positively charged nitrogen in general, substrates had positively charged nitrogen with four, three, two, and one non-hydrogen bond in 18, 11, 45, and 13%, respectively, as compared to 2, 34, 27, and 15% in non-substrates, respectively.

DISCUSSION AND CONCLUSIONS

Here, we will discuss the usefulness of our model for prediction of further OCT1 substrates specifically and the importance of virtual screening in search of OCT1 substrates in general. Furthermore, we will discuss new substrates with regard to potential clinical implications.

Usefulness of Model-Based Searches for New OCT1 Substrates. The model was successful in enriching substrates among tested candidates. Given that only about 200 freely available substances were tested with the same methodology, we consider the addition of 23 substances with many of them way above average substrates as substantial (overall, we actually added 97 substances to the data previously used by Baidya et al.[19]). A confirmation rate of 84% substrates among the tested substances, as found among the newly tested substances in this publication, is above what is usually experienced in screening for OCT1 substrates. Prior to use of the model, only 40% of the substances among the subset
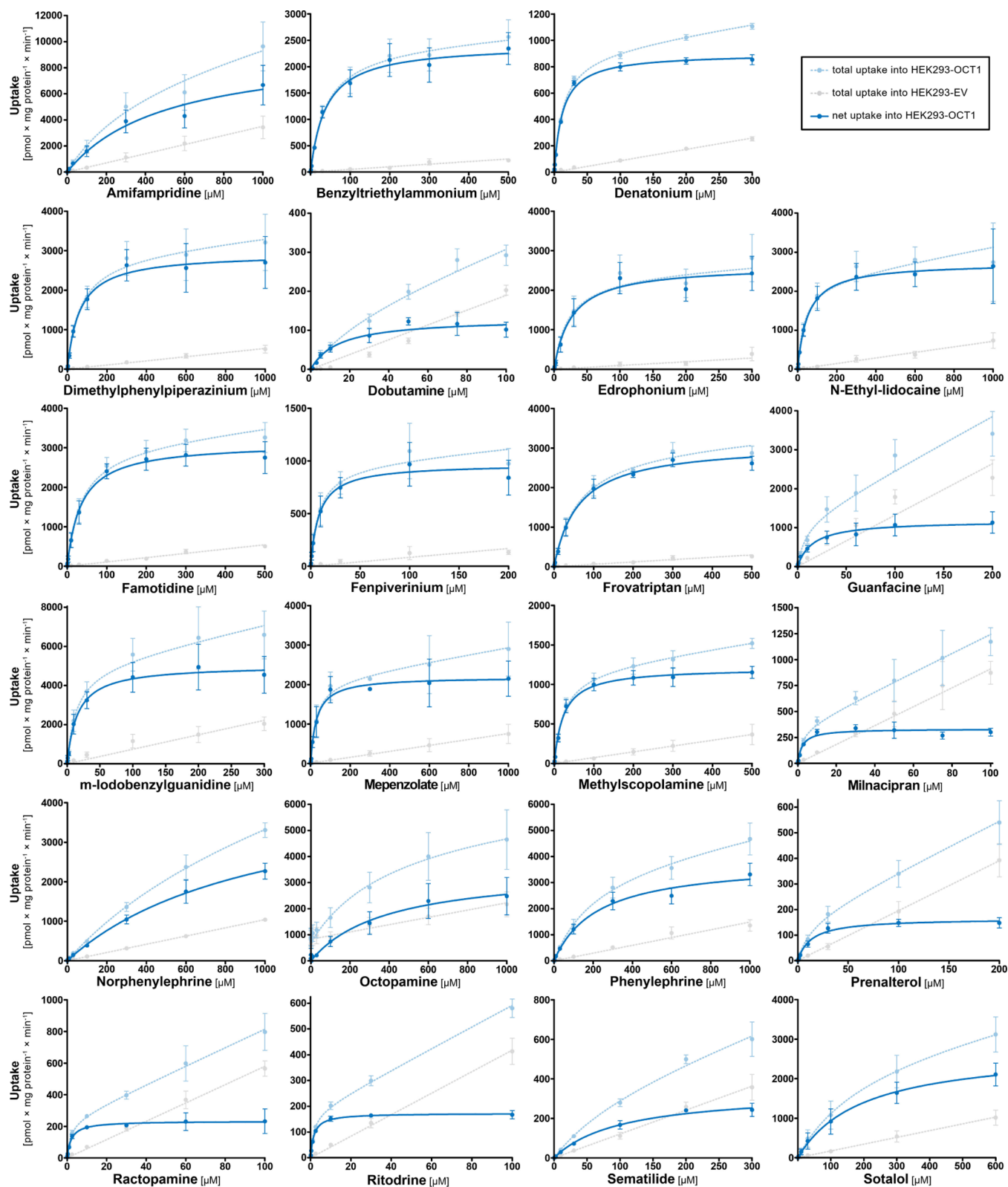
Figure 3. Total and net uptake into empty vector-transfected HEK293 cells ("HEK293-EV") and HEK293 cells overexpressing OCT1 ("HEK293-OCT1") reveal transport kinetics of known and newly identified substrates, listed in alphabetical order (octopamine: intrinsic/endogenous concentrations affect total uptake).

with a single positive charge, a log $D_{7.4}$ below 1, and a molecular weight between 104 and 766 g × mol^{-1} were substrates (using our strict criteria for the ratio and Cl$_{int}$). Simple binomial testing proves that given an expected success

rate of 40%, 16 or more substrates within 19 tested substances is not considered coincidence ($p = 0.0001$). One might object that searching handedly for structures similar to known substrates would have also increased the success rate, but it
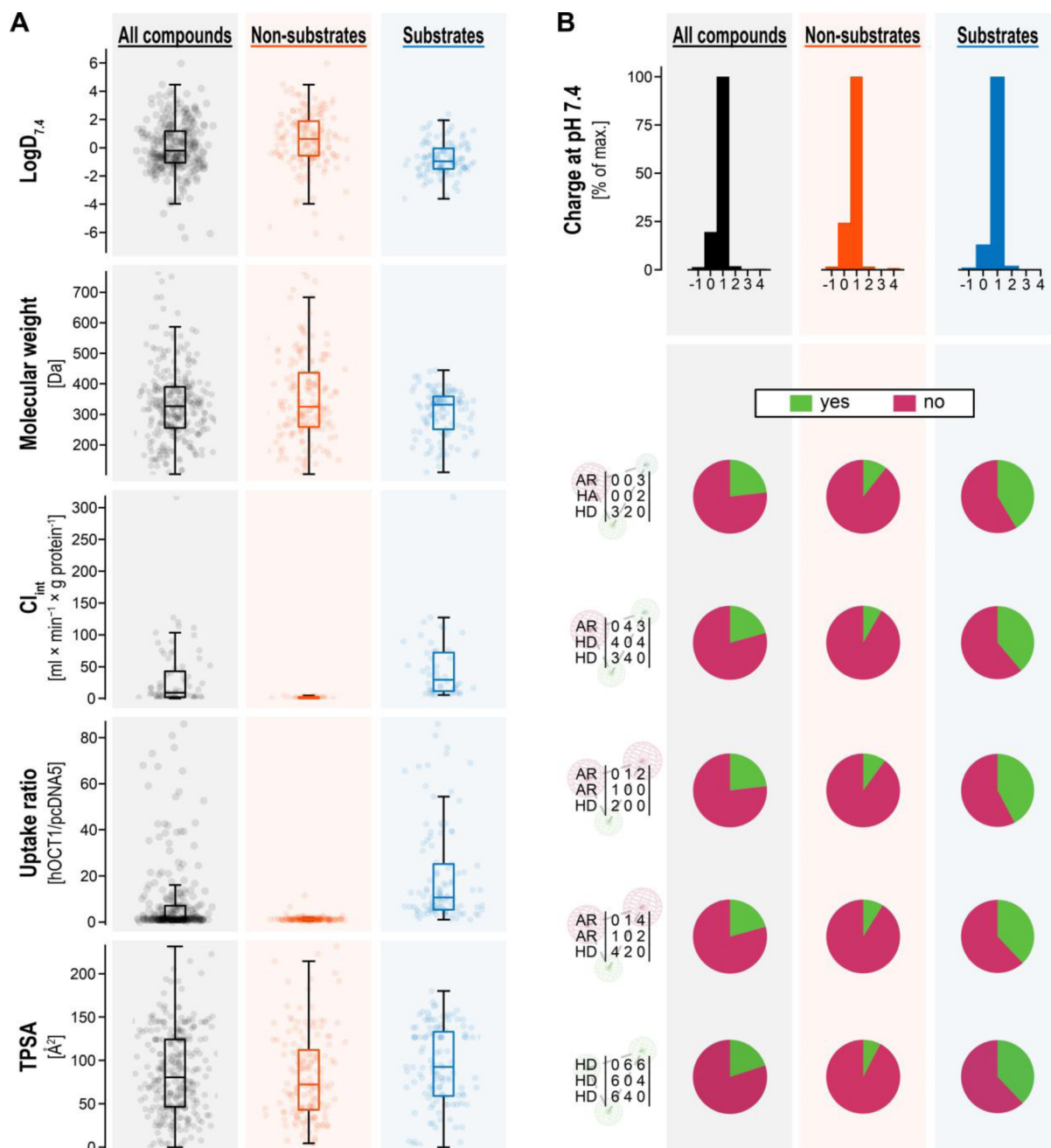
Figure 4. (A) Distribution of the general descriptors, log $D_{7.4}$ and molecular weight; the transport properties Cl_{int} and uptake ratio; and the total polar surface area for all compounds included in the data set as well as the OCT1 non-substrates and substrates. (B) Distribution of total charge at pH 7.4, given as percentage of the most represented group, and distribution of the top five pharmacophore features (given as matrices of their two-dimensional configurations) in the data set as well as the OCT1 non-substrates and substrates (AR—aromatic ring, HA—hydrogen acceptor, HD—hydrogen donor; numbers describe the binned spatial distance between the features according to RDKit[60]).

is nevertheless exciting that the algorithm could do similarly well or even better than an experienced investigator. Obviously, the overall database of 263 substances before our screening was no result of purely random testing either. The previous selection of tested substances will have already been biased by similarity searches.

Screening only drugs from groups already proven to include OCT1 substrates might also improve the success rate, but neither do we assume that this was never done while contributing to the data set before nor will manual search for drug classes be as efficient and complete. Finally, while some newly identified substrates were structurally very similar

to known substrates (e.g., methylscopolamine to butylscopolamine), for the majority, this was not the case. Either they were not highly similar to the training set, for example, N-ethyllidocaine (as lidocaine was not a part of the training set) or they were not highly similar to any known substrate and do not belong to substance classes majorly associated with OCT1, for example, edrophonium as a cholinesterase inhibitor.

Using a model within a limited chemical space comes with disadvantages as well. As opposed to Baidya and colleagues,[19] we restricted the scope of model predictions on cationic substances with a net charge of +1. Baidya and colleagues applied their model to newly FDA-approved drugs in general.
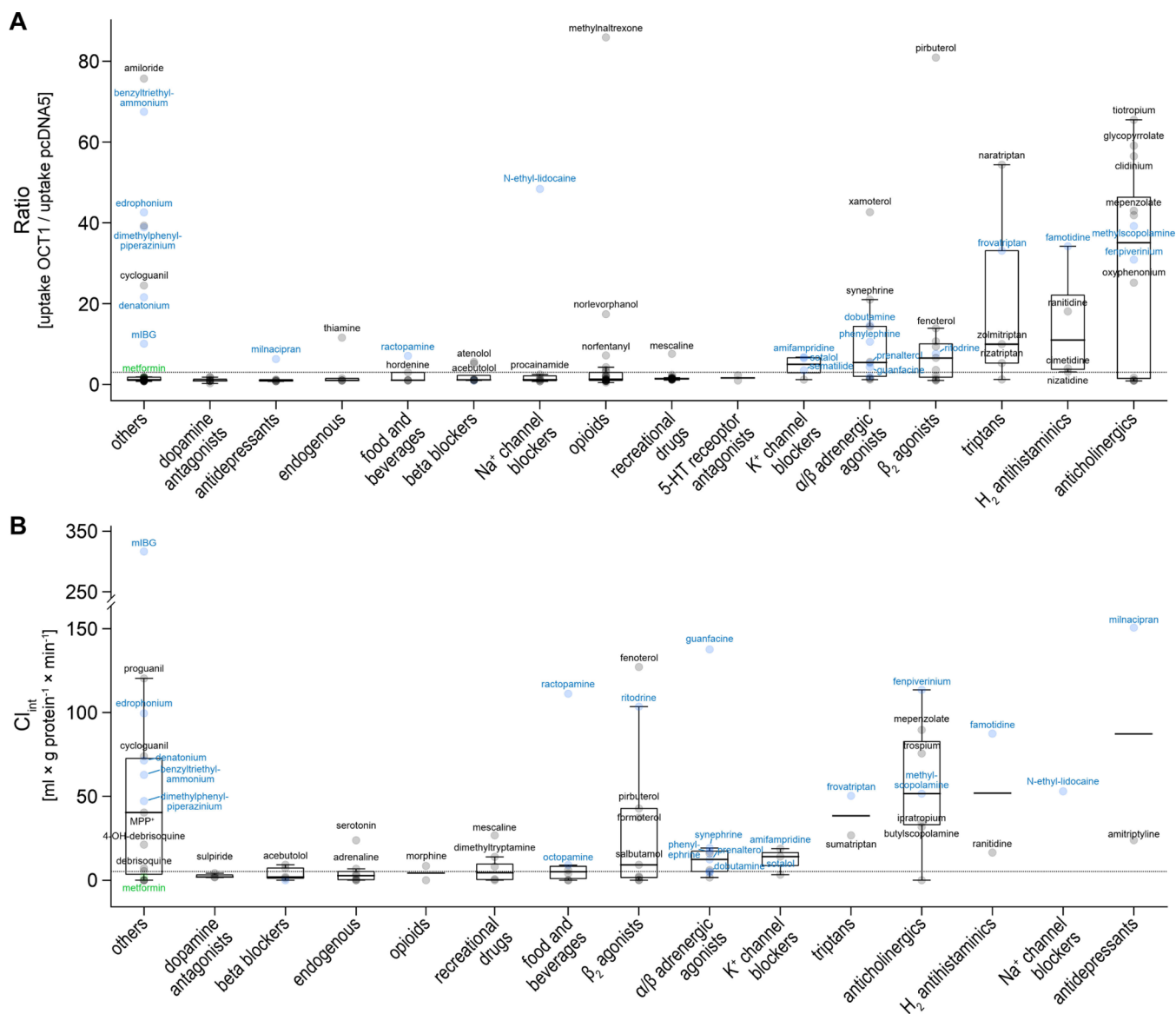
Figure 5. Uptake ratios (A) and intrinsic clearances (B) by drug classes. A classification according to PubChem PharmAction categories was used, and substances known earlier as substrates of OCT1 are printed in black, while substances newly identified are printed in blue. The antidiabetic drug metformin, as the best-known but obviously not the "best" substrate of OCT1, is highlighted in green.

While we see problems with usage in a broad chemical space and within extrapolation from the chemical space a model was built on, it is of course in no way sure that this is doomed to fail. The methods used might actually also help to find non-charged or even negatively charged substrates. Therefore, we also find expanding the horizon of OCT1 toward less probable candidate substrates appealing.

As great science is (at least sometimes) guided by coincidence, reducing coincidence by a systematic search will deprive us from finding some surprisingly great results. Therefore, we consider model-guided search for OCT1 substrates useful but emphasize that we also find random testing beyond the scope of known substrates extremely important. This was what, for example, led to identification of amifampridine and milnacipran as interesting OCT1 substrates.

Most probably guided by the high threshold we used for the distinction of substrates and non-substrates (clearance ≥ 5 mL × g protein^{-1} × min^{-1} and/or ratio ≥ 3), the novel substrates presented here were mostly extraordinarily good substrates. This will be beneficial for future search of high-Cl_{int} substrates and might generally contribute to a better understanding of the substrate binding sites of OCT1. A regression model not only predicting substrates but also hinting at the respective clearance/ratio is an obvious next step. With the initial data set, one major problem was a lack of high-Cl_{int} substrates, at least when fenoterol with a clearance of 120 was considered the benchmark of high Cl_{int}.

Not in focus of this study was the differentiation of substrates of OCT1 and the highly similar organic cation transporters, such as OCT2, OCT3, OCTN1, and OCTN2, and also efflux transporters like MATE1 and MATE2-K. Therefore, in spite of the high transport rates, firm conclusions about OCT1 selectivity of the newly identified substrates of OCT1 cannot be drawn. Our approach was to identify OCT1 substrates irrespective of their selectivity. This is especially medically relevant in situations when the substrate is known to be metabolized in the liver (and a significant renal elimination
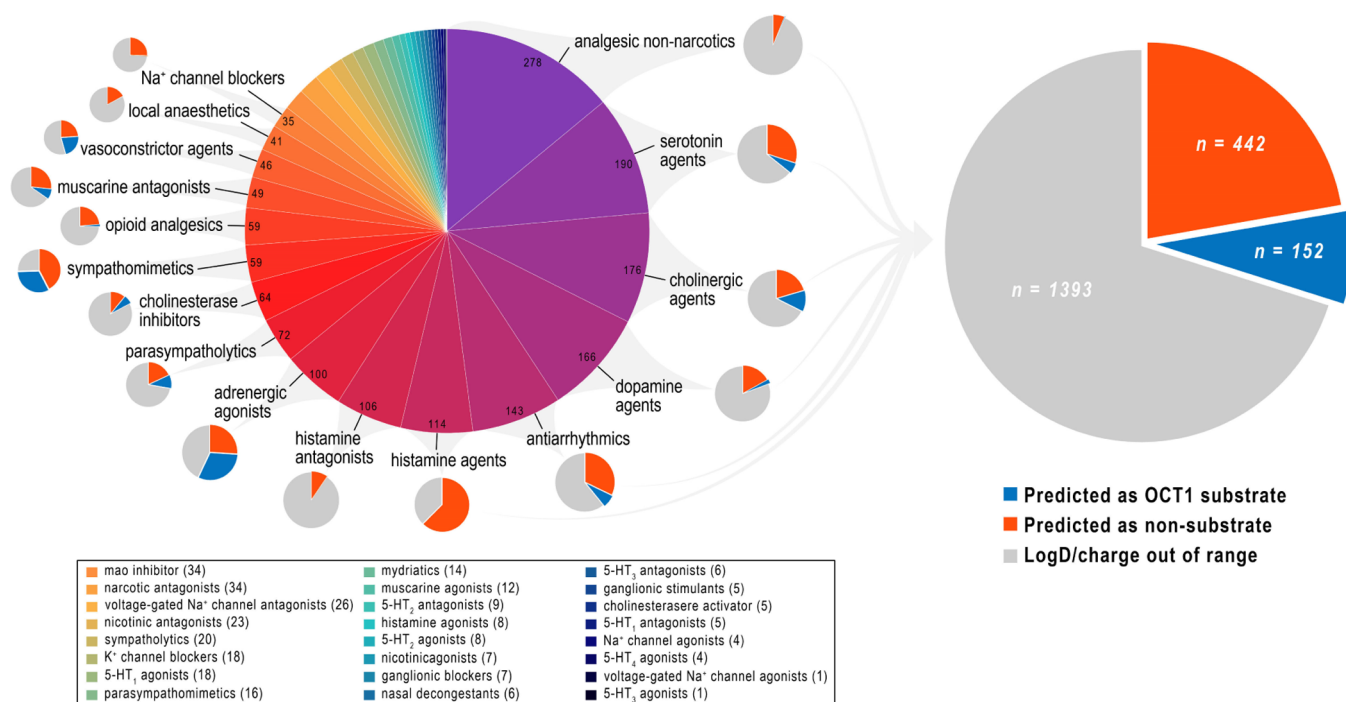
Figure 6. (Left) Illustration of the database composition. Small pie charts around show the same information separately by drug class. Histamine antagonists did not include any suggested substrates as the non-screening database only included H_1-antagonists. (Right) Underlying database consisted of drugs outside the range of charge (=+1) and log $D_{7.4}$ (<1) considered for testing (gray) as well as those within the range predicted as non-substrates (orange) and those within the range predicted as substrates (blue).

has been excluded). Further modeling of the differential selectivity of transporters and experimental validation is an important future perspective. It is especially important as it points toward structural differences of closely related transporters, having in mind that with stereoisomers, there was quite an astonishing partial selectivity between OCT1- and OCT2-mediated transport.[49] For differential modeling, as a starting point, it has to be known that a substance is at least a substrate of one of the transporters in question. This usually requires hierarchical modeling, even though in some cases, this problem has been solved creatively by the use of *in vivo* phenotyping.[22]

Of course, machine learning and other *in silico* approaches have not only been used for the prediction of substrates for organic cation transporters but for other transporters as well.[20,22,23] For all transporters, machine learning approaches have not been the only successful *in silico* methods for predicting new substrates/inhibitors. Long-established non-machine-learning approaches, such as knowledge-based pharmacophore modeling and others, should not be disregarded as they have delivered and will deliver valuable results.[20,21,23] Of course, it is of value not only to quantitatively predict ligand activities but also to develop a further understanding of the structural mechanisms upon ligand binding and translocation. Transport is not the same uniform process for each substrate. Especially, considering evidence for different binding sites in transporters,[26,50] it is important to continue with elucidation of their true molecular structures and with structural modeling. This knowledge cannot singularly be derived from ligand-based approaches. The ligands presented in this study might fall into groups of already known binding modes and might further elucidate the understanding of those when combined with structure-based approaches.[24]

We are aware that we have proven the usefulness of the model only for a chemical subspace (log $D_{7.4}$ < 1, charge = 1). It will be interesting to expand the validation onto substances not associated with cation transporters, implying more lipophilic and/or non-cationic compounds. However, at present, the database of experimentally well-characterized non-cationic substrates of OCT1 is relatively small, making reliable predictions in this part of the chemical space difficult. The future goal is to expand the database toward more diverse and maybe even better substrates and to elucidate the structural basis for efficient transport based on them. Our enrichment of this set with high-affinity substrates will hopefully assist in finding even better substrates, implying higher clearance, possibly higher affinity, higher transport capacity, and higher clinical relevance.

Clinical Implications of Newly Found OCT1 Substrates. Here, we tested potential substrates of OCT1 based on the model's suggestion to learn more about structure–activity relationships. When searching for clinically relevant substrates of OCT1, one has to consider additional factors: (1) is the drug commonly used? (2) Does the drug require transporter-mediated uptake into the liver for biliary secretion or hepatic biotransformation with subsequent renal elimination, and/or does the liver accumulate relevant amounts of the drug serving as a reservoir? If (1) and (2) hold true, one has to answer the question whether common OCT1 polymorphisms or OCT1-inhibiting comedication influences the patients' exposure to the drug. While none of the substances tested here are blockbuster drugs, some are prescribed frequently and shall be discussed.

Radiolabeled *m*IBG is used for diagnostic purposes and treatment of neuroendocrine tumors. While some guanidines are long known to be substrates of OCT1,[3,51] for *m*IBG, some but no conclusive evidence had been reported.[47] While writing
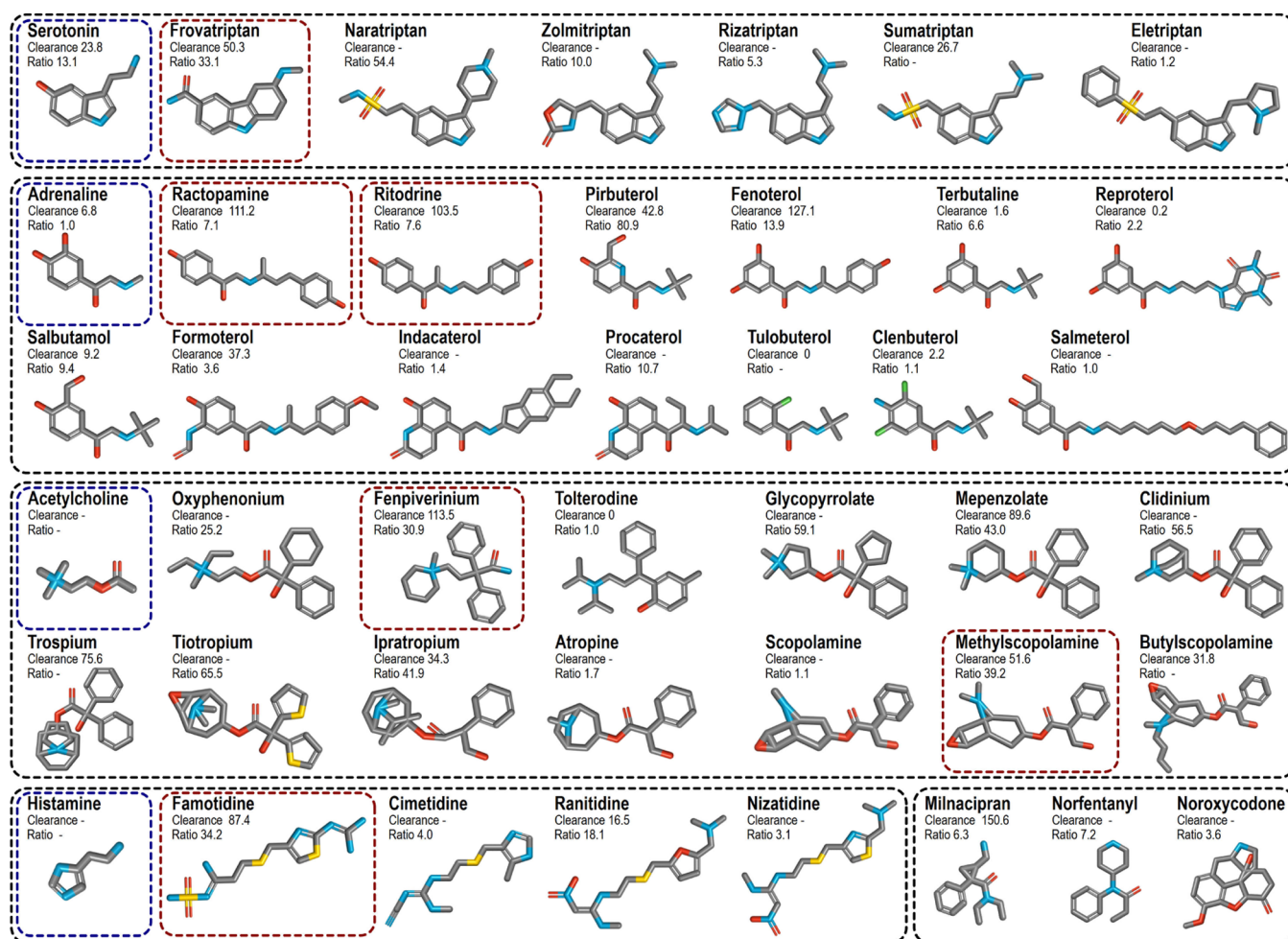
Figure 7. Overview of structural relation of the newly identified substrates (encircled in red) to previously tested substances and the endogenous agonist (encircled in blue).

Table 2. Characteristics of the OCT1 Substrate Set and the Non-substrate Set[a]

	OCT1 substrates	OCT1 non-substrates
count	117	166
molecular weight (g/mol)	332 (110−444)	325 (104−766)
number of hydrogen donors	3 (0−6)	2 (0−8)
number of hydrogen acceptors	4 (0−8)	4 (0−12)
number of rings	2 (0−6)	3 (0−8)
number of aromatic rings	2 (0−3)	2 (0−6)
percentage of substances with the guanidinium group (within substrates/non-substrates)	9%	2%
percentage of substances with charged nitrogen and four non-hydrogen bonds (within substrates/non-substrates)	18%	2%
percentage of substances with charged nitrogen and three non-hydrogen bonds (within substrates/non-substrates)	11%	34%
percentage of substances with charged nitrogen and two non-hydrogen bonds (within substrates/non-substrates)	45%	27%
percentage of substances with charged nitrogen and one non-hydrogen bond (within substrates/non-substrates)	13%	15%

[a]All data are provided as the median (minimum−maximum).

this article, OCT1-conclusive evidence has been reported elsewhere.[38] Therefore, *m*IBG validates our model, while our data now only add to a very recent publication proving *m*IBG as a substrate.[38] Uptake of *m*IBG by OCT1 is interesting because one might be able to reduce its unwanted and potentially harmful accumulation in normal tissues by OCT1 inhibition.[38,48] We furthermore want to add that OCT1 polymorphisms should also be studied with regard to their influence on *m*IBG pharmacokinetics, pharmacodynamics, and adverse effects. From a purely structural point of view, one might also be interested in *in vitro* testing of benzylguanidine as a substrate of OCT1 to further examine if iodine contributes to the high OCT1 clearance.

Frovatriptan is now an additional triptan proven as an OCT1 substrate. Regarding potential influences of OCT1 polymorphisms on its pharmacokinetics, frovatriptan is an interesting candidate as it is metabolized in the liver[52] and with 26 h, it already has a very long half-life compared to other triptans.[53] This long half-life might even increase with polymorphisms leading to OCT1 deficiency, and carriers may suffer from more and prolonged adverse effects.

Sotalol is mainly excreted unchanged via the kidneys.[54] If at all, OCT polymorphisms may influence pharmacokinetics only as they might exclude the liver as a reservoir. This phenomenon of hepatic storage was impressively shown for sumatriptan by autoradiography as well as by positron emission

tomography scans.[55] It has also been shown for metformin.[56] Milnacipran is also mainly excreted unchanged via the kidneys so that polymorphisms may influence pharmacokinetics only as they might exclude the liver as a reservoir here as well.[57]

Systemic amifampridine exposure has been shown to be dependent on *N*-acetyltransferase 2 (NAT2) activity, with up to 8.8-fold increase in AUC dependent on the kidney function.[58] NAT2 is highly expressed in the liver. The influence of OCT1 polymorphisms on liver uptake could further modulate systemic exposure to amifampridine.

In summary, we expanded the database of substances with directly proven OCT1 transport by a double-digit percentage and contributed high-affinity substrates, which might allow for future regression modeling and for analyses of different binding modes. Additionally, effects of polymorphisms on the *in vitro* transport of the new substrates are worth studying. The same holds true for *in vivo* pharmacokinetics and pharmacodynamics in the case of some of these novel substrates. Apparently, the algorithms currently available may significantly accelerate our knowledge about the substrate spectrum of not only OCT1 but also many other solute carrier transporters and beyond.

■ EXPERIMENTAL SECTION

Database Creation. Only data from transporter assays using HEK293 cells overexpressing human OCT1 were added to our database. We included ratio data (OCT1-overexpressing over control) of transport experiments from Hendrickx et al. (ratios determined at a concentration of 2.5 μM),[13] a publication from Meyer and colleagues (ratios determined at a concentration of 0.5 μM),[14] and ratio and clearance data from our lab. We did not include inhibition data.

Hendrickx and colleagues reported transport assay results for 354 substances, with 81 of them with a clear name and 273 experimental substances with aliases.[13] Baidya and colleagues used the clear-name substances and additional 100 of the experimental substances for successful modeling.[19] The clear-named drugs used by Hendrickx et al. and the experimental substances used by Baidya and colleagues were added to our database. The additional experimental substances were not added to not shift the focus of modeling and prediction too much on this very specific subset. Adding 21 test substances from the Meyer publication[14] and ratio and clearance data from our laboratory, we created a database of 286 drugs (this also includes the newly tested substrates from this publication) with complete structural information and data on transport via OCT1 either as ratios or as clearances. In summary, we added around 100 substances to the database used by Baidya earlier.[19] The resulting data set still had the advantage that it comprises data from highly homogeneous sources. The cell lines used in the Meyer publication[14] are of the same origin as ours. For the Hendrickx[13] results, we have shown a good overlap over years, and an ad hoc analysis showed a high correlation of observed ratios ($r^2 = 0.94$, $n = 6$). Files with structure information were downloaded as structure data files (.sdf) from either the ZINC database[59] or PubChem. Drugs with only SMILES information were converted into the .sdf format using the chemical identifier resolver from the NIH website.

For screening of new substrates, libraries of structural files were obtained from PubChem. The screening database included 2055 drug-like substances from PubChem (~1500 after curation with, for example, removal of duplicates).

A chemical database was created using Instant JChem (ChemAxon, Budapest, Hungary), transport data were included, and molecular descriptors were calculated.

The overall database was imported into RDKit (Python).[60] Additional molecular descriptors and pharmacophore fingerprints based on the definitions by Gobbi[61] as well as Morgan fingerprints (radius = 2, 2048 bits) were added.

Machine Learning. All steps were performed in Python using pandas, scikit-learn, and *XGBoost*.[62−64] At an initial stage, only the originally accessible Hendrickx data set and our lab data were used. In the later stages, the data from the Meyer publication as well as data from substrates predicted by the model and already tested in our lab were added. This was done to perform the prediction based on the best data available at each point in time.

Consistent cutoff values for clearance and ratio were derived from drugs with both measurements available (clearance ≥ 5 mL × g protein^{-1} × min^{-1} and/or ratio ≥ 3 was set as the substrate definition, and supporting data are presented in the first Results section and in Figure S1).

The data set was split randomly into the training set (80%) and holdout validation set (20%) using a stratified split (stratified with regard to the proportion of substrates and non-substrates). The initial model was built based on the training set and included all features and descriptors calculated. The features were then reduced to those with good predictive performance in repeated 5-fold cross-validation only using the training set. The performance of the reduced models was assessed based on AUCs in repeated 5-fold cross-validation still only using the training set. Hyperparameters were also tuned based on AUCs in repeated 5-fold cross-validation of the training set only. The final model performance was then assessed using the holdout validation set. Virtual screening was subsequently performed using the validated model and the screening database.

***In Vitro* Uptake Experiments.** Transport experiments were performed as described earlier.[49,65] In brief, 600,000 HEK293 cells stably transfected with the empty pcDNA5 vector or to overexpress human OCT1 were plated in poly-D-lysine pre-coated 12-well plates 48 h prior to the transport experiment. For this, cells were washed once with 37 °C Hanks' balanced salt solution (HBSS, Thermo Fisher Scientific, Darmstadt, Germany) supplemented with 10 mM 4-(2-hydroxyethyl)-1-piperazineethanesulfonic acid pH 7.4 (Sigma-Aldrich, Taufkirchen, Germany)—from here on termed HBSS+. Cells were incubated with increasing concentrations of the respective drug in HBSS+ at 37 °C. After 2 min, cells were washed with ice-cold HBSS+ twice and lyzed with 500 μL of 80% (v/v) acetonitrile (LGC Standards, Wesel, Germany) including an internal standard. The intracellular accumulation of tested substances was measured by liquid chromatography with tandem mass spectrometry (LC−MS/MS). Normalization of cell numbers was performed by measuring the total protein via a standard bicinchoninic acid assay. All tested compounds suggested by virtual screening were tested negative for pan assay interference (online filter: http://zinc15.docking.org/patterns/home/).[66] Among the substances presented in this study, only dobutamine was reported as a possibly interfering compound. This might be of minor relevance because normalization of uptake is performed, controls were used, and uptake experiments are less prone to interference compared to inhibition experiments.

LC−MS/MS Concentration Analyses. Cellular concentrations were determined by high-performance liquid chromatography (HPLC)−MS/MS using a Shimadzu Nexera HPLC system with an LC-30AD pump, a SIL-30AC autosampler, a CTO-20AC column oven, and a CBM-20A controller (all Shimadzu, Kyoto, Japan). Liquid chromatography was performed on a Brownlee SPP RP-Amide column (4.6 × 100 mm inner dimensions with a 2.7 μm particle size) with a C18 pre-column. The aqueous mobile phase contained 0.1% (v/v) formic acid and 3% (v/v) organic additive [acetonitrile/methanol 6:1 (v/v)] in the case of edrophonium (Santa Cruz Biotechnology, Heidelberg, Germany), amifampridine, norphenylephrine, octopamine, and phenylephrine (all Sigma-Aldrich, Taufkirchen, Germany); 8% (v/v) in the case of benzyltriethylammonium, dimethylphenylpiperazinium, frovatriptan, sematilide (Sigma-Aldrich, Taufkirchen, Germany), famotidine, prenalterol, and sotalol (Santa Cruz Biotechnology, Heidelberg, Germany); 20% (v/v) in the case of dobutamine (Eli Lilly, Indianapolis, USA), fenpiverinium, *m*-IBG, methylscopolamine, milnacipran (Santa Cruz Biotechnology, Heidelberg, Germany), *N*-ethyl-lidocaine, labetalol, ractopamine, ritodrine (Sigma-Aldrich, Taufkirchen, Germany); or 35% (v/v) in the case of denatonium (Sigma-Aldrich, Taufkirchen, Germany), and chromatography was carried out with a flow of 0.3 mL/min. The HPLC system was coupled to an API 4000 tandem mass spectrometer

(AB SCIEX, Darmstadt, Germany), and detection was performed in the MRM mode with parameters given in Table S1. Quantification was performed using the Analyst software (version 1.6.2, AB SCIEX, Darmstadt, Germany) and determined by the simultaneous measurement of a standard curve with known concentrations. The net uptake by OCT1 was calculated as the difference between the uptake by OCT1 overexpressing and empty vector-transfected HEK293 cells. If not stated otherwise, the results are given as mean values ± standard errors of the mean (SEM). All compounds used were purchased with purity > 95%.

ASSOCIATED CONTENT

Supporting Information

The Supporting Information is available free of charge at https://pubs.acs.org/doi/10.1021/acs.jmedchem.0c02047.

> Definition of criteria for OCT1 substrates and non-substrates and performance of the model; wallpaper of clustering of OCT1 substrates by fingerprint similarity; and LC−MS/MS parameters for detection of substances tested in this study (PDF)
>
> Overall data set (including the results of previous publications, unpublished data from our lab, and the results of this publication) (PDF)
>
> Molecular formula strings of all compounds of the data set in the .csv format (CSV)
>
> Predicted substrates not tested in this publication (XLSX)
>
> Overall data set (including the results of previous publications, unpublished data from our lab, and the results of this publication) (TXT)

AUTHOR INFORMATION

Corresponding Author

Christof Dücker − Institute of Clinical Pharmacology, University Medical Center Göttingen, D-37075 Göttingen, Germany; orcid.org/0000-0002-4776-138X; Phone: +49 551 39 65776; Email: christof.duecker@med.uni-goettingen.de; Fax: +49 551 39 12767

Authors

Ole Jensen − Institute of Clinical Pharmacology, University Medical Center Göttingen, D-37075 Göttingen, Germany; orcid.org/0000-0001-9903-4769

Jürgen Brockmöller − Institute of Clinical Pharmacology, University Medical Center Göttingen, D-37075 Göttingen, Germany

Complete contact information is available at:
https://pubs.acs.org/10.1021/acs.jmedchem.0c02047

Author Contributions

O.J., J.B., and C.D. conceptualized the study; C.D. performed the chemoinformatics analyses; O.J. and C.D. developed the model; O.J. and C.D. designed the experiments; O.J. performed the wet-lab experiments; O.J. and C.D. analyzed the data; and O.J., J.B., and C.D. wrote the manuscript. All authors have given approval to the final version of the manuscript.

Notes

The authors declare no competing financial interest.

ACKNOWLEDGMENTS

ABBREVIATIONS USED

Cl_{int}, intrinsic clearance; H_2-receptor, histamine 2 receptor; HBSS, Hanks' balanced salt solution; HEPES, 4-(2-hydroxyethyl)-1-piperazineethanesulfonic acid; log D, logarithm of distribution coefficient; mIBG, meta-iodobenzylguanidine; MPP^+, 1-methyl-4-phenylpyridinium; MRM, multiple reaction monitoring; NAT2, N-acetyltransferase 2; SEM, standard error of the mean; SLC, solute carrier; TAS22, taste receptor 22; TEA, tetraethylammonium; TPSA, total polar surface area

REFERENCES

(1) Nies, A. T.; Koepsell, H.; Winter, S.; Burk, O.; Klein, K.; Kerb, R.; Zanger, U. M.; Keppler, D.; Schwab, M.; Schaeffeler, E. Expression of organic cation transporters OCT1 (SLC22A1) and OCT3 (SLC22A3) is affected by genetic factors and cholestasis in human liver. Hepatology 2009, 50, 1227−1240.

(2) Hilgendorf, C.; Ahlin, G.; Seithel, A.; Artursson, P.; Ungell, A.-L.; Karlsson, J. Expression of thirty-six drug transporter genes in human intestine, liver, kidney, and organotypic cell lines. Drug Metab. Dispos. 2007, 35, 1333−1340.

(3) Koepsell, H. Organic cation transporters in health and disease. Pharmacol. Rev. 2020, 72, 253−319.

(4) Suhre, K.; Shin, S. Y.; Shin, S.-Y.; Petersen, A.-K.; Mohney, R. P.; Meredith, D.; Wägele, B.; Altmaier, E.; Deloukas, P.; Erdmann, J.; Grundberg, E.; Hammond, C. J.; de Angelis, M. H.; Köttgen, A.; Kronenberg, F.; Mangino, M.; Meisinger, C.; Meitinger, T.; Mewes, H.-W.; Milburn, M. V.; Prehn, C.; Raffler, J.; Ried, J. S.; Römisch-Margl, W.; Samani, N. J.; Small, K. S.; Wichmann, H.-E.; Zhai, G.; Illig, T.; Spector, T. D.; Adamski, J.; Soranzo, N.; Gieger, C.; Gieger, C. Human metabolic individuality in biomedical and pharmaceutical research. Nature 2011, 477, 54−60.

(5) Meyer, M. J.; Seitz, T.; Brockmöller, J.; Tzvetkov, M. V. Effects of genetic polymorphisms on the OCT1 and OCT2-mediated uptake of ranitidine. PLoS One 2017, 12, No. e0189521.

(6) Liang, X.; Yee, S. W.; Chien, H.-C.; Chen, E. C.; Luo, Q.; Zou, L.; Piao, M.; Mifune, A.; Chen, L.; Calvert, M. E.; King, S.; Norheim, F.; Abad, J.; Krauss, R. M.; Giacomini, K. M. Organic cation transporter 1 (OCT1) modulates multiple cardiometabolic traits through effects on hepatic thiamine content. PLoS Biol. 2018, 16, No. e2002907.

(7) Shu, Y.; Brown, C.; Castro, R.; Shi, R.; Lin, E.; Owen, R.; Sheardown, S.; Yue, L.; Burchard, E.; Brett, C.; Giacomini, K. Effect of genetic variation in the organic cation transporter 1, OCT1, on metformin pharmacokinetics. Clin. Pharmacol. Ther. 2008, 83, 273−280.

(8) Venkatasubramanian, R.; Fukuda, T.; Niu, J.; Mizuno, T.; Chidambaran, V.; Vinks, A. A.; Sadhasivam, S. ABCC3 and OCT1 genotypes influence pharmacokinetics of morphine in children. Pharmacogenomics 2014, 15, 1297−1309.

(9) Matthaei, J.; Kuron, D.; Faltraco, F.; Knoch, T.; Dos Santos Pereira, J.; Abu Abed, M.; Prukop, T.; Brockmöller, J.; Tzvetkov, M. OCT1 mediates hepatic uptake of sumatriptan and loss-of-function OCT1 polymorphisms affect sumatriptan pharmacokinetics. Clin. Pharmacol. Ther. 2016, 99, 633−641.

(10) Tzvetkov, M. V.; Matthaei, J.; Pojar, S.; Faltraco, F.; Vogler, S.; Prukop, T.; Seitz, T.; Brockmöller, J. Increased systemic exposure and stronger cardiovascular and metabolic adverse reactions to fenoterol in individuals with heritable OCT1 deficiency. Clin. Pharmacol. Ther. 2018, 103, 868−878.

(11) Tzvetkov, M. V.; dos Santos Pereira, J. N.; Meineke, I.; Saadatmand, A. R.; Stingl, J. C.; Brockmöller, J. Morphine is a substrate of the organic cation transporter OCT1 and polymorphisms in OCT1 gene affect morphine pharmacokinetics after codeine administration. *Biochem. Pharmacol.* **2013**, *86*, 666−678.

(12) Stamer, U. M.; Musshoff, F.; Stüber, F.; Brockmöller, J.; Steffens, M.; Tzvetkov, M. V. Loss-of-function polymorphisms in the organic cation transporter OCT1 are associated with reduced postoperative tramadol consumption. *Pain* **2016**, *157*, 2467−2475.

(13) Hendrickx, R.; Johansson, J. G.; Lohmann, C.; Jenvert, R.-M.; Blomgren, A.; Börjesson, L.; Gustavsson, L. Identification of novel substrates and structure-activity relationship of cellular uptake mediated by human organic cation transporters 1 and 2. *J. Med. Chem.* **2013**, *56*, 7232−7242.

(14) Meyer, M. J.; Neumann, V. E.; Friesacher, H. R.; Zdrazil, B.; Brockmöller, J.; Tzvetkov, M. V. Opioids as substrates and inhibitors of the genetically highly variable organic cation transporter OCT1. *J. Med. Chem.* **2019**, *62*, 9890−9905.

(15) Chen, E. C.; Khuri, N.; Liang, X.; Stecula, A.; Chien, H.-C.; Yee, S. W.; Huang, Y.; Sali, A.; Giacomini, K. M. Discovery of competitive and noncompetitive ligands of the organic cation transporter 1 (OCT1; SLC22A1). *J. Med. Chem.* **2017**, *60*, 2685−2696.

(16) Dakal, T. C.; Kumar, R.; Ramotar, D. Structural modeling of human organic cation transporters. *Comput. Biol. Chem.* **2017**, *68*, 153−163.

(17) Popp, C.; Gorboulev, V.; Müller, T. D.; Gorbunov, D.; Shatskaya, N.; Koepsell, H. Amino acids critical for substrate affinity of rat organic cation transporter 1 line the substrate binding region in a model derived from the tertiary structure of lactose permease. *Mol. Pharmacol.* **2005**, *67*, 1600−1611.

(18) Liu, H. C.; Goldenberg, A.; Chen, Y.; Lun, C.; Wu, W.; Bush, K. T.; Balac, N.; Rodriguez, P.; Abagyan, R.; Nigam, S. K. Molecular properties of drugs interacting with SLC22 transporters OAT1, OAT3, OCT1, and OCT2: a machine-learning approach. *J. Pharmacol. Exp. Ther.* **2016**, *359*, 215−229.

(19) Baidya, A. T. K.; Ghosh, K.; Amin, S. A.; Adhikari, N.; Nirmal, J.; Jha, T.; Gayen, S. In silico modelling, identification of crucial molecular fingerprints, and prediction of new possible substrates of human organic cationic transporters 1 and 2. *New J. Chem.* **2020**, *44*, 4129−4143.

(20) Wu, J.-w.; Yin, L.; Liu, Y.-q.; Zhang, H.; Xie, Y.-f.; Wang, R.-l.; Zhao, G.-l. Synthesis, biological evaluation and 3D-QSAR studies of 1,2,4-triazole-5-substituted carboxylic acid bioisosteres as uric acid transporter 1 (URAT1) inhibitors for the treatment of hyperuricemia associated with gout. *Bioorg. Med. Chem. Lett.* **2019**, *29*, 383−388.

(21) Wolman, A. T.; Gionfriddo, M. R.; Heindel, G. A.; Mukhija, P.; Witkowski, S.; Bommareddy, A.; Vanwert, A. L. Organic anion transporter 3 interacts selectively with lipophilic beta-lactam antibiotics. *Drug Metab. Dispos.* **2013**, *41*, 791−800.

(22) Nigam, A. K.; Li, J. G.; Lall, K.; Shi, D.; Bush, K. T.; Bhatnagar, V.; Abagyan, R.; Nigam, S. K. Unique metabolite preferences of the drug transporters OAT1 and OAT3 analyzed by machine learning. *J. Biol. Chem.* **2020**, *295*, 1829−1842.

(23) Ahn, S.-Y.; Eraly, S. A.; Tsigelny, I.; Nigam, S. K. Interaction of organic cations with organic anion transporters. *J. Biol. Chem.* **2009**, *284*, 31422−31430.

(24) Türková, A.; Zdrazil, B. Current advances in studying clinically relevant transporters of the solute carrier (SLC) family by connecting computational modeling and data science. *Comput. Struct. Biotechnol. J.* **2019**, *17*, 390−405.

(25) Ahlin, G.; Karlsson, J.; Pedersen, J. M.; Gustavsson, L.; Larsson, R.; Matsson, P.; Norinder, U.; Bergström, C. A. S.; Artursson, P. Structural requirements for drug inhibition of the liver specific human organic cation transport protein 1. *J. Med. Chem.* **2008**, *51*, 5932−5942.

(26) Schlessinger, A.; Welch, M. A.; van Vlijmen, H.; Korzekwa, K.; Swaan, P. W.; Matsson, P. Molecular modeling of drug-transporter

(27) FDA. *In Vitro Drug Interaction Studies—Cytochrome P450 Enzyme- and Transporter-Mediated Drug Interactions*, 2020.

(28) Liu, X.; Grandy, D. K.; Janowsky, A. Ractopamine, a livestock feed additive, is a full agonist at trace amine-associated receptor 1. *J. Pharmacol. Exp. Ther.* **2014**, *350*, 124−129.

(29) Mantegazza, R. Amifampridine tablets for the treatment of Lambert-Eaton myasthenic syndrome. *Expert Rev. Clin. Pharmacol.* **2019**, *12*, 1013−1018.

(30) Meyerhof, W.; Batram, C.; Kuhn, C.; Brockhoff, A.; Chudoba, E.; Bufe, B.; Appendino, G.; Behrens, M. The molecular receptive ranges of human TAS2R bitter taste receptors. *Chem. Senses* **2010**, *35*, 157−170.

(31) Page, I. H.; McCubbin, J. W. Cardiovascular action of 1,1-dimethyl-4-phenylpiperazinium iodide (DMPP); a ganglion stimulating agent useful in the diagnosis of pheochromocytoma. *Am. J. Med.* **1953**, *15*, 675−683.

(32) Sonnenblick, E. H.; Frishman, W. H.; LeJemtel, T. H. Dobutamine: a new synthetic cardioactive sympathetic amine. *N. Engl. J. Med.* **1979**, *300*, 17−22.

(33) Naji, A.; Owens, M. L. Edrophonium. In *StatPearls [Internet]*; StatPearls Publishing LLC: Treasure Island, FL, 2020.

(34) Bourdet, D. L.; Pritchard, J. B.; Thakker, D. R. Differential substrate and inhibitory activities of ranitidine and famotidine toward human organic cation transporter 1 (hOCT1; SLC22A1), hOCT2 (SLC22A2), and hOCT3 (SLC22A3). *J. Pharmacol. Exp. Ther.* **2005**, *315*, 1288−1297.

(35) Sanahuja, J.; Corbera, G.; Garau, J.; Plá, R.; Carré, M. C. Intramuscular diclofenac sodium versus intravenous baralgin in the treatment of renal colic. *DICP, Ann. Pharmacother.* **1990**, *24*, 361−364.

(36) Huss, M.; Chen, W.; Ludolph, A. G. Guanfacine extended release: a new pharmacological treatment option in Europe. *Clin. Drug Invest.* **2016**, *36*, 1−25.

(37) Miller, M.; Kerndt, C. C.; Maani, C. V. Labetalol. In *StatPearls [Internet]*; StatPearls Publishing LLC: Treasure Island, FL, 2020.

(38) López Quiñones, A. J.; Wagner, D. J.; Wang, J. Characterization of meta-iodobenzylguanidine (mIBG) transport by polyspecific organic cation transporters: implication for mIBG therapy. *Mol. Pharmacol.* **2020**, *98*, 109−119.

(39) Kasper, S.; Pail, G. Milnacipran: a unique antidepressant? *Neuropsychiatr. Dis. Treat.* **2010**, *6*, 23−31.

(40) Brenneis, C.; Kistner, K.; Puopolo, M.; Jo, S.; Roberson, D.; Sisignano, M.; Segal, D.; Cobos, E. J.; Wainger, B. J.; Labocha, S.; Ferreirós, N.; von Hehn, C.; Tran, J.; Geisslinger, G.; Reeh, P. W.; Bean, B. P.; Woolf, C. J. Bupivacaine-induced cellular entry of QX-314 and its contribution to differential nerve block. *Br. J. Pharmacol.* **2014**, *171*, 438−451.

(41) Leclerc, G.; Bizec, J. C.; Bieth, N.; Schwartz, J. Synthesis and structure-activity relationships among alpha-adrenergic receptor agonists of the phenylethanolamine type. *J. Med. Chem.* **1980**, *23*, 738−744.

(42) Stohs, S. J.; Shara, M.; Ray, S. D. p-Synephrine, ephedrine, p-octopamine and m-synephrine: comparative mechanistic, physiological and pharmacological properties. *Phytother. Res.* **2020**, *34*, 1838−1846.

(43) Mayer, C.; Apodaca-Ramos, I. Tocolysis. In *StatPearls [Internet]*; StatPearls Publishing LLC: Treasure Island, FL, 2020.

(44) Shi, J.; Lasser, T.; Koziol, T.; Hinderling, P. H. Kinetics and dynamics of sematilide. *Ther. Drug Monit.* **1995**, *17*, 437−444.

(45) Anderson, J. L.; Prystowsky, E. N. Sotalol: An important new antiarrhythmic. *Am. Heart J.* **1999**, *137*, 388−409.

(46) Grube, M.; Ameling, S.; Noutsias, M.; Köck, K.; Triebel, I.; Bonitz, K.; Meissner, K.; Jedlitschky, G.; Herda, L. R.; Reinthaler, M.; Rohde, M.; Hoffmann, W.; Kühl, U.; Schultheiss, H.-P.; Völker, U.; Felix, S. B.; Klingel, K.; Kandolf, R.; Kroemer, H. K. Selective regulation of cardiac organic cation transporter novel type 2

(OCTN2) in dilated cardiomyopathy. *Am. J. Pathol.* **2011**, *178*, 2547−2559.

(47) Bayer, M.; Kuçi, Z.; Schömig, E.; Gründemann, D.; Dittmann, H.; Handgretinger, R.; Bruchelt, G. Uptake of mIBG and catecholamines in noradrenaline- and organic cation transporter-expressing cells: potential use of corticosterone for a preferred uptake in neuroblastoma- and pheochromocytoma cells. *Nucl. Med. Biol.* **2009**, *36*, 287−294.

(48) Chen, X.; Kudo, T.; Lapa, C.; Buck, A.; Higuchi, T. Recent advances in radiotracers targeting norepinephrine transporter: structural development and radiolabeling improvements. *J. Neural Transm.* **2020**, *127*, 851−873.

(49) Jensen, O.; Rafehi, M.; Tzvetkov, M. V.; Brockmöller, J. Stereoselective cell uptake of adrenergic agonists and antagonists by organic cation transporters. *Biochem. Pharmacol.* **2020**, *171*, 113731.

(50) Koepsell, H. Multiple binding sites in organic cation transporters require sophisticated procedures to identify interactions of novel drugs. *Biol. Chem.* **2019**, *400*, 195−207.

(51) Kimura, N.; Masuda, S.; Katsura, T.; Inui, K.-i. Transport of guanidine compounds by human organic cation transporters, hOCT1 and hOCT2. *Biochem. Pharmacol.* **2009**, *77*, 1429−1436.

(52) Balbisi, E. A. Frovatriptan: a review of pharmacology, pharmacokinetics and clinical potential in the treatment of menstrual migraine. *Ther. Clin. Risk Manage.* **2006**, *2*, 303−308.

(53) Buchan, P.; Keywood, C.; Wade, A.; Ward, C. Clinical pharmacokinetics of frovatriptan. *Headache* **2002**, *42*, S54−S62.

(54) Hanyok, J. J. Clinical pharmacokinetics of sotalol. *Am. J. Cardiol.* **1993**, *72*, A19−A26.

(55) Dixon, C. M.; Saynor, D. A.; Andrew, P. D.; Oxford, J.; Bradbury, A.; Tarbit, M. H. Disposition of sumatriptan in laboratory animals and humans. *Drug Metab. Dispos.* **1993**, *21*, 761−769.

(56) Wang, D.-S.; Jonker, J. W.; Kato, Y.; Kusuhara, H.; Schinkel, A. H.; Sugiyama, Y. Involvement of organic cation transporter 1 in hepatic and intestinal distribution of metformin. *J. Pharmacol. Exp. Ther.* **2002**, *302*, 510−515.

(57) Puozzo, C.; Leonard, B. E. Pharmacokinetics of milnacipran in comparison with other antidepressants. *Int. Clin. Psychopharmacol.* **1996**, *11*, 15−28.

(58) Haroldsen, P. E.; Sisic, Z.; Datt, J.; Musson, D. G.; Ingenito, G. Acetylator status impacts amifampridine phosphate (firdapse) pharmacokinetics and exposure to a greater extent than renal function. *Clin. Ther.* **2017**, *39*, 1360−1370.

(59) Sterling, T.; Irwin, J. J. ZINC 15—ligand discovery for everyone. *J. Chem. Inf. Model.* **2015**, *55*, 2324−2337.

(60) Landrum, G. RDKit: open-source cheminformatics software. https://www.rdkit.org/ (accessed Feb 1, 2021).

(61) Gobbi, A.; Poppinger, D. Genetic optimization of combinatorial libraries. *Biotechnol. Bioeng.* **1998**, *61*, 47−54.

(62) McKinney, W. Data structures for statistical computing in python. *Proceedings of the 9th Python in Science Conference*, Austin, TX, USA, 2010; Vol. *445*, pp 51−56.

(63) Pedregosa, F.; Varoquaux, G.; Gramfort, A.; Michel, V.; Thirion, B.; Grisel, O.; Blondel, M.; Prettenhofer, P.; Weiss, R.; Dubourg, V.; Vanderplas, J.; Passos, A.; Cournapeau, D.; Brucher, M.; Perrot, M.; Duchesnay, E. Scikit-learn: machine learning in python. *J. Mach. Learn. Res.* **2011**, *12*, 2825−2830.

(64) Chen, T.; Guestrin, C. *XGBoost: A Scalable Tree Boosting System*; ACM: New York, NY, USA, 2016.

(65) Jensen, O.; Matthaei, J.; Blome, F.; Schwab, M.; Tzvetkov, M. V.; Brockmöller, J. Variability and heritability of thiamine pharmacokinetics with focus on OCT1 effects on membrane transport and pharmacokinetics in humans. *Clin. Pharmacol. Ther.* **2020**, *107*, 628−638.

(66) Baell, J. B.; Holloway, G. A. New substructure filters for removal of pan assay interference compounds (PAINS) from screening libraries and for their exclusion in bioassays. *J. Med. Chem.* **2010**, *53*, 2719−2740.

Identification of novel high-affinity substrates of OCT1 using machine learning-guided virtual screening and experimental validation

Ole Jensen, Jürgen Brockmöller, and Christof Dücker*

Institute of Clinical Pharmacology, University Medical Center Göttingen, D-37075 Göttingen, Germany

Supporting Information

Table of Contents

Figure S1

A

Ratio and Cl_{int} of substrates with cutoffs indicated

y-axis: Ratio [uptake OCT1/uptake pcDNA5] (90, 80, 50, 40, 30, 20, 10)

x-axis: Cl_{int} [mL × g protein^{-1} × min^{-1}] (0, 10, 20, 30, 40, 50, 90, 120, 130)

B

Fourfold table of Figure S1A

y-axis: Ratio [uptake OCT1/uptake pcDNA5] (90, 80, 60, 50, 40, 30, 20, 10)

x-axis: Cl_{int} [mL × g protein^{-1} × min^{-1}] (0, 1, 2, 3, 5, 50, 100, 130)

C

Fourfold table of substances assigned by ratio and Cl_{int}

	clearance-based non-substrate	clearance-based substrate
ratio-based substrate	terbutalin, thiamine	acebutolol, atenolol, cycloguanil, dobutamine, etilefrine, fenoterol, formoterol, metaproterenol, morphine, pirbuterol, salbutamol, serotonin, synephrine, methylnaltrexone, norfentanyl, noroxycodone, phenylephrine, octopamine, amifampridine, N-ethyl-lidocaine, mepenzolate, hordenine
ratio-based non-substrate	betaine, bisoprolol, caffeine, choline, clenbuterol, cocaine, esmolol, methylamphetamine, paraxanthine, reproterol, theophylline, tolterodine, urapidil, valine, hydromorphone, mirabegron, midodrine	adrenaline, diethyltryptamine, dimethyltryptamine, amitriptyline

D

Performance of the final model

y-axis: True Positive Rate (0.0, 0.2, 0.4, 0.6, 0.8, 1.0)

x-axis: False Positive Rate (0.0, 0.2, 0.4, 0.6, 0.8, 1.0)

AUC = 0.88

random performance = 0.5

E

Hyperparameters and model performance

Model parameters	Value
Estimators	1000
Learning rate	0.01
Subsample	0.7
Max. depth	1
Feature sample per tree	0.5
AUC training set	0.96
AUC holdout validation set	0.88
AUC training set (in repeated 5-fold crossvalidation)	0.95 – 0.98 (median 0.96)
AUC test set (in repeated 5-fold crossvalidation)	0.76 – 0.98 (median 0.87)

F

Ranking of predictors (reduced model)

16822phore
18339phore
13217phore
13233phore
33680phore
18272phore
Strongest acidic pKa
16684phore
LogD
Chi1
Ipc
Chi4n
65phore
16973phore
119morgan
18383phore
MolMR
HeavyAtomCount
Strongest basic pKa
182phore
Chi3n
NumHDonors
SlogP_VSA2
LabuteASA
Chi2n
VSA_EState4
Chi0
28603phore
Kappa1
MaxEStateIndex
MaxAbsEStateIndex
MolWt
chargeatph7_4

Legend: (A) Plot of ratio (uptake in OCT1 overexpressing cells divided by uptake in mock-transfected cells) against Cl_{int}, with lines indicating cutoffs at a clearance of 5 ml × g protein^{-1} × min^{-1} and a ratio of 3. **(B)** Plot of scatters from Figure S1A as detailed view highlighting the cutoff and **(C)** providing the compound names. Green squares indicating substrates and non-substrates congruently assigned by ratio <u>and</u> Cl_{int}, red squares indicate non-congruent classification. **(D)** Performance of the final model as quantified by area under the curve (AUC) for the holdout validation set. **(E)** Model parameters and performance, as well as **(F)** predictors of the reduced model in descending order of importance. Phores and fingerprints enumeration according to RDKit assignment.

Figure S2

Jensen, O, Brockmöller J, Dücker C: Identification of novel and high-affinity substrates of OCT1 using machine learning-guided virtual screening and experimental validation, Figure S2

Page S3

Clustering by fingerprint similarity

Dendrogram labels (top to bottom):
debrisoquine, 4-OH-debrisoquine, substance 1, substance 2, meptazinol, norlevorphanol, morphine, noroxycodone, methylnaltrexone, thiamine, dimethylphenylpiperazinium, famotidine, cimetidine, ranitidine, nizatidine, amifampridine, cycloguanil, amiloride, substance 3, proguanil, guanfacine, phenformin, m-iodobenzylguanidine, frovatriptan, naratriptan, MPP, amitriptyline, oxyphenonium, fenpiverinium, glycopyrrolate, mepenzolate, clidinium, trospium, tiotropium, ipratropium, methylscopolamine, butylscopolamine, norfentanyl, milnacipran, tetraethylammonium, benzyltriethylammonium, N-ethyl-lidocaine, denatonium, procainamide, sematilide, sotalol, procaterol, zolmitriptan, rizatriptan, sumatriptan, dimethyltryptamine, diethyltryptamine, prenalterol, serotonin, ractopamine, ritodrine, phenylephrine, norphenylephrine, octopamine, edrophonium, pirbuterol, metaproterenol, fenoterol, terbutalin, salbutamol, etilefrine, synephrine, adrenaline, hordenine, dobutamine, formoterol, xamoterol, atenolol, acebutolol, substance 4, ZINC96932953, substance 5, substance 6, substance 7, substance 8, substance 9, substance 10, substance 11, substance 12, substance 13, substance 14, substance 15, ZINC96932958, substance 16, substance 17, ZINC000096933793, ZINC96933138, ZINC96932960, ZINC96932955, substance 18, substance 19, ZINC96932951, substance 20, substance 21, substance 22, substance 23, substance 24, substance 25, substance 26, substance 27, substance 28, substance 29, substance 30, substance 31, substance 32, substance 33, substance 34, substance 35, substance 36, substance 37, substance 38, substance 39, substance 40, substance 41, substance 42, substance 43, substance 44, substance 45, substance 46

Substrate	Structure	CI$_{int}$	Ratio
debrisoquin		7.1	-
4-hydroxydebrisoquine		21.2	-
substance 1		-	12.6
substance 2		-	3.7
meptazinol		-	3.2
norlevorphanol		-	17.4
morphine		8.5	4.3
noroxycodone		-	3.6
methylnaltrexone		-	85.9
thiamine		2.7	11.6
dimethylphenylpiperazinium		47.2	38.9
famotidine		87.4	34.2
cimetidine		-	4.0
ranitidine		16.5	18.1
nizatidine		-	3.1
amifampridine		18.8	6.8
cycloguanil		73.9	24.5
amiloride		-	75.7
substance 3		-	20.6
proguanil		120.3	-
guanfacine		137.6	4.3
phenformin		-	39.3
m-iodobenzylguanidine		316.5	10.1
frovatriptan		50.3	33.1
naratriptan		-	54.4
MPP		40.4	-
amitriptyline		23.9	1.2
oxyphenonium		-	25.2
fenpiverinium		113.5	30.9
glycopyrrolate		-	59.1
mepenzolate		89.6	43.0
clidinium		-	56.5
trospium		75.6	-
tiotropium		-	65.5
ipratropium		34.3	41.9
methylscopolamine		51.6	39.2
butylscopolamine		31.8	-
norfentanyl		-	7.2
milnacipran		150.6	6.3

Substrate	Structure	CI$_{int}$	Ratio
tetraethylammonium		5.5	
benzyltriethylammonium		62.8	67.5
N-ethyl-lidocaine		53.0	48.4
denatonium		71.4	21.6
procainamide		-	2.5
sematilide		3.3	3.5
sotalol		14.1	6.5
procaterol		-	10.7
zolmitriptan		-	10.0
rizatriptan		-	5.3
sumatriptan		26.7	-
dimethyltryptamine		13.9	1.5
diethyltryptamine		8.2	1.6
prenalterol		12.4	5.3
serotonin		23.8	-
ractopamine		111.2	7.1
ritodrine		103.5	7.6
phenylephrine		17.3	10.6
norphenylephrine		4.6	2.1
octopamine		9.1	-
edrophonium		99.5	42.6
pirbuterol		42.8	80.9
metaproterenol		16.0	14.3
fenoterol		127.1	13.9
terbutalin		1.6	6.6
salbutamol		9.2	9.4
etilefrine		6.0	5.6
synephrine		19.2	21
adrenaline		6.8	1.0
hordenine		6.0	3.0
dobutamine		5.2	14.7
formoterol		37.3	3.6
xamoterol		-	42.7
atenolol		7.2	5.6
acebutolol		9.2	5.2

Substrate	Structure	CI$_{int}$	Ratio
substance 4		-	10.7
ZINC96932953		-	12.7
substance 5		-	13.9
substance 6		-	6.6
substance 7		-	7.1
substance 8		-	21.5
substance 9		-	11.3
substance 10		-	4.6
substance 11		-	16.7
substance 12		-	5.3
substance 13		-	8.0
substance 14		-	35.4
substance 15		-	3.0
ZINC96932958		-	38.6
substance 16		-	10.0
substance 17		-	9.1
ZINC000096933793		-	68.0
ZINC96933138		-	73.1
ZINC96932960		-	11.4
ZINC96932955		-	25.9
substance 18		-	17.0
substance 19		-	12.5
ZINC96932951		-	52.7
substance 20		-	5.2
substance 21		-	2.5
substance 22		-	4.5
substance 23		-	8.6
substance 24		-	3.4

Substrate	Structure	CI$_{int}$	Ratio
substance 25		-	69.1
substance 26		-	11.3
substance 27		-	13.9
substance 28		-	6.8
substance 29		-	2.7
substance 30		-	2.9
substance 31		-	23.5
substance 32		-	5.3
substance 33		-	5.1
substance 34		-	3.6
substance 35		-	14.6
substance 36		-	4.5
substance 37		-	7.2
substance 38		-	6.5
substance 39		-	8.4
substance 40		-	3.4
substance 41		-	6.5
substance 42		-	16.1
substance 43		-	3.0
substance 44		-	6.6
substance 45		-	13.4
substance 46		-	6.7

⭐ - substrates tested in this publication

Legend: Wallpaper of substrates with a ratio ≥ 3 or CI$_{int}$ ≥ 5 clustered based on Tanimoto similarity of Morgan fingerprints (radius = 2, 2048 bits) using SciPy hierarchical clustering, showing molecular structures with the respective ratio and CI$_{int}$ values.
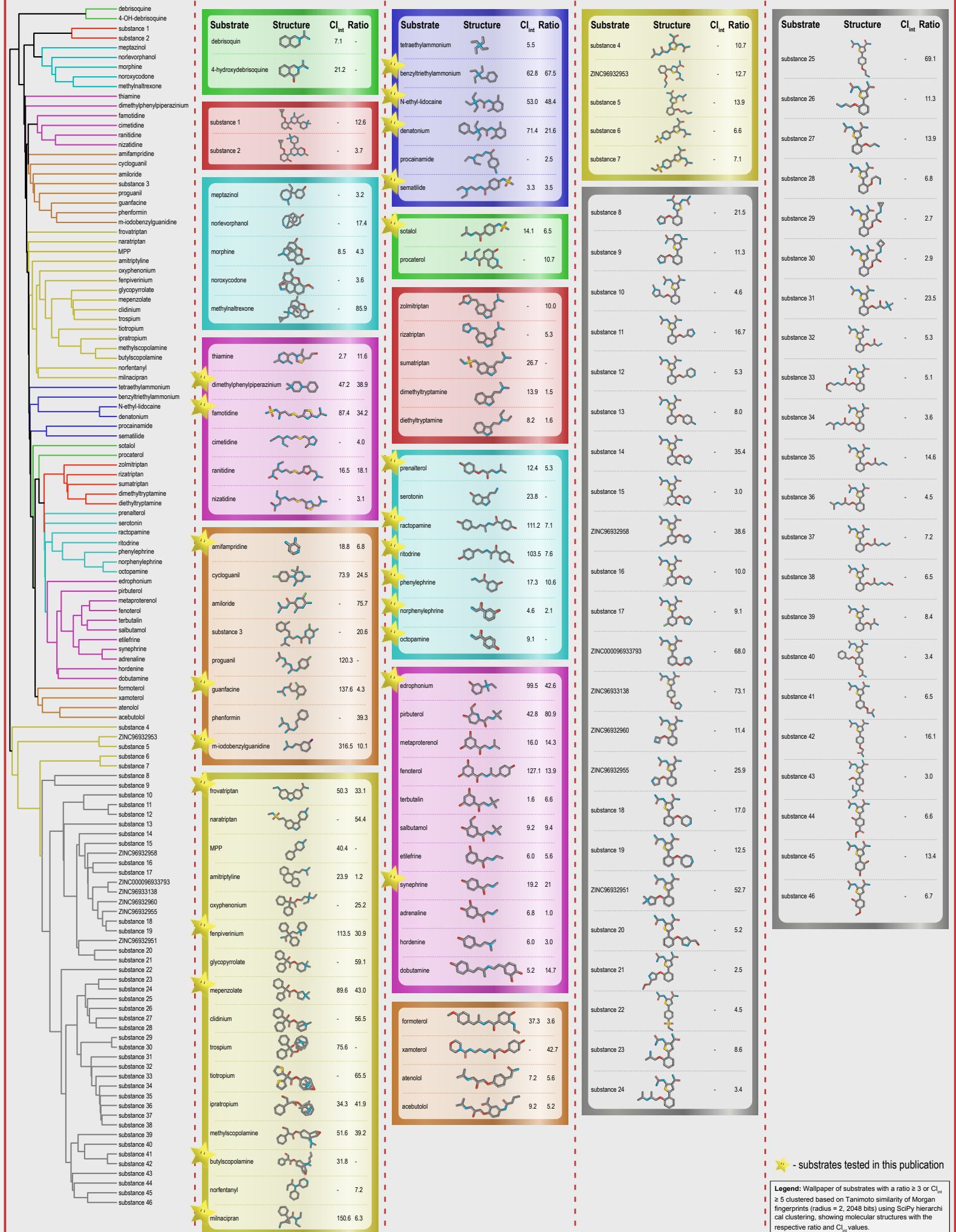
Table S1: Mass spectrometry detection parameters

Substance	RT (min)	Mass Q1 (Da)	Mass Q3 (Da)	DP (V)	CE (V)	CXP (V)	Internal standard
Dobutamine	4.0	302.2	137.0 (106.9)	66	30 (37)	10 (6)	desvenlafaxine
Milnacipran	4.5	247.2	230.2 (100.1)	51	27 (38)	8 (14)	metoclopramide
Amifampridine	2.9	113.1	69.1 (66.1)	66	27 (44)	12 (12)	choline-d9
Octopamine	2.9	154.1	136.0 (91.1)	36	11 (29)	8 (16)	choline-d9
Phenylephrine	3.9	168.2	91.0 (77.0)	41	30 (56)	11 (4)	choline-d9
N-Ethyl-lidocaine	4.5	264.2	86.0 (58.0)	81	36 (64)	16 (11)	nadolol
Denatonium	3.8	326.5	91.0 (86.1)	71	51 (29)	16 (16)	cortisone
DPP	5.3	192.3	72.1 (58.0)	96	34 (54)	13 (10)	ranitidine-d6
Frovatriptan	4.9	244.3	170.1 (213.0)	56	34 (19)	10 (14)	ranitidine-d6
Benzyltriethylammonium	5.7	193.3	92.1 (101.0)	56	28 (23)	17 (18)	ranitidine-d6
Sematilide	5.4	314.4	240.9 (162.1)	79	27 (39)	16 (10)	ranitidine-d6
Prenalterol	4.3	226.3	149.1 (56.0)	81	23 (39)	10 (10)	ranitidine-d6
Sotalol	4.0	273.4	255.1 (133.1)	61	17 (37)	16 (8)	ranitidine-d6
Famotidine	4.4	338.5	189.0 (155.0)	54	27 (43)	12 (10)	ranitidine-d6
Ritodrine	3.6	288.4	270.1 (121.1)	59	19 (31)	18 (8)	tulobuterol
Ractopamine	4.1	302.4	107.0 (91.0)	56	43 (58)	6 (16)	tulobuterol
Methylscopolamine	3.5	319.4	152.0 (45.1)	109	37 (49)	10 (8)	tulobuterol
mIBG	5.7	276.1	217.0 (90.0)	76	29 (54)	14 (16)	tulobuterol
Fenpiverinium	6.1	338.5	239.1 (77.0)	69	24 (111)	16 (14)	tulobuterol
Labetalol	8.2	329.4	311.2 (162.0)	71	19 (35)	15 (10)	tulobuterol
Norphenylephrine	3.3	154.2	136.0 (91.1)	39	11 (29)	8 (16)	buformin
Edrophonium	4.7	167.2	137.0 (139.0)	76	37 (23)	8 (9)	buformin
Tulobuterol	4.5	228.1	153.9 (119.1)	60	23 (41)	10 (8)	-
Ranitidine-d6	4.1	321.2	176.0 (130.1)	65	25 (35)	15 (15)	-
Cortisone	8.1	361.2	163.0 (121.2)	71	33 (43)	12 (9)	-
Desvenlafaxine	4.1	264.3	58.1 (107.2)	60	47 (50)	8 (8)	-
Metoclopramide	3.5	300.2	227.0 (184.0)	65	25 (42)	14 (12)	-
Choline-d9	2.9	113.1	69.1 (66.1)	66	27 (44)	12 (12)	-
Nadolol	3.5	310.1	254.1 (201.0)	66	23 (31)	16 (16)	-
Buformin	3.8	158.0	60.0 (47.0)	40	35 (66)	10 (8)	-

RT - retention time; DP - declustering potential; CE - collision energy; CXP - collision cell exit potential

3.3 Publication 3

Stereoselective cell uptake of adrenergic agonists and antagonists

by organic cation transporters

Ole Jensen[a], Muhammad Rafehi[a], Mladen V. Tzvetkov[a,b], Jürgen Brockmöller[a]

[a] Institute of Clinical Pharmacology, University Medical Center Göttingen, Georg-August University, D-37075 Göttingen, Germany

[b] Center of Drug Absorption and Transport (C_DAT), Department of Pharmacology, University Medical Center, Ernst-Moritz-Arndt-University, D-17487 Greifswald, Germany

Stereoselective cell uptake of adrenergic agonists and antagonists by organic cation transporters

Ole Jensen[a,*], Muhammad Rafehi[a], Mladen V. Tzvetkov[a,b], Jürgen Brockmöller[a]

[a] *Institute of Clinical Pharmacology, University Medical Center Göttingen, Georg-August University, D-37075 Göttingen, Germany*
[b] *Center of Drug Absorption and Transport (C_DAT), Department of Pharmacology, University Medical Center, Ernst-Moritz-Arndt-University, D-17487 Greifswald, Germany*

A R T I C L E I N F O

Keywords:
Beta-adrenergic drugs
Enantiomers
Organic cation transporters
SLC22A1
Solute carriers

A B S T R A C T

Stereoselectivity is well described for receptor binding and enzyme catalysis, but so far has only been scarcely investigated in carrier-mediated membrane transport. We thus studied transport kinetics of racemic (anti) adrenergic drugs by the organic cation transporters OCT1 (wild-type and allelic variants), OCT2, OCT3, MATE1, and MATE2-K with a focus on stereospecificity.

OCT1 showed stereoselective uptake with up to 2-fold higher v_{max} over their corresponding counterpart enantiomers for (R,R)-fenoterol, (R,R)-formoterol, (S)-salbutamol, (S)-acebutolol, and (S)-atenolol. Orciprenaline and etilefrine were also transported stereoselectively. The K_m was 2.1-fold and 1.5-fold lower for the (S,S)-enantiomers of fenoterol and formoterol, while no significant difference in K_m was seen for the other aforementioned drugs. Common OCT1 variants showed similar enantiopreference to wild-type OCT1, with a few notable exceptions (e.g. a switch in enantiospecificity for fenoterol in OCT1*2 compared to the wild-type). Other cation transporters showed strong differences to OCT1 in stereoselectivity and transport activity: The closely related OCT2 displayed a 20-fold higher v_{max} for (S,S)-fenoterol compared to (R,R)-fenoterol and OCT2 and OCT3 showed 3.5-fold and 4.6-fold higher v_{max} for the pharmacologically active (R)-salbutamol over (S)-salbutamol. MATE1 and MATE2-K generally mediated transport with a higher capacity but lower affinity compared to OCT1, with moderate stereoselectivity.

Our kinetic studies showed that significant stereoselectivity exists in solute carrier-mediated membrane transport of racemic beta-adrenergic drugs with surprising, and in some instances even opposing, preferences between closely related organic cation transporters. This may be relevant for drug therapy, given the strong involvement of these transporters in hepatic and renal drug elimination.

1. Introduction

While receptor binding and enzymatic catalysis are widely known to often be highly stereospecific processes, stereoselectivity in membrane transport by polyspecific solute carriers (SLC) is not so evident and often not considered in research. Given the very broad substrate spectrum of many of these transporters, it may predominantly be the physicochemical properties of a substance that determine which transporter is relevant [1]. In this study, we focus on stereospecificity in organic cation transport of adrenergic and antiadrenergic drugs, since many of these have chiral centres and are often administered as racemic mixtures.

The importance of stereospecificity in pharmacodynamics has already been thoroughly studied for several (anti)adrenergic drugs. For instance, the prototypic adrenergic substance (R)-adrenaline is over 20-fold more potent than (S)-adrenaline. Also, the spasmolytic actions of salbutamol (albuterol) and formoterol were attributed solely to (R)-salbutamol and (R,R)-formoterol, while the counterpart enantiomers showed significantly less agonist activity at the beta$_2$-adrenergic receptor [2,3]. Stereoselectivity has also been extensively studied with respect to drug metabolism [4], and it was strongly observed in the sulfation of some beta-adrenergic drugs [5]. Before sulfate conjugation or other metabolic reactions can take place in enterocytes, hepatocytes, or renal tubular cells, these relatively hydrophilic drugs must first enter the cell. Organic cation transporters (OCTs) are predominantly responsible for the transport of more hydrophilic cationic substances in the liver and kidneys for metabolism and excretion [6]. Transport via OCT1 and OCT3 may be particularly relevant in the context of hepatic

---
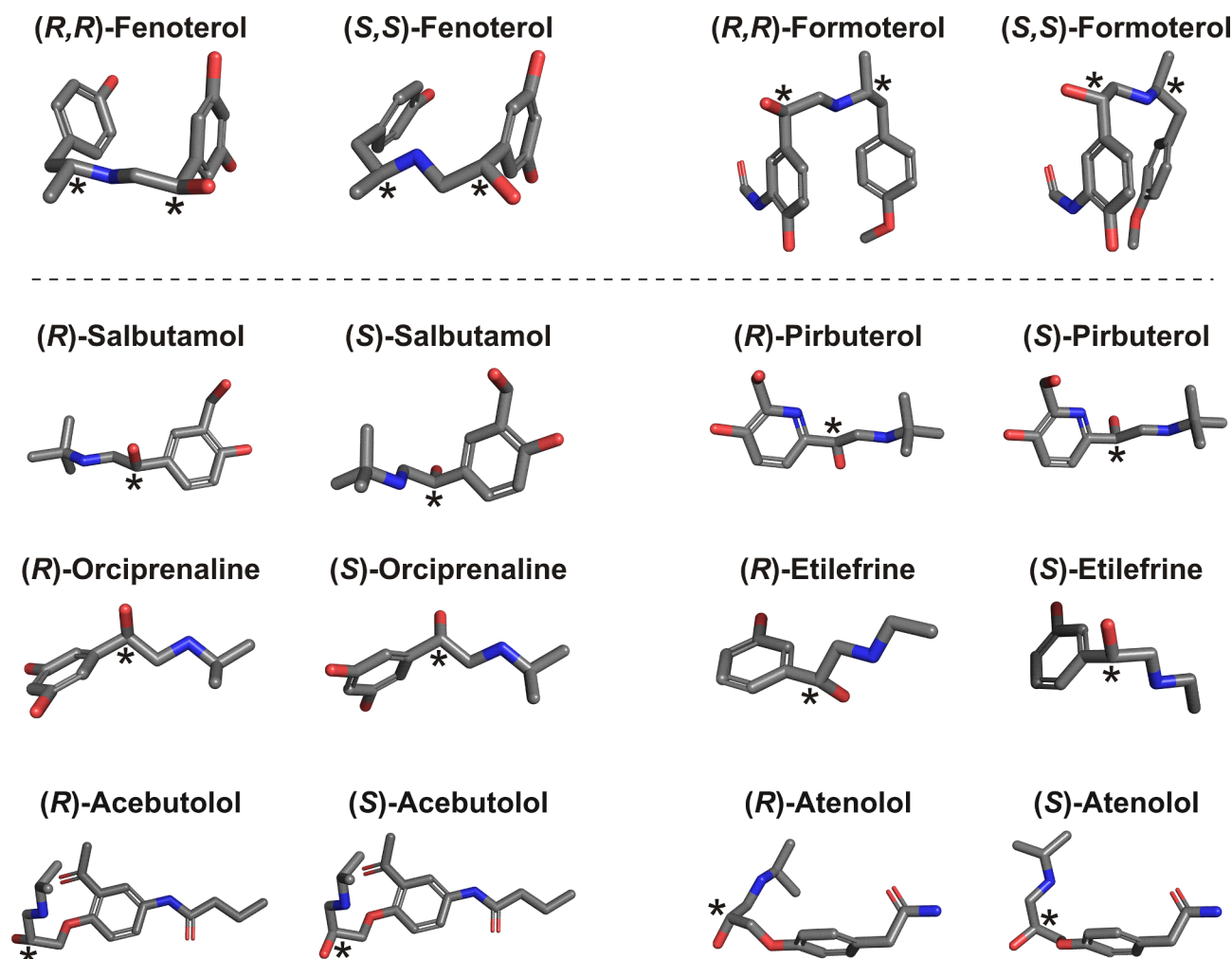
Fig. 1. Beta-adrenergic receptor agonists and antagonists investigated for stereoselective transport by OCTs and transporters of the MATE-family. These were selected for physicochemical properties ($pK_a > 8.0$ and $logD_{pH7.4} < 1$) that renders them likely transporter substrates. Chiral centres are indicated by an asterisk.

metabolism [7], whereas OCT2 and MATE2-K are often involved in renal elimination.

Only few studies investigating stereoselectivity in drug membrane transport have been published so far [8]. For example, for the beta₁-adrenergic receptor partial agonist xamoterol, the (S)-enantiomer was found to be 2-fold preferentially transported by OCT1 [1]. With regard to other substrates of OCT1, literature data on stereoselectivity is scarce. Here, we report a comprehensive characterisation of the extent of stereospecificity in the transport of different beta-adrenergic receptor agonists and antagonists (Fig. 1) by wild-type and genetic variants of OCT1 as well as by the related transporters OCT2, OCT3, MATE1, and MATE2-K.

2. Materials and methods

2.1. In vitro uptake experiments

Transport experiments were performed with HEK293 cells stably transfected to overexpress OCT1*1 (wild-type), OCT1*2 (M420del), OCT1*3 (R61C), OCT1*4 (G401S), OCT1*5 (M420del/G465R), OCT1*6 (C88R/M420del), OCT1*7 (S14F), OCT1*8 (R488M), OCT2, OCT3, MATE1, or MATE2-K. All cell lines were generated using the Flp-In system (Thermo Fisher Scientific, Darmstadt, Germany) as previously described [7,9,10], except for the OCT3-overexpressing HEK293 cells that were a kind gift from Drs. Koepsell and Gorbulev (University of Würzburg, Germany). Cells were kept in culture for no more than 30

passages. Tested drugs were purchased as racemates from Sigma-Aldrich (Darmstadt, Germany; catalogue numbers: fenoterol, F1016; formoterol, F9552; salbutamol, S8250; orciprenaline, M2398; acebutolol, A3669; atenolol, A7655) or Santa Cruz Biotechnology (Heidelberg, Germany; pirbuterol, sc-476485; etilefrine, sc294579A). Internal standards were purchased from Sigma-Aldrich (desvenlafaxine, D-2069; metoprolol, 80337), Santa Cruz Biotechnology (tulobuterol, sc-213131; (S)-propranolol, sc-294579A), or Biozol Diagnostica (Eching, Germany; fenoterol-d6, TRC-F248852).

Cells were seeded on 12-well plates coated with poly-D-lysine 48 h before the transport experiments and incubated at 37 °C, 95% relative humidity, and 5% CO_2. Cell lines overexpressing MATE1 and MATE2-K were incubated with 30 mM NH_4Cl in HBSS+ (10 mM HEPES in HBSS, pH 7.4; Thermo Fisher Scientific, Darmstadt, Germany) for 30 min prior to the assay to invert the direction of transport. All cell lines were washed with 37 °C HBSS+ and subsequently incubated with the prewarmed substrate in HBSS+ for one (MATE1, MATE2-K) or two (OCTs) minutes at 37 °C. The reaction was stopped by adding ice-cold HBSS+, and the cells were washed twice with ice-cold HBSS+ before lysis with 80% acetonitrile (LGC Standards, Wesel, Germany). Subsequently, the intracellular substrate accumulation was determined using LC-MS/MS.

2.2. Stereoselective concentration analyses

Cell uptake was quantified by stereoselective HPLC and tandem mass spectrometric detection using a Shimadzu Nexera™ HPLC system

Table 1

HPLC settings for the separation of (anti)adrenergic drug enantiomers.

Drug	Column[a]	Mobile phase[b]	Flow rate [µl × min^{-1}]	Retention time A [min]	Retention time B [min]
Fenoterol	Chiral-CBH	10 mM NH$_4$Ac, pH 5.8, 5% IPA	500	5.3 (*R,R*)	6.1 (*S,S*)
Formoterol	Chiral-CBH	10 mM NH$_4$Ac, 10% ACN	300	15.4 (*R,R*)	17.0 (*S,S*)
Salbutamol	Chirobiotic T	20 mM NH$_4$Ac, pH 4.5, 96% MeOH	1000	6.8 (*R*)	7.7 (*S*)
Pirbuterol	Chiral-CBH	10 mM NH$_4$Ac, pH 5.8, 5% IPA	300	3.3 (P1)	3.5 (P2)
Orciprenaline	Chirobiotic T	20 mM NH$_4$Ac, pH 4.5, 93% MeOH	500	9.2 (P1)	10.7 (P2)
Etilefrine	Chirobiotic T	20 mM NH$_4$Ac, pH 4.5, 93% MeOH	500	10.8 (P1)	11.6 (P2)
Acebutolol	Chiral-CBH	10 mM NH$_4$Ac, pH 5.8, 10% ACN	500	2.9 (*R*)	4.8 (*S*)
Atenolol	Chiral-CBH	10 mM NH$_4$Ac, pH 5.8, 5% IPA	300	3.8 (*R*)	5.1 (*S*)

[a] CBH, cellobiohydrolase

[b] ACN, acetonitrile; IPA, isopropanol; MeOH, methanol; NH$_4$Ac, ammonium acetate

Table 2

Chemical properties pK$_a$ and logD$_{pH7.4}$ and relevant data for mass-spectrometric detection of the substrates and analytical internal standards.

Drug	pK$_a$	logD$_{pH7.4}$	Q1 Mass[a] [Da]	Q3 Mass[b] [Da]	DP[c] [V]	CE[d] [V]	CXP[e] [V]
Substrates							
Fenoterol[1]	9.63	0.33	304.1 (304.1)	107.1 (135.2)	70 (70)	44 (24)	12 (12)
Formoterol[1]	9.81	0.04	345.2 (345.2)	149.1 (121.1)	70 (70)	28 (42)	15 (15)
Salbutamol[2]	9.40	−1.32	240.2 (240.2)	148.2 (222.2)	60 (60)	24 (24)	15 (15)
Pirbuterol[1]	9.59	−1.78	241.3 (241.3)	149.1 (167.2)	65 (65)	30 (24)	15 (15)
Orciprenaline[3]	9.70	−0.94	212.1 (212.1)	152.0 (107.0)	56 (56)	23 (39)	10 (8)
Etilefrine[4]	9.73	−1.07	182.1 (182.1)	164.0 (91.0)	51 (51)	17 (37)	10 (6)
Acebutolol[2]	9.65	−0.68	337.2 (337.2)	116.0 (98.1)	91 (91)	31 (29)	8 (8)
Atenolol[5]	9.67	−1.80	267.2 (267.2)	145.2 (74.0)	130 (1 3 0)	38 (35)	10 (14)
Internal standards							
Fenoterol-d6	–	–	310.3 (310.3)	109.1 (141.0)	70 (70)	40 (26)	12 (12)
Desvenlafaxine	–	–	264.3 (264.3)	58.1 (107.2)	60 (60)	47 (50)	8 (8)
Metoprolol	–	–	268.2 (268.2)	116.1 (74.0)	86 (86)	27 (35)	8 (14)
(*S*)-Propranolol	–	–	260.2	116.2	85	30	10
Tulobuterol	–	–	228.1 (228.1)	153.9 (119.1)	60 (60)	23 (41)	10 (8)

[a] Q1, first quadrupole (qualifiers below in parentheses);

[b] Q3, third quadrupole (qualifiers in parentheses);

[c] DP, declustering potential;

[d] CE, collision energy;

[e] CXP, collision cell exit potential;

[1] quantified with internal standard fenoterol-d6;

[2] quantified with internal standard desvenlafaxine;

[3] quantified with internal standard metoprolol;

[4] quantified with internal standard (*S*)-propranolol;

[5] quantified with internal standard tulobuterol

that included a LC-30AD pump, a SIL-30AC autosampler, a CTO-20AC column oven, and a CBM-20A controller (Shimadzu, Kyoto, Japan). A Chiral-CBH column (100 × 3 mm, 4.6 µm; Sigma-Aldrich, Darmstadt, Germany) with a corresponding 10 × 3 mm guard column or an Astec Chirobiotic T (15 cm × 2.1 mm, 5 µm; Sigma-Aldrich, Darmstadt, Germany) column with a corresponding 2 cm × 1 mm guard column was used (Table 1). Oven temperature was 25 °C for all methods, and separation was achieved by isocratic elution. The order of enantiomer elution was inferred from available literature, where the investigated substrates had been separated by HPLC using identical columns and similar mobile phases [11–15]. However, no reference literature was found for etilefrine, orciprenaline, and pirbuterol. In these cases, the enantiomers were only named by the order of elution, as the identification of the enantiomers was not the focus of this study. Tested substrates and suitable internal standards were detected using an API 4000 tandem mass spectrometer (AB SCIEX, Darmstadt, Germany) with the parameters listed in Table 2.

2.3. Calculations

The net active transport by overexpressed transporters was calculated by subtracting the uptake measured in an empty vector control cell line. The parameters K$_m$ and v$_{max}$ were estimated by regression analysis using the Michaelis-Menten equation. Means and standard

errors were calculated from individual K$_m$ and v$_{max}$ values of at least three independent experiments. The intrinsic clearance Cl$_{int}$ was calculated as the ratio of v$_{max}$ over K$_m$. The kinetic parameters v$_{max}$, K$_m$, and Cl$_{int}$ were tested for statistical significance using Student's *t*-test with an alpha-value of 0.05.

3. Results

3.1. Stereoselective OCT1-mediated cellular uptake of adrenergic drugs

First, we analysed the extent of stereoselectivity in the OCT1-mediated transport of eight clinically relevant beta-adrenergic receptor agonists and antagonists. The test compounds were selected based on their physicochemical properties (pk$_A$ > 8.0 and logD$_{pH7.4}$ < 1), because more lipophilic or acidic substances are mostly not transported by OCTs to a relevant extent.

We observed a 1.9- and 1.7-fold (calculated as the ratio of the larger over the smaller parameter) higher maximum transport velocity (v$_{max}$) for the (*R,R*)-enantiomers of fenoterol and formoterol in comparison to the corresponding (*S,S*)-enantiomers (Figs. 2, 3, Table 3). The K$_m$ values were also higher for (*R,R*)-fenoterol and (*R,R*)-formoterol. We observed a 1.1- to 1.7-fold difference in v$_{max}$ between the enantiomers of salbutamol, pirbuterol, orciprenaline (metaproterenol), etilefrine, acebutolol, and atenolol (Figs. 2, 3, Table 3). However, no notable differences
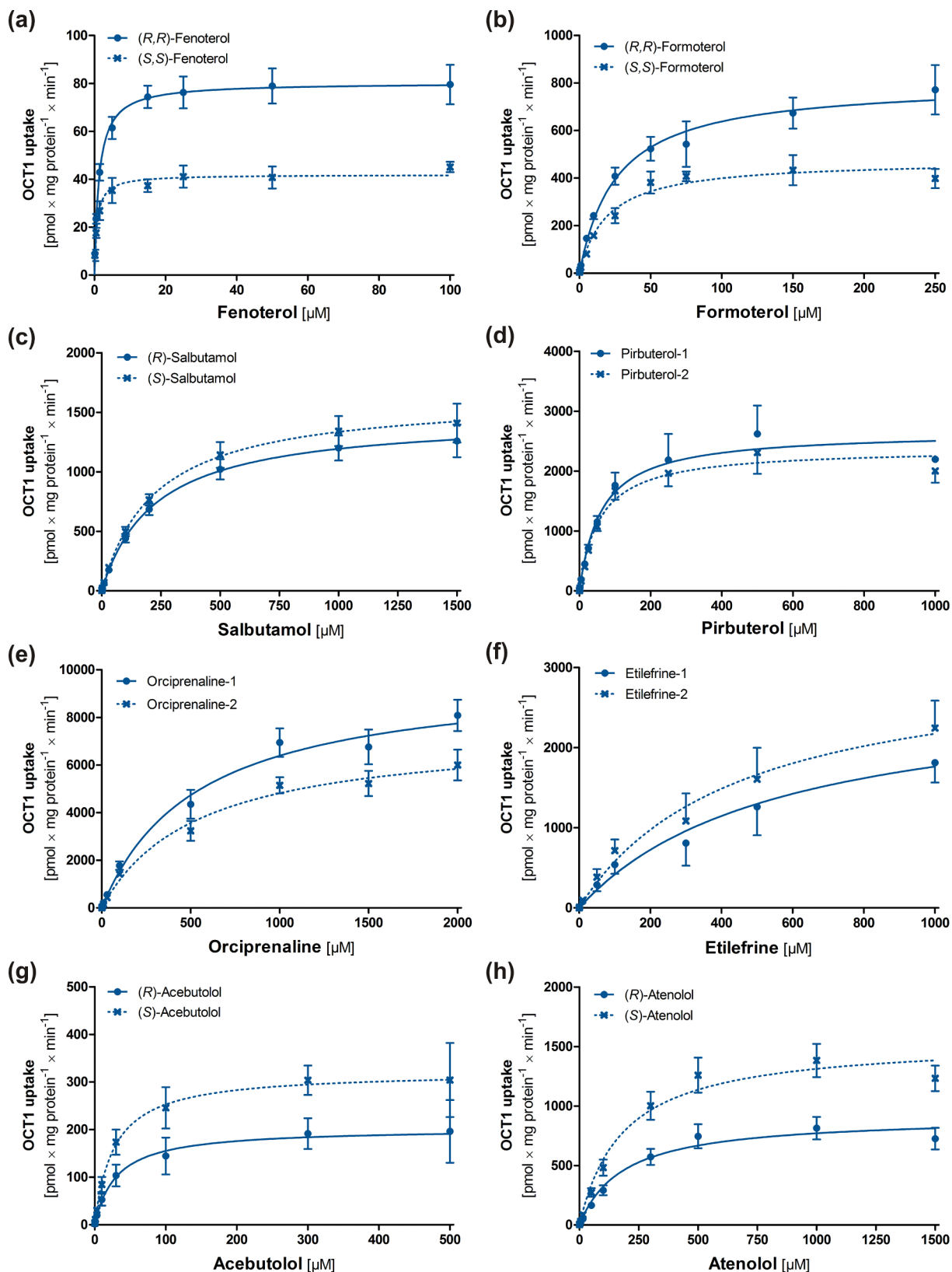
Fig. 2. Transport of (anti)adrenergic drug enantiomers by wild-type OCT1, determined using stably transfected HEK293 cells. Shown are the mean ± SEM of at least three independent experiments for each drug. Enantiomers that could not be identified were numbered according to the order of HPLC elution.

in K_m between the enantiomers of these drugs were seen. The intrinsic clearance differed 1.1- to 1.7-fold between the enantiomers of salbutamol, orciprenaline, etilefrine, acebutolol, and atenolol, whereas no significant difference was seen between the enantiomers of pirbuterol.

To summarise, remarkable differences, particularly in the maximum uptake velocity, were seen between the enantiomers of structurally related (anti)adrenergic drugs, which is notably indicative of stereospecificity in the molecular interaction between substrate and
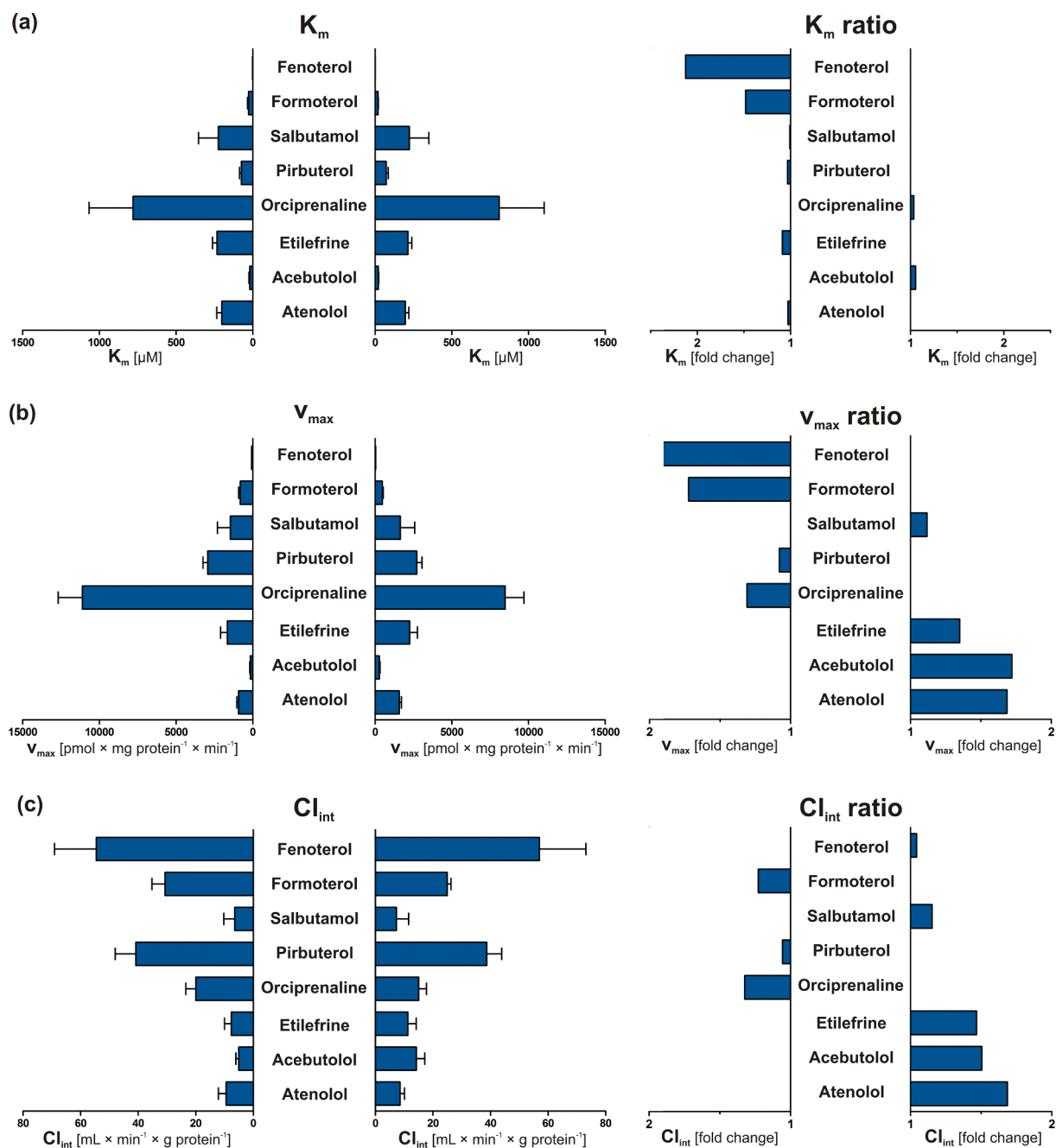
Fig. 3. Stereoselectivity in the OCT1-mediated transport of sympathomimetic and sympatholytic drugs. The ratios on the right were calculated as the quotients of the higher and the lower values.

transporter. However, general conclusions about stereoselective uptake by OCT1 cannot be deduced at present, and stereoselectivity must be determined for every substrate individually.

3.2. Differential stereoselective transport among genetic variants of OCT1

Next, we investigated possible differences in stereospecific membrane transport of a subset of (anti)adrenergic drugs with particular clinical importance, namely fenoterol, formoterol, salbutamol, and atenolol, between common naturally occurring variants of OCT1 (OCT1*2 to OCT1*8). With the exception of fenoterol uptake via OCT1*4, a reduction in the transport velocity was observed for all substrates in the variants OCT1*2, *3, *4, and *7 (Table 4). No transport activity was detected in OCT1*5 and *6 (data not shown), which are known to be non-functional [7]. In contrast, OCT1*8 showed a

transport capacity similar to wild-type (for salbutamol) or higher (for fenoterol, formoterol, and atenolol). Generally, the stereoselectivity of transport did not differ strongly between any of these common OCT1 variants, with a few notable exceptions further outlined below.

For fenoterol, the observed v_{max} but also the K_m were approximately twice as high for the pharmacologically active (R,R)-fenoterol in comparison to (S,S)-fenoterol in wild-type OCT1. Interestingly, for the worldwide most common variant OCT1*2, the enantioselectivity was completely opposite: the v_{max} was 1.6-fold higher and the K_m almost 5-fold higher for (S,S)-fenoterol. Notable is also the switch in affinity from wild-type (2.1-fold lower K_m for (S,S)-fenoterol) to OCT1*7 (3.1-fold lower K_m for (R,R)-fenoterol). There is little difference in the intrinsic clearance between the two enantiomers of fenoterol for wild-type OCT1 and all studied variants, except for OCT1*4, where it is 1.7-fold higher for (R,R)-fenoterol.

Table 3
Kinetic parameters for the transport of racemic (anti)adrenergic drugs by wild-type OCT1.

Transporter	Substrate	K_m (± SEM) [μM]	v_{max} (± SEM) [pmol × mg protein^{-1} × min^{-1}]	Cl_{int} (± SEM) [ml × min^{-1} × g protein^{-1}]	Stereoselectivity		
					K_m	v_{max}	Cl_{int}
OCT1	(R,R)-Fenoterol	1.7* (± 0.3)	81.5** (± 2.6)	54.6 (± 14.6)	2.13-fold for (R,R)	1.94-fold for (R,R)	1.04-fold for (S,S)
	(S,S)-Fenoterol	0.8* (± 0.2)	42.0** (± 3.5)	57.0 (± 16.2)			
	(R,R)-Formoterol	28.3 (± 6.2)	820.4* (± 102.8)	30.7 (± 4.5)	1.48-fold for (R,R)	1.72-fold for (R,R)	1.23-fold for (R,R)
	(S,S)-Formoterol	19.1 (± 2.0)	476.1* (± 54.5)	25.0 (± 1.3)			
	(R)-Salbutamol	224.2 (± 18.4)	1464.3* (± 157.6)	6.5** (± 3.8)	1.01-fold for (R)	1.12-fold for (S)	1.12-fold for (S)
	(S)-Salbutamol	222.5 (± 20.5)	1637.3* (± 192.6)	7.3** (± 4.2)			
	Pirbuterol-1	75.3 (± 11.4)	2942.7 (± 307.2)	40.9 (± 7.2)	1.03-fold for (1)	1.08-fold for (1)	1.06-fold for (1)
	Pirbuterol-2	72.9 (± 12.3)	2724.3 (± 337.4)	38.7 (± 5.3)			
	Orciprenaline-1	780.5 (± 285.9)	11106.3 (± 1579.8)	20.0* (± 3.5)	1.04-fold for (2)	1.31-fold for (1)	1.32-fold for (1)
	Orciprenaline-2	808.8 (± 292.6)	8482.0 (± 1224.2)	15.1* (± 2.7)			
	Etilefrine-1	232.9 (± 29.8)	1667.1** (± 432.9)	7.7* (± 2.3)	1.08-fold for (2)	1.35-fold for (2)	1.47-fold for (2)
	Etilefrine-2	214.0 (± 24.9)	2253.8** (± 506.8)	11.3* (± 2.9)			
	(R)-Acebutolol	19.9 (± 5.7)	161.5*** (± 41.9)	9.5** (± 2.7)	1.05-fold for (S)	1.72-fold for (S)	1.51-fold for (S)
	(S)-Acebutolol	21.0 (± 2.5)	277.9*** (± 45.1)	14.3** (± 2.9)			
	(R)-Atenolol	201.9 (± 33.1)	929.7*** (± 115.3)	5.1** (± 1.0)	1.03-fold for (R)	1.69-fold for (S)	1.69-fold for (S)
	(S)-Atenolol	196.4 (± 23.1)	1567.4*** (± 143.6)	8.6** (± 1.5)			

SEM, standard error of the mean; asterisks indicate statistical significance of the differences between the two enantiomers (Student's t-test; * $p < 0.05$, ** $p < 0.01$, and *** $p < 0.001$).

Table 4
Kinetic parameters for the transport of racemic (anti)adrenergic drugs by genetic variants of OCT1.

Transporter	Substrate	K_m (± SEM) [μM]	V_{max} (± SEM) [pmol × mg protein^{-1} × min^{-1}]	Cl_{int} (± SEM) [ml × min^{-1} × g protein^{-1}]	Stereoselectivity		
					K_m	v_{max}	Cl_{int}
OCT1*2	(R,R)-Fenoterol	11.4 (± 5.9)	49.6 (± 14.4)	28.9* (± 25.3)	4.85-fold for (S,S)	1.55-fold for (S,S)	1.09-fold for (R,R)
	(S,S)-Fenoterol	55.3 (± 36.8)	77.0 (± 34.0)	26.4* (± 25.0)			
	(R,R)-Formoterol	22.3* (± 5.6)	278.5 (± 107.3)	12.1 (± 1.8)	2.53-fold for (R,R)	2.51-fold for (R,R)	1.08-fold for (S,S)
	(S,S)-Formoterol	8.8* (± 5.1)	111.1 (± 61.6)	13.1 (± 0.4)			
	(R)-Salbutamol	338.2 (± 139.2)	597.6 (± 216.0)	2.2* (± 1.2)	1.30-fold for (R)	1.03-fold for (S)	1.23-fold for (S)
	(S)-Salbutamol	260.8 (± 94.6)	614.7 (± 204.0)	2.7* (± 1.6)			
	(R)-Atenolol	410.1 (± 256.6)	536.0 (± 264.3)	1.7* (± 0.4)	1.83-fold for (R)	1.28-fold for (S)	2.12-fold for (S)
	(S)-Atenolol	223.8 (± 79.8)	687.8 (± 190.6)	3.6* (± 0.8)			
OCT1*3	(R,R)-Fenoterol	no transport	no transport	no transport	–	–	–
	(S,S)-Fenoterol						
	(R,R)-Formoterol	77.8 (± 27.5)	162.7 (± 43.6)	2.2 (± 0.2)	2.29-fold for (S,S)	1.27-fold for (S,S)	1.05-fold for (R,R)
	(S,S)-Formoterol	178.5 (± 162.1)	205.9 (± 155.4)	2.1 (± 1.0)			
	(R)-Salbutamol	no transport	no transport	no transport	–	–	–
	(S)-Salbutamol						
	(R)-Atenolol	no transport	no transport	no transport	–	–	–
	(S)-Atenolol						
OCT1*4	(R,R)-Fenoterol	9.6 (± 0.8)	151.7* (± 11.8)	16.3** (± 2.1)	1.07-fold for (S,S)	1.72-fold for (R,R)	1.70-fold for (R,R)
	(S,S)-Fenoterol	10.3 (± 1.6)	88.4* (± 1.5)	9.6** (± 2.2)			
	(R,R)-Formoterol	52.8 (± 7.4)	161.4* (± 35.9)	3.0 (± 0.4)	2.07-fold for (R,R)	1.74-fold for (R,R)	1.60-fold for (S,S)
	(S,S)-Formoterol	24.5 (± 19.7)	92.6* (± 63.3)	4.8 (± 1.3)			
	(R)-Salbutamol	no transport	no transport	no transport	–	–	–
	(S)-Salbutamol						
	(R)-Atenolol	no transport	no transport	no transport	–	–	–
	(S)-Atenolol						
OCT1*7	(R,R)-Fenoterol	1.1 (± 0.5)	32.9 (± 8.0)	38.7 (± 14.9)	3.09-fold for (S,S)	1.20-fold for (R,R)	1.10-fold for (S,S)
	(S,S)-Fenoterol	3.4 (± 3.0)	27.5 (± 7.4)	42.6 (± 25.8)			
	(R,R)-Formoterol	78.6 (± 42.6)	788.7 (± 229.9)	14.3 (± 4.5)	2.00-fold for (R,R)	2.11-fold for (R,R)	1.28-fold for (R,R)
	(S,S)-Formoterol	39.3 (± 14.9)	373.8 (± 107.3)	11.2 (± 2.2)			
	(R)-Salbutamol	494.7 (± 222.4)	898.8 (± 218.3)	2.8** (± 1.6)	1.35-fold for (R)	1.01-fold for (R)	1.18-fold for (S)
	(S)-Salbutamol	365.8 (± 136.9)	888.4 (± 154.0)	3.3** (± 1.9)			
	(R)-Atenolol	148.4 (± 63.9)	296.1** (± 53.2)	2.9* (± 1.0)	1.01-fold for (R)	2.01-fold for (S)	1.66-fold for (S)
	(S)-Atenolol	146.6 (± 41.0)	596.0** (± 57.6)	4.8* (± 1.3)			
OCT1*8	(R,R)-Fenoterol	3.1* (± 0.5)	204.2* (± 32.7)	68.8 (± 15.1)	1.48-fold for (R,R)	1.95-fold for (R,R)	1.17-fold for (R,R)
	(S,S)-Fenoterol	2.1* (± 0.8)	104.7* (± 20.4)	58.9 (± 16.3)			
	(R,R)-Formoterol	44.5 (± 5.6)	1589.3** (± 188.1)	35.8* (± 1.0)	1.14-fold for (S,S)	1.45-fold for (R,R)	1.64-fold for (R,R)
	(S,S)-Formoterol	50.8 (± 3.4)	1099.0** (± 200.8)	21.8* (± 4.3)			
	(R)-Salbutamol	210.9 (± 21.9)	1424.7** (± 203.9)	6.8* (± 3.9)	1.06-fold for (S)	1.19-fold for (S)	1.12-fold for (S)
	(S)-Salbutamol	223.4 (± 13.7)	1701.3** (± 195.4)	7.6* (± 4.4)			
	(R)-Atenolol	299.3 (± 91.1)	1059.9** (± 79.0)	4.0** (± 0.8)	1.10-fold for (S)	2.05-fold for (S)	1.73-fold for (S)
	(S)-Atenolol	328.4 (± 49.7)	2177.0** (± 60.8)	6.9** (± 0.9)			

SEM, standard error of the mean; asterisks indicate statistical significance of the differences between the two enantiomers (Student's t-test; * $p < 0.05$, ** $p < 0.01$, and *** $p < 0.001$).

With regard to formoterol, allelic OCT1 variants with the exception of OCT1*3 showed, similar to wild-type OCT1, a preference for the pharmacologically active (*R,R*)-formoterol.

The uptake of salbutamol enantiomers by wild-type OCT1 and allelic variants showed only minor stereoselectivity. It was reduced in OCT1*2 and *7, and similar, or marginally higher, to the wild-type in *8. An interesting observation was the markedly different substrate affinity for OCT1*3 and *4: whereas fenoterol was transported to a significant extent by *4, transport of salbutamol and atenolol was completely absent in *3 and *4.

With atenolol, we observed a general preference for the pharmacologically active (*S*)-atenolol, both in terms of maximum transport velocity and lower K_m.

Our results indicate that stereoselectivity in transport is for the OCT1 variants in most cases relatively similar to the wild-type, but a few notable exceptions were found.

3.3. Differences in stereoselectivity between different organic cation transporters

Beside OCT1, other cation transporters may also be involved in cellular uptake and hepatic or renal elimination. We therefore studied the extent of stereoselectivity in the transport of fenoterol, formoterol, salbutamol, and atenolol by the related solute carriers OCT2, OCT3, MATE1, and MATE2-K as well (Fig. 4, Table 5).

Fenoterol transport by OCT2 revealed the most drastic differences in stereoselectivity: OCT1 showed an almost 2-fold higher v_{max} for (*R,R*)-fenoterol. In contrast, OCT2 transported (*S,S*)-fenoterol with a 20-fold higher v_{max}, while (*R,R*)-fenoterol transport was, in comparison,

negligibly low. This resulted in a 37-fold higher intrinsic clearance for the presumably inactive (*S,S*)-enantiomer. The strong difference is particularly surprising given the high (70%) protein sequence identity shared between OCT1 and OCT2. For OCT3, the maximum transport velocity for both fenoterol enantiomers was similar to that of OCT1, while the K_m was about 10-fold higher. The antiporters MATE1 and MATE2-K transported fenoterol with significantly higher capacity but also higher K_m, whereby they showed a modest preference for the (*R,R*)-enantiomer.

Transport of formoterol by OCT2, OCT3, MATE1, and MATE2-K was completely absent or too low to determine pharmacokinetic parameters reliably.

With salbutamol, a differential enantiopreference was observed for both OCT2 and OCT3: While OCT1 and all OCT1 variants showed no stereoselectivity or only a minor degree of stereoselectivity towards (*S*)-salbutamol, OCT2 and OCT3 displayed significantly higher (3.5-fold and 4.6-fold) v_{max} values for (*R*)-salbutamol relative to (*S*)-salbutamol. This resulted in 1.9- and 5.9-fold greater intrinsic clearances for the pharmacologically active (*R*)-enantiomer. Comparable to fenoterol, MATE transporters showed a low affinity-high capacity transport of salbutamol, in this case with a preference for (*S*)-salbutamol.

Transport of atenolol by OCT2 was characterised by a lower v_{max} compared to OCT1 and a similar preference for (*S*)-atenolol. While MATE2-K exhibited OCT1-like atenolol transport, it was particularly surprising that MATE1 transported atenolol with a strongly increased capacity and a preference for the pharmacologically inactive (*R*)-atenolol.

In conclusion, unlike the relatively moderate differences in stereoselectivity among allelic variants of OCT1, a more complex picture
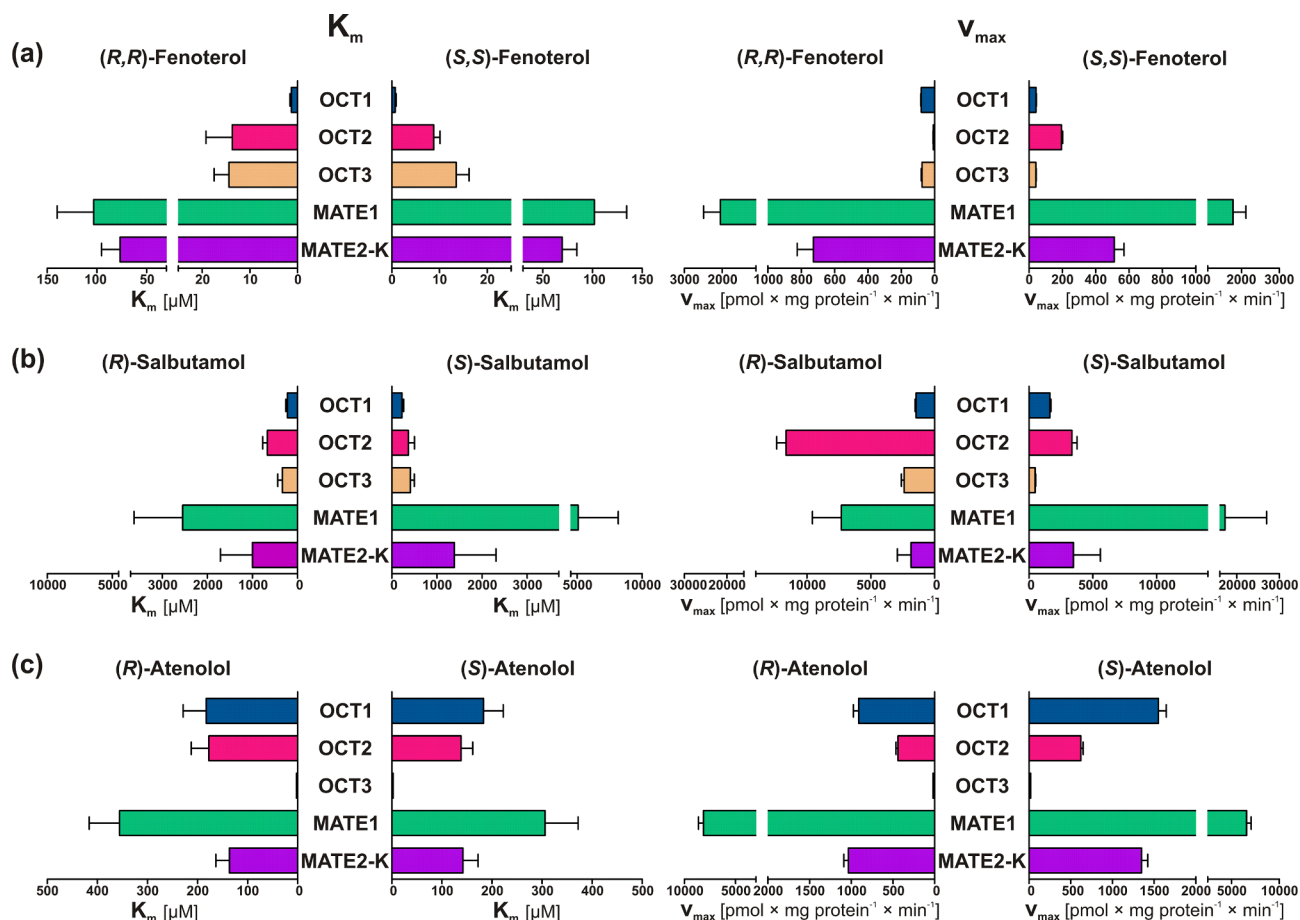
Fig. 4. Comparison of K_m (left) and v_{max} (right) between wild-type OCT1 and related cation transporters for **(a)** fenoterol, **(b)** salbutamol, and **(c)** atenolol. Formoterol transport kinetic parameters could not be determined with high precision and are given in Table 5 only.

Table 5

Kinetic parameters for the transport of racemic (anti)adrenergic drugs by OCT1-related transporters.

Transporter	Substrate	K_m (± SEM) [μM]	V_{max} (± SEM) [pmol × mg protein^{-1} × min^{-1}]	Cl_{int} (± SEM) [ml × min^{-1} × g protein^{-1}]	Stereoselectivity		
					K_m	v_{max}	Cl_{int}
OCT2	(R,R)-Fenoterol	21.2 (± 10.6)	9.9** (± 2.7)	0.6** (± 0.2)	2.37-fold for (R,R)	19.6-fold for (S,S)	36.7-fold for (S,S)
	(S,S)-Fenoterol	8.9 (± 0.6)	194.1** (± 11.6)	22.0** (± 2.6)			
	(R,R)-Formoterol	no transport	no transport	no transport	–	–	–
	(S,S)-Formoterol						
	(R)-Salbutamol	679.0* (± 92.5)	11766.7** (± 1256.3)	17.5** (± 0.7)	1.88-fold for (R)	3.45-fold for (R)	1.86-fold for (R)
	(S)-Salbutamol	361.1* (± 66.9)	3407.3** (± 682.2)	9.4** (± 0.2)			
	(R)-Atenolol	290.6 (± 92.9)	609.0* (± 149.5)	2.4* (± 0.6)	1.68-fold for (R)	1.23-fold for (S)	1.96-fold for (S)
	(S)-Atenolol	172.9 (± 35.7)	749.3* (± 113.8)	4.7* (± 0.9)			
OCT3	(R,R)-Fenoterol	15.2 (± 2.5)	76.5** (± 7.4)	5.3* (± 0.8)	1.07-fold for (R,R)	1.85-fold for (R,R)	1.71-fold for (R,R)
	(S,S)-Fenoterol	14.2 (± 2.9)	41.3** (± 4.1)	3.1* (± 0.5)			
	(R,R)-Formoterol	no transport	no transport	no transport	–	–	–
	(S,S)-Formoterol						
	(R)-Salbutamol	356.8 (± 62.7)	2418.7* (± 317.4)	7.1* (± 1.3)	1.45-fold for (S)	4.60-fold for (R)	5.92-fold for (R)
	(S)-Salbutamol	518.9 (± 195.1)	526.3* (± 81.0)	1.2* (± 0.3)			
	(R)-Atenolol	no transport	no transport	no transport	–	–	–
	(S)-Atenolol						
MATE1	(R,R)-Fenoterol	111.3 (± 16.3)	2091.3 (± 133.7)	19.8 (± 3.5)	1.08-fold for (R,R)	1.15-fold for (R,R)	1.14-fold for (R,R)
	(S,S)-Fenoterol	103.5 (± 18.0)	1822.3 (± 360.6)	17.4 (± 1.4)			
	(R,R)-Formoterol	231.5 (± 114.7)	301.5 (± 152.3)	2.6 (± 1.6)	1.49-fold for (S)	1.48-fold for (S,S)	1.04-fold for (R,R)
	(S,S)-Formoterol	343.8 (± 321.0)	447.3 (± 363.4)	2.5 (± 1.2)			
	(R)-Salbutamol	2545.7 (± 1079.7)	7313.3 (± 2260.4)	3.1* (± 0.4)	2.00-fold for (R)	2.35-fold for (S)	1.19-fold for (S)
	(S)-Salbutamol	5081.0 (± 3073.9)	17216.7 (± 9812.9)	3.7* (± 0.4)			
	(R)-Atenolol	381.5 (± 68.7)	8326.3** (± 775.1)	22.6 (± 2.4)	1.01-fold for (S)	1.19-fold for (R)	1.07-fold for (R)
	(S)-Atenolol	384.7 (± 137.9)	7009.3** (± 916.5)	21.2 (± 4.3)			
MATE2-K	(R,R)-Fenoterol	76.4 (± 4.1)	728.6* (± 92.9)	9.5** (± 0.8)	1.10-fold for (R,R)	1.42-fold for (R,R)	1.28-fold for (R,R)
	(S,S)-Fenoterol	69.5 (± 1.1)	511.7* (± 47.0)	7.4** (± 0.7)			
	(R,R)-Formoterol	181.7 (± 158.1)	77.6 (± 38.5)	1.0 (± 0.7)	5.09-fold for (R,R)	2.30-fold for (R,R)	1.10-fold for (S,S)
	(S,S)-Formoterol	35.7 (± 12.5)	33.7 (± 6.1)	1.1 (± 0.6)			
	(R)-Salbutamol	999.4 (± 709.7)	1855.8 (± 1069.2)	2.2 (± 0.5)	1.39-fold for (S)	1.88-fold for (S)	1.23-fold for (S)
	(S)-Salbutamol	1386.2 (± 921.9)	3487.0 (± 2105.0)	2.7 (± 0.3)			
	(R)-Atenolol	150.1 (± 40.5)	1060.9* (± 128.7)	7.6* (± 1.1)	1.04-fold for (S)	1.30-fold for (S)	1.26-fold for (S)
	(S)-Atenolol	155.7 (± 45.2)	1383.7* (± 200.7)	9.6* (± 1.2)			

SEM, standard error of the mean; asterisks indicate statistical significance of the differences between the two enantiomers (Student's t-test; * p < 0.05, ** p < 0.01, and *** p < 0.001).

with, in some instances, very strong degrees of stereoselectivity was seen with other solute carriers. Particularly interesting was the observed opposite stereoselectivity between the highly homologous (70% shared amino acid sequence identity) transporters OCT1 and OCT2 for some substrates. In addition, large changes in transport activity and stereoselectivity were observed between the two hepatic uptake transporters OCT1 and OCT3. These results indicate a completely non-uniform behaviour among relatively similar transporters with relatively similar chemical compounds.

4. Discussion

In a comprehensive study on stereospecificity in OCT-mediated transport, we have assessed a selection of beta-adrenergic receptor-targeting drugs that are always or often administered as racemates in clinical drug therapy. Our data is indicative of notable stereospecificity in OCT1-mediated transport, with the most common genetic variants of OCT1 showing similar enantiomer preferences to the wild-type in overall but with exceptions. A general trend, however, was not evident, and at present, stereoselective uptake by organic cation transporters must be determined for every substrate individually. Enantiospecificity between different solute carriers differed surprisingly strongly, with the partially opposing enantiomer preferences between the closely related OCT1, OCT2, and OCT3 being of particular interest. As proposed recently, multiple substrate binding sites might contribute to the observed stereoselectivity in transport by organic cation transporters [16,17], and the amino acids in the substrate binding cleft are crucial for OCT substrate recognition and transport [18]. Moreover, pharmacophore modelling showed that organic cation transporters interact with molecules with pronounced three-dimensional structures [19], compared to organic anion transporters. The stereoselectivity in transport of some of the substrates analysed in our study is compatible with a three-dimensional substrate recognition site.

Generally, the therapeutic effects for almost all beta$_2$-adrenergic receptor agonists currently in clinical use are attributed to the (R)-enantiomers, while the (S)-enantiomers were found to be almost inactive at the beta$_2$-adrenergic receptor [20]. Accordingly, for the anti-adrenergic drugs atenolol and acebutolol, it is the (S)-enantiomers that function as beta-adrenergic receptor antagonists [21].

As the pharmacokinetics of a drug are dependent on a number of stereoselective processes in the organism, it is of great relevance to compare how our in vitro results relate to clinical findings and data on stereoselectivity in the biotransformation of the studied drugs.

For fenoterol, no data was found in the literature regarding stereoselective pharmacokinetics in humans. However, in vitro sulfo-conjugation of fenoterol was stereoselective, with the preferred enantiomer depending on the sulfotransferase and the site of sulfation [22]. Our data showed that wild-type OCT1 transports the pharmacologically active enantiomer, (R,R)-fenoterol, with almost double the maximum transport velocity compared to the (S,S)-enantiomer but with proportionally lower affinity. Interestingly, this was nearly the opposite for OCT1*2, a variant that is particularly common in people of Central and South American origin [7]. However, for both wild-type OCT1 and the *2 variant, no stereoselectivity was seen in the intrinsic clearance. Thus, it is difficult to predict from this data which implication the OCT1 related stereoselectivity will have on clinical pharmacokinetics and

pharmacodynamics. At the very low therapeutic concentrations, the differences in K_m may have a stronger effect than those in v_{max} or intrinsic clearance. Very interesting is the large degree of stereospecificity (37-fold higher intrinsic clearance for (S,S)-fenoterol) observed for OCT2, a transporter that is highly expressed in the kidneys. However, given the relatively low renal clearance of fenoterol, this may not be of greater relevance in clinical therapy.

Formoterol plasma concentrations were 1.5-fold higher for the (S,S)-enantiomer than for the (R,R)-enantiomer one hour following inhalative dosing of the 1:1 mixture of (R,R)- and (S,S)-formoterol in humans [23]. Both after inhalative and oral administration, the excretion of unchanged drug in urine was greater for (S,S)- than for (R,R)-formoterol, but excretion as formoterol glucuronide conjugate was greater for (R,R)- over (S,S)-formoterol [14,24,25]. The latter is particularly interesting in light of the fact that glucuronide conjugation in liver microsomes was found to be more than 2-fold higher for the (S,S)-enantiomer [14]. The total excretion (unchanged and as glucuronide conjugate) after oral dosage was greater for (R,R)-formoterol. There appeared to be a significant difference between male and female participants [26]. The enantiopreference for (R,R)-formoterol in metabolism and the 1.2-fold higher OCT1-mediated intrinsic clearance of (R,R)-formoterol could together contribute to higher plasma concentrations of (S,S)-formoterol.

Salbutamol is probably the most widely-used short-acting beta-mimetic drug. Upon administration of the racemate, significant differences in pharmacokinetics were found, with up to 8-fold higher systemic exposure (AUC) for the (S)- versus the (R)-enantiomer after inhalative dosage, and more than 20-fold following oral administration [27–29]. The larger systemic (S):(R) ratio after oral dosage is mostly a result of a stereoselective first-pass metabolism, but pH-dependent chiral inversion of the (R)- to the (S)-enantiomer was also found to occur to a smaller extent (ca. 6%) in the stomach but not following inhalation [27,30–33]. The plasma levels of (R)- and (S)-salbutamol were higher when given in enantiopure form compared to the racemate, suggesting a possible influence of each enantiomer on the clearance of the opposite enantiomer when administered as racemic mixture [28]. With respect to the biotransformation, sulphate conjugation in the intestine and liver was 12-fold higher for (R)-salbutamol [33–36]. Stereospecificity in presystemic metabolism in the lungs was observed *in vitro* but not confirmed in humans [36,37]. A common single nucleotide polymorphism (rs1975350) in SULT1A3, the main metabolising enzyme, had no significant effect on the stereospecificity of the pharmacokinetics [33,38]. We observed a small but probably negligible enantiopreference for the (S)-enantiomer by OCT1, MATE1, and MATE2-K, which, hence, do not appear to contribute to the higher systemic exposure for (S)-salbutamol. However, the almost 6-fold higher intrinsic clearance of (R)-salbutamol observed for OCT3, another hepatic uptake transporter, is in line with the clinical observations. In accordance is also the almost 2-fold higher intrinsic clearance of (R)-salbutamol for OCT2, which may very well be of relevance, given the comparatively high renal clearance of unchanged salbutamol (46% for (R)-salbutamol; 55% for (S)-salbutamol [39]).

Acebutolol plasma and urine concentrations were both 1.2-fold higher for the (S)-enantiomer following oral administration of racemic acebutolol, which corresponded to a 1.2-fold higher oral clearance of (R)-acebutolol. This may be explained by stereoselectivity in first-pass metabolism and renal excretion of the main metabolite diacetolol. For diacetolol, C_{max} and renal clearance was greater for the (R)-enantiomer; no significant difference was seen with respect to plasma AUC [40]. The (S):(R) ratio for urinary excretion correlated with age in a subsequent study involving elderly participants, possibly as a result of altered stereoselectivity in tubular secretion [41]. A different study preceding the above two found no stereoselectivity in the disposition of acebutolol and diacetolol following single and repeated oral administration [42]. Plasma protein binding of acebutolol appears not to be stereoselective and the majority of the drug (greater than 85%) is found in the

unbound fraction [21]. Our data showed a 1.5-fold higher intrinsic clearance of (S)-acebutolol for OCT1.

With respect to atenolol, it was found in several independent studies that the plasma AUCs were slightly (1.1-fold) higher for (R)-atenolol following a single oral dose of the racemate [43–46]. In the study conducted by Mehvar et al., a slightly (1.1-fold) but statistically significantly higher renal clearance of the (S)-enantiomer was proposed as possible underlying reason; however, no significant difference in the renal clearance was seen in the study by Boyd et al. [43,45]. Intriguingly, exercise appeared to alter the stereoselectivity of atenolol pharmacokinetics, as the (R):(S) ratio of the mean plasma concentrations changed from 1.1 at rest to 0.7 following exercise [47]. Given its more hydrophilic structure, atenolol is almost exclusively eliminated unchanged in urine, a process that appears to be modestly stereoselective towards the (R)-enantiomer [21,43,45]. A possible interaction between the enantiomers in a racemic mixture, as seen for salbutamol, apparently does not occur with atenolol [44,46]. A high degree of stereoselectivity was observed in the glucuronidation of atenolol, as 3.1-fold more of the (S)-glucuronide conjugate was formed after incubation of the racemate with UGT1A9 [48]. These clinical observations may partially be explained by the higher intrinsic clearance of the (S)-enantiomer via OCT1 (including variants) and OCT2, but the almost 2-fold difference in cell uptake via OCT2 is apparently not fully reflected by the pharmacokinetic data.

Altogether, our *in vitro* data on stereospecificity in organic cation transporter-mediated drug transport is in accordance with, and may partially account for, stereospecificity in clinical pharmacokinetics, especially with respect to formoterol, salbutamol, and atenolol. It is notable that, for many racemic drugs, the pharmacokinetics were not analysed with regard to stereospecificity, despite receptor interactions being stereoselective in most cases. Here we showed that membrane transport of several beta-(anti)adrenergic drugs can be stereospecific, but it appears that stereoselectivity is more pronounced in biotransformation of some of the studied drugs. From a molecular perspective, the observed stereoselectivity in membrane transport may indicate a relatively tight interaction between solute carriers and some substrates. This could be explored in more detail using computational molecular modelling as a follow-up to this study.

CRediT authorship contribution statement

Ole Jensen: Methodology, Formal analysis, Investigation, Writing - original draft, Writing - review & editing, Visualization. **Muhammad Rafehi:** Writing - original draft, Writing - review & editing. **Mladen V. Tzvetkov:** Conceptualization, Resources. **Jürgen Brockmöller:** Conceptualization, Resources, Writing - original draft, Writing - review & editing, Project administration, Supervision.

Declaration of Competing Interest

The authors declare that they have no known competing financial interests or personal relationships that could have appeared to influence the work reported in this paper.

Acknowledgements

References

[1] R. Hendrickx, J.G. Johansson, C. Lohmann, R.M. Jenvert, A. Blomgren, L. Borjesson, L. Gustavsson, Identification of novel substrates and structure-activity relationship of cellular uptake mediated by human organic cation transporters 1 and 2, J. Med. Chem. 56 (18) (2013) 7232–7242.

[2] D.A. Handley, C.H. Senanayake, W. Dutczak, J.L. Benovic, T. Walle, R.B. Penn, H.S. Wilkinson, G.J. Tanoury, R.G. Andersson, F. Johansson, J. Morley, Biological actions of formoterol isomers, Pulm. Pharmacol. Ther. 15 (2) (2002) 135–145.

[3] J. Lötvall, M. Palmqvist, P. Arvidsson, A. Maloney, G.P. Ventresca, J. Ward, The therapeutic ratio of R-albuterol is comparable with that of RS-albuterol in asthmatic patients, J. Allergy Clin. Immunol. 108 (5) (2001) 726–731.

[4] T. Niwa, N. Murayama, H. Yamazaki, Stereoselectivity of human cytochrome p450 in metabolic and inhibitory activities, Curr. Drug Metab. 12 (6) (2011) 549–569.

[5] U.K. Walle, T. Walle, Stereoselective sulfation of terbutaline by the rat liver cytosol: evaluation of experimental approaches, Chirality 1 (2) (1989) 121–126.

[6] M.J. Dresser, M.K. Leabman, K.M. Giacomini, Transporters involved in the elimination of drugs in the kidney: organic anion transporters and organic cation transporters, J. Pharm. Sci. 90 (4) (2001) 397–421.

[7] T. Seitz, R. Stalmann, N. Dalila, J. Chen, S. Pojar, J.N. Dos Santos Pereira, R. Kratzner, J. Brockmöller, M.V. Tzvetkov, Global genetic analyses reveal strong inter-ethnic variability in the loss of activity of the organic cation transporter OCT1, Genome Med 7(1) (2015) 56.

[8] Q. Zhou, L.S. Yu, S. Zeng, Stereoselectivity of chiral drug transport: a focus on enantiomer-transporter interaction, Drug Metab. Rev. 46 (3) (2014) 283–290.

[9] A.R. Saadatmand, S. Tadjerpisheh, J. Brockmöller, M.V. Tzvetkov, The prototypic pharmacogenetic drug debrisoquine is a substrate of the genetically polymorphic organic cation transporter OCT1, Biochem. Pharmacol. 83 (10) (2012) 1427–1434.

[10] J. Chen, J. Brockmöller, T. Seitz, J. König, M.V. Tzvetkov, X. Chen, Tropane alkaloids as substrates and inhibitors of human organic cation transporters of the SLC22 (OCT) and the SLC47 (MATE) families, Biol. Chem. 398 (2) (2017) 237–249.

[11] H. Jiang, C. Randlett, H. Junga, X. Jiang, Q.C. Ji, Using supported liquid extraction together with cellobiohydrolase chiral stationary phases-based liquid chromatography with tandem mass spectrometry for enantioselective determination of acebutolol and its active metabolite diacetolol in spiked human plasma, J. Chromatogr. B 877 (3) (2009) 173–180.

[12] T. Fornstedt, A.M. Hesselgren, M. Johansson, Chiral assay of atenolol present in microdialysis and plasma samples of rats using chiral CBH as stationary phase, Chirality 9 (4) (1997) 329–334.

[13] M. Sanghvi, A. Ramamoorthy, J. Strait, I.W. Wainer, R. Moaddel, Development and validation of a sensitive LC-MS/MS method for the determination of fenoterol in human plasma and urine samples, J. Chromatogr. B Analyt. Technol. Biomed. Life Sci. 933 (2013) 37–43.

[14] M. Zhang, J.P. Fawcett, J.M. Kennedy, J.P. Shaw, Stereoselective glucuronidation of formoterol by human liver microsomes, Br. J. Clin. Pharmacol. 49 (2) (2000) 152–157.

[15] A. Halabi, C. Ferrayoli, M. Palacio, V. Dabbene, S. Palacios, Validation of a chiral HPLC assay for (R)-salbutamol sulfate, J. Pharm. Biomed. Anal. 34 (1) (2004) 45–51.

[16] T. Keller, V. Gorboulev, T.D. Mueller, V. Dotsch, F. Bernhard, H. Koepsell, Rat organic cation transporter 1 contains three binding sites for substrate 1-methyl-4-phenylpyridinium per monomer, Mol. Pharmacol. 95 (2) (2019) 169–182.

[17] H. Koepsell, Multiple sites in organic cation transporters require sophisticated procedures to identify interactions of novel drugs, Biol. Chem. (2019) 195.

[18] D.C. Li, C.G. Nichols, M. Sala-Rabanal, Role of a hydrophobic pocket in polyamine interactions with the polyspecific organic cation transporter OCT3, J. Biol. Chem. 290 (46) (2015) 27633–27643.

[19] H.C. Liu, A. Goldenberg, Y. Chen, C. Lun, W. Wu, K.T. Bush, N. Balac, P. Rodriguez, R. Abagyan, S.K. Nigam, Molecular properties of drugs interacting with SLC22 transporters OAT1, OAT3, OCT1, and OCT2: A machine-learning approach, J. Pharmacol. Exp. Ther. 359 (1) (2016) 215–229.

[20] B. Waldeck, Enantiomers of bronchodilating beta2-adrenoceptor agonists: is there a cause for concern? J. Allergy Clin. Immunol. 103 (5 Pt 1) (1999) 742–748.

[21] R. Mehvar, D.R. Brocks, Stereospecific pharmacokinetics and pharmacodynamics of beta-adrenergic blockers in humans, J. Pharm. Pharm. Sci. 4 (2) (2001) 185–200.

[22] A.A. Wilson, J. Wang, P. Koch, T. Walle, Stereoselective sulphate conjugation of fenoterol by human phenolsulphotransferases, Xenobiotica 27 (11) (1997) 1147–1154.

[23] M. Hostrup, C.K. Narkowicz, S. Habib, D.S. Nichols, G.A. Jacobson, Beta2 -adrenergic ligand racemic formoterol exhibits enantioselective disposition in blood and skeletal muscle of humans, and elicits myocellular PKA signaling at therapeutic inhaled doses, Drug Test. Anal. 11 (7) (2019) 1048–1056.

[24] J.B. Lecaillon, G. Kaiser, M. Palmisano, J. Morgan, G. Della Cioppa, Pharmacokinetics and tolerability of formoterol in healthy volunteers after a single high dose of Foradil dry powder inhalation via Aerolizer, Eur. J. Clin. Pharmacol. 55 (2) (1999) 131–138.

[25] G.A. Jacobson, M. Hostrup, C.K. Narkowicz, D.S. Nichols, E.H. Walters, Enantioselective disposition of (R, R)-formoterol, (S, S)-formoterol and their respective glucuronides in urine following single inhaled dosing and application to doping control, Drug Test. Anal. 11 (7) (2019) 950–956.

[26] M. Zhang, J.P. Fawcett, J.P. Shaw, Stereoselective urinary excretion of formoterol and its glucuronide conjugate in human, Br. J. Clin. Pharmacol. 54 (3) (2002) 246–250.

[27] M. Vakily, R. Mehvar, D. Brocks, Stereoselective pharmacokinetics and pharmacodynamics of anti-asthma agents, Ann. Pharmacother. 36 (4) (2002) 693–701.

[28] B.J. Lipworth, D.J. Clark, P. Koch, C. Arbeeny, Pharmacokinetics and extrapulmonary beta 2 adrenoceptor activity of nebulised racemic salbutamol and its R and S isomers in healthy volunteers, Thorax 52 (10) (1997) 849–852.

[29] G.A. Jacobson, F.V. Chong, R. Wood-Baker, (R, S)-Salbutamol plasma concentrations in severe asthma, J. Clin. Pharm. Ther. 28 (3) (2003) 235–238.

[30] D.W. Boulton, J.P. Fawcett, Enantioselective disposition of salbutamol in man following oral and intravenous administration, Br. J. Clin. Pharmacol. 41 (1) (1996) 35–40.

[31] T. Zhou, J. Zeng, S. Liu, T. Zhao, J. Wu, W. Lai, M. He, B. Xu, S. Qu, L. Xu, W. Tan, Study on the determination and chiral inversion of R-salbutamol in human plasma and urine by liquid chromatography-tandem mass spectrometry, J. Chromatogr. B Analyt. Technol. Biomed. Life Sci. 1002 (2015) 218–227.

[32] K. Gumbhir-Shah, D.J. Kellerman, S. DeGraw, P. Koch, W.J. Jusko, Pharmacokinetic and pharmacodynamic characteristics and safety of inhaled albuterol enantiomers in healthy volunteers, J. Clin. Pharmacol. 38 (12) (1998) 1096–1106.

[33] D.W. Boulton, J.P. Fawcett, The pharmacokinetics of levosalbutamol: what are the clinical implications? Clin. Pharmacokinet. 40 (1) (2001) 23–40.

[34] U.K. Walle, G.R. Pesola, T. Walle, Stereoselective sulphate conjugation of salbutamol in humans: comparison of hepatic, intestinal and platelet activity, Br. J. Clin. Pharmacol. 35 (4) (1993) 413–418.

[35] T. Nakpheng, S. Songkarak, T. Suwandecha, R. Sritharadol, C. Chunhachaichana, T. Srichana, Evidences for salbutamol metabolism by respiratory and liver cell lines, Drug Metab. Pharmacokinet. 32 (2) (2017) 127–134.

[36] J.K. Ward, J. Dow, N. Dallow, P. Eynott, S. Milleri, G.P. Ventresca, Enantiomeric disposition of inhaled, intravenous and oral racemic-salbutamol in man–no evidence of enantioselective lung metabolism, Br. J. Clin. Pharmacol. 49 (1) (2000) 15–22.

[37] T. Walle, E.A. Eaton, U.K. Walle, G.R. Pesola, Stereoselective metabolism of RS-albuterol in humans, Clin. Rev. Allergy Immunol. 14 (1) (1996) 101–113.

[38] G.A. Jacobson, K.C. Yee, R. Wood-Baker, E.H. Walters, SULT 1A3 single-nucleotide polymorphism and the single dose pharmacokinetics of inhaled salbutamol enantiomers: are some athletes at risk of higher urine levels? Drug Test. Anal. 7 (2) (2015) 109–113.

[39] D.W. Boulton, J.P. Fawcett, Enantioselective disposition of albuterol in humans, Clin. Rev. Allergy Immunol. 14 (1) (1996) 115–138.

[40] M. Piquette-Miller, R.T. Foster, C.T. Kappagoda, F. Jamali, Pharmacokinetics of acebutolol enantiomers in humans, J. Pharm. Sci. 80 (4) (1991) 313–316.

[41] M. Piquette-Miller, R.T. Foster, C.T. Kappagoda, F. Jamali, Effect of aging on the pharmacokinetics of acebutolol enantiomers, J. Clin. Pharmacol. 32 (2) (1992) 148–156.

[42] M.G. Sankey, A. Gulaid, C.M. Kaye, Preliminary study of the disposition in man of acebutolol and its metabolite, diacetolol, using a new stereoselective hplc method, J. Pharm. Pharmacol. 36 (4) (1984) 276–277.

[43] R. Mehvar, M.E. Gross, R.N. Kreamer, Pharmacokinetics of atenolol enantiomers in humans and rats, J. Pharm. Sci. 79 (10) (1990) 881–885.

[44] K. Stoschitzky, G. Egginger, G. Zernig, W. Klein, W. Lindner, Stereoselective features of (R)- and (S)-atenolol: clinical pharmacological, pharmacokinetic, and radioligand binding studies, Chirality 5 (1) (1993) 15–19.

[45] R.A. Boyd, S.K. Chin, O. Don-Pedro, R.L. Williams, K.M. Giacomini, The pharmacokinetics of the enantiomers of atenolol, Clin. Pharmacol. Ther. 45 (4) (1989) 403–410.

[46] G. Egginger, W. Lindner, S. Kahr, K. Stoschitzky, Stereoselective HPLC bioanalysis of atenolol enantiomers in plasma: application to a comparative human pharmacokinetic study, Chirality 5 (7) (1993) 505–512.

[47] K. Stoschitzky, W. Lindner, W. Klein, Stereoselective release of (S)-atenolol from adrenergic nerve endings at exercise, Lancet 340 (8821) (1992) 696–697.

[48] S. Xie, S. Zeng, Stereoselective glucuronidation of propafenone and its analogues by human recombinant UGT1A9, Chem Pharm Bull (Tokyo) 58 (6) (2010) 879–883.

3.4   Publication 4

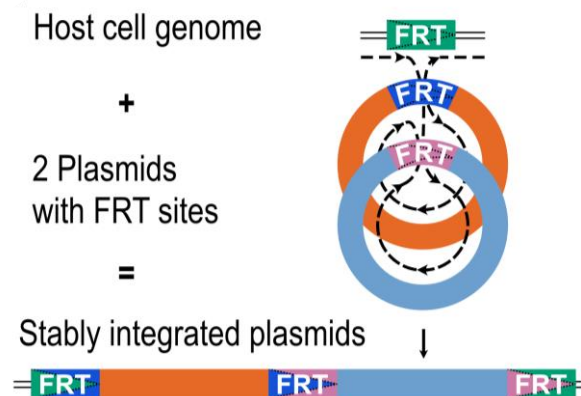**A double-Flp-In method for stable overexpression of two genes**

Ole Jensen[1,4], Salim Ansari[1,4], Lukas Gebauer[1,4], Simon F. Müller[2], Kira A. A. T. Lowjaga[2], Joachim Geyer[2], Mladen V. Tzvetkov[1,3] & Jürgen Brockmöller[1]

[1] Institute of Clinical Pharmacology, University Medical Center Göttingen, Georg-August University, Robert-Koch-Str. 40, 37075 Göttingen, Germany.

[2] Institute of Pharmacology and Toxicology, Faculty of Veterinary Medicine, Justus Liebig University Giessen, 35392 Giessen, Germany.

[3] Institute of Pharmacology, Center of Drug Absorption and Transport (C_DAT), University Medical Center Greifswald, 17489 Greifswald, Germany.

[4] These authors contributed equally: Ole Jensen, Salim Ansari, and Lukas Gebauer.

SCIENTIFIC
REPORTS
natureresearch

Check for updates

OPEN

A double-Flp-in method for stable overexpression of two genes

Ole Jensen[1,4]✉, Salim Ansari[1,4], Lukas Gebauer[1,4], Simon F. Müller[2], Kira A. A. T. Lowjaga[2], Joachim Geyer[2], Mladen V. Tzvetkov[1,3] & Jürgen Brockmöller[1]

Overexpression of single genes in mammalian cells is widely used to investigate protein function in basic and applied biosciences and in drug research. A better understanding of interactions of two proteins is an important next step in the advancement of our understanding of complex biological systems. However, simultaneous and robust overexpression of two or more genes is challenging. The Flp-In system integrates a vector into cell lines at a specific genomic locus, but has not been used for integration of more than one gene. Here we present a modification of the Flp-In system that enables the simultaneous targeted integration of two genes. We describe the modification and generation of the vectors required and give the complete protocol for transfection and validation of correct genomic integration and expression. We also provide results on the stability and reproducibility, and we functionally validated this approach with a pharmacologically relevant combination of a membrane transporter facilitating drug uptake and an enzyme mediating drug metabolism.

The use of immortal cell lines has become an indispensable tool in basic and applied biomedical research in the last decades. In vitro experiments with cell lines are often used to generate new hypotheses, or to validate in vivo findings with the possibility to manipulate under well-defined conditions[1,2]. In drug research, cell lines over-expressing specific genes are an important screening tool. Overexpression can be achieved via numerous ways, with transient or stable expression of the gene of interest[3,4]. However, many transgene-introducing techniques come along with obvious disadvantages: Reproducibility, efficiency, and anisogeneity are only a few of them. Stable transfection, based on non-viral site-specific recombination circumvents these disadvantages[5–8]. This can be accomplished by the use of recombinases, such as Cre from the P1 bacteriophage or Flp from *Saccharomyces cerevisiae*. These enzymes can catalyze the recombination of two DNA strands at specific recognition sequences, making it possible to insert, excise, invert, or translocate DNA segments[9,10]. The Flp-In system (Thermo Fisher Scientific, Darmstadt, Germany) uses the Flp recombinase to generate isogenic cell lines, in which the gene of interest integrates at a single well-defined locus within the host cell genome[11–15]. One highlight of the Flp-In system is the fact that the promoter, which drives the expression of the resistance against the selection antibiotic hygromycin, is present upstream of the recombination site in the host cell genome. This ensures the expression of the resistance gene only in successfully transfected cells that carry and stably overexpress the gene of interest. Since the promoter and the locus of genomic integration are the same for all constructed cell lines, the expression level of the genes of interest and general isogeneity are well comparable[11].

The Flp-In system, so far, was not applicable when two or more genes of interest are to be overexpressed in a controlled manner, although that option actually exists. The Flp recombination target (FRT) site not only persists after the integration of a vector, but even a second FRT site is introduced upon vector integration (Fig. 1a). Modifying the Flp-In vector with internal ribosomal entry sites (IRES) would be one option to integrate and overexpress several genes[16], but the expression efficiency has been shown to depend strongly on the distance between IRES element and translation start site. The expression of the genes is highly dependent on the order in the operon and requires a precise design[17,18]. The simple transfection of two kinds of the same vector is also a feasible approach[19]. However, without a second selection antibiotic resistance gene, there is no easy way to select cell clones successfully transfected with both vectors. Excessive and sophisticated validation would be needed to ensure the presence of both genes of interest and their expression levels.

[1]Institute of Clinical Pharmacology, University Medical Center Göttingen, Georg-August University, Robert-Koch-Str. 40, 37075 Göttingen, Germany. [2]Institute of Pharmacology and Toxicology, Faculty of Veterinary Medicine, Justus Liebig University Giessen, 35392 Giessen, Germany. [3]Institute of Pharmacology, Center of Drug Absorption and Transport (C_DAT), University Medical Center Greifswald, 17489 Greifswald, Germany. [4]These authors contributed equally: Ole Jensen, Salim Ansari, and Lukas Gebauer. ✉email: ole.jensen@med.uni-goettingen.de
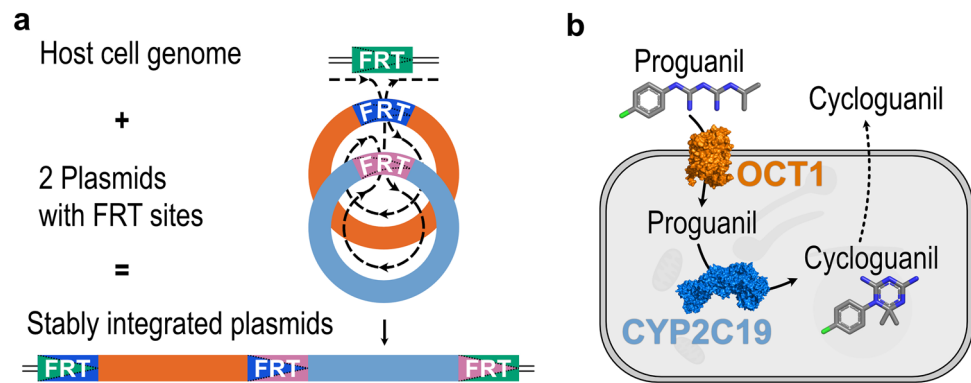
Figure 1. The principle and an application example of the Double-Flp-In technique. (**a**) The integration of two simultaneously transfected plasmids encoding two genes of interest can be achieved into a single Flp recombination target (FRT) site. (**b**) As a proof of concept, we transfected HEK293 cells with the coding sequences for the human organic cation transporter 1 (OCT1) and cytochrome P450 isoform 2C19 (CYP2C19). Together, these proteins will facilitate the uptake of the anti-malarial prodrug proguanil and the metabolism to its active metabolite cycloguanil. Protein icons of OCT1 and CYP2C19 and chemical structures were created using The PyMOL Molecular Graphics System, Version 1.3, Schrödinger, LLC, www.pymol.org.
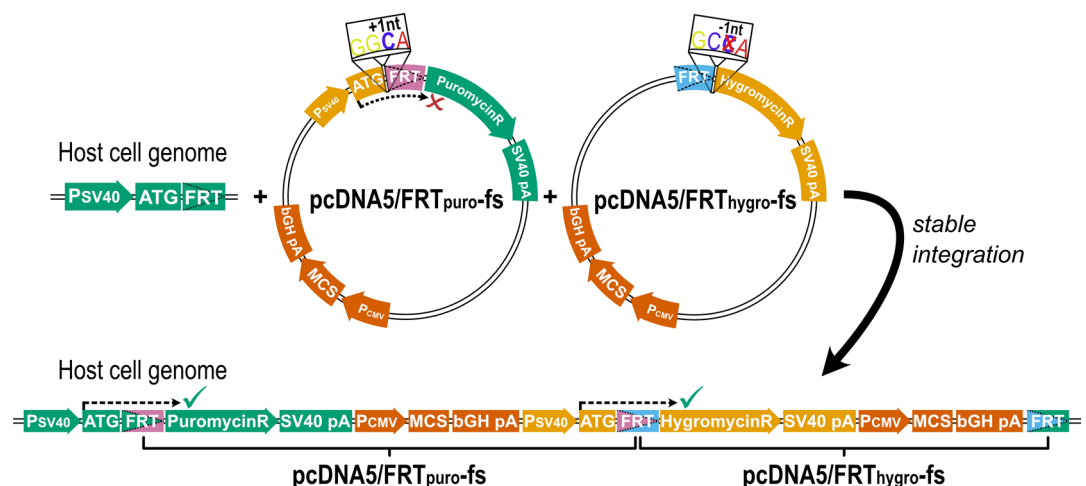
Figure 2. Illustration of the total construct and the reading frame shift introduced to ensure expression of both resistance genes only in case of successful double transfection. The reading frame shift introduced into the both FRT vectors leads to expression of both resistance genes only after successful stable integration (green ticks), and not before (red x). The introduction of an additional C between the start codon (ATG) and the FRT site is indicated. This allows reliable selection of double-transfected cell clones (sequence elements for bacterial expression are not shown) and expression of genes of interest cloned into the multiple cloning sites (MCS) from identical promoters. (*PSV40* SV40 promoter, *SV40 pA* polyA signal of SV40, *PCMV* CMV promoter; *bGH pA* polyA signal of bovine growth hormone).

Our goal was to develop a simple and robust protocol to transfect two different genes in a modular concept (Fig. 1). To achieve this, we introduced a one-nucleotide deletion into the original pcDNA5/FRT vector, which was necessary for correct expression of the hygromycin resistance gene from the promoter of the second vector. The second vector did not only include the promoter to drive hygromycin expression after correct integration but also the gene for puromycin resistance. To exclude that the puromycin resistance was already expressed upon transient presence of the vector, we inserted one nucleotide between the translation start site and the coding sequence of the puromycin resistance gene, which leads to a frame shift and to early termination of translation. After successful integration in the correct order, the deletion and the insertion will neutralize themselves and expression of both resistance genes will ensure proper selection (Fig. 2). These vectors can be used for the easy and replicable transfection of two genes for multifarious applications to study interactive actions of almost any two proteins. As proof of concept, we show the stability of the double transfection with two pairs of fluorescent proteins, we compare expression levels of single- to double-transfected genes, and we provide a scientifically relevant example for the application of this method to study the interaction between cell uptake transport and metabolism of the anti-malarial prodrug proguanil (Fig. 1). The scope of this technique, however, is much broader

and includes any combination of substance uptake and metabolism, substance metabolism and efflux, or any other interaction in intermediary metabolism or cell signaling.

Results

Below, we recapitulate the principles of our approach and explain some critical items in the generation of the stable double transfection. The system was then tested and validated by three gene pairs, a pair of two membrane bound fluorescently labeled transport proteins, a pair of two cytosolic fluorescent proteins used particularly to prove the stability of stable expression, and as a pharmacologically relevant application a pair of a membrane transporter (OCT1) and a drug-metabolizing enzyme (CYP2C19).

Strategy for the Double-Flp-In and the generation of the required vectors. To generate the Double Flp-In system we took advantage from the fact that by the integration of a single plasmid in the classical Flp-In system, the FRT site is not destroyed, but is even duplicated. This enables the integration of at least one additional expression vector in one of the FRT sites.

Therefore, we engineered a second expression vector (pcDNA5/FRT$_{puro}$-fs) carrying a puromycin resistance gene. This additional expression vector was created based on the backbone of the existing pcDNA5/FRT vector by replacing the hygromycin with a puromycin resistance gene (Fig. S1). Additionally, a SV40 promoter region, as present in the host cell genome, was included in the vector to facilitate the expression of the hygromycin resistance gene after chromosomal integration of both vectors. To ensure that this promoter will not drive expression of the puromycin resistance gene in the non-integrated transient state, we generated a reading-frame shift by introducing a single base between the start codon ATG and the puromycin resistance coding sequence. In addition, a one-base deletion was introduced into the original pcDNA5/FRT vector, resulting in the pcDNA5/FRT$_{hygro}$-fs plasmid (Fig. 2). This frame shift was necessary to restore the distance between the ATG from the pcDNA5/FRT$_{puro}$-fs and the hygromycin resistance coding sequence from the pcDNA5/FRT$_{hygro}$-fs. This enables the expression of the hygromycin resistance of the downstream plasmid by the SV40 promoter introduced by the upstream plasmid.

Transfection protocol optimization. Since the main difference between the transfection protocol for one vector as provided by the manufacturer and our approach is the second vector and the requirement of a second antibiotic, we had to titrate the antibiotics concentrations required to eliminate non-resistant (i.e. not correctly transfected) HEK293 cells by a simple checkerboard approach[20]. The result was a slightly reduced concentration of hygromycin compared to the one typically used for single transfection of HEK293 cells in our laboratory for initial selection of cell clones (200 µg/mL instead of 300 µg/mL). During initial cultivation of cell clones, we also used a reduced hygromycin concentration of 50 µg/mL instead of typically 100 µg/mL. The concentration of puromycin was more difficult to obtain, because the HEK293 cells were highly sensitive to puromycin treatment. The final concentration used for the double transfection was 0.25 µg/mL during selection and 0.025 µg/mL during the cultivation period until complete validation of the cell clones.

Regarding the amounts of DNA used for transfection, initial experiments showed that an increased amount of transfected vector DNA, compared to the single transfection protocol, is not required and only leads to unwanted multiple integrations due to the surplus of vector DNA (data not shown). The ratio of 400 ng pcDNA5 vector(s) to 3.6 µg pOG44 (encoding the transient expression of the Flp recombinase) was maintained as stated in the original transfection protocol by the manufacturer. In case of double transfections, the plasmids were mixed and transfected in an equimolar ratio.

In a preliminary experiment, selection of double-transfected cells was performed with only hygromycin and 22 out of 25 cell clones showed proper expression of both genes of interest (eGFP and tdTomato).

Double transient vs. double stable transfection. For the initial testing of the created plasmids, we double-transfected the cyan or the yellow fluorescent protein (CFP, YFP) tagged sodium/bile acid cotransporter (NTCP) into HEK293 cells and compared the transient to the stable transfection. The fluorescent cells were analyzed by microscopy (Fig. 3a). The stable transfection and clonal selection of cells provided a homogeneous signal with highly comparable signals per individual cell. Moreover, the cells were positive for both transfected fluorescent proteins. On the other side, transiently transfected cells were characterized by a limited efficiency as not all cells showed a fluorescence signal and by a high signal variability within the fluorescent cells, making it difficult to find microscopy settings for an average signal.

Stability of the genomic integration. The stability of double transfection was determined by flow cytometry and confocal microscopy. Cells validated by flow cytometry had been transfected with pcDNA5/FRT$_{puro}$-fs::tdTomato and pcDNA5/FRT$_{hygro}$-fs::eGFP and double-positivity was compared to empty vector-transfected cells (Fig. 3b). Results showed a stable expression and presence of both fluorescence proteins over 30 passages, regardless of whether the selection antibiotics used for clonal selection was present in the cell culture medium or not. After 25 passages, 99.95% (± 0.03% SEM) of the cells cultivated in medium containing hygromycin and puromycin, and 99.5% (± 0.03% SEM) of the cells cultivated in medium without selection antibiotics were double-positive (Fig. 3c). Similar results were obtained when the stability of the integration was analyzed in the cells double-transfected with CFP- and YFP-tagged NTCP. Here, the signals were analyzed by fluorescence microscopy. After 25 passages, the amount of double-positive cells was not significantly different (unpaired t-test, $p > 0.05$, GraphPad Prism version 5.01 for Windows, GraphPad Software, La Jolla, California, USA), in cells cultured with and without selection antibiotics (98.0% ± 1.2% SEM and 96.7% ± 1.8% SEM) (Fig. 3d). Alto-
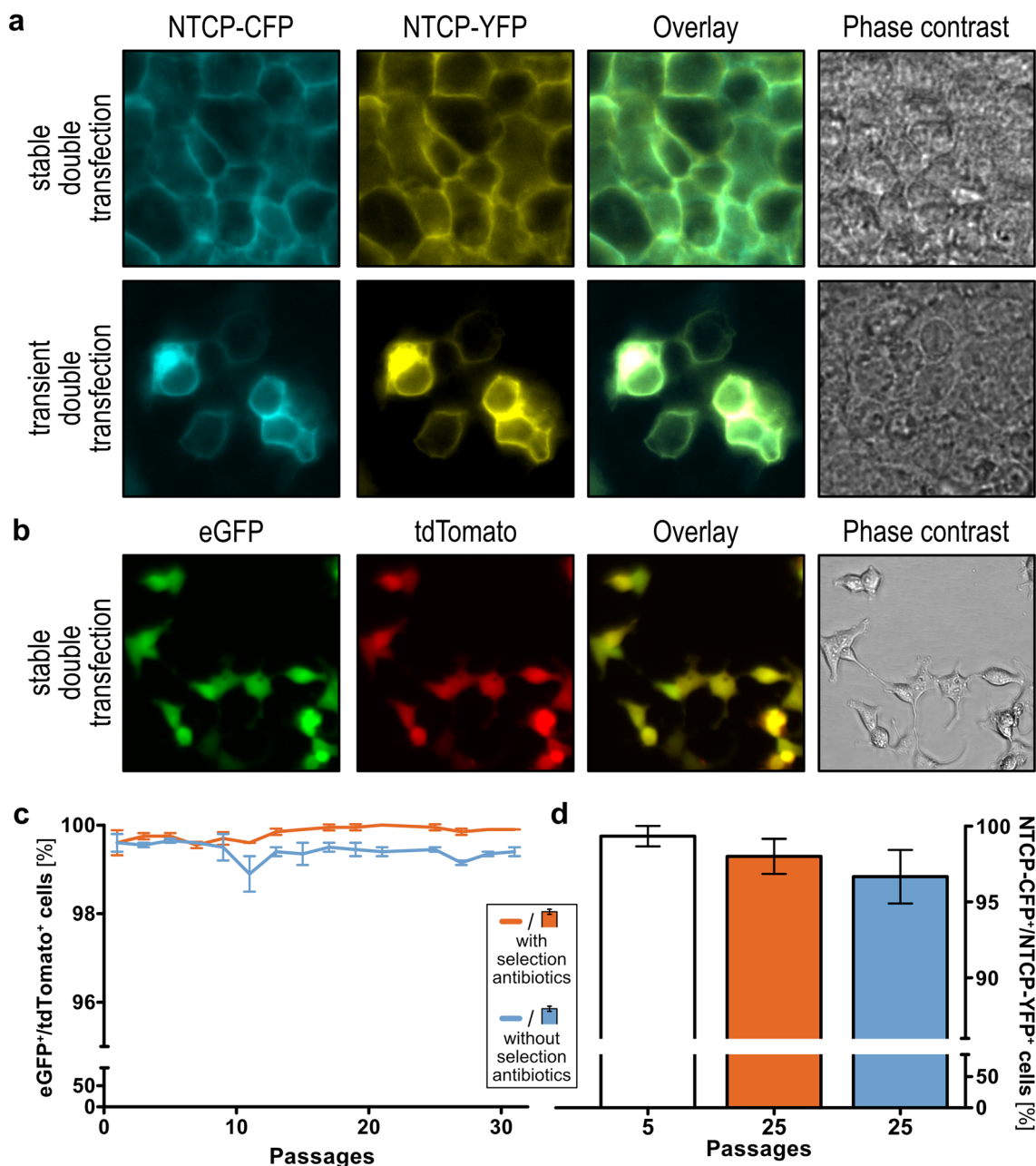
Figure 3. Microscopic and flow cytometric analyses of double-transfected cell lines overexpressing fluorophores. (**a**) Simultaneous co-transfection of the sodium/bile acid cotransporter (NTCP) tagged with cyan or yellow fluorescent protein (CFP, YFP) into HEK293 cells reveals an even expression in virtually all cells. Transient co-transfection of NTCP-CFP and NTCP-YFP illustrates the heterogeneity in strength and distribution of transient transfections, compared to the stably integrated double-transfection. (**b**) HEK293 cells showed consistent overexpression of tdTomato and eGFP during the early selection process by live-cell imaging. (**c**) Flow cytometric analysis of the integration of the genes encoding eGFP and tdTomato showed a high stability over 30 passages (mean ± SEM). (**d**) Stability of genomic integration of simultaneously transfected CFP- and YFP-tagged sodium/bile acid cotransporter (NTCP) was additionally confirmed by microscopic analysis (mean ± SEM). Figures (**c**) and (**d**) were created using GraphPad Prism version 5.01 for Windows, GraphPad Software, La Jolla, California, USA, www.graphpad.com.

gether, although a very minor decline appeared to exist according to the nominal values (Fig. 3c,d), this decline was not significant.

Genomic validation. The integration of both vectors in the intended order was confirmed and different cases of multiple integrations were analyzed by PCR. The PCRs were established to detect all possible different arrangements of the two integrated vectors. For this, primers were designed binding at specific elements only

present in the FRT locus of the host cell line or in one of the two expression vectors. This led to two reactions confirming the successful integration of both vectors in the intended order and three reactions detecting all setups of multiple integrations (Fig. 4a). This genomic validation assay was planned in a way which allowed to perform four of the reactions simultaneously as part of a multiplex polymerase chain reaction since these four reactions share in total two forward and two reverse primers, and their amplicons differ sufficiently in length. This provides a suitable basis for initial screening of cell lines covering one integration PCR and all three multiple integration PCRs.

Next, we generated OCT1/CYP2C19 overexpressing cell lines in several combinations to perform functional studies later. For each cell line, a number of cell clones were screened by multiplex PCR. The result of this screening is shown in Fig. 4b for all cell clones used for transport experiments in this study. Considering the known limitations of multiplex PCR, we subsequently confirmed the results by performing single PCRs for each reaction and each cell line. Figure 4c shows the exemplary result of this single analysis for one of the analyzed clones which confirmed the findings of the multiplex reaction. Single PCRs for all other double-transfected cell clones used in this study are shown in Fig. S2. Sanger sequencing of the regions around the three FRT sites showed proper arrangement (Fig. S3), as indicated by PCR screening.

Quantification of gene expression. In a next step, we addressed the question of whether the integration of a second expression vector and the expression of a second gene of interest affects the expression of the first gene of interest and vice versa. For this, we analyzed the gene expression of selected cell clones, which had passed the genomic validation process. In particular, we compared the expression of OCT1 and CYP2C19 of single transfected cell lines to the double transfected ones and moreover analyzed whether the order of integration of both vectors affects the expression of the genes of interest (Fig. 4d). The OCT1 expression levels were highly similar among all analyzed cell lines. In the first place, the number of integrated vectors did not significantly affect the OCT1 expression (One-way ANOVA with post-hoc Tukey test) and secondly, the order of integration as shown by comparison of the OCT1/CYP2C19 (OCT1 in the pcDNA/FRT$_{puro}$ and CYP2C19 in pcDNA/FTR$_{hygro}$) and the CYP2C19/OCT1 (CYP2C19 in the pcDNA/FRT$_{puro}$ and OCT1 in pcDNA/FTR$_{hygro}$) cell lines did also not alter the level of gene expression. The same findings were made for the expression of CYP2C19. Its relative expression in all double-transfected cell lines shows no significant difference in comparison to the CYP2C19 only transfected cell line and the order of integration did not affect its expression as well. Moreover, the basal expression of OCT1 and CYP2C19 genes was negligible (not detected) in empty vector-transfected cell lines (data not shown) and cell lines not overexpressing these genes.

Functional validation. For the functional validation of this novel overexpression system, we performed cellular uptake and metabolism experiments with the OCT1/CYP2C19 generated cell lines. For this, the uptake via OCT1 and the metabolic activation of proguanil to cycloguanil via CYP2C19 were analyzed (Fig. 5). Both, the transporter and the phase I enzyme were previously known to be involved in the uptake and metabolism of proguanil[21,22]. Uptake of proguanil was remarkably increased in OCT1 overexpressing compared to non-overexpressing cell lines. However, the uptake as indicated by the reduction of extracellular proguanil as well as the accumulation of intracellular proguanil was highly similar in all different OCT1 overexpressing cell lines. This could be regardless of whether the cells were single or double transfected, of the order of integration (OCT1/CYP2C19 or CYP2C19/OCT1) and of whether the second expression vector was empty or carrying CYP2C19. Accumulation of cycloguanil was only observed in cell lines overexpressing CYP2C19. Nevertheless, it was highly increased in double-transfected cell lines co-overexpressing OCT1 as compared to cell lines overexpressing CYP2C19 alone. Additionally, a time-dependent increase of extracellular cycloguanil was also observed as a result of passive diffusion or the presence of endogenous transporters facilitating the export of cycloguanil. Both, the intracellular accumulation as well as the extracellular increase of cycloguanil, were indistinguishable within the two OCT1 and CYP2C19 overexpressing cell lines, but also within the single CYP2C19 and CYP2C19/mock-double transfected cell lines. Pharmacologically, these experiments demonstrate how remarkable a drug metabolic activity in a cell system is enhanced by combined overexpression of the relevant transport protein with the drug-metabolizing enzyme, compared to the enzyme alone.

Discussion

We established a robust transfection system for simultaneous overexpression of two different genes using several modifications of the Flp-In system[5–8], and confirmed the long-term stability of gene expression even in the absence of selection antibiotics. We demonstrated that the integration of a second expression vector in the Flp-In locus is not only possible, but also that expression of two genes of interest does not affect each other's expression, and expression levels are highly similar to single-overexpressing cells. Our protocol allows the generation and validation of isogenic cell lines within approximately four weeks. This system provides an ideal tool for studying the interaction of two proteins under well-defined conditions.

As one application from the area of pharmacogenomics pathway analysis, we demonstrated its value for understanding the distinct interactions between transporter mediated drug cell uptake and drug metabolism on the example of the uptake of proguanil and its metabolomic activation to cycloguanil. The obtained results were highly comparable to experiments performed with primary human hepatocytes[22], indicating our system might be suitable to partially replace drug metabolism analysis in primary human tissue. Moreover, only in the combination with the right transporter, the CYP2C19 overexpressing cells are highly efficient in biotransformation. Such systems may even be further developed for biosynthetic production purposes.

In previous publications, researchers showed the possibilities of multigene expression using the Flp-In system by two succeeding transfections[19]. This approach, however, is not just more laborious, since it requires two
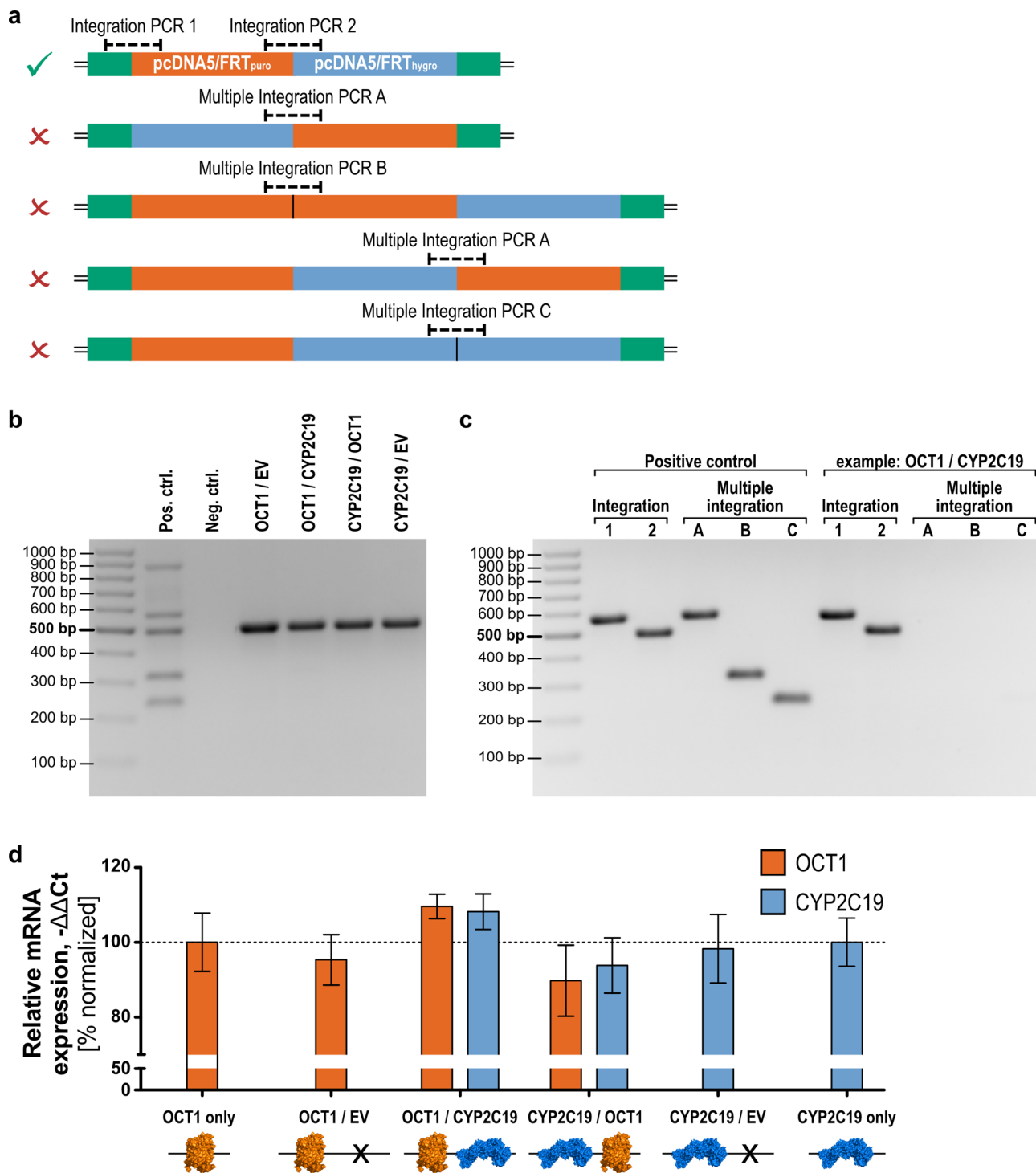
Figure 4. Validation of the double-Flp-In cell clones on genomic and transcriptional level. (**a**) Simultaneous integration of two vectors my lead to at least four unwanted combinations (red 'x') besides the intended one (green tick). (**b**) Screening of cell clones by multiplex PCR allowed verification of single integration of each vector (*EV* empty vector; primers as given in Table 1). (**c**) More precise single PCRs were used to validate correct integration for each cell clone, as shown here using one representative example. (**d**) OCT1 and CYP2C19 gene expression analysis of double-Flp-In cell clones compared to single transfected cell lines. Results of n = 3 independent experiments are shown. Gene expression was normalized to the OCT1 only or CYP2C19 only transfected cell lines, respectively. Figure (**d**) was created using GraphPad Prism version 5.01 for Windows, GraphPad Software, La Jolla, California, USA, www.graphpad.com. Protein icons of OCT1 and CYP2C19 were created using The PyMOL Molecular Graphics System, Version 1.3, Schrödinger, LLC, www.pymol.org.
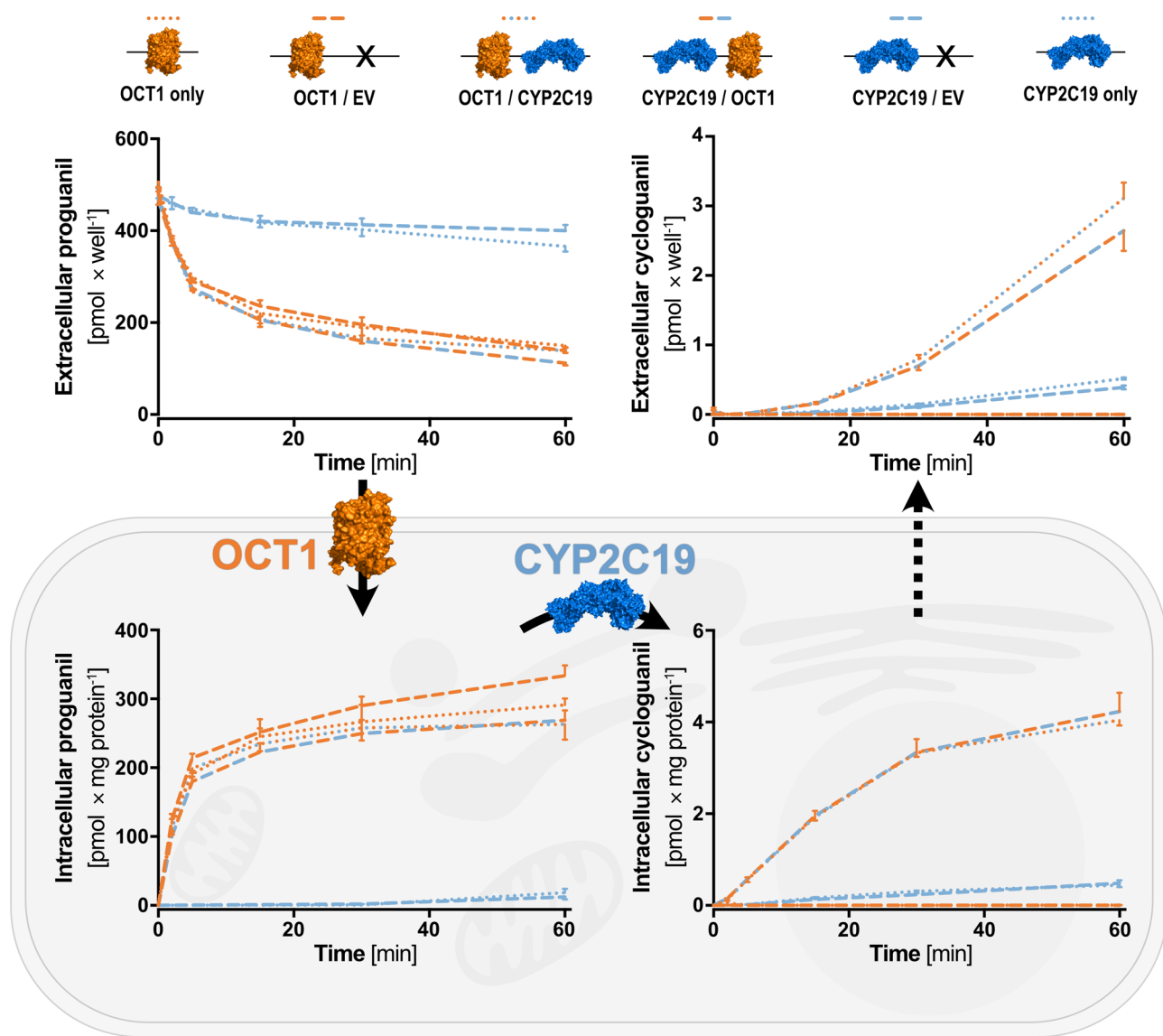
Figure 5. Transport and metabolism of proguanil via two simultaneously transfected genes. Overexpression of OCT1 facilitates the uptake of the anti-malarial prodrug proguanil, while overexpression of CYP2C19 catalyzes the metabolism of proguanil to cycloguanil. Accumulation of cycloguanil was only present in cells overexpressing OCT1 as well as CYP2C19. Results of n = 3 independent experiments are shown. Figure was created using GraphPad Prism version 5.01 for Windows, GraphPad Software, La Jolla, California, USA, www.graphpad.com. Protein icons of OCT1 and CYP2C19 were created using The PyMOL Molecular Graphics System, Version 1.3, Schrödinger, LLC, www.pymol.org.

consecutive transfections, it also goes along with clear disadvantages, when a single vector backbone is used: the lack of specific selection antibiotics for each gene of interest and the lack of validation on genomic level (and the early exclusion of clones with multiple integrated vectors from the validation process). The new vectors with novel frame shift matches could be conveniently used by other scientists, who used the Flp-In system as one part of their strategy for generating multiple transfectants[23,24]. These projects could profit from the simultaneous transfection of two Flp-In vectors, since the intermediate validation and screening procedure after conventional transfection could be skipped. In contrast to IRES-dependent expression of two genes of interest from a bicistronic vector, there is no effect on the expression level in our system[18].

Depending on the purpose, the here presented method can easily be modified or refined. The Flp-mediated recombination could be complemented by other recombination enzymes using specific integration sites. Also, modification of the FRT site could modulate specificity of the location of vector integration[25]. This means that several divergent genomic FRT sites could serve as target sites for analogously divergent FRT sites in vector, and recombination could be facilitated by the same enzyme at different sites simultaneously. The frame-dependent expression of the resistance gene only in the case of successful genomic integration is limited to two frames in the case of the FRT site—the third frame leads to a premature stop within the recombination site. Sequence

modifications or the use of other recombination enzymes with needs for different recombination sites could solve this issue potentially.

Limitations of the here presented method, such as the treatment with two antibiotics simultaneously, could apply to very sensitive cell lines. However, the use of only hygromycin could be sufficient to select double-transfected cells, because the resistance gene is only expressed after integration downstream to the pcDNA5/FRT$_{puro}$-fs vector. In preliminary experiments, 22 out of 25 cell clones with fluorescent genes of interest showed integration of both vectors after selection with only hygromycin. This might be useful when adapting the here presented protocol to different cell systems. A general problem of stable integration by site-specific recombinases (SSRs) is the integration in pseudosites with high homology to the recombination target site. This off-target activity of SSRs, however, is lower than by other site-specific DNA integration systems[10].

Double transfections using the method shown here or possible further adoptions to triple or quadruple transfections may serve a scientifically very important bridging between the study of single genes and complex systems biology studies of a large number of genes. Overall we believe that this technique will be helpful in the near future to not only investigate the associations among pharmacogenes, but will be useful when studying gene interactions, and could be extended to three or more genes of interest.

Methods

Modification of the original vector pcDNA5/FRT.   To match the introduced frame shift between the promoter and the FRT site, the original Flp-In vector pcDNA5/FRT (Thermo Fisher Scientific, Darmstadt, Germany) was modified by deletion of one cytosine (C1590del) and termed pcDNA5/FRT$_{hygro}$-fs here. This modification was achieved by site-directed mutagenesis[26]. For this, 1.0 µL (50 ng) of the pcDNA5/FRT vector was mixed with 5 µL Q-Solution (Qiagen, Hilden, Germany), 2.5 µL 10×KOD buffer (KOD Hot Start DNA Polymerase Kit; Merck, Darmstadt, Germany), 2.5 µL dNTPs (2 mM each), 1 µL MgSO$_4$ (25 mM), 0.65 µL forward primer SDM_hygro_fwd (5′-GTATAGGAACTTCCTTGGCAAAAAGCCTGAACTCACC-3′), 0.65 µL reverse primer SDM_hygro_rev (5′-GGTGAGTTCAGGCTTTTTGCCAAGGAAGTTCCTATAC-3′), 0.5 µL HotStart KOD Polymerase and 11.2 µL H$_2$O, and PCR was carried out at 95 °C for 3 min, followed by 20 cycles of 95 °C for 30 s, 63 °C for 45 s, and 72 °C for 4 min. The product was digested with DpnI. For this, 25 µL of the PCR product were mixed with 3 µL cut smart buffer (New England Biolabs, Ipswich, USA) and 1.5 µL DpnI (20 units/mL; New England Biolabs) and incubated at 37 °C for 1 h. After this, further 1 µL DpnI was added and the mixture was incubated at 37 °C for one more hour. The product was dialyzed and transformed into E.coli using an *Electroporator Gene Pulser II* (Bio-Rad Laboratories, Hercules, California, USA) for clonal amplification prior to sequence validation.

Generation of second vector (pcDNA5/FRT$_{puro}$).   The second vector was built to include the same promoter as in the Flp-In host cell line (from vector pcDNA5/lacZeo, Thermo Fisher Scientific) including the FRT site, the puromycin resistance gene, and the backbone of the regular pcDNA5/FRT vector. To distinguish the two vectors by PCR, we also introduced a unique sequence, at which primers could bind for the eventual validation. For cloning, the three different fragments were generated by PCR using hybrid primers to generate overlapping amplicons (Fig. S1). The fragments of the puromycin resistance gene and the SV40 promoter/FRT region were then fused by overlap-extension PCR[27] and recombined with the pcDNA5 backbone by sequence and ligation independent cloning[28–30].

To amplify the pcDNA5 backbone, 10 µL Q-solution (Qiagen, Hilden, Germany), 5 µL 10×KOD buffer (KOD Hot Start DNA Polymerase Kit; Merck, Darmstadt, Germany), 5 µL dNTPs (2 mM each), 3 µL MgSO$_4$ (25 mM), 1.5 µL forward primer PuroR_p5_fwd (5′-ᴄᴀᴄɢᴀᴄᴄᴄᴄᴀᴛɢGGCTGGATGATCCTCCAGCG-3′), 1.5 µL reverse primer SV40/FRT_p5_rev (5′-ɢᴀᴄᴀᴄɢᴛᴀᴄɢᴛᴀᴄɢᴛGGCGAACGTGGCGAGAAAGG-3′), 1 µL HotStart KOD polymerase, 1.5 µL pcDNA5/FRT DNA (100 ng) and 21.5 µL H$_2$O were mixed and PCR was carried out at 95 °C for 2 min, followed by 35 cycles of 95 °C for 30 s, 68.1 °C for 30 s, 72 °C for 5 min and completed at 72 °C for 10 min. The PCR product was DpnI digested to remove template DNA interfering with subsequent cloning steps as described above. The PCR for the amplification of the SV40 promoter region and the FRT site was composed of 10 µL Q-solution, 5 µL 10×KOD buffer, 5 µL dNTPs (2 mM each), 3 µL MgSO$_4$ (25 mM), 1.5 µL forward primer p5_SV40/FRT_fwd (5′-ɢᴄᴄᴀᴄɢᴛᴀᴄɢᴛᴀᴄɢᴛGTCAGTTAGGGTGTGGAAAG-3′), 1.5 µL reverse primer PuroR_SV40/FRT_rev (5′-ᴛᴄɢɢᴛɢɢᴄᴄᴀᴀɢGAAGTTCCTATACTTTCTAGAG-3′), 1 µL HotStart KOD polymerase, 1.5 µL pcDNA5/lacZeo DNA (100 ng) and 21.5 µL H$_2$O and carried out at 95 °C for 2 min, followed by 35 cycles of 95 °C for 30 s, 64.9 °C for 30 s, 72 °C for 1 min and completed at 72 °C for 10 min. To amplify the puromycin resistance gene, 10 µL Q-solution, 5 µL 10×KOD buffer, 5 µL dNTPs (2 mM each), 3 µL MgSO$_4$ (25 mM), 1.5 µL forward primer SV40/FRT_PuroR_fwd (5′-ᴛᴛᴄᴄᴛᴛɢɢᴄᴄACCGAGTACAAGCCCACGG-3′), 1.5 µL reverse primer p5_PuroR_rev (5′-ᴛᴄᴀᴛᴄᴄᴀɢᴄᴄCATGGGGTCGTGCGCTCC-3′), 1 µL HotStart KOD polymerase, 1.5 µL of a puromycin resistance gene-containing vector (100 ng) and 21.5 µL H$_2$O were mixed and PCR was carried out at 95 °C for 2 min, followed by 35 cycles of 95 °C for 30 s, 68.1 °C for 30 s, 72 °C for 2 min and completed at 72 °C for 10 min.

For the recombination of the 'SV40 promoter-FRT' region and the puromycin resistance gene, overlap-extension PCR composed of 10 µL Q-Solution, 5 µL 10×KOD buffer, 5 µL dNTPs (2 mM each), 3 µL MgSO$_4$ (25 mM), 5 µL purified PCR product of SV40/FRT PCR (60 ng/µL), 5 µL purified PCR product of puromycin resistance gene (109 ng/µL; equimolar ratio), 1 µL HotStart KOD polymerase and 17 µL H$_2$O was performed at 95 °C for 2 min, followed by 35 cycles of 95 °C for 30 s, 50 °C for 45 s, 72 °C for 2 min and completed at 72 °C for 10 min. Subsequently, 2 µL of the PCR product were mixed with 10 µL Q-Solution, 5 µL 10×KOD buffer, 5 µL dNTPs (2 mM each), 3 µL MgSO$_4$ (25 mM), 1.3 µL forward primer p5_SV40/FRT_fwd (5′-ɢᴄᴄᴀᴄɢᴛᴀᴄɢᴛᴀᴄɢᴛ-GTCAGTTAGGGTGTGGAAAG-3′), 1.3 µL reverse primer p5_PuroR_rev (5′-ᴛᴄᴀᴛᴄᴄᴀɢᴄᴄCATGGGGTCGTG

CGCTCC-3′), 1 µL HotStart KOD polymerase and 22.4 µL H$_2$O and incubated at 95 °C for 2 min, followed by 35 cycles of 95 °C for 30 s, 50 °C for 45 s, 72 °C for 3 min and completed at 72 °C for 10 min.

The final vector was recombined by sequence and ligation independent cloning[28–30]. For this, 6 µL of the purified pcDNA5/FRT backbone (60 ng) were mixed with 1.44 µL purified product of the overlap-extension PCR (1:3 vector to insert molar ratio), 1 µL 10 × BSA (New England Biolabs, Ipswich, USA), 1 µL 10 × NEB Buffer 2.1 (New England Biolabs), 0.56 µL H$_2$O and 0.5 µL T4 DNA polymerase (3 units/µL; New England Biolabs), incubated at 50 °C for 40 s and subsequently kept on ice for 10 min. After this, dialysis was performed and the dialyzed product was electroporated into One Shot TOP10 Electrocomp *E. coli*. Obtained bacterial clones were screened via colony PCR and correct assembly of the plasmid was confirmed by sequencing.

The created plasmid pcDNA5/FRT$_{puro}$ was modified by site-directed mutagenesis to correct the FRT site, since the FRT site present in the provided pcDNA5/lacZeo differs in one nucleotide from the one present in the original pcDNA5/FRT vector, and to introduce a frame shift (C1757ins) matching the reading frame of the pcDNA5/FRT$_{hygro}$-fs vector. For this, 0.6 µL (50 ng) of the pcDNA5/FRT$_{puro}$ vector were mixed with 5 µL Q-Solution, 2.5 µL 10 × KOD buffer, 2.5 µL dNTPs (2 mM each), 1 µL MgSO$_4$ (25 mM), 0.65 µL forward primer SDM_puro_fwd (5′-CATGG**C**AGAAGTT**C**CTATTCCGAAGTTCC-3′), 0.65 µL reverse primer SDM_puro_rev (5′-AATAG**G**AACTTCT**G**CCATGGTAGCCTCC-3′), 0.5 µL HotStart KOD Polymerase and 11.2 µL H$_2$O and PCR was carried out at 95 °C for 3 min, followed by 20 cycles of 95 °C for 30 s, 58.1 °C for 45 s, 72 °C for 3 min and completed at 72 °C for 10 min. The product was DpnI digested as described above and transformed into E.coli prior to sequence validation. The obtained vector was termed pcDNA5/FRT$_{puro}$-fs hereafter.

Cloning CYP2C19 from human liver RNA.   Human liver total RNA (TaKaRa Bio, Kusatsu, Japan) was used to clone CYP2C19. For this, 1 µL RNA (1 µg) was diluted by adding 16.75 µL RNase-free water, mixed with 1 µL gene-specific primers (5′-GAGGAAAGAGAGCTGCAGGG-3′), incubated at 72 °C for 10 min and subsequently cooled down to room temperature. After this, 6 µL 5 × RT buffer (SuperScript II Reverse Transcriptase Kit; Thermo Fisher Scientific, Darmstadt, Germany), 3.5 µL DTT (0.1 M), 1 µL dNTPs (2 mM each), 0.5 µL RNase inhibitor (40 U/µL) and 0.25 µL SuperScript II Reverse Transcriptase (200 U/µL) were added and reverse transcription was carried out at 42 °C for 1 h before temperature was raised to 75 °C for 15 min. Synthesized cDNA was amplified with primers containing restriction sites for eventual cloning with HindIII and EcoRV (see Table 1). The PCR for the amplification was composed of 10 µL Q-solution, 5 µL 10 × KOD buffer, 5 µL dNTPs (2 mM each), 2 µL MgSO$_4$ (25 mM), 1.3 µL forward primer CYP2C19_HindIII_fwd (5′-AAGAGGAGaagcttACCATGGATCCTTTTGTGGTCCTTG-3′), 1.3 µL reverse primer CYP2C19_EcoRV_rev (5′-CATCTGTgatatcTCAGACAGGAATGAAGCACAGC-3′), 1 µL HotStart KOD polymerase, 2.0 µL cDNA template and 22.4 µL H$_2$O and carried out at 95 °C for 3 min, followed by 35 cycles of 95 °C for 30 s, 61 °C for 30 s, 72 °C for 2:30 min and completed at 72 °C for 10 min. After amplification, the CYP2C19 was subcloned by TOPO cloning using the TOPO XL PCR Cloning Kit (Thermo Fisher Scientific, Darmstadt, Germany) following the instructions of the manufacturer. Sequencing revealed two single nucleotide polymorphisms: c.99C>T (rs17885098; synonymous) and c.991A>G (rs3758581, p.ile331val). Both polymorphisms define the *1B variant of CYP2C19, which is not associated with changes in its in vitro catalytic activity[31] and additionally the most abundant variant in the global population[32–34]. It was therefore used for further cloning into the expression vectors and for performing transport and metabolism experiments.

Transfection protocol.   Generally, cell lines used in this study were cultivated in DMEM culture medium (Thermo Fisher Scientific, Darmstadt, Germany) which was supplemented with 10% fetal calf serum (FCS; Thermo Fisher Scientific, Darmstadt, Germany) and penicillin/streptomycin (100 units/mL, 100 µg/mL; Thermo Fisher Scientific, Darmstadt, Germany) unless explicitly described differently. Cells were cultured at 37 °C in a humidified atmosphere (5% CO$_2$, 95% relative humidity). All experiments were carried in HEK293 T-REx cells (Thermo Fisher Scientific, Darmstadt, Germany).

For transfection of HEK293 T-REx cells, one million cells were plated for each transfection in a 6-well plate 24 h in advance. On the day of transfection, for double transfections, 200 ng of each expression plasmid in midi-prep quality were mixed with 3.6 µg pOG44 encoding the Flp recombinase in 100 µL DMEM. For single transfections, 400 ng of expression plasmid was mixed with 3.6 µg pOG44 encoding the Flp recombinase in 100 µL DMEM. Additionally, 12 µL *FuGene 6* transfection reagent (Promega Corporation, Walldorf, Germany), were added to 100 µL DMEM. After an incubation period of 5 min at room temperature, both solutions were mixed by repetitive pipetting and incubated for another 15 min at room temperature. In the meantime, the cells were washed once with 2 mL DMEM with 10% FCS and 1.8 mL fresh DMEM with 10% FCS were added to the cells. After incubation, the 200 µL DNA-*FuGene 6* was pipetted dropwise onto the cells. After 24 h, the cell culture medium was replaced by DMEM with 10% FCS and penicillin–streptomycin. On the next day (48 h post transfection), cells were transferred to a 100 mm petri dish. After 24 h, the selection was performed by adding hygromycin B (final concentration 200 µg/mL; Thermo Fisher Scientific, Darmstadt, Germany) and puromycin (final concentration 0.25 µg/mL; Thermo Fisher Scientific, Darmstadt, Germany). Five days later, the supernatant was replaced by fresh cell culture medium containing hygromycin and puromycin. Around ten days after selection started, single colonies were picked. For this, cells were washed once with culture medium to remove dead cells and finally the medium was completely removed. Single colonies were resuspended in 2 µL medium and transferred to a 24-well-plate, where 1 mL culture medium with a reduced concentration of the selection antibiotics (hygromycin: 50 µg/mL, puromycin: 0.025 µg/mL) had been placed in advance. After reaching a confluence of 70–80%, cells were transferred to a 6 well plate and later to a T25 culture flask. When cells were passaged the first time, 40% of cells were used to prepare cell pellets for DNA and RNA extraction each, to allow validation

Primers used for generation of pcDNA5/FRT$_{puro}$ vector			
Fragment	**Primer**	**Sequene (5′–3′)**	**Amplicon size (bp)**
pcDNA5 backbone	PuroR_p5_fwd	cacgaccccaTGGGCTGGATGATCCTCCAGCG	3,834
	SV40/FRT_p5_rev	gacacgtacgtacgtGGCGAACGTGGCGAGAAAGG	
Puromycin resistance	SV40/FRT_PuroR_fwd	ttccttggccACCGAGTACAAGCCCACGG	669
	p5_PuroR_rev	tcatccagccCATGGGGTCGTGCGCTCC	
SV40 promotor-FRT region	p5_SV40/FRT_fwd	gccacgtacgtacgtGTCAGTTAGGGTGTGGAAAG	395
	PuroR_SV40/FRT_rev	tcggtggccaagGAAGTTCCTATACTTTCTAGAG	
Primers used for site-directed mutagenesis			
Vector	**Primer**	**Sequence (5′–3′)**	**Amplicon size (bp)**
pcDNA5/FRT$_{hygro}$	SDM_hygro_fwd	GTATAGGAACTTCCTTGGC-AAAAAGCCTGAACTCACC	N/A
	SDM_hygro_rev	GGTGAGTTCAGGCTTTTT-GCCAAGGAAGTTCCTATAC	
pcDNA5/FRT$_{puro}$	SDM_puro_fwd	CATGG**C**AGAAGTT**C**CTATTCCGAAGTTCC	N/A
	SDM_puro_rev	AATAG**G**AACTTCT**G**CCATGGTAGCCTCC	
Primers used for cloning of CYP2C19			
Reaction	**Primer**	**Sequence (5′–3′)**	**Amplicon size (bp)**
Reverse transcription	CYP2C19_GSP_rev	GAGGAAAGAGAGCTGCAGGG	N/A
Introduction of restriction sites	CYP2C19_HindIII_fwd	AAGAGGAGaagcttACCATGGATCCTTTTGTGGTCCTTG	1516
	CYP2C19_EcoRV_rev	CATCTGTgatatcTCAGACAGGAATGAAGCACAGC	
Primers used for Validation PCRs			
Reaction	**Primer**	**Sequence (5′–3′)**	**Amplicon size (bp)**
Integration PCR 1	P$_{SV40}$	AGCTGTGGAATGTGTGTCAGTTAGG	559
	P$_{puro\_r}$	CGACGCGCGTGAGGAAGAGTTCTTG	
Integration PCR 2	P$_{uni\_f}$	CGTTCGCCACGTACGTACGTGTCAG	489
	P$_{hyr\_r}$	CTTCGCCCTCCGAGAGCTGCATCAG	
Multiple Integration PCR A	P$_{uni\_f}$	CGTTCGCCACGTACGTACGTGTCAG	564
	P$_{puro\_r}$	CGACGCGCGTGAGGAAGAGTTCTTG	
Multiple Integration PCR B	P$_{FRT\_f}$	AATCGGGGGCTCCCTTTAGGGTTCC	313
	P$_{puro\_r}$	CGACGCGCGTGAGGAAGAGTTCTTG	
Multiple Integration PCR C	P$_{FRT\_f}$	AATCGGGGGCTCCCTTTAGGGTTCC	238
	P$_{hyr\_r}$	CTTCGCCCTCCGAGAGCTGCATCAG	
Primers used for quantitative RT-PCR			
Gene	**Primer**	**Sequence (5′-3′)**	**Amplicon size (bp)**
CYP2C19	P$_{CYP2C19\_f}$	CCTGATCAAAATGGAGAAGGAAAAG	99
	P$_{CYP2C19\_r}$	TCTGTCCCAGCTCCAAGTAAG	
HPRT1	P$_{HPRT1\_f}$	TGACACTGGCAAAACAATGCA	94
	P$_{HPRT1\_r}$	GGTCCTTTTCACCAGCAAGCT	
OCT1	P$_{OCT1\_f}$	TGTCACCGAAAAGCTGAGCC	96
	P$_{OCT1\_r}$	TCCGTGAACCACAGGTACATC	

Table 1. Primers used for PCR. The 5′-hybrid part of primers used for generation of overlapping amplicons for creation of the pcDNA5/FRT$_{puro}$ vector is shown by nucleotides in small capital letters. The unique sequence introduced into the generated vector is underscored. The newly introduced base into the pcDNA5/FRT$_{puro}$ vector for frame shift generation is marked in bold, the nucleotide substitution for the correction of the FRT site is highlighted by an italic, bold letter. The position of the single nucleotide deletion introduced into the pcDNA5/FRT$_{hygro}$ vector is shown by a hyphen. Endonuclease restriction sites are indicated by lower case letters.

of generated cell lines on genomic as well as on transcriptional level. Transfections were usually carried out in duplicates to ensure a sufficient number of clones to analyze.

The same protocol was independently performed in the Institute of Pharmacology and Toxicology at the Justus Liebig University in Giessen to stably transfect two versions of the sodium/bile acid transporter (NTCP) tagged with yellow or cyan fluorescent protein (NTCP-YFP, NTCP-CFP).

Validation of correct integration by PCR. The stable, genomic integration of both plasmids was validated by PCR. For this, the genomic DNA of 2×10^6 cells was isolated using the QIAGEN DNeasy Blood &

Tissue Kit (Qiagen, Hilden, Germany) in a QIACube robot (Qiagen) following the manufacturer's protocol. The isolated DNA was analyzed by multiplex PCR using the QIAGen Multiplex PCR Kit (Qiagen). This reaction covered the *Integration PCR 2* as well as the *Multiple Integration PCRs A-C* (for detailed primer information see Table 1). Multiplex PCR was composed of 5 μL 2×QIAGEN Multiplex PCR Master mix, 2 μL Q-Solution, 1 μL 10×primer mix (2 μM each), 1 μL genomic DNA (100 ng) and 1 μL H_2O. PCR was carried out at 95 °C for 15 min, followed by 35 cycles of 95 °C for 30 s, 62.7 °C for 90 s, 72 °C for 90 s and completed at 72 °C for 10 min. As a positive control, the genomic DNA of a cell clone validated for all types of multiple integrations was used. Cell clones passing the multiplex PCR screening were validated again by single PCRs (*Integration PCRs 1 and 2, Multiple Integration PCRs A-C*) composed of 5 μL 2×QIAGEN Multiplex PCR Master mix, 2 μL Q-Solution, 0.25 μL forward primer (10 μM), 0.25 μL reverse primer (10 μM), 1 μL genomic DNA (100 ng) and 1.5 μL ddH_2O using the same thermocycler conditions.

Sanger sequencing was performed on the products including the FRT sites. For the third FRT site, the primers P_{FRT_f} and P_{LacZ} (5′-CCTTCCTGTAGCCAGCTTTCATCAA-3′) under the same conditions as mentioned for single PCRs above. The resulting amplicons were separated on a 0.8% agarose gel, cut out and extracted using the QIAquick Gel Extraction Kit (Qiagen, Hilden, Germany). For sanger sequencing, 100 ng DNA were pre-mixed with 30 pmol of one of the primers used for amplification and sent to external sequencing by Microsynth Seqlab, Göttingen.

Tracking of eGFP/tdTomato double-transfected cells by flow cytometry. The stability of stable transfection was tracked by analyzing fluorescence signals of eGFP/tdTomato double-transfected cell lines over 30 passages. Two independently generated cell lines were cultured in parallel in DMEM cell culture medium with or without the culturing concentrations of hygromycin (50 μg/mL) and puromycin (0.025 μg/mL). Every second passage, cells were analyzed using a LSR II (BD Bioscience, Heidelberg, Germany) flow cytometer and the software BD FACSDiva (Version 6.1.3, BD Bioscience). Fluorescence intensities of green channel (laser excitation wavelength 488 nm) and red channel (laser excitation wavelength 561 nm) were plotted to determine double-positive cells. Thresholds for classifying cells as positive were set by comparing the fluorophore expressing cells to a mock-transfected control cell line.

Expression analyses. The RNeasy Plus Mini Kit (Qiagen, Hilden, Germany) was used according to the manufacturer's instructions for total RNA isolation. Briefly, 1 to 2×10^6 cells were harvested by centrifugation at 500×*g* for 5 min at RT. The pellet was dissolved in 350 μL of RLT buffer supplemented with 1% β-mercaptoethanol (v/v). The automatic isolation was performed using a QIAcube (Qiagen, Hilden, Germany), in which the genomic DNA eliminator spin column removed the genomic DNA and total RNA was eluted in 50 μL of RNAse free ddH_2O.

The cDNA synthesis from isolated RNA was performed using the SuperScript II Reverse Transcriptase Kit (Thermo Fisher Scientific, Darmstadt, Germany). Three μg RNA was diluted in 17.75 μL of RNAse free ddH_2O. Primer annealing was initiated with the addition of 1 μL anchored-dT primer (10 μM) and incubation at 70 °C for 10 min. To initiate cDNA synthesis, 11.25 μL of a reverse transcription reaction mix [6 μl 5×Superscript RT buffer, 3.5 μL DTT (0.1 M), 1 μL dNTPs (10 mM), 0.5 μL RNase Inhibitor P/N (40 U/μL), 0.25 μL SuperScript II Reverse Transcriptase (200 U/μL)] were added and incubated at 42 °C for one hour. Afterward, enzyme denaturation was done by increasing the temperature to 75 °C for 15 min. To this 30 μL synthesized cDNA, 70 μL of RNAse free ddH_2O were added and concentration was further adjusted to 3 ng/μL cDNA by 1:10 dilution.

HOT FIREPol EvaGreen qPCR Mix Plus (ROX) kit (Solis BioDyne, Tartu, Estonia) was used to perform the real-time qPCR. Briefly, the reaction mixture constituted 2 μL 5×EvaGreen qPCR Mix, 5.6 μL ddH_2O, 0.4 μL primer mix (10 μM each; HPRT1: forward (5′-TGACACTGGCAAAACAATGCA-3′), reverse (5′-GGTCCTTTT CACCAGCAAGCT-3′); OCT1: forward (5′-TGTCACCGAAAAGCTGAGCC-3′), reverse (5′-TCCGTGAAC CACAGGTACATC-3′), CYP2C19: forward (5′-CCTGATCAAAATGGAGAAGGAAAAG-3′), reverse (5′-TCT GTCCCAGCTCCAAGTAAG-3′)), 2 μL cDNA (6 ng total). Standard curve analysis for each primer pair was performed to check the primer efficiency and amplification of a single specific amplicon. To do so, five concentrations of a cDNA pool in a 1:5 dilution series were distributed in a 384 well-plate and amplification was performed in TaqMan 7900HT (Applied Biosystems, Darmstadt, Germany) machine. SDS 1.2 software (Applied Biosystems, Darmstadt, Germany) was used to identify the Cycle threshold (Ct) value. The Primer efficiency was well within the accepted range, namely 107% (HPRT1), 101% (OCT1), and 99% (CYP2C19)[35]. Subsequently, expression levels of OCT1 and CYP2C19 genes, along with the housekeeping gene HPRT1, were measured in technical and biological triplicate manner. The ΔΔCt method was used for expression analysis[36]. Relative expression against single transfected OCT1 and CYP2C19 cell lines were calculated based on this equation:

$$\text{Relative expression} = 2^{-\left[(\text{Ct experimental} - \text{Ct housekeeping experimental}) - (\text{Ct control} - \text{Ct housekeeping control})\right]} = 2^{-[\Delta\Delta Ct]}$$

Transport experiments. Functional validation of the stably integrated genes was performed via transport and metabolism of proguanil. Two days ahead of the transport experiment, 600,000 cells were plated in poly-ᴅ-lysine pre-coated 12-well-plates. On the day of experiment, cells were washed once with 2 mL 37 °C pre-warmed Hanks buffered saline solution (Thermo Fisher Scientific, Darmstadt, Germany) containing 10 mM HEPES (Sigma-Aldrich, Taufkirchen, Germany; from here on named HBSS+) followed by incubation with HBSS+ containing 1 μM Proguanil (Sigma-Aldrich, Taufkirchen, Germany). After 2, 5, 15, 30 and 60 min, the incubation was stopped by collecting the supernatant and cells were immediately washed twice with 1 mL ice-cold HBSS+ and cells were lysed by adding 500 μL lysis buffer [acetonitrile:water 4:1 (v/v)] containing 10 ng/μL

proguanil-d6 (Toronto Research Chemicals, North York, Canada) and 10 ng/µL desvenlafaxine (Sigma-Aldrich, Taufkirchen, Germany) as an internal standard for mass spectrometry analysis. For sample preparation, cell lysates were centrifuged in a desktop centrifuge at maximum speed for 15 min, 400 µL were transferred into a collection plate, evaporated at 40 °C under nitrogen flow and the dry residues were dissolved in 250 µL 0.1% formic acid. For the processing of cell supernatant, samples were centrifuged at 400×g for 5 min. After this, 400 µL was transferred to a new reaction tube and 800 µL of precipitation reagent [acetonitrile:methanol 10:1 (v/v) containing the same internal standards as described above] were added and the mixture was incubated for 15 min on a rotation shaker. Precipitated protein was pelleted by centrifugation at full-speed in a desktop centrifuge for 15 min, 800 µL of the supernatant was used for evaporation and dry residues were dissolved in 250 µL 0.1% formic acid for analysis as well.

LC–MS/MS determination of proguanil transport and metabolism. Concentrations of proguanil and cycloguanil were quantified by high-performance liquid chromatography coupled to mass spectrometry. For sample separation, we used a Shimadzu Nexera 2 UHPLC system containing an auto-sampler SIL-30AC, a communications bus module CBM-20A, a liquid chromatograph LC-30AD, a column oven CTO-20AC and a Brownlee SPP RP-Amide column (4.6×100 mm inner dimension with 2.7 µm particle size) with a C18 pre-column. For chromatography, an aqueous mobile phase containing 20% organic additive (acetonitrile:methanol 6:1 (v/v)) was used with a flow gradient starting with 0.3 mL/min for the first 4.5 min, increased to 0.7 mL/min at 4.6 min and back to 0.3 mL/min from 9.0 to 9.1 min, which was left for another two minutes to reconstitute the original conditions for the next measurement. The HPLC system was coupled with an API 4000 tandem mass spectrometer (AB SCIEX, Darmstadt, Germany), which enabled the detection of substrates via specific LC retention times and mass transitions in MRM mode with parameters given in Table S1. The quantification was performed by integration of the peak areas using the Analyst software (Version 1.6.2, AB SCIEX, Darmstadt, Germany). Concentrations of proguanil and cycloguanil (Santa Cruz Biotechnology, Heidelberg, Germany) were determined by simultaneous measurement of a standard curve with known concentrations. To calculate the net uptake of proguanil, the measurement of an empty vector-transfected cell line was subtracted from the other cell lines to take passive diffusion and endogenous transporters into account.

Total protein quantification. Results of cellular transport experiments were normalized to the total amount of protein per well to compensate differences in cell density. For this, the total protein of one well per cell line in each transport experiment was quantified using a BCA assay. Cells were lysed by incubation with 500 µL RIPA buffer for 10 min. Five microliter of each sample were incubated after adding 200 µL bicinchoninic acid with 0.008% copper sulfate at 37 °C for 30 min. Subsequently, the absorbance at a wavelength of 570 nm was measured using a *Tecan Ultra microplate reader* (Tecan Group, Männedorf, Switzerland). The protein concentration was quantified by comparison to a standard curve using bovine serum albumin.

Tracking of double-transfected cells by microscopy. HEK293-Flp-In cells stably transfected by our Double-Flp-In Method with NTCP-CFP and NTCP-YFP, a classical Foerster Resonance Energy Transfer (FRET) pair, were seeded onto IBIDI chamber-slides to reach confluency at the day of microscopy. For comparison HEK293-MSR cells were seeded like above and were transiently transfected with Lipofectamine 2000 (Thermo Fisher Scientific, Darmstadt, Germany) with an equimolar number of premixed plasmids of pcDNA5 vectors coding for NTCP-CFP or NTCP-YFP both under the control of the identical CMV-promoter, which is also applied by the Double-Flp-In Method. After 48 h of standard incubation, slides were washed twice with PBS and transferred to microscopy at room temperature covered in PBS. Images were taken with a Leica DMI6000 B inverted fluorescent microscope at 40× objective magnification. For qualitative analysis and comparison of expression levels and patterns of the fluorescent proteins CFP and YFP channels were adjusted to yield similar signal intensities. Phase contrast channel was applied to demonstrate the confluency of the cell layer and transfection rates. Staining of the cell nuclei and the fixation of the cells was deliberately avoided to not interfere with CFP and YFP signals.

References

1. Drexler, H. G. & Matsuo, Y. Guidelines for the characterization and publication of human malignant hematopoietic cell lines. *Leukemia* **13**, 835–842. https://doi.org/10.1038/sj.leu.2401428 (1999).
2. Mirabelli, P., Coppola, L. & Salvatore, M. Cancer cell lines are useful model systems for medical research. *Cancers* https://doi.org/10.3390/cancers11081098 (2019).
3. Adamson, A. D., Jackson, D. & Davis, J. R. Novel approaches to in vitro transgenesis. *The Journal of endocrinology* **208**, 193–206. https://doi.org/10.1677/JOE-10-0417 (2011).
4. Prelich, G. Gene overexpression: uses, mechanisms, and interpretation. *Genetics* **190**, 841–854. https://doi.org/10.1534/genetics.111.136911 (2012).
5. O'Gorman, S., Fox, D. T. & Wahl, G. M. Recombinase-mediated gene activation and site-specific integration in mammalian cells. *Science* **251**, 1351–1355. https://doi.org/10.1126/science.1900642 (1991).
6. Turan, S. & Bode, J. Site-specific recombinases: from tag-and-target- to tag-and-exchange-based genomic modifications. *FASEB J.* **25**, 4088–4107. https://doi.org/10.1096/fj.11-186940 (2011).
7. Akopian, A. & Marshall Stark, W. *Advances in Genetics* 1–23 (Academic Press, New York, 2005).

8. Hallet, B. & Sherratt, D. J. Transposition and site-specific recombination: adapting DNA cut-and-paste mechanisms to a variety of genetic rearrangements. *FEMS Microbiol. Rev.* **21**, 157–178. https://doi.org/10.1111/j.1574-6976.1997.tb00349.x (1997).

9. Turan, S. *et al.* Recombinase-mediated cassette exchange (RMCE): traditional concepts and current challenges. *J. Mol. Biol.* **407**, 193–221. https://doi.org/10.1016/j.jmb.2011.01.004 (2011).

10. Olorunniji, F. J., Rosser, S. J. & Stark, W. M. Site-specific recombinases: molecular machines for the genetic revolution. *Biochem. J.* **473**, 673–684. https://doi.org/10.1042/bj20151112 (2016).

11. Seitz, T. *et al.* Global genetic analyses reveal strong inter-ethnic variability in the loss of activity of the organic cation transporter OCT1. *Genome Med.* **7**, 56. https://doi.org/10.1186/s13073-015-0172-0 (2015).

12. Bakhaus, K. *et al.* The polymorphism L204F affects transport and membrane expression of the sodium-dependent organic anion transporter SOAT (SLC10A6). *J. Steroid Biochem. Mol. Biol.* **179**, 36–44. https://doi.org/10.1016/j.jsbmb.2017.09.017 (2018).

13. Wen, X., Joy, M. S. & Aleksunes, L. M. In vitro transport activity and trafficking of MRP2/ABCC2 polymorphic variants. *Pharm. Res.* **34**, 1637–1647. https://doi.org/10.1007/s11095-017-2160-0 (2017).

14. Lu, H. *et al.* A rapid Flp-In system for expression of secreted H5N1 influenza hemagglutinin vaccine immunogen in mammalian cells. *PLoS ONE* **6**, e17297. https://doi.org/10.1371/journal.pone.0017297 (2011).

15. Niss Arfelt, K. *et al.* Signaling via G proteins mediates tumorigenic effects of GPR87. *Cell. Signal.* **30**, 9–18. https://doi.org/10.1016/j.cellsig.2016.11.009 (2017).

16. Pelletier, J. & Sonenberg, N. Internal initiation of translation of eukaryotic mRNA directed by a sequence derived from poliovirus RNA. *Nature* **334**, 320–325. https://doi.org/10.1038/334320a0 (1988).

17. Attal, J., Theron, M. C., Puissant, C. & Houdebine, L. M. Effect of intercistronic length on internal ribosome entry site (IRES) efficiency in bicistronic mRNA. *Gene Exp.* **8**, 299–309 (1999).

18. Mizuguchi, H., Xu, Z., Ishii-Watabe, A., Uchida, E. & Hayakawa, T. IRES-dependent second gene expression is significantly lower than cap-dependent first gene expression in a bicistronic vector. *Mol. Ther.* **1**, 376–382. https://doi.org/10.1006/mthe.2000.0050 (2000).

19. Ward, R. J., Alvarez-Curto, E. & Milligan, G. Using the Flp-In T-Rex system to regulate GPCR expression. *Methods Mol. Biol.* **746**, 21–37. https://doi.org/10.1007/978-1-61779-126-0_2 (2011).

20. Bonapace, C. R., Bosso, J. A., Friedrich, L. V. & White, R. L. Comparison of methods of interpretation of checkerboard synergy testing. *Diagn. Microbiol. Infect. Dis.* **44**, 363–366. https://doi.org/10.1016/S0732-8893(02)00473-X (2002).

21. Wright, J., Helsby, N. & Ward, S. The role of S-mephenytoin hydroxylase (CYP2C19) in the metabolism of the antimalarial biguanides. *Br. J. Clin. Pharmacol.* **39**, 441–444. https://doi.org/10.1111/j.1365-2125.1995.tb04474.x (1995).

22. Matthaei, J. *et al.* OCT1 deficiency affects hepatocellular concentrations and pharmacokinetics of cycloguanil, the active metabolite of the antimalarial drug proguanil. *Clin. Pharmacol. Ther.* **105**, 190–200. https://doi.org/10.1002/cpt.1128 (2019).

23. Liu, X. *et al.* Establishment of Flp-In(TM) CHO cell lines with double expression of CYP2A13 and MRP2. *Chin. J. Cell. Mol. Immunol.* **35**, 865–871 (2019).

24. Tamura, A. *et al.* Genetic polymorphisms of human ABC transporter ABCG2: development of the standard method for functional validation of SNPs by using the Flp recombinase system. *J. Exp. Ther. Oncol.* **6**, 1–11 (2006).

25. Thieme, F., Engler, C., Kandzia, R. & Marillonnet, S. Quick and clean cloning: a ligation-independent cloning strategy for selective cloning of specific PCR products from non-specific mixes. *PLoS ONE* **6**, e20556. https://doi.org/10.1371/journal.pone.0020556 (2011).

26. Weiner, M. P. *et al.* Site-directed mutagenesis of double-stranded DNA by the polymerase chain reaction. *Gene* **151**, 119–123. https://doi.org/10.1016/0378-1119(94)90641-6 (1994).

27. Horton, R. M., Hunt, H. D., Ho, S. N., Pullen, J. K. & Pease, L. R. Engineering hybrid genes without the use of restriction enzymes: gene splicing by overlap extension. *Gene* **77**, 61–68. https://doi.org/10.1016/0378-1119(89)90359-4 (1989).

28. Li, M. Z. & Elledge, S. J. Harnessing homologous recombination in vitro to generate recombinant DNA via SLIC. *Nat. Methods* **4**, 251–256. https://doi.org/10.1038/nmeth1010 (2007).

29. Islam, M. N. *et al.* Optimizing T4 DNA polymerase conditions enhances the efficiency of one-step sequence- and ligation-independent cloning. *Biotechniques* **63**, 125–130. https://doi.org/10.2144/000114588 (2017).

30. Stevenson, J., Krycer, J. R., Phan, L. & Brown, A. J. A practical comparison of ligation-independent cloning techniques. *PLoS ONE* **8**, e83888. https://doi.org/10.1371/journal.pone.0083888 (2013).

31. Richardson, T. H. *et al.* A universal approach to the expression of human and rabbit cytochrome P450s of the 2C subfamily in *Escherichia coli. Arch. Biochem. Biophys.* **323**, 87–96. https://doi.org/10.1006/abbi.1995.0013 (1995).

32. Shirasaka, Y. *et al.* Interindividual variability of CYP2C19-catalyzed drug metabolism due to differences in gene diplotypes and cytochrome P450 oxidoreductase content. *Pharmacogenom. J.* **16**, 375–387. https://doi.org/10.1038/tpj.2015.58 (2016).

33. Jin, T. *et al.* Genotypephenotype analysis of CYP2C19 in the Tibetan population and its potential clinical implications in drug therapy. *Mol. Med. Rep.* **13**, 2117–2123. https://doi.org/10.3892/mmr.2016.4776 (2016).

34. Zhou, Q. *et al.* Genetic polymorphism, linkage disequilibrium, haplotype structure and novel allele analysis of CYP2C19 and CYP2D6 in Han Chinese. *Pharmacogenom. J.* **9**, 380–394. https://doi.org/10.1038/tpj.2009.31 (2009).

35. Bustin, S. & Huggett, J. qPCR primer design revisited. *Biomol. Detect Quant.* **14**, 19–28. https://doi.org/10.1016/j.bdq.2017.11.001 (2017).

36. Livak, K. J. & Schmittgen, T. D. Analysis of relative gene expression data using real-time quantitative PCR and the 2(-Delta Delta C(T)) Method. *Methods* **25**, 402–408. https://doi.org/10.1006/meth.2001.1262 (2001).

Acknowledgements

Author contributions

O.J., J.G., M.V.T. and J.B. designed the research. O.J., S.A., L.G., K.A.A.T.L. and S.F.M. performed the research and contributed to figure content. O.J., L.G., S.A., S.F.M. and J.B. wrote the article. All authors edited the manuscript.

Competing interests

The authors declare no competing interests.

Additional information

Supplementary information is available for this paper at https://doi.org/10.1038/s41598-020-71051-5.

Supplementary Information for:

A Double-Flp-In Method for Stable Overexpression of Two Genes

Ole Jensen[1#*], Salim Ansari[1#], Lukas Gebauer[1#], Simon F. Müller[2], Kira A. A. T. Lowjaga[2], Joachim Geyer[2], Mladen V. Tzvetkov[1,3], and Jürgen Brockmöller[1]

[#] These authors contributed equally to the work.

[1] Institute of Clinical Pharmacology, University Medical Center Göttingen, D-37075 Göttingen, Germany

[2] Institute of Pharmacology and Toxicology, Faculty of Veterinary Medicine, Justus Liebig University Giessen, D-35392 Giessen, Germany

[3] Institute of Pharmacology, Center of Drug Absorption and Transport (C_DAT), University Medical Center Greifswald, D-17489 Greifswald, Germany

Address for correspondence:

Ole Jensen
Institute of Clinical Pharmacology
University Medical Center Göttingen, Georg-August University
Robert-Koch-Str. 40
37075 Göttingen, Germany
E-Mail: ole.jensen@med.uni-goettingen.de
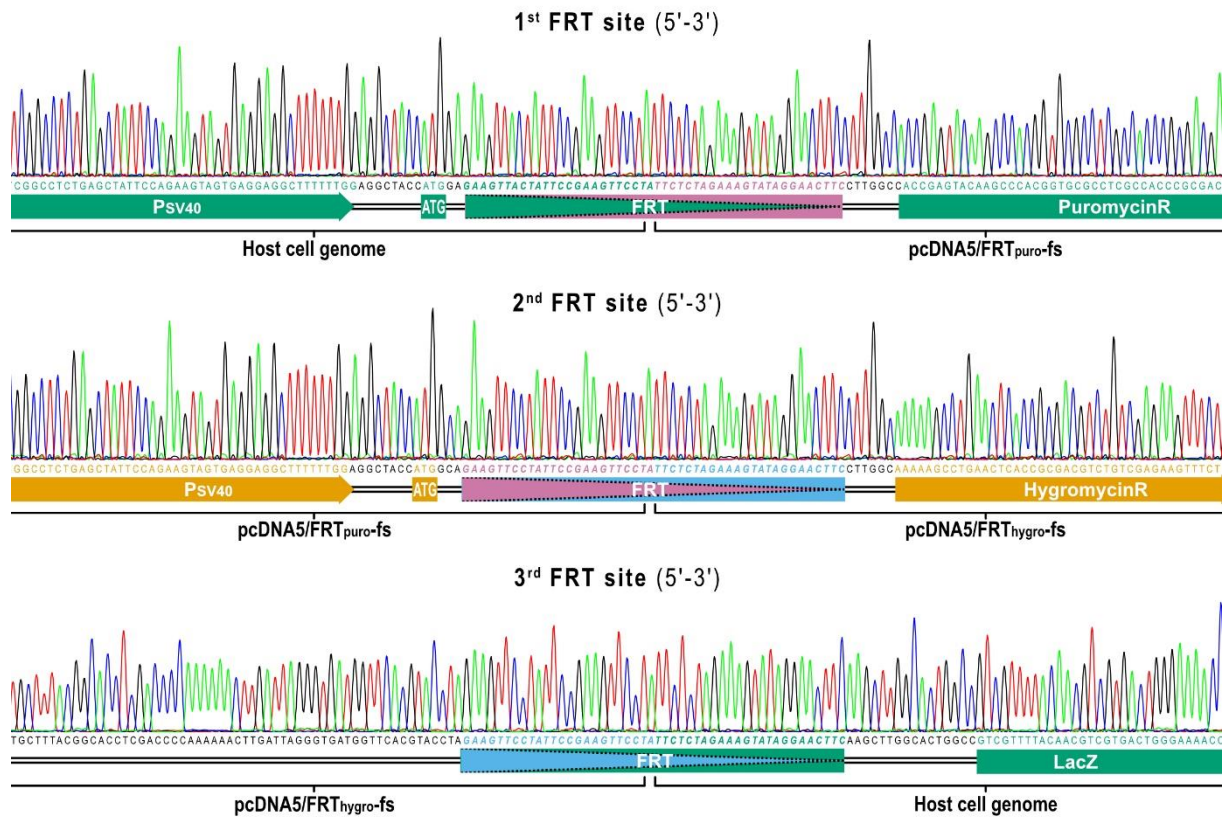Telephone: +49 551 39 65776
Fax: +49 551 39 12767
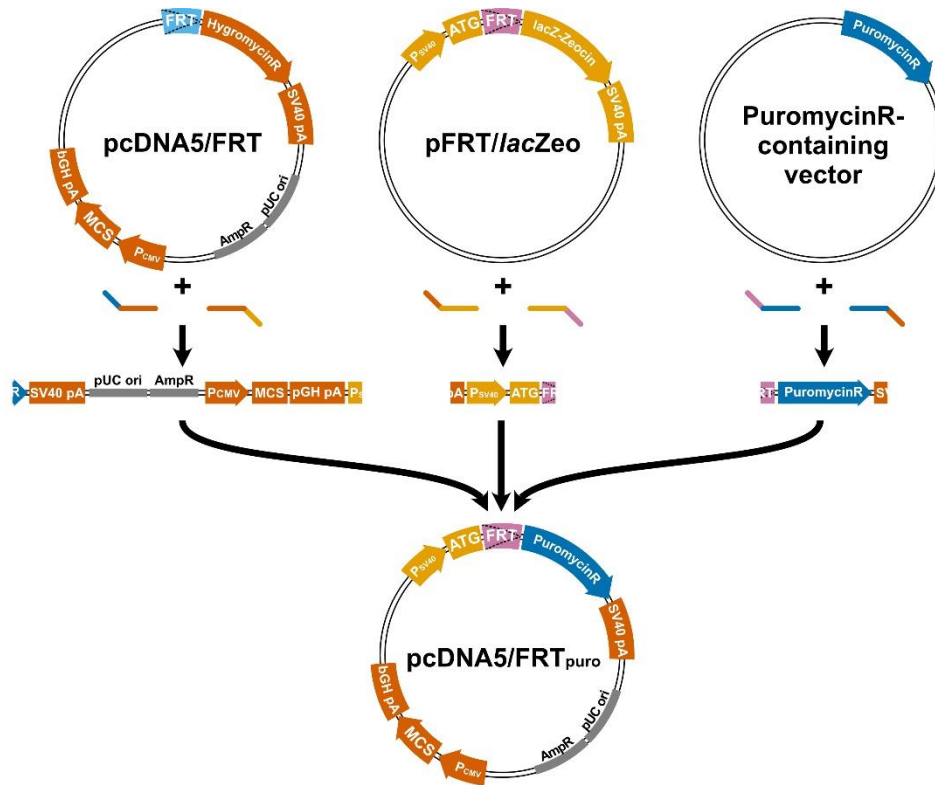
Figure S1: Illustration of vector creation. The newly generated vector pcDNA5/FRT$_{puro}$ was created by PCR amplification with primers including overhangs from two of the vectors that belong to the Flp-In™ system, pcDNA5/FRT and pFRT/lacZeo. The puromycin resistance cassette was cloned from a third puromycin resistance-containing vector by PCR amplification and sequence and ligation-independent cloning (SLIC).
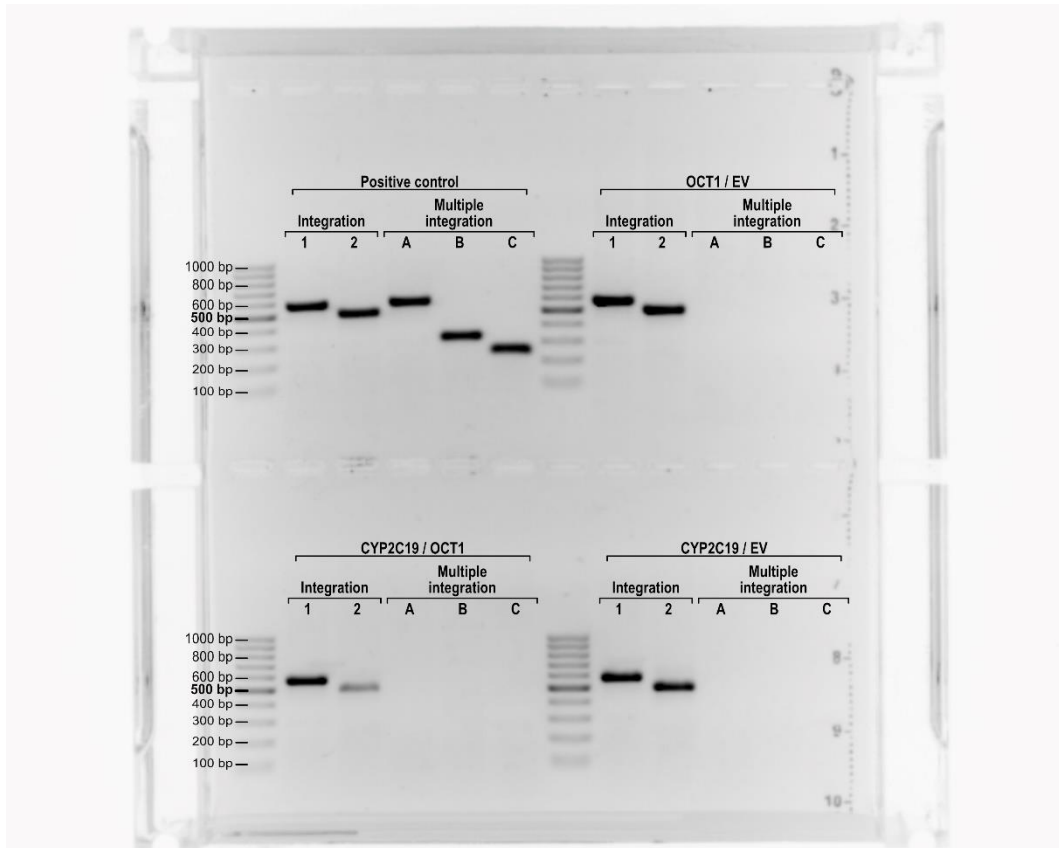
Figure S2: Validation of used cell clones by PCR. In addition to the initial screening by multiplex PCR (see Figure 4), the finally employed cell clones (OCT1/EV, CYP2C19/OCT1, CYP2C19/EV) were validated by single PCRs.

1st FRT site (5'-3')

`'CGGCCTCTGAGCTATTCCAGAAGTAGTGAGGAGGCTTTTTTGGAGGCTACCATGGAGAAGTTACTATTCCGAAGTTCCTATTCTCTAGAAAGTATAGGAACTTCCTTGGCCACCGAGTACAAGCCCACGGTGCGCCTCGCCACCCGCGAC`

Psv40 — ATG — *AAGTTACTATTCCGAAGTTCCTA* — FRT — PuromycinR

Host cell genome | pcDNA5/FRT_puro-fs

2nd FRT site (5'-3')

`GGCCTCTGAGCTATTCCAGAAGTAGTGAGGAGGCTTTTTTGGAGGCTACCATGGCAGAAGTTCCTATTCCGAAGTTCCTATTCTCTAGAAAGTATAGGAACTTCCTTGGCAAAAAGCCTGAACTCACCGCAGCGTCTGTCGAGAAGTTTCT`

Psv40 — ATG — *AAGTTCCTATTCCGAAGTTCCTA* — FRT — HygromycinR

pcDNA5/FRT_puro-fs | pcDNA5/FRT_hygro-fs

3rd FRT site (5'-3')

`TGCTTTACGGCACCTCGACCCCAAAAAACTTGATTAGGGTGATGGTTCACGTACCTAGAAGTTCCTATTCCGAAGTTCCTATTCTCTAGAAAGTATAGGAACTTCAAGCTTGGCACTGGCCGTCGTTTTACAACGTCGTGACTGGGAAAACC`

FRT — *AAGTTCCTATTCCGAAGTTCCTA* — LacZ

pcDNA5/FRT_hygro-fs | Host cell genome

Figure S3: Sequence validation of the three FRT sites including flanking regions. Sanger sequencing was performed on the cell clone OCT1/CYP2C19 to validate correct integration on nucleotide level. Sequences of the FRT sites are highlighted in ***bold italic***, while other functional elements are indicated in their respective color, as shown in Figure 2.

Table S1: Mass spectrometry detection parameters

Substance	Retention time (min)	Mass (Da) Q1	Mass (Da) Q3	DP (V)	CE (V)	CXP (V)
Cycloguanil	4.2	252.2	195.1 (153.0)	75	25 (41)	10 (10)
O-Desmethyl-venlafaxine	4.0	264.3	58.1 (107.2)	75	47 (50)	10 (10)
Proguanil	8.7	254.2	170.2 (153.1)	75	24 (40)	10 (10)
Proguanil-d6	8.6	260.3	170.2 (153.1)	75	25 (41)	10 (10)

DP - declustering potential; CE - collision energy; CXP - collision cell exit potential
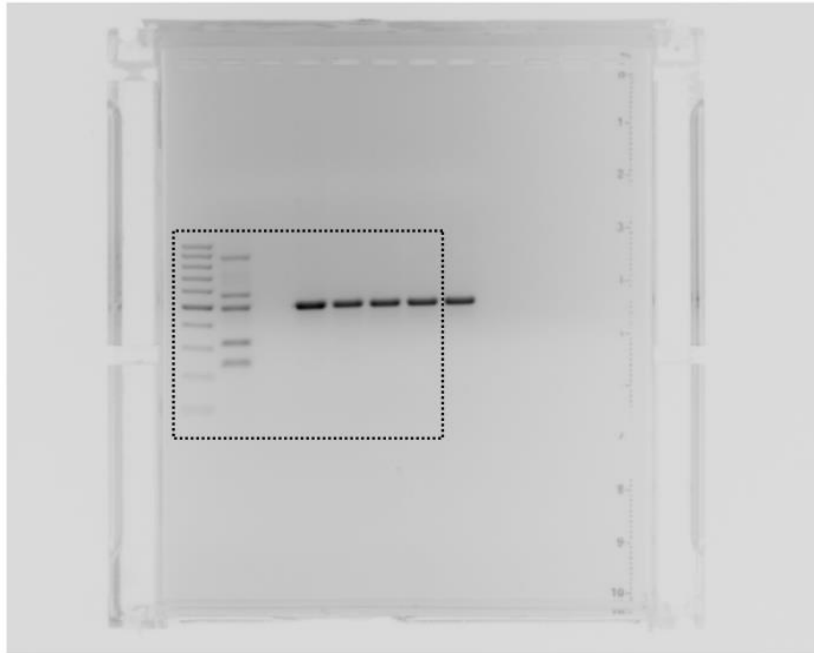
Original gel: Fig. 4b (additional band shows amplification of EV / EV control by multiplex PCR)
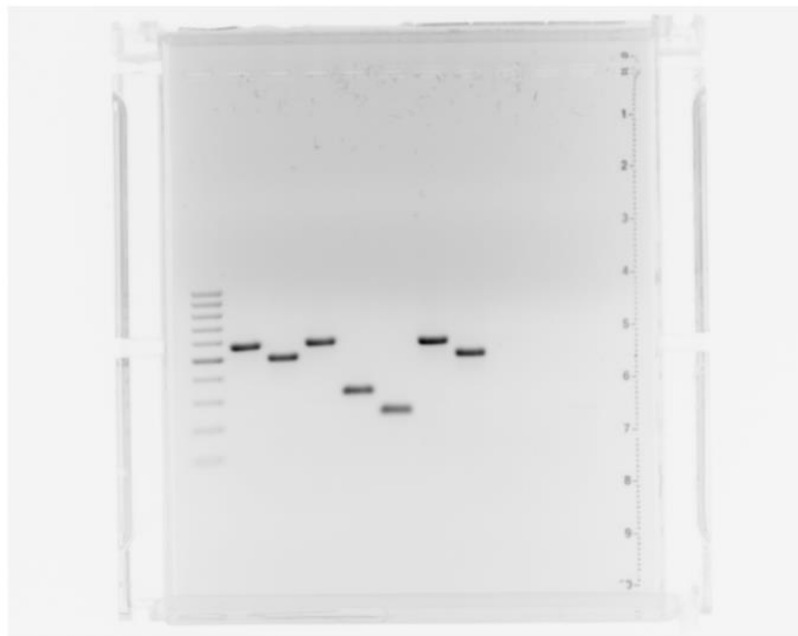
Original gel: Fig. 4c

3.5 Publication 5

Variability and Heritability of Thiamine Pharmacokinetics With Focus on OCT1

Effects on Membrane Transport and Pharmacokinetics in Humans

Ole Jensen[1], Johannes Matthaei[1], Felix Blome[1], Matthias Schwab[2,3,4], Mladen V. Tzvetkov[1,5] and Jürgen Brockmöller[1]

[1] Department of Clinical Pharmacology, University Medical Center, Georg August University, Goettingen, Germany

[2] Dr. Margarete Fischer-Bosch Institute of Clinical Pharmacology, University of Tübingen, Stuttgart, Germany

[3] iFIT Cluster of Excellence, University of Tübingen, Tübingen, Germany

[4] Departments of Clinical Pharmacology, Pharmacy, and Biochemistry, University Tübingen, Tübingen, Germany

[5] Department of Pharmacology, University Medical Center, Ernst-Moritz-Arndt-University, Greifswald, Germany

Variability and Heritability of Thiamine Pharmacokinetics With Focus on OCT1 Effects on Membrane Transport and Pharmacokinetics in Humans

Ole Jensen[1],* (iD) , Johannes Matthaei[1], Felix Blome[1], Matthias Schwab[2,3,4] (iD) , Mladen V. Tzvetkov[1,5] and Jürgen Brockmöller[1]

Thiamine is substrate of the hepatic uptake transporter organic cation transporter 1 (OCT1), and pathological lipid metabolism was associated with OCT1-dependent thiamine transport. However, it is unknown whether clinical pharmacokinetics of thiamine is modulated by OCT1 genotype. We analyzed thiamine transport *in vitro*, thiamine blood concentrations after high-dose and low-dose (nutritional) intake, and heritability of thiamine and thiamine-phosphate blood concentrations. The variant *OCT1*2* had reduced and *OCT1*3* to *OCT1*6* had deficient thiamine uptake activity. However, pharmacokinetics of thiamine did not differ depending on OCT1 genotype. Further studies in primary human hepatocytes indicated that several cation transporters, including OCT1, OCT3, and THTR-2, contribute to hepatic uptake of thiamine. As much as 54% of the variation in thiamine and 75% in variation of thiamine monophosphate plasma concentrations was determined by heritable factors. Apparently, thiamine is not useful as a probe drug for OCT1 activity, but the high heritability, particularly of thiamine monophosphate, may stimulate further genomic research.

Study Highlights

WHAT IS THE CURRENT KNOWLEDGE ON THE TOPIC?
☑ Human organic cation transporter 1 (OCT1) can mediate cell uptake of thiamine and OCT1-genotype-dependent differences in hepatic metabolism may be caused by OCT1-mediated thiamine transport.

WHAT QUESTION DID THIS STUDY ADDRESS?
☑ Do human thiamine blood concentrations differ depending on the OCT1 genotype? Can thiamine blood concentrations serve as a biomarker for *in vivo* OCT1 activity? How much of the variation of thiamine blood concentrations is heritable?

WHAT DOES THIS STUDY ADD TO OUR KNOWLEDGE?
☑ Thiamine pharmacokinetics does not depend on OCT1 genotypes but variation in thiamine plasma concentrations

is determined by heritable factors. Combined clinical and *in vitro* data indicate that hepatic thiamine uptake is mediated by multiple transporters with a minor contribution of OCT1. Translation from murine OCT models to humans may be difficult.

HOW MIGHT THIS CHANGE CLINICAL PHARMACOLOGY OR TRANSLATIONAL SCIENCE?
☑ Thiamine is not suitable as a probe drug for OCT1 activity. Associations of cardiometabolic phenotypes with OCT1 genotype may be mediated by mechanisms other than OCT1-mediated thiamine transport. Apparently, thiamine pharmacokinetics is modulated by genomic variation but the underlying genes are not yet identified.

The organic cation transporter 1 (OCT1) mediates hepatic uptake of typically cationic substances with a molecular weight below 400 Dalton.[1–4] In humans, OCT1 shows strong expression in the sinusoidal membrane of hepatocytes[5] and only minor, if any, expression in other organs.[6,7] OCT1 can be relevant for the hepatic uptake and pharmacokinetics of numerous drugs, including metformin, morphine, O-desmethyltramadol, sumatriptan, fenoterol, trospium, and ranitidine.[3,8–14] Beyond that, OCT1 may

also be relevant for hepatic uptake of numerous naturally occurring cations, including dopamine, epinephrine, serotonin, tyramine, and thiamine.[15] OCT1 activity is highly variable between individuals due to numerous naturally occurring synonymous and nonsynonymous variants. Five alleles are rather common in the European population (**Figure 1b**) and cause deficient or strongly reduced transport activity.[16,17] Activity of OCT1*2 is substrate dependent and there is some remaining but low activity of *3 and *4, whereas proteins coded by alleles *5 and *6 have no activity at all. Thus, depending on the substrate, between 2% and 9% of Europeans are deficient in OCT1-mediated transport.

Compared with other solute carriers and ABC transporters, OCT1 has a very high hepatic expression[12,18] suggesting a physiological role of OCT1, but only a few endogenous substrates are known. Recent data demonstrate a role of OCT1 in membrane transport of thiamine (vitamin B1).[15] In cell culture, thiamine uptake was inhibited by structurally unrelated organic cations like 1-methyl-4-phenylpyridinium (MPP+) (an OCT1 model substrate and inhibitor) and by serotonin and other OCT inhibitors as well. Human OCT1 is a high capacity but low affinity transporter for thiamine. Transgenic mice expressing human OCT1 showed enlarged livers and hepatic steatosis upon high-fat diets, whereas in knockout mice, the lack of OCT1 resulted in decreased hepatic concentrations of thiamine and the active metabolite thiamine diphosphate.[15] Most interestingly, in this model OCT1-mediated thiamine uptake correlated with hepatic steatosis.[19] Recent human genomewide association study data indicate a possible correlation between metabolic phenotypes and OCT1 genotype in humans as well.[20] Beyond that and because of its very low toxicity, thiamine might be an excellent *in vivo* probe drug for human OCT1 activity, if one could show a correlation between thiamine pharmacokinetics and OCT1 genotype.

Here, we wanted to further elucidate the role of OCT1 and its naturally occurring variants for thiamine disposition in humans. Therefore, we first compared thiamine cellular uptake via OCT1 with uptake via other cation transporters, including the thiamine transporters thiamine transporter 1 (THTR-1) and thiamine transporter 2 (THTR-2) using overexpressing cell lines and human hepatocytes. We then analyzed the effects of OCT1 and its variants on clinical pharmacokinetics of high-dose thiamine and low-dose thiamine in humans. In this clinical study, we took advantage of the common low or zero-activity variants of OCT1 to elucidate the quantitative contribution of OCT1 deficiency to thiamine pharmacokinetics in humans. Furthermore, we analyzed the overall heritability of thiamine and thiamine monophosphate plasma concentrations in humans using the repeated measurements approach and the twin study design.

RESULTS

Thiamine uptake via OCT1 and effects of common polymorphisms in human OCT1

First, we confirmed the high-capacity thiamine transport by wild-type OCT1*1. At 15 µM thiamine, cells expressing the variant OCT1*2 (a variant found almost worldwide) showed only about 50% of the uptake compared with the wild-type allele (**Figure 1a,b**). Cells expressing variants *3 and *4 had only 6% of the transport capacity of OCT1*1. The alleles OCT1*7

and OCT1*8, which are more common in African populations, showed 111% and 132%, respectively, of the wild-type activity. The intrinsic clearance by the common variant OCT1*2 was about 60% of that of OCT1*1 but uptake via OCT1*3 and OCT1*4 was so small and not saturating that no reliable transport kinetic constants could be estimated (**Table 1**). OCT1*5 and OCT1*6 (known as nonfunctional) did not produce any uptake above the control. The variants OCT1*7 and OCT1*8 showed similar or insignificantly increased maximum transport capacity, compared with the wild-type allele. Affinity was increased for the OCT1*7 variant compared with the wild-type allele ($P < 0.05$, Student t-test, no adjustment for multiple testing; **Figure 1a,d**, **Table 1**).

Pharmacokinetics of thiamine and its phosphate esters after a high dose of 200 mg

As a high capacity thiamine transporter, OCT1 should be most relevant at very high doses and high extracellular concentrations. To confirm that clinically, we administered thiamine orally to 18 healthy volunteers preselected according to their OCT1 genotype. Both groups, those with low activity or deficiency of OCT1 and those with high OCT1 activity, had a comparable sex proportion (4 women and 5 men each in both groups), similar age (mean 25.6 vs. 25.2 years) and similar body mass index (22.8 vs. 22.1 kg/m^2). Per study protocol, we classified OCT1 alleles *2 to *6 as inactive and all homozygous and compound-homozygous carriers of alleles *2 to *6 as inactive. Alleles *6, *7, and *8 were not found among the volunteers screened for the present study. As illustrated in **Figure 2**, the concentration time curves after the end of the absorption phase tended to be higher in carriers of zero OCT1 activity alleles. However, none of the pharmacokinetic parameters differed statistically significantly between the groups with high vs. low OCT1 activity (**Table 2**). Pharmacokinetic parameters for thiamine monophosphate and thiamine diphosphate did also not significantly differ between the subgroups defined by OCT1 genotype. Because more detailed transport kinetics measurements revealed that OCT1*2 still retained some transport activity (**Table 1**), the plasma and whole blood thiamine area under the curves (AUCs) were analyzed depending on the OCT1 *in vitro* activity score, which was calculated based on an additive model of inheritance using the activity score from transport experiments (**Figure 1a**). The *in vitro* activity score was assigned per allele, relative to wild-type OCT1*1. Alleles OCT1*2 was classified as 0.51, OCT1*3 and OCT1*4 as 0.07, and OCT1*5 and OCT1*6 as zero. However, also using this classification, there was not even a trend of increasing plasma or whole blood thiamine AUCs with increasing genotype-predicted OCT1 activity (**Figure 3**).

Effect of OCT1 deficiency on thiamine trough concentrations

We further tested whether morning trough thiamine blood concentrations after overnight fasting may be influenced by the OCT1 genotype, both after low-dose nutritional thiamine intake and 24 hours after 200 mg high-dose thiamine. At that time, thiamine and thiamine monophosphate plasma concentrations were still significantly above those concentrations measured with
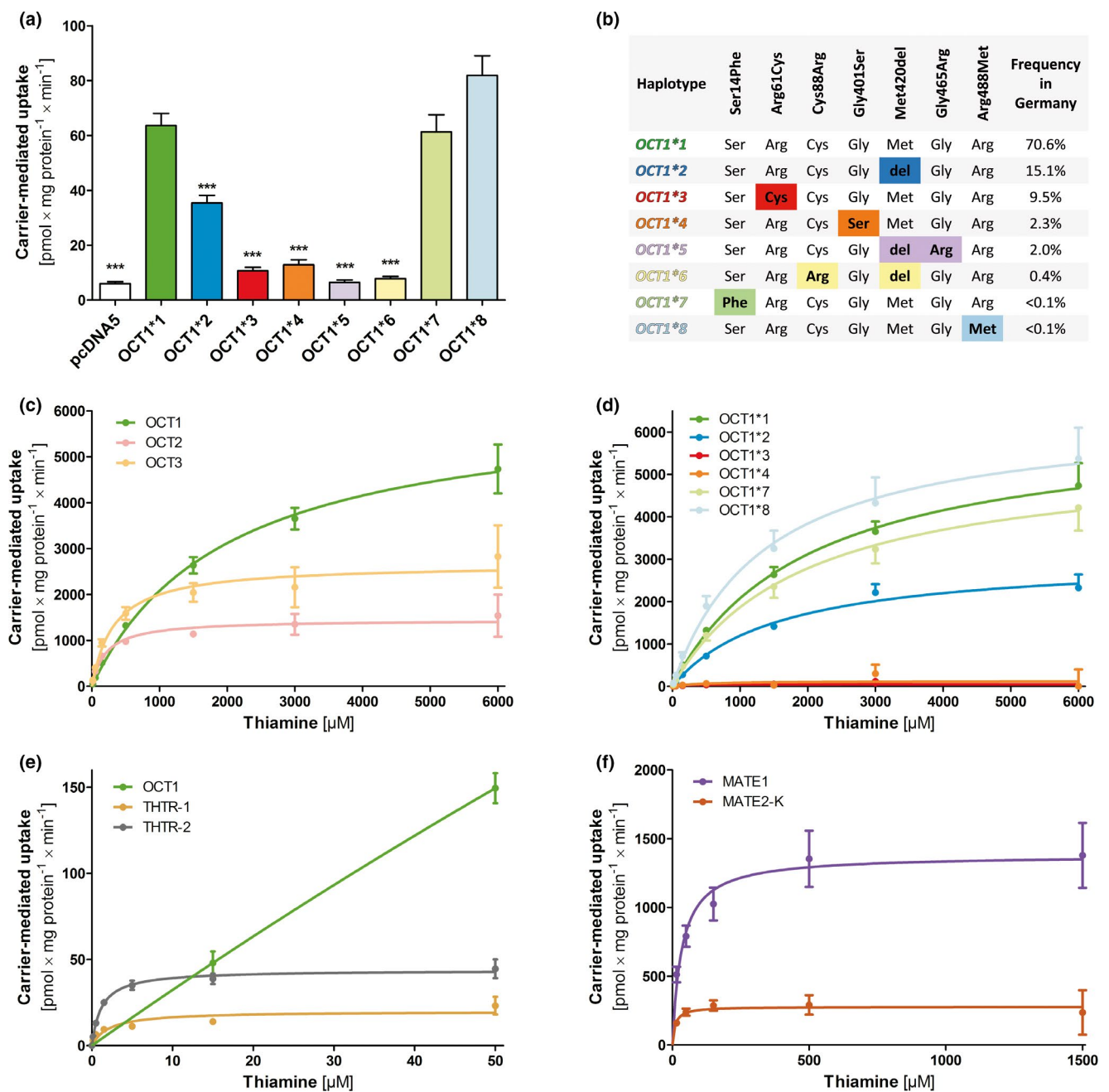
Figure 1 Thiamine uptake by wild-type and variant organic cation transporter (OCT)1 and by other organic cation transporters. At 15 µM thiamine, uptake was significantly reduced in variants *2 to *6 compared with wild-type OCT1*1 ($P < 0.05$ (**a**)). Thiamine uptake with variants *5 and *6 not statistically significantly different from the empty vector (pcDNA5). Common haplotypes result from combinations of six amino acid substitutions and the methionine420 deletion (**b**). Thiamine transport was analyzed under the same conditions in cells overexpressing THTR-1 and THTR-2 (**e**), as well as MATE1 and MATE2-K (**f**). (**c–f**) In these panels, carrier-mediated uptake is illustrated, that is the difference between uptake measured in the respective transfected cell lines minus the uptake into HEK cells transfected with the empty plasmid.

nutritional thiamine intake only. However, none of the concentrations differed significantly between the OCT1 active and deficient genotypes (**Table S1**). Similarly, thiamine monophosphate blood concentrations did also not differ between OCT1 genotypes (**Table S1**). Single values are illustrated in relation to the two classifications of OCT1 genotypes in **Figure 3**, but none of the differences were significant according to one-way analysis of variance.

Thiamine uptake by other solute carriers

The lack of significant differences in thiamine pharmacokinetics between active and deficient OCT1 genotypes was unexpected. To further clarify the reasons for that, we first characterized the uptake of thiamine via OCT1 in comparison to its known high-affinity transporters THTR-1 and THTR-2 (**Figure 1e**). The two thiamine transporters THTR-1 and THTR-2 exhibited high-affinity transport with limited capacity (**Table 1**). The

Table 1 Thiamine transport kinetic constants (mean ± SEM) studied in HEK cells

Transporter	K_m (µM)	V_{max} (pmol/mg protein/minute)	Cl_{int} (V_{max}/K_m) (µL/mg protein/minute)
OCT1*1	1,997 ± 174	5,750 ± 388	3.0 ± 0.1
OCT1*2	2,729 ± 1,228	3,761 ± 964	2.1 ± 0.4
OCT1*3	—[a]	—[a]	—[a]
OCT1*4	—[a]	—[a]	—[a]
OCT1*5	—[a,b]	—[a,b]	—[a,b]
OCT1*6	—[a,b]	—[a,b]	—[a,b]
OCT1*7	1,348 ± 201	4,293 ± 704	2.9 ± 0.5
OCT1*8	1,577 ± 390	6,747 ± 1,061	4.8 ± 1.2
OCT2	163 ± 20	1,336 ± 93	8.4 ± 0.6
OCT3	443 ± 158	2,840 ± 616	8.2 ± 1.7
MATE1	44.7 ± 8.5	1,496 ± 205	38.9 ± 9.1
MATE2-K	5.2 ± 1.3	245 ± 38	50.5 ± 5.7
THTR-1	1.2 ± 0.2	16.6 ± 1.6	15.1 ± 2.5
THTR-2	1.2 ± 0.1	43.4 ± 4.2	37.1 ± 2.1

HEK, human embryonic kidney; K_m, Michaelis constant; MATE1, multidrug and toxin extrusion protein 1; MATE2-K, multidrug and toxin extrusion protein 2-K; THTR-1, thiamine transporter 1; THTR-2 , thiamin transporter 2; OCT, organic cation transporter; V_{max}, maximal rate of metabolism.
[a]No saturating transport observed and therefore K_m and V_{max} could not be determined. [b]Variants OCT1*5 and OCT1*6 are known to result in complete transport deficiency.

organic cation transporter 3 (OCT3), which is also expressed in the liver, showed a higher affinity but lower capacity compared to OCT1 (**Table 1**). However, compared with the high-affinity thiamine transporters, OCT3 also had low affinity.

Primary human hepatocytes in combination with inhibitors of the transporters are more suitable to estimate the relative contribution of the specific transporters to overall cellular uptake. Therefore, we analyzed the inhibitory potency of the relatively OCT1-specific inhibitors dextrorphan and desipramine, and the relatively THTR-2-specific inhibitor amprolium together with an unspecific inhibitor of cation transporters, MPP+. Concentrations leading to at least 90% reduction in transport activity in human embryonic kidney 293 cells (HEK293) cells overexpressing OCT1 or THTR-2 were used to inhibit thiamine uptake in hepatocytes (50 µM dextrorphan; 100 µM desipramine; 100 µM amprolium; and 1 mM MPP+; **Figure 4**). By using low and high thiamine concentrations, we modeled trough concentrations from our clinical study and estimated maximum concentrations in the portal vein according to Ito *et al*.[21] We could indeed show a bigger impact of OCT1 on cellular uptake of thiamine if thiamine concentration was high (40 µM) compared with low thiamine (0.15 µM). Inhibition of the thiamine transporter THTR-2 resulted only in a moderate reduction of cellular uptake.

Altogether, these experiments indicate that thiamine hepatocellular uptake may be mediated by multiple transporters. OCT1-mediated thiamine transport could be relevant at very high concentrations only, whereas at typical thiamine blood concentrations other transporters are responsible for thiamine uptake into the liver. Quantitative expression data in different tissues confirmed the almost exclusive hepatic expression of OCT1 (**Figure S2**). In contrast, THTR-1 and THTR-2 were expressed at low to moderate levels in other tissues, as well as in HEK293 cells. The very high

hepatic expression of OCT1 may not compensate for the more than 1,000-fold higher affinity of thiamine transporters (**Figure S2**).

Heritability of morning fasting thiamine plasma concentrations

To explore overall heritability in thiamine membrane transport and metabolism, we used two independent samples and approaches, first, data from repeated measurements and, second, data from a study in monozygotic and dizygotic twins. In the first study, on average four samples were drawn per person ($n = 40$) with a time interval of at least 1 week between the samplings. From those data we estimated the genetic component by the approach suggested by Kalow *et al*.[22] Mean SD of thiamine concentration within the same subjects was 0.194 and mean SD between the subjects was 0.220. From that, a genetic component of 0.226 was calculated, thus, only 22.6% of the variation may be due to heritable factors. However, heritability might be much higher for thiamine monophosphate. With mean within and between SDs of 0.321 and 0.670, the genetic component was 0.770, thus, up to 77% of the variation in thiamine monophosphate concentrations may be due to heritable factors.

In the second study, to further investigate the heritability of thiamine in the blood, we determined basal plasma thiamine and thiamine monophosphate concentrations in 86 monozygotic and 28 dizygotic twins. All were healthy and had taken no drugs. Further details about the study have been described earlier.[23] In the twin study, variation could be attributed to additive genetic effects, dominant genetic effects, common environmental effects, and unique environmental effects. As summarized in **Table S2**, variation in thiamine and thiamine monophosphate plasma concentrations could be described best by a model including additive genetic and unique environmental effects. Thus, according to this analysis, broad heritability of plasma thiamine was 54% (95% confidence
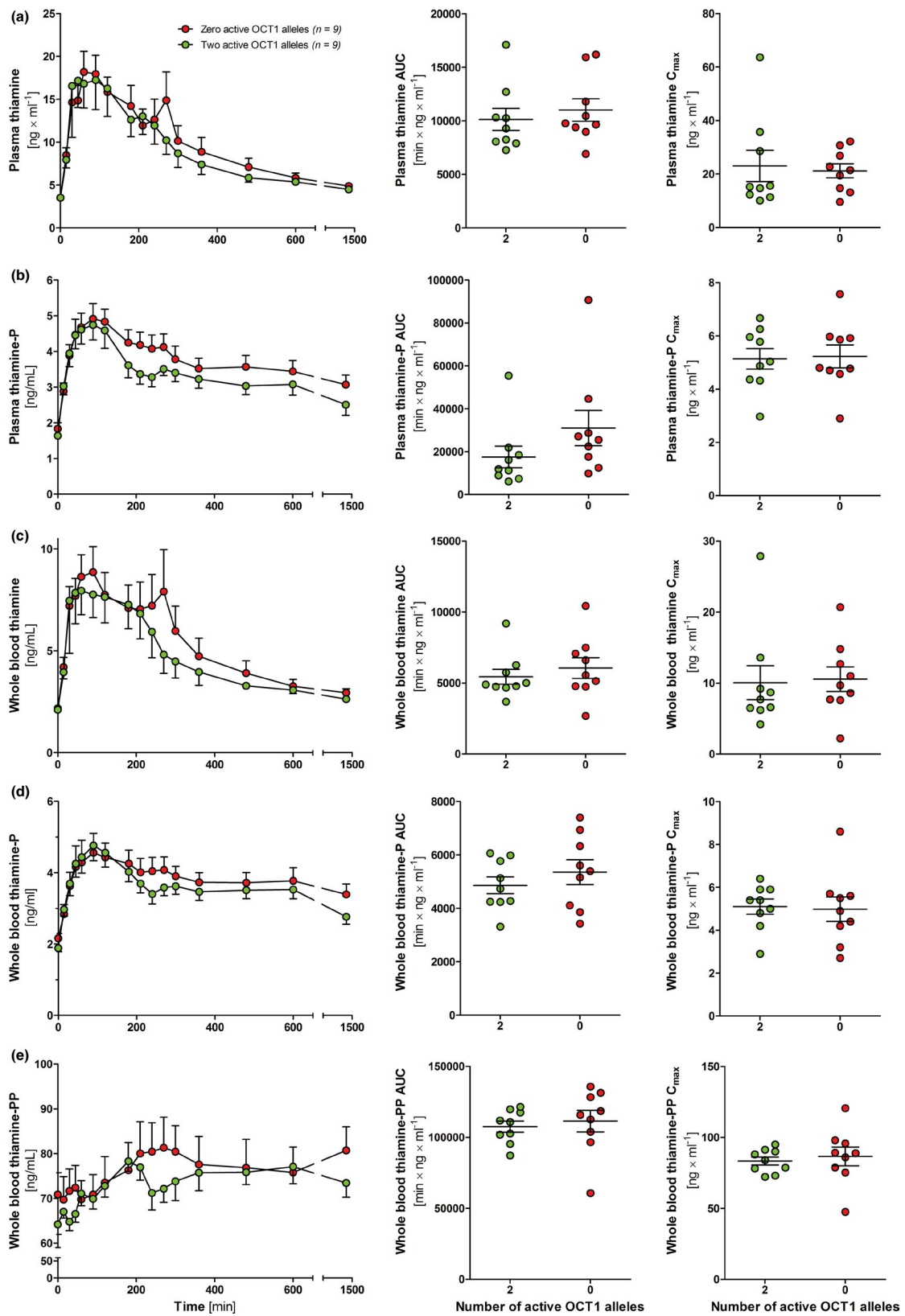
Figure 2 Pharmacokinetics of thiamine and its phosphate esters in human plasma and in whole blood after 200 mg thiamine orally. As defined in the study protocol, carriers of two organic cation transporter (OCT)1 active alleles were exclusively carriers of OCT1*1, thus allele OCT1*2 was classified as inactive. Carriers of two inactive alleles had homozygous or compound homozygous genotypes with alleles *2, *3, *4, and *5. As known, thiamine diphosphate is not found in relevant concentrations in plasma. AUC, area under the curve; C_{max}, peak plasma concentration.

**Table 2 Pharmacokinetics of high-dose thiamine in human plasma and whole blood**

	Plasma		Whole blood	
	Number of active OCT1 alleles		Number of active OCT1 alleles	
	Zero ($n = 9$)	Two ($n = 9$)	Zero ($n = 9$)	Two ($n = 9$)
Thiamine				
AUC (minute µg/mL)	11.2 ± 1.0	10.4 ± 1.1	6.1 ± 0.7	5.6 ± 0.5
Clearance/F (L/minute)	8.1 ± 0.8	10.0 ± 1.3	13.4 ± 2.1	15.1 ± 1.5
C_{max} (ng/mL)	21.2 ± 2.6	23.0 ± 5.8	10.6 ± 1.7	10.1 ± 2.4
T_{max} (hour)	2.2 ± 0.5	1.4 ± 0.3	2.2 ± 0.6	1.9 ± 0.3
Half-life (hour)	41.3 ± 10.0	35.5 ± 9.3	45.0 ± 11.1	40.0 ± 4.6
V_Z/F (L)	24,546 ± 3,855	24,526 ± 2,378	41,215 ± 5,250	48,754 ± 3,108
C_{24h} (ng/mL)	4.9 ± 0.2	4.5 ± 0.2	2.9 ± 0.2	2.6 ± 0.1
Thiamine monophosphate				
AUC (minute µg/mL)	5.2 ± 0.4	4.6 ± 0.4	5.5 ± 0.5	5.0 ± 0.3
C_{max} (ng/mL)	5.2 ± 0.4	5.1 ± 0.4	5.0 ± 0.6	5.1 ± 0.3
T_{max} (hour)	3.0 ± 0.9	4.6 ± 2.6	3.1 ± 0.8	2.8 ± 0.8
Thiamine diphosphate				
AUC (minute µg/mL)	—	—	113.5 ± 7.5	111.2 ± 4.5
C_{max} (ng/mL)	—	—	86.7 ± 6.6	83.4 ± 2.7
T_{max} (hour)	—	—	11.0 ± 3.5	6.3 ± 2.4

All data provided as arithmetic means ± SEM.
AUC, area under the curve; C_{24h}, 24-hour drug concentration; C_{max}, peak plasma concentration; OCT, organic cation transporter; T_{max}, time of maximum plasma concentration; Vz/F, volume of distribution based on the terminal phase.
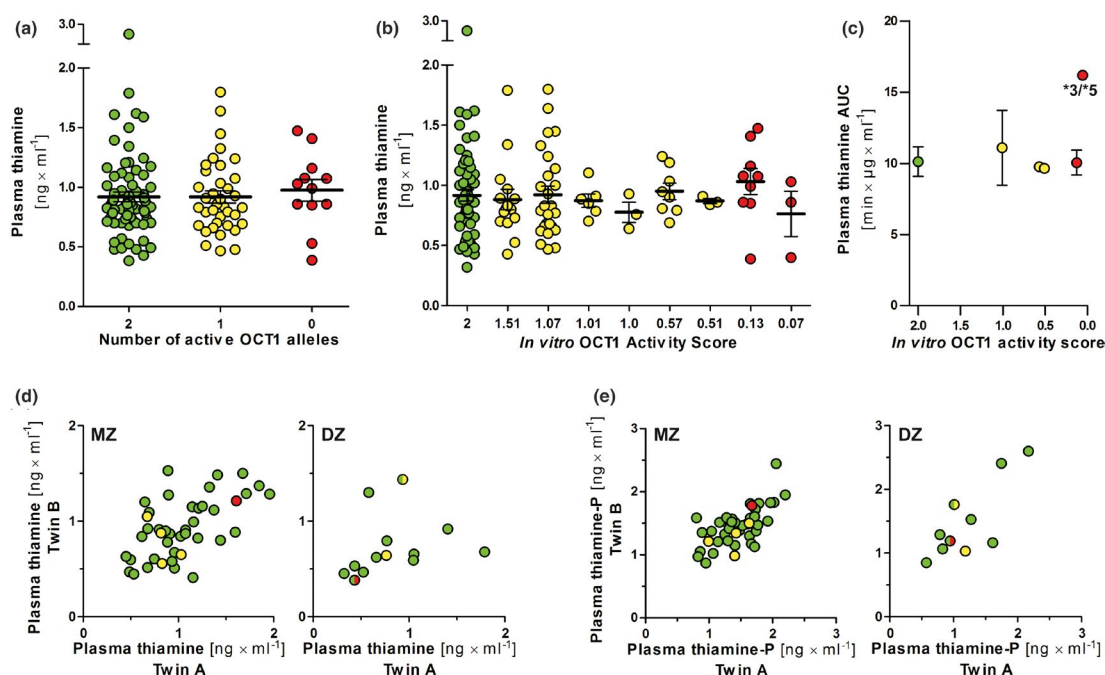
Figure 3 Plasma thiamine trough concentrations and area under the curve (AUC) in relation to organic cation transporter (OCT)1 genotypes and correlation of plasma thiamine and thiamine monophosphate concentrations in monozygotic (MZ) and dizygotic (DZ) twins. Plasma thiamine trough concentrations in healthy volunteers grouped by their OCT1 genotypes showed no significant differences. Classification according to the number of active OCT1 alleles ((**a**); classifying OCT1*2 as active) or by their *in vitro* activity score (**b**) also revealed no statistically significant differences (one-way analysis of variance). (**c**) In addition, the plasma thiamine AUC showed no dependency on the *in vitro* OCT1 activity score. (**d, e**) These panels show correlations of thiamine and thiamine monophosphate in MZ and DZ twins. The higher correlation in MZ twins (100% genotypes identical) compared with DZ twins (50% genotypes identical) indicates heritability. A detailed analysis using structural equation modeling is provided in **Table S2**. Green, yellow, and red dots refer to carriers of two, one, and zero active alleles. DZ twins having different genotypes are indicated by the respective semicircles.
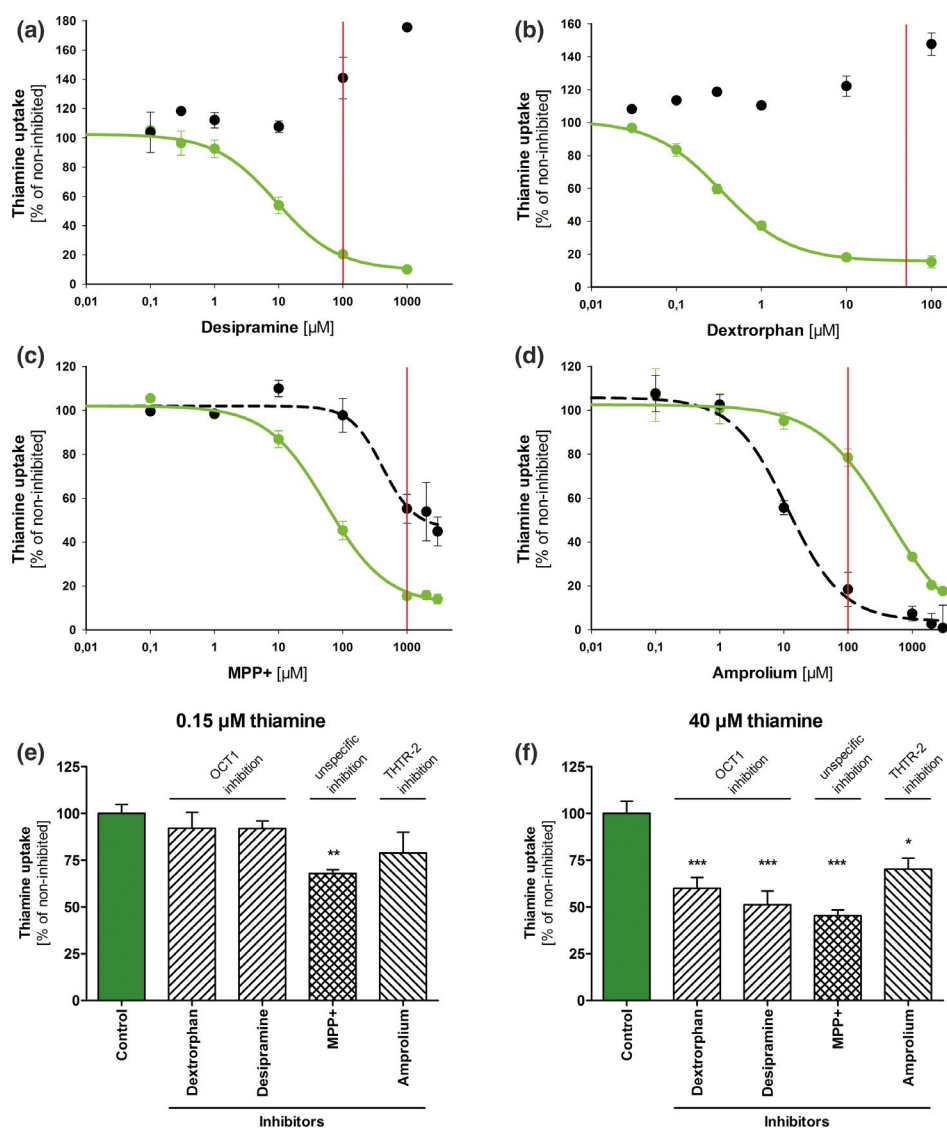
Figure 4 Inhibitor specificity and inhibitor effects on thiamine uptake in primary human hepatocytes. Inhibition of thiamine uptake with increasing concentrations of desipramine, dextrorphan, MPP+, and amprolium for organic cation transporter (OCT)1 and THTR-2. Red lines indicate concentrations used for experiments in primary human hepatocytes (**a–d**). Thiamine uptake into human hepatocytes was performed at low and high concentrations and revealed inhibitor-specific reduction (**e, f**). As seen, inhibitor concentrations resulting in < 20% uptake in the transfected cells resulted only in moderate inhibition of uptake in primary hepatocytes, indicating that still other transporters may be involved. MPP+, 1-methyl-4-phenylpyridinium; THTR-2, thiamine transporter 2.

interval (CI) 0.34–0.75), whereas 46% (95% CI 0.25–0.66) was due to random environmental effects. Broad heritability of thiamine monophosphate was 75% (95% CI 0.62–0.88), whereas 25% (95% CI 0.12–0.38) was due to environmental effects. Estimates of heritability in thiamine monophosphate corresponded particularly well with the estimate of a genetic component of 0.77 in the other independent study.

DISCUSSION

Our data confirm earlier findings in mice and human cell culture showing that OCT1 unequivocally can serve as a thiamine uptake transporter. However, in humans, the pharmacokinetics of thiamine and its phosphate esters were modulated only to a minor extent by naturally existing loss-of-function OCT1

variants. When considering the huge liver concentrations observed after injection of ^{11}C thiamine in rats,[24] it was particularly surprising that even peak plasma concentration (C_{max}) of thiamine was not significantly different between the OCT1 genotypes (**Figure 2**). In humans, parallel uptake via the thiamine transporters THTR-1 and THTR-2 may partially explain why there was no significant effect of OCT1 genotypes on blood and plasma thiamine concentrations. Chemical inhibition of THTR-1 and OCT1 reduced cellular uptake only moderately, indicating that even other uptake transporters may exist, one of which may be OCT3 (**Figure 5**).

Analysis of thiamine plasma concentrations in two independent study samples clearly indicated that a relevant fraction of variation in thiamine concentrations was due to heritable factors.
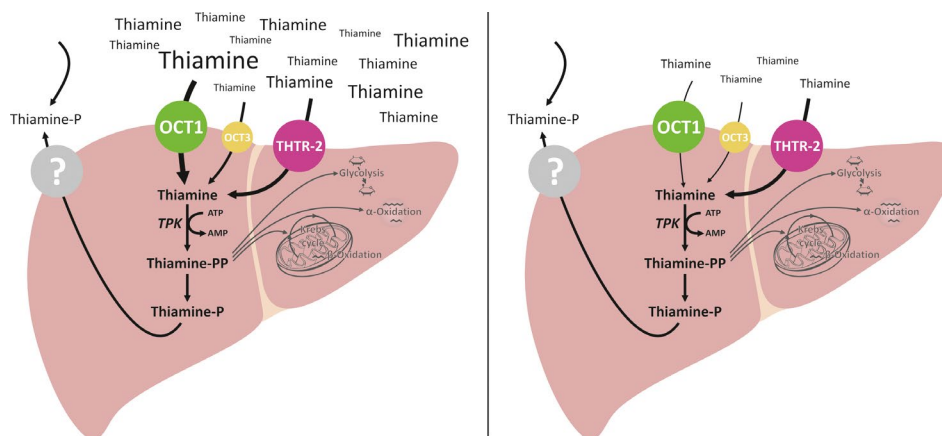
Figure 5 Pathways of thiamine in high and low dose. A moderately bigger impact of organic cation transporter (OCT)1 for hepatic thiamine uptake with high extracellular thiamine compared with low extracellular thiamine was concluded from the *in vitro* experiments with primary human hepatocytes, but was not reflected by the thiamine blood concentrations measured in healthy volunteers, where even peak plasma concentration was not different depending on OCT1 genotype (**Figure** 2). ATP, adenosine triphosphate; AMP, adenosine monophosphate; TPK, thiamine pyrophosphokinase; THTR-2, thiamine transporter 2.

Considering that low-dose nutritional thiamine intake was not specifically defined except for excluding any vitamin supplements, the intraindividual constancy and heritability in thiamine pharmacokinetics was most likely even underestimated. However, again, the existing interindividual variation could not be explained by the well-defined OCT1 variants (**Figure 3**). Interestingly, heritability of thiamine monophosphate was much higher than that of free thiamine, possibly indicating heritability in other enzymes and transporters in the thiamine cycle.[25] The significant heritability in the variation of thiamine monophosphate is particularly notable considering that the phosphate esters serve important functions in the intermediate-term thiamine storage.

Thiamine might have been an ideal probe drug to test *in vivo* human OCT1 activity, but in contrast to expectations from *in vitro* data (**Table 1**)[15] and Oct1 knockout mice,[20] thiamine blood and plasma concentrations did not reflect individual OCT1 genotypes. In addition, the thiamine phosphate esters did not correlate with the loss-of-function OCT1 genotypes. Apparently, it is not always possible to predict from *in vitro* experiments or from genetically modified mice whether or not human pharmacokinetics of an OCT1 substrate is dependent on OCT1 genotypes. Similar as with thiamine, also pharmacokinetics of some other prototypical substrates of OCT1 like metformin or proguanil did not depend in a significant fashion on OCT1 genotypes,[26,27] although intrahepatic metformin concentrations and pharmacodynamics did depend on OCT1 genotypes.[28,29] In the case of thiamine, several other organs also contribute to storage of thiamine and its phosphate esters even more than the liver.[30] Particularly the relatively high muscle, heart, kidney, or lung thiamine concentrations are not expected to depend on OCT1 genotypes because there is only negligible OCT1 expression outside the liver (**Figure S2**). In contrast, some other substances, including sumatriptan and fenoterol, did differ depending on OCT1 genotype most likely to be explained by a more selective accumulation of these two drugs in the human liver with only small accumulation in other organs.

At low concentrations, thiamine cell uptake should be mostly mediated by the high affinity transporters THTR-1 and THTR-2.[31,32] In our experiments using primary human hepatocytes, this was reflected by an almost negligible effect of OCT1 inhibitors with 0.15 µM thiamine but a clearly detectable effect of OCT1 inhibitors at 40 µM (**Figure 4**). However, in both conditions, inhibitors reduced the hepatocellular thiamine uptake only moderately, at least much less than that observed in the HEK cells transfected with OCT1. One interpretation of that may be the existence of other thiamine transporters, such as THTR-1 or solute carrier 35F3,[33] but also OCT3 may contribute to hepatic uptake of thiamine. Intrinsic thiamine clearance mediated by OCT3 was higher than that mediated by OCT1 so that even in the situation that OCT3 is expressed at a 10-fold lower concentration than OCT1 in the human liver, OCT3 may nevertheless contribute in a relevant manner to hepatic uptake of thiamine.

There seems to be an exciting association between OCT1 activity and OCT1 genotypes and hepatic lipid metabolism in mice and also in humans.[15,19,20] However, whether or not this is solely mediated by thiamine may be questionable. Considering that the relevant thiamine diphosphate ester concentrations in the cells are between 10-fold and 100-fold higher than those of free thiamine[30] (**Table 2**), phosphorylation and dephosphorylation, but also possibly transport of the phosphate esters, may play an even bigger role than hepatocellular uptake for the intrahepatic thiamine concentrations.

As indicated by our experiments with primary hepatocytes (**Figure 4**), OCT1 inhibition led to an about twofold reduction of hepatic uptake. Assuming a similar effect caused by OCT1 deficiency, reduced uptake probably could be more than compensated by providing much higher doses of thiamine. Although our experiments do not contribute to the question whether or not high intrahepatic thiamine concentrations result in metabolic disturbances, other quite ancient data on 70 humans who received a > 50-fold excess of thiamine compared with recommended nutritional intake over a period of 3 years did not result in major toxicity.[34] Nevertheless, it might be interesting to repeat such experiments now with more refined biomarkers of liver toxicity and lipid metabolism. Our experiments do not support, but also do not exclude, relevance of OCT1 for hepatic thiamine-related metabolism

under more challenging conditions, such as starvation, or alcoholic and nonalcoholic steatosis and hepatitis. Even if the contribution of OCT1 to hepatic thiamine uptake is moderate only, in the long term it may be relevant. According to the simple principle of additivity of partial clearances, a higher or lower hepatic uptake in humans with high or low/deficient OCT1 activity should usually not be compensated by other transporters but results in higher or lower thiamine concentrations.

Next steps in human clinical research might include more detailed analyses of OCT1 genotypes on hepatic metabolism in thiamine deficiency and thiamine oversupply with and without optimal conditions for thiamine phosphorylation and thiamine requirements. Conditions of malnutrition with thiamine deficiency are not infrequent[35] and the roles of specific hepatic transporters and intracellular phosphorylation are still not completely understood. In addition, the source of thiamine monophosphate in human plasma may deserve further investigation, it is conceivable that this is already formed in the gut wall and released from the enterocytes, but it may also be released from erythrocytes and other cells. Although the clinical studies were not sufficiently powered to study the effects of OCT2 polymorphisms for renal secretion, THTR-2 or SLC5F3,[33] polymorphisms, this may be an interesting topic for further research.

In conclusion, thiamine plasma concentrations under high-dose and low-dose exposures did not indicate a major impact of OCT1 for human thiamine pharmacokinetics but can also not exclude moderate and, in the long term, relevant OCT1 genotype-dependent differences in hepatic thiamine-dependent metabolism. Apparently, genomic variation is most relevant for thiamine pharmacokinetics but many underlying genes are not yet known.

MATERIALS AND METHODS

In vitro uptake of thiamine

Thiamine uptake was characterized in all the HEK293 cells stably transfected to overexpress the cation transporters included in the present study. In addition, thiamine uptake was studied in cryopreserved human hepatocytes (Gibco; Thermo Fisher Scientific, Darmstadt, Germany) from donors with active OCT1 alleles (donor a: OCT1*1/OCT1*1; donor b: OCT1*1/OCT1*2). Thiamine uptake in HEK293 cells or hepatocytes was performed for 2 minutes at 37°C and pH 7.4 after a preceding fasting period. Cell lysates were reconstituted and thiamine and its phosphate esters were quantified after oxidation to the fluorescent thiochrome with $K_3[Fe(CN)_6]$. High-performance liquid chromatography (HPLC) was performed on an XBridge C18 column (2.1 × 50 mm, 3.5 μm, Waters) and gradient elution. The detailed description of the experimental procedures and thiamine quantification can be found in the **Supplementary Material**.

OCT1 genotyping

Genotyping for OCT1 was performed on DNA extracted from blood samples via automated solid-phase extraction (EZ1 DNA Blood Kit; Qiagen, Hilden, Germany). Genotyping was described in detail elsewhere.[36] Briefly, a single-base primer extension assay was performed to genotype following common genetic variants: Ser14Phe (rs34447885), Arg61Cys (rs12208357), Cys88Arg (rs55918055), Pro117Leu (rs200684404), Ser189Leu (rs34104736), Gly401Ser (rs34130495), Met420del (rs202220802), and Gly465Arg (rs34059508). Almost all samples included in the study were genotyped in duplicate, with 100% concordant results.

Clinical studies

A high dose of 200 mg thiamine was administered to 18 unrelated healthy male and female volunteers with European ancestry. The participating volunteers were selected from a database of healthy volunteers according to their OCT1 genotype (9 carriers of 2 wild type alleles and 9 homozygous or compound heterozygous carriers of alleles *2, *3, and *4). Health was verified by medical history, common clinical biochemistry and hematology tests, and by a clinical examination, including echocardiogram recording. After overnight fasting, each volunteer took a single oral dose of 200 mg thiamine (Ratiopharm, Neu-Ulm, Germany). Intake of any vitamin supplements was forbidden for 7 days prior to the study day and also intake of any drugs except for oral contraceptives for 2 weeks prior to the study day was an exclusion criterion. Plasma and whole blood concentrations of thiamine were measured predose, and 15, 30, 45, 60, 90, 120, 180, 210, 240, 270, 300, 360, 480, 600, and 1,440 minutes after administration.

In another series of experiments, thiamine and thiamine monophosphate plasma concentrations were analyzed at the morning after overnight fasting in each subject on 3–5 separate occasions with intervals of at least 1 week. The aim of this study was to compare intraindividual vs. interindividual variation.[37]

In a third study, thiamine was analyzed in 28 dizygotic and 86 monozygotic twins to assess the overall heritability of thiamine blood concentrations. All participants were healthy men and women younger than 55 years. Details of that study have been described earlier.[23] All participants had given written informed consent and the clinical studies were approved by the ethics committee of the University Medical Center Göttingen. The thiamine pharmacokinetics study was registered at ClinicalTrials.gov (NCT02054299) and in the European Clinical Trials Database (EudraCT 2012-003546-33).

Thiamine blood concentration analyses

Plasma and whole blood concentrations of thiamine, thiamine monophosphate, and thiamine diphosphate were quantified with HPLC and fluorescence detection after oxidation to the respective thiochromes using potassium ferricyanide. Calibrators, thiamine, thiamine monophosphate, and thiamine diphosphate, were from Sigma. In brief, 300 μL plasma samples were mixed with 300 μL 10% trichloroacetic acid, thoroughly mixed, incubated on ice for 15 minutes, and centrifuged at 13,000 rpm for 15 minutes. Four hundred μL of the supernatant were washed with 1.5 mL water-saturated methyl-butyl-ether and 240 μL of the aqueous phase were mixed with 60 μL methanol and 150 μL derivatization reagent (0.6 mM potassium ferricyanide in 15% NaOH). Then, 10 μL of the reaction mixture were injected into the HPLC system. For chromatography, an X-Bridge C18 column (2.1 × 50 mm, 3.5 μm, Waters) was used with gradient elution. Plasma calibration range was 1–30 ng/mL for thiamine and 16 ng/mL for the thiamine phosphates, the whole blood calibration range was 0.5–25 ng for thiamine, 1–10 ng/mL for thiamine monophosphate, and 1–40 ng/mL for thiamine diphosphate.

Pharmacokinetic data analysis

Noncompartmental pharmacokinetic parameters were estimated with Phoenix WinNonlin version 6.3 (Certara USA, Princeton, NJ). The AUC was the predefined primary parameter and was calculated with the linear/log trapezoidal rule from time of thiamine administration and extrapolated to infinity based on the last predicted concentrations. The time of maximum concentration (T_{max}) and the corresponding concentration (C_{max}) were given as measured.

Statistical analyses

Primary parameters were plasma AUC of thiamine. For the pharmacokinetic study, the number of volunteers per genotype was calculated to give 80% power to identify a presumed 50% increase in the area under the time-concentration curve in the poor compared with the extensive

OCT1 transporters. The Student t-test was used with a type-I (alpha) error of 5% and assuming 35% SD of AUC in both groups based on published data.[38] Comparison of intraindividual vs. interindividual variation may provide important hints on possible heritability. Repeated analysis in each subject was used to calculate the genetic component, as described by Kalow et al.[22,37] Variance within (V_w) the subjects and variance between (V_b) the subjects were calculated and repeated genetic component was calculated as $(V_b - V_w)/V_b$. This metric is often interpreted as an indicator of heritability but would also reflect individually constant environmental factors.

To unambiguously differentiate between individually constant acquired factors vs. heritable factors, we analyzed thiamine and thiamin monophosphate concentrations in blood samples of monozygotic and dizygotic twins. Using monovariate structural equation modeling, we compared models with additive and dominant genetic factors, common environmental factors, and unique environmental factors. For structural equation analysis, the mets package in R was used.[39]

SUPPORTING INFORMATION
Supplementary information accompanies this paper on the *Clinical Pharmacology & Therapeutics* website (www.cpt-journal.com).

Supinfo Supplementary Methods
Figure S1. PCRs validating integration of THTR-1 or THTR-2 by the Flp-In system. THTR-1, thiamine transporter 1; THTR-2, thiamine transporter 2.
Figure S2. Expression of OCT1, THTR-1, and THTR-2 in 20 tissues and HEK293 cells. HEK293, human embryonic kidney 293 cells; OCT1, organic cation transporter 1; THTR-1, thiamine transporter 1; THTR-2, thiamine transporter 2.
Table S1. Plasma trough concentrations after low (nutritional) doses and high 200 mg doses of thiamine.
Table S2. Heritable and acquired determinants of thiamine and thiamine monophosphate plasma concentrations.

CONFLICT OF INTEREST
The authors declared no competing interests for this work.

AUTHOR CONTRIBUTIONS
O.J. and J.B. wrote the manuscript. J.M., M.S., M.V.T., and J.B. designed the research. O.J., J.M., and F.B. performed the research. O.J., J.M., M.V.T., and J.B. analyzed the data.

1. Grundemann, D., Gorboulev, V., Gambaryan, S., Veyhl, M. & Koepsell, H. Drug excretion mediated by a new prototype of polyspecific transporter. *Nature* **372**, 549–552 (1994).

2. Zhang, L., Dresser, M.J., Gray, A.T., Yost, S.C., Terashita, S. & Giacomini, K.M. Cloning and functional expression of a human liver organic cation transporter. *Mol. Pharmacol.* **51**, 913–921 (1997).
3. Hendrickx, R. *et al.* Identification of novel substrates and structure-activity relationship of cellular uptake mediated by human organic cation transporters 1 and 2. *J. Med. Chem.* **56**, 7232–7242 (2013).
4. Chen, E.C. *et al.* Discovery of competitive and noncompetitive ligands of the organic cation transporter 1 (OCT1; SLC22A1). *J. Med. Chem.* **60**, 2685–2696 (2017).
5. Meyer-Wentrup, F., Karbach, U., Gorboulev, V., Arndt, P. & Koepsell, H. Membrane localization of the electrogenic cation transporter rOCT1 in rat liver. *Biochem. Biophys. Res. Commun.* **248**, 673–678 (1998).
6. Gorboulev, V. *et al.* Cloning and characterization of two human polyspecific organic cation transporters. *DNA Cell Biol.* **16**, 871–881 (1997).
7. Nishimura, M. & Naito, S. Tissue-specific mRNA expression profiles of human ATP-binding cassette and solute carrier transporter superfamilies. *Drug Metab. Pharmacokinet.* **20**, 452–477 (2005).
8. Bourdet, D.L., Pritchard, J.B. & Thakker, D.R. Differential substrate and inhibitory activities of ranitidine and famotidine toward human organic cation transporter 1 (hOCT1; SLC22A1), hOCT2 (SLC22A2), and hOCT3 (SLC22A3). *J. Pharmacol. Exp. Ther.* **315**, 1288–1297 (2005).
9. Wenge, B., Geyer, J. & Bönisch, H. Oxybutynin and trospium are substrates of the human organic cation transporters. *Naunyn-Schmiedebergs Arch. Pharmacol.* **383**, 203–208 (2011).
10. Stamer, U.M., Musshoff, F., Stuber, F., Brockmoller, J., Steffens, M. & Tzvetkov, M.V. Loss-of-function polymorphisms in the organic cation transporter OCT1 are associated with reduced postoperative tramadol consumption. *Pain* **157**, 2467–2475 (2016).
11. Fukuda, T. *et al.* OCT1 genetic variants influence the pharmacokinetics of morphine in children. *Pharmacogenomics* **14**, 1141–1151 (2013).
12. Tzvetkov, M.V., dos Santos Pereira, J.N., Meineke, I., Saadatmand, A.R., Stingl, J.C. & Brockmoller, J. Morphine is a substrate of the organic cation transporter OCT1 and polymorphisms in OCT1 gene affect morphine pharmacokinetics after codeine administration. *Biochem. Pharmacol.* **86**, 666–678 (2013).
13. Wang, D.S., Jonker, J.W., Kato, Y., Kusuhara, H., Schinkel, A.H. & Sugiyama, Y. Involvement of organic cation transporter 1 in hepatic and intestinal distribution of metformin. *J. Pharmacol. Exp. Ther.* **302**, 510–515 (2002).
14. Dresser, M.J., Xiao, G., Leabman, M.K., Gray, A.T. & Giacomini, K.M. Interactions of n-tetraalkylammonium compounds and biguanides with a human renal organic cation transporter (hOCT2). *Pharm. Res.* **19**, 1244–1247 (2002).
15. Chen, L. *et al.* OCT1 is a high-capacity thiamine transporter that regulates hepatic steatosis and is a target of metformin. *Proc. Natl. Acad. Sci. USA* **111**, 9983–9988 (2014).
16. Kerb, R. *et al.* Identification of genetic variations of the human organic cation transporter hOCT1 and their functional consequences. *Pharmacogenetics* **12**, 591–595 (2002).
17. Seitz, T. *et al.* Global genetic analyses reveal strong inter-ethnic variability in the loss of activity of the organic cation transporter OCT1. *Genome Med.* **7**, 56 (2015).
18. Wang, L. *et al.* Interspecies variability in expression of hepatobiliary transporters across human, dog, monkey, and rat as determined by quantitative proteomics. *Drug Metab. Dispos.* **43**, 367–374 (2015).
19. Chen, L., Yee, S.W. & Giacomini, K.M. OCT1 in hepatic steatosis and thiamine disposition. *Cell Cycle* **14**, 283–284 (2015).
20. Liang, X. *et al.* Organic cation transporter 1 (OCT1) modulates multiple cardiometabolic traits through effects on hepatic thiamine content. *PLoS Biol.* **16**, e2002907 (2018).
21. Ito, K., Iwatsubo, T., Kanamitsu, S., Ueda, K., Suzuki, H. & Sugiyama, Y. Prediction of pharmacokinetic alterations caused by drug-drug interactions: metabolic interaction in the liver. *Pharmacol. Rev.* **50**, 387–412 (1998).
22. Kalow, W., Tang, B.K. & Endrenyi, L. Hypothesis: comparisons of inter- and intra-individual variations can substitute for twin studies in drug research. *Pharmacogenetics* **8**, 283–289 (1998).

23. Matthaei, J. *et al*. Heritability of metoprolol and torsemide pharmacokinetics. *Clin. Pharmacol. Ther.* **98**, 611–621 (2015).

24. Doi, H. *et al*. Synthesis of 11C-labeled thiamine and fursultiamine for in vivo molecular imaging of vitamin B1 and its prodrug using positron emission tomography. *J. Org. Chem.* **80**, 6250–6258 (2015).

25. Manzetti, S., Zhang, J. & van der Spoel, D. Thiamin function, metabolism, uptake, and transport. *Biochemistry* **53**, 821–835 (2014).

26. Tzvetkov, M.V. *et al*. The effects of genetic polymorphisms in the organic cation transporters OCT1, OCT2, and OCT3 on the renal clearance of metformin. *Clin. Pharmacol. Ther.* **86**, 299–306 (2009).

27. Matthaei, J. *et al*. OCT1 deficiency affects hepatocellular concentrations and pharmacokinetics of cycloguanil, the active metabolite of the antimalarial drug proguanil. *Clin. Pharmacol. Ther.* **105**, 190–200 (2019).

28. Sundelin, E. *et al*. Genetic polymorphisms in organic cation transporter 1 attenuates hepatic metformin exposure in humans. *Clin. Pharmacol. Ther.* **102**, 841–848 (2017).

29. Shu, Y. *et al*. Effect of genetic variation in the organic cation transporter 1 (OCT1) on metformin action. *J. Clin. Invest.* **117**, 1422–1431 (2007).

30. Gangolf, M. *et al*. Thiamine status in humans and content of phosphorylated thiamine derivatives in biopsies and cultured cells. *PLoS One* **5**, e13616 (2010).

31. Said, H.M., Balamurugan, K., Subramanian, V.S. & Marchant, J.S. Expression and functional contribution of hTHTR-2 in thiamin absorption in human intestine. *Am. J. Physiol. Gastrointest. Liver Physiol.* **286**, G491–G498 (2004).

32. Eudy, J.D., Spiegelstein, O., Barber, R.C., Wlodarczyk, B.J., Talbot, J. & Finnell, R.H. Identification and characterization of the human and mouse SLC19A3 gene: a novel member of the reduced folate family of micronutrient transporter genes. *Mol. Genet. Metab.* **71**, 581–590 (2000).

33. Zhang, K. *et al*. Genetic implication of a novel thiamine transporter in human hypertension. *J. Am. Coll. Cardiol.* **63**, 1542–1555 (2014).

34. Leitner, Z.A. Toxicity of thiamine. *Lancet* **249**, 345–346 (1947).

35. Whitfield, K.C. *et al*. Thiamine deficiency disorders: diagnosis, prevalence, and a roadmap for global control programs. *Ann. NY Acad. Sci.* **1430**, 3–43 (2018).

36. Matthaei, J. *et al*. OCT1 mediates hepatic uptake of sumatriptan and loss-of-function OCT1 polymorphisms affect sumatriptan pharmacokinetics. *Clin. Pharmacol. Ther.* **99**, 633–641 (2016).

37. Kalow, W., Endrenyi, L. & Tang, B.K. Repeat administration of drugs as a means to assess the genetic component in pharmacological variability. *Pharmacology* **58**, 281–284 (1999).

38. Smithline, H.A., Donnino, M. & Greenblatt, D.J. Pharmacokinetics of high-dose oral thiamine hydrochloride in healthy subjects. *BMC Clin. Pharmacol.* **12**, 4 (2012).

39. Holst, K. & Scheike, T.mets: analysis of multivariate event times, R package version 1.1.1. <http://CRAN.R-project.org/package=mets> (2015).

Supplementary Methods

Creation and validation of cell lines

Thiamine cellular uptake was analyzed in HEK293 cells overexpressing wild-type OCT1 and its common variants or OCT2, OCT3, MATE1, MATE2-K, and the thiamine transporters THTR-1 or THTR-2, and in cryopreserved primary human hepatocytes. Generation and validation of the of cell lines overexpressing OCT1 isoforms was described elsewhere [1, 2]. Gene constructs of thiamine transporters THTR-1 and THTR-2 were generated via reverse transcription from HEK293 cell RNA via gene specific primers (SLC19A2: ATCCAGGCAGTTGCTGTGC; SLC19A3: ACTTTGAAAGCCACTGTTGCG). The cDNA thus obtained was cloned into pCR-XL-TOPO vectors (Invitrogen, Thermo Fisher Scientific) and wild-type sequence was confirmed by Sanger sequencing. Gene sequences were amplified via PCR (KOD Hot Start DNA Polymerase Kit, Merck Millipore) with primers introducing restriction sites for *Hind*III and *EcoR*V and subsequently cloned into the pcDNA5.1 plasmid. The obtained constructs were integrated into HEK293 T-REx™ cells using the Flp-In™ system (Invitrogen) following to the manufacturer's protocol. Briefly, each transfection was conducted on 1×10^6 cells, which were plated per well in a 6-well plate 24 hours before. Four hundred ng of the pcDNA5.1::THTR-1 or pcDNA5.1::THTR-2 plasmid were co-transfected with 3.6 µg of the helper plasmid pOG44 using 12 µL FuGene6 transfection reagent. Cells were incubated for 24 hours and on the next day the supernatant medium was replaced by DMEM supplemented with 10% FCS, penicillin (50 U/mL) and streptomycin (50 µg/mL). Forty-eight hours after transfection, cells were transferred from the 6-well plate to a 100 mm Petri dish in 20 mL cell culture medium. Cells were then incubated overnight to ensure attachment. Next day, 120 µL hygromycin B (50 mg/mL) were added to the cell medium (final concentration: 300 µg/mL). The medium was renewed 4 days later again with fresh DMEM supplemented with 10% FCS, penicillin, streptomycin and hygromycin B (300 µg/mL). Approximately 10 days after the initial hygromycin B treatment colonies deriving from single cells appeared. Single colonies were selected and transferred to 12-well plates and cultured in 2 mL DMEM supplemented with 10% FCS, penicillin, streptomycin and hygromycin B (100 µg/mL). As the cells reached a confluence of about 70 to 80%,

1

they were transferred into a 6-well plate and further cultivated in DMEM supplemented with 10% FCS, penicillin, streptomycin and hygromycin B (100 µg/mL). Upon confluence of 70 to 80%, cells were transferred to a T25 (Sarstedt) cell culture flask with a ventilated cap.

Correct integration of transfected plasmids was validated by three independent PCR reactions (Fig. S1 A). For this, genomic DNA was extracted from pellets of cultured cells using the *DNeasy Blood & Tissue Kit* (Qiagen) with the QIACube robot. An *Integration PCR* (Fwd. primer: AGCTGTGGAATGTGTGTCAGTTAGG; Rev. primer: ACGCCCTCCTACATCGAAGCTGAAA; 518 bp amplicon) was used to detect the integration of the vector into the host cell genome in general by amplification of the hygromycin B resistance gene provided by pcDNA5. A second PCR (*Multiple Integration PCR;* Fwd: AATCGGGGGGCTCCCTTTAGGGTTCC; Rev: CTTCGCCCTCCGAGAGCTGCATCAG; 238 bp amplicon) was carried out to exclude multiple vector integration. The outcome of this PCR should be negative when only a single vector integrated into the FRT site, but multiple, subsequent integrations will lead to amplification of a PCR product. A third PCR was performed to amplify and thereby detect the gene of interest (*GOI PCR*; Fwd: CCATGGTGATGCGGTTTTGGCAGTA; Rev: CCTTCCTGTAGCCAGCTTTCATCAA; 2965 (THTR-1) / 2962 (THTR-2) / 3137 (OCT1) bp amplicon). Gene-unspecific primers were used to bind in the CMV promoter and LacZ-Zeocin region, both neighboring the inserted gene, and the correct size of the insert was validated on an agarose gel (Fig. S1 B).

In cell clones, which passed the PCR validation process, overexpression of the gene of interest was validated via quantitative RT-PCR using TaqMan™ assays (SLC22A1: Hs00427550_m1; SLC19A2: Hs00949693_m1; SLC19A3: Hs00228858_m1 ; TBP: 4326322E; Thermo Fisher Scientific). For this purpose, RNA from cultured cells was extracted using the *RNeasy Plus Mini Kit* (Qiagen) with the QIACube robot according to the manufacturer's instructions. Normalization of expression of different transporter genes was performed with the help of plasmids carrying one gene copy per plasmid molecule. The molecular weight of each plasmid was approximated via its length, and from measured concentrations, standard curves with known plasmid quantities were create. Through this, the number copies of transcripts in unknown samples could be determined and compared (Fig. S1 C).

Finally, stably transfected cells were functionally validated via thiamine transport in concentration-dependent uptake experiments (Fig. S1 D). OCT1 variant cell lines had been validated with numerous other substrates known to be transported by wild-type OCT1 and some of its common naturally occurring variants [2].

Uptake experiments

Concentration-dependent uptake was analyzed in HEK293 cells overexpressing OCT1, THTR-1 or THTR-2 at varying thiamine concentrations. For this purpose, 12-well plates were pre-coated with poly-D-lysine and 6×10^5 cells were plated 48 hours ahead of each uptake measurement per well to reach 95 to 100% confluency on the day of the experiment. Human hepatocytes (Gibco, Thermo Fisher Scientific) were thawed and processed rapidly according to the manufacturer's protocol. One hundred thousand hepatocytes were plated per well of a collagen-pre-coated 24-well plate (Gibco, Thermo Fisher Scientific) and let adhere for 4 hours before further use in uptake experiments. In order to reduce intracellular thiamine concentrations, HEK293 cells were incubated for 30 minutes in HBSS+ before each uptake experiment. The optimized plating medium of hepatocytes was replaced by thiamine-free DMEM (Gibco, Thermo Fisher Scientific) after 2 hours.

Uptake in HEK293 cells or hepatocytes was performed for two minutes at 37 °C and pH 7.4, and stopped with ice-cold HBSS supplemented with 10 mM HEPES. Cells were lyzed with 80% acetonitrile and the lysate was evaporated under nitrogen flow at 40 °C until dry. Standard curve samples for transport experiments were prepared simultaneously in 100% MeOH to minimize evaporation time. The dry lysates of unknown as well as standard were reconstituted in 200 µL 20% methanol and 100 µL 0.6 mM $K_3[Fe(CN)_6]$ in 15% NaOH were added and the intracellularly accumulated thiamine was quantified via HPLC with fluorescence detection.

Thiamine quantification

Thiamine was quantified via HPLC-coupled fluorescence detection of pre-column derivatized samples. The Nexera 2 HPLC system (Shimadzu) was used with the SIL 30-AC autosampler to process samples from a 96 deep well plate. Substance separation was achieved with a XBridge™ C18 column (2.1 x 50 mm, 3.5 µm, Waters) and a Phenomonex C18 pre-column and gradient elution. Mobile phase A (25 mM Na_2HPO_4, pH 7) and B (60% 25 mM Na_2HPO_4, pH 7, 40% MeOH) were used at a constant flow of 0.5 mL/min with following gradient: 0% mobile phase B at 0 min, 30% B at 1 min, 30% B at 1.5 min, 100% B at 3 min, 0% B at 3.1 min, and 0% B at 8 min to restore initial conditions. Fluorescence of derivatized thiamine (retention time 6.22 min), thiamine-P (RT 5.19 min) and thiamine-PP (RT 4.74 min) were detected with 375 nm excitation and 435 nm emission wavelengths.

Legends to supplementary Figures and Tables

Figure S1: PCRs validating integration of THTR-1 or THTR-2 by the Flp-In™ system. The schematic depiction of the three conducted validation PCRs (A) and results of these PCRs for two newly generated cell clones overexpressing THTR-1 or THTR-2 (B) are shown. Absolute quantification reveals strong differences in expression levels of OCT1, THTR-1 and THTR-2 in HEK293 cells after stable transfection (C). Function of thiamine transporter was verified with thiamine uptake experiment (D). Thiamine uptake was calculated as the difference between uptake measured in the respective transfected cell lines minus the uptake into HEK cells transfected with the empty plasmid.
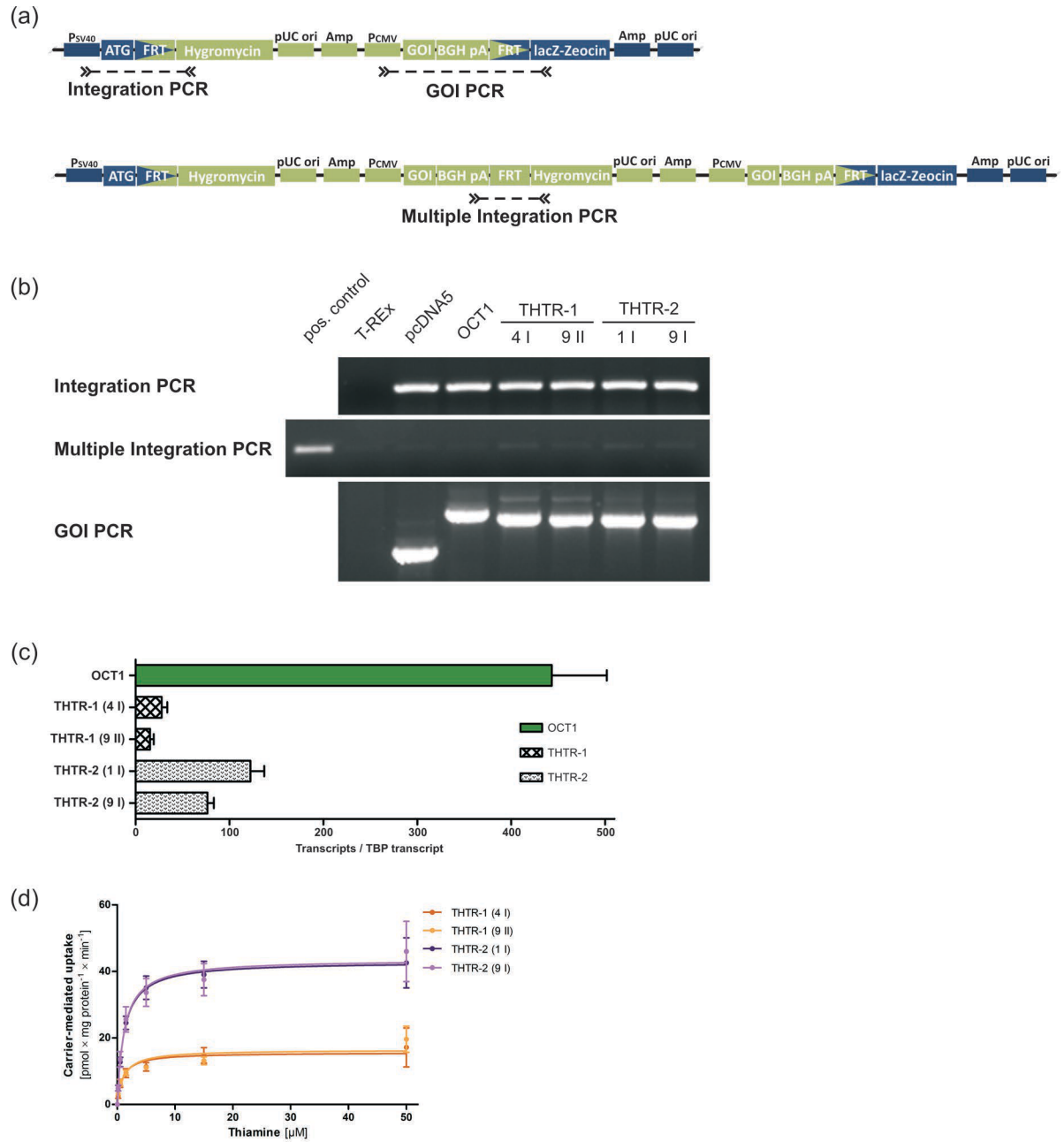
Fig. S2: Expression of OCT1, THTR-1 and THTR-2 in 20 tissues and HEK293 cells. Expression analysis revealed high OCT1 mRNA levels in the liver, compared to THTR-1 and THTR-2. In contrast to OCT1, both thiamine transporters were low to moderately expressed in other tissues, and HEK293 cells.

Table S1: Plasma trough concentrations after low (nutritional) doses and high 200 mg dose of thiamine. Thiamine morning trough levels measured after usual nutritional intake and at least 10 hours overnight fasting (low dose) and 24 hours after 200 mg thiamine orally. Depending on assay conditions in cell culture, OCT1*2 has about 30 to 50% of the normal transport activity conferred by wild-type OCT1*1, thus, both classifications may be justified. Further differentiation is given in Fig. 3.

Table S2: Heritable and acquired determinants of thiamine and thiamine monophosphate plasma concentrations. Estimates and of additive genetic effects (A), dominant genetic effects (D), shared environmental effects (C) and unshared environmental effects (E) are presented under different genetic models. Both, for thiamine and thiamine monosphate the best model according to the Akaike criterion (AIC) was the model with additive genetic effects and environmental effects (AE). Thus, according to this analysis, broad heritability of plasma thiamine was 54% and broad heritability of thiamine monophosphate was 0.75, which is quite high considering that nutritional intake was not standardized.

(1)   Saadatmand, A.R., Tadjerpisheh, S., Brockmöller, J. & Tzvetkov, M.V. The prototypic pharmacogenetic drug debrisoquine is a substrate of the genetically polymorphic organic cation transporter OCT1. *Biochemical Pharmacology* **83**, 1427–34 (2012).
(2)   Seitz, T. *et al.* Global genetic analyses reveal strong inter-ethnic variability in the loss of activity of the organic cation transporter OCT1. *Genome Med* **7**, 56 (2015).

Figure S1. PCRs validating integration of THTR-1 or THTR-2 by the Flp-In system. THTR-1, thiamine transporter 1; THTR-2, thiamine transporter 2.

Figure S2. Expression of OCT 1, THTR-1, and THTR-2 in 20 tissues and HEK293 cells. HEK293, human embryonic kidney 293 cells; OCT 1, organic cation transporter 1; THTR-1, thiamine transporter 1; THTR-2, thiamine transporter 2.
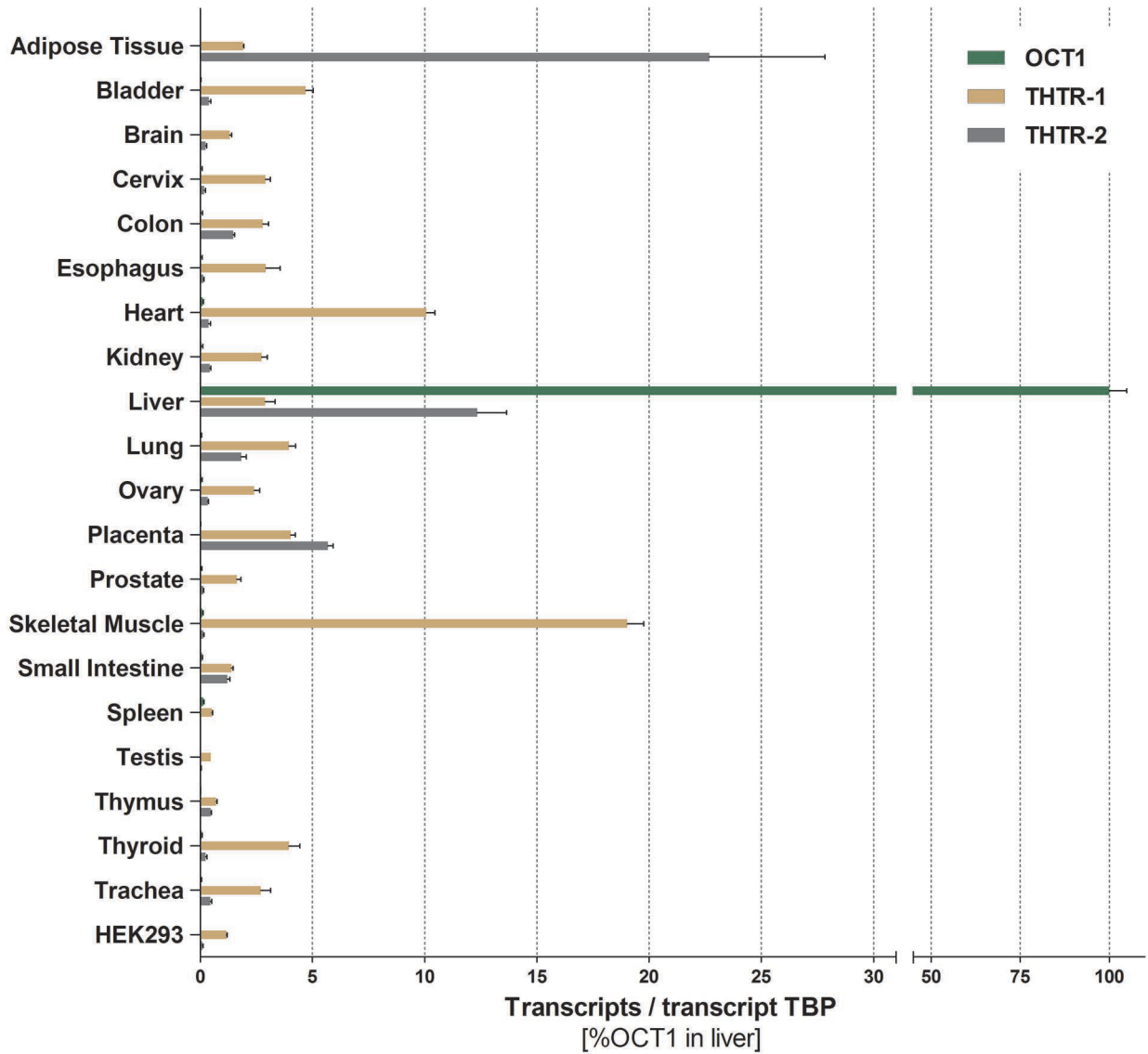
Table S1: Plasma trough concentrations after low (nutritional) doses and a high 200 mg dose of thiamine

Genotype classification assuming that OCT1 allele *2 is deficient[#]

Thiamine trough concentrations in plasma [ng/ml]

No. of active OCT1 alleles	2	1	0
Low doses (n = 152)	0.92 (0.32 – 2.50)	0.90 (0.43 – 1.80)	0.92 (0.39 – 1.47)
200 mg dose (n=18)	4.49 (3.03 – 5.25)	-	2.51 (1.43 – 4.32)

Thiamine monophosphate in plasma

No. of active OCT1 alleles	2	1	0
Low doses	1.65 (0.55 – 5.20)	1.51 (0.73 – 2.60)	1.73 (1.00 – 3.13)
200 mg dose	2.51 (1.43 – 4.32)	-	3.07 (1.66 – 4.15)

Genotype classification assuming that OCT1 allele *2 is active

Thiamine in plasma [ng/ml]

No. of active OCT1 alleles	2	1	0
Low doses (n = 152)	0.91 (0.32 – 2.50)	0.91 (0.47 – 1.80)	0.94 (0.39 – 1.47)
200 mg dose (n=18)	4.53 (3.03 – 5.45)	4.97 (4.59 – 5.36)	5.01 (4.28 – 5.57)

Thiamine monophosphate in plasma [ng/ml]

No. of active OCT1 alleles	2	1	0
Low doses	1.62 (0.55 – 5.20)	1.61 (0.90 – 2.60)	1.71 (1.00 – 3.13)
200 mg dose	2.53 (1.43 – 4.32)	3.51 (2.90 – 4.11)	3.22 (2.19 – 4.15)

Thiamine morning trough levels measured after usual nutritional intake and at least 10 hours overnight fasting (low dose) and 24 hours after 200 mg thiamine orally. Depending on assay conditions in cell culture, OCT1*2 has about 30 to 50% of the normal transport activity conferred by wild-type OCT1*1, thus, both classifications may be justified. Further differentiation is given in Fig. 3. All data provided as mean and range (minimum – maximum)

Table S2:

Heritable and acquired determinants of thiamine and thiamine monophosphate plasma concentrations

Thiamine								
	Pearson Correlation		A	D	C	E	AIC	p-value (with respect to saturated model)
	MZ	DZ	Estimate 95% CI	Estimate 95% CI	Estimate 95% CI	Estimate 95% CI		
ACE			0.48 (-0.45 – 1.41)	-	0.06 (-0.80 – 0.93)	0.46 (0.25 – 0.67)	86.13	0.011
ADE			0.54 (0.34 – 0.75)	0	-	0.46 (0.25 – 0.66)	86.15	0.011
AE*	0.58	0.27	**0.54 (0.34 – 0.75)**	-	-	**0.46 (0.25 – 0.66)**	**84.15**	**0.017**
CE			-	-	0.47 (0.27 – 0.67)	0.53 (0.33 – 0.73)	85.35	0.012
Thiamine Monophosphate								
	Pearson Correlation		A	D	C	E	AIC	p-value (with respect to saturated model)
	MZ	DZ	Estimate 95% CI	Estimate 95% CI	Estimate 95% CI	Estimate 95% CI		
ACE			0.43 (-0.12 – 1.00)	-	0.30 (-0.22 – 0.81)	0.27 (0.12 – 0.41)	80.56	0.004
ADE			0.75 (0.62 – 0.88)	0	-	0.25 (0.12 – 0.38)	81.57	0.003
AE*	0.67	0.66	**0.75 (0.62 – 0.88)**	-	-	**0.25 (0.12 – 0.38)**	**79.57**	**0.005**
CE			-	-	0.63 (0.48 – 0.79)	0.37 (0.33 – 0.73)	81.28	0.003

Estimates and of additive genetic effects (A), dominant genetic effects (D), shared environmental effects (C) and unshared environmental effects (E) are presented under different genetic models. Both, for thiamine and thiamine monophosphate the best model according to the Akaike criterion (AIC) was the model with additive genetic effects and environmental effects (AE). Thus, according to this analysis, broad heritability of plasma thiamine was 54% and broad heritability of thiamine monophosphate was 0.75, which is quite high considering that nutritional intake was not standardized.

4 Discussion

Translational pharmacology includes target finding, drug screening, lead optimization, preclinical testing with functional assays in functional models, *in vitro*-to-*in vivo* extrapolation, and subsequent *in vivo* validation. The five publications, on which this thesis is built, include several of these tasks as illustrated in Figure 8.
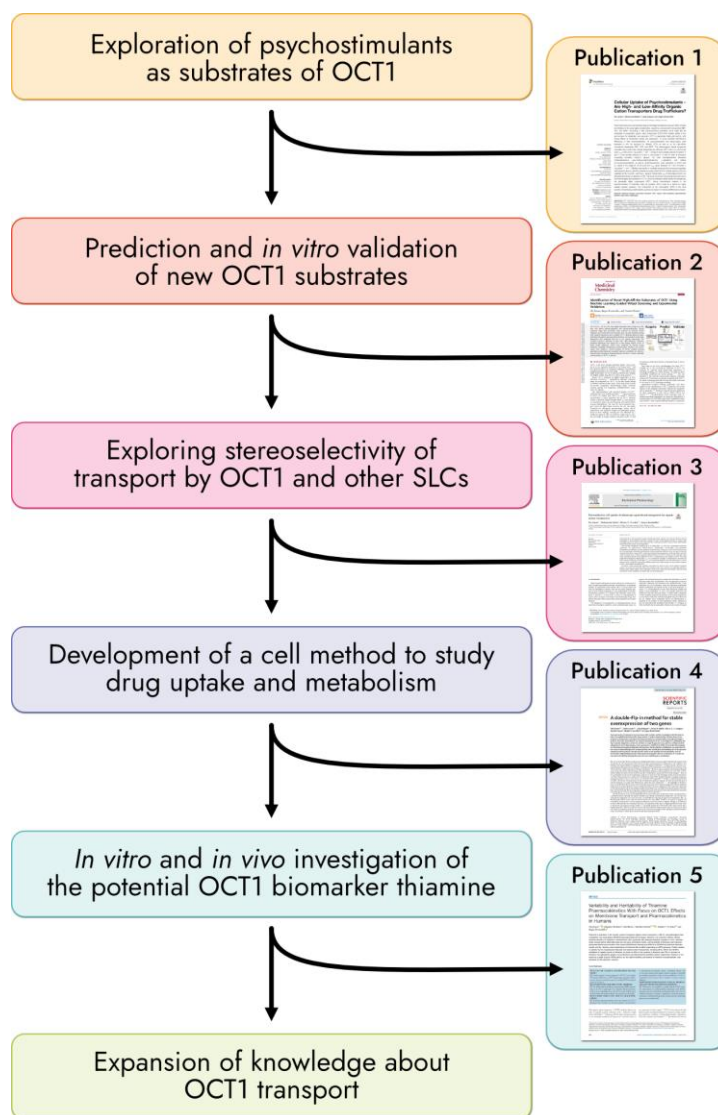
Figure 8: Integrative overview of the publications in this thesis.

Data about OCT1 substrates is plenteously available, and traditional substrate criteria comprise a molecular weight below 600 Da, predominantly positive charge at pH 7.4 and lipophilicity. To expand the knowledge about OCT1 substrates and non-substrates exploratively, 18 psychostimulants or hallucinogens, all of which meet the just-mentioned conventional criteria, were investigated. Out of these, only mescaline was identified as an OCT1 substrate, while other compounds were only transported by OCT2 or the high-affinity monoamine transporters NET

and DAT. Unlike the exploration of molecules with a different structure, an exploitational approach was used to predict novel OCT1 substrates on the basis of known ones. Results showed that a machine learning-based model is a suitable method for predicting substrates with high reliability. Since the use of two-dimensional models for machine learning-based prediction of substrates (as applied in our work) are not or only poorly able to predict the interaction of racemates with OCT1, stereoselective transport was investigated *in vitro*. Results of eight investigated known OCT1 substrates indicated that transport by polyspecific transporters, such as OCT1, facilitates translocation of enantiomers with significant stereoselectivity.

The *in vitro* investigation of combined effects of uptake and metabolism, be it in the case of racemates, pure enantiomers, or substances without a stereocenter, requires the presence of a transporter and a metabolizing enzyme. Therefore, a method for the stable overexpression of two genes was developed. Testing substances for uptake and metabolism might be one way to investigate metabolic pathways integratively prior to clinical studies and improve the *in vitro*-to-*in vivo* extrapolation. The search for a suitable biomarker that indicates OCT1 activity has been running for some time and several substances have already been proposed for this purpose. In a clinical study, we showed that thiamine might be transported by OCT1 *in vitro*, but does not serve as a biomarker for OCT1 activity.

4.1 Cellular Uptake of Psychostimulants

Screening for new substrates can be based on random selection of test compounds. It can also be guided by physicochemical and/or structural characteristics of known substrates. Here, we selected test compounds based on a single positive charge at pH 7.4 and a $logD_{7.4}$ value of < 1. The low success rate in our study with regard to OCT1 substrates found (1 out of 18) is surprising, as in other datasets about 40 % of all test compounds were substrates (Hendrickx et al. 2013). It was surprising that despite its scaffold identity to the tested non-substrates, mescaline turned out to be an extraordinarily good OCT1 substrate. Specific structural properties of mescaline may set it apart from the other substances. This so-called *activity cliff* might provide further insights in OCT1 binding and translocation processes (Stumpfe und Bajorath 2012). Previous studies did not find uptake of amphetamine or methamphetamine by OCT1 either (Wagner et al. 2017). The same study also reported the uptake of both compounds by OCT2, which was in part confirmed by our findings. The interaction of OCT1 with other substances from the group of psychostimulants cannot be ruled out, as these are diverse. Official regulations make working with these legally restricted substances more difficult, which means that there is a comparatively limited amount of data. Nonetheless, it is conceivable that other hallucinogens or psychostimulants can be transported by OCT1. In light of astonishingly different *in vitro* results for the structurally similar compounds tested, further exploration of this drug class might reveal more interesting insights.

The proposed native role of OCT1 includes the elimination of endogenous amines (Zhang L. et al. 1997). Psychostimulants, such as the here investigated amphetamine or cocaine are known to

increase extracellular levels of monoamines norepinephrine, dopamine, and serotonin, by inhibition of the high-affinity monoamine transporters NET, DAT, and SERT (Di Chiara und Imperato 1988; Kuczenski und Segal 1997; Ritz et al. 1990). These neurotransmitters have also been shown to be substrates of OCT1 (Boxberger et al. 2014; Busch et al. 1996). In addition, also so-called false neurotransmitters have been described to be increased in blood and in the brain upon hepatic failure. These include β-hydroxylated phenylethylamines mimicking norepinephrine without respective effect (Fischer und Baldessarini 1971; Fischer et al. 1965). Some of these false neurotransmitters of endogenous or natural origin, such as hordenine, octopamine, phenylephrine, and synephrine have been described as OCT1 substrates for the first time during this work (see *Publication 1*). Overall, this context gives sufficient reason to further investigate the interaction of OCT1 with biogenic amines that can reach the CNS and interact with other transporters. For a better understanding of the interaction, psychostimulants and biogenic amines should be investigated with regard to their functions as substrates or inhibitors of OCT1 and monoamine transporters. Interestingly, OCT3 has been studied as a target for antidepressive medication (Hu et al. 2016; Zhu et al. 2012), further underlining the possible therapeutic value of insights into the substrate overlap of OCTs and MATs.

4.2 Identification of novel OCT1 substrates by machine learning

The machine learning-aided search for additional OCT1 substrates on the bases of known and published substrates and non-substrates led to the identification of additional high-affinity substrates. More then 80% of predicted substrates were experimentally confirmed. Previously published studies on screenings have already led to a general understanding of the characteristics of OCT1 substrates and inhibitors (Ahlin et al. 2008; Chen EC et al. 2017; Hendrickx et al. 2013). *In silico* prediction was used earlier to predict OCT1 inhibitors on a limited data basis only (Moaddel et al. 2007).

Earlier screening for OCT1 substrates mainly focused on physicochemical properties. As shown in *Publication 1*, this can lead to a low success rate. Our approach combined both, the already existing knowledge about physicochemical properties of known substrates and the power of machine learning-aided prediction. This was done by using the machine learning model for substances inside the confined physicochemical space of already known substrates only. Of course, such an approach, which includes filtering the prediction set by molecular weight, $logD_{7.4}$ and charge at pH 7.4, reduces the number of substrates predicted, but the rate of false-positively predicted substrates is reduced even more. For our study, the best available dataset of OCT1 substrates was expanded by addition of in-house transport data from the last couple of years and comparable data from other recent sources (Baidya et al. 2020; Hendrickx et al. 2013; Meyer et al. 2019). One crucial aspect for the quality of the prediction model is size and uniformity of the dataset. Respectable sizes have previously been achieved by testing OCT1 inhibition quantified by reduction of transport of a model substrate (Ahlin et al. 2008; Chen EC et al. 2017). However, an

inhibitor is not necessarily a substrate, as already discussed in early OCT1 studies (Grundemann et al. 1999; Koepsell 2020; Schlessinger et al. 2018). Inhibition can be achieved by several mechanisms and can also be allosteric only. We therefore solely relied on a smaller, pure transport dataset, committing to quality and specificity more than to quantity.

The approach used in our study was prospective in contrast to previous studies which did validations with a subset of the initial data instead of acquiring a new validation set of thus far unknown substrates (Baidya et al. 2020). The success rate of predicted compounds was > 80 %, instead of around 40 % (percentage of substrate among substances in the dataset so far) (Baidya et al. 2020; Meyer et al. 2019). Approaches, such as the presented one, can very well be used for virtual screening to guide biological testing towards the more promising lead compounds (Kapetanovic 2008).

Many of the compounds predicted and tested in our study belong to substance groups, which have previously been investigated (Koepsell 2020). The procedure we used can be described as an exploitation of previous findings and is contrary to an approach in which entirely new structures are tested and thus 'explored'. This kind of exploitation does most probably not identify completely new, unrelated ligands. Therefore, additional random testing of compounds is still advisable. On the other hand, the computer-supported search seems to have filtered the positive properties of substrates exceptionally well, so that more high-affinity substrates were found than expected.

For many years, there have been several reports about non-cationic OCT1 substrates, such as acyclovir or lamivudine (Dickens et al. 2012; Minuesa et al. 2009; Takeda et al. 2002). It is currently difficult to make predictions for neutral substances because there is too little information on transport and non-transport for substances from this chemical space for a model to learn from (Koepsell 2020). The set of compounds tested in our study was highly restricted (charge at pH 7.4 = +1, $logD_{7.4} < 1$), caused by the limited chemical space of the training set. It would therefore make sense to expand this space in the future by testing more 'improbable' substances. Even if the reward for this work is not guaranteed, predictions and insights beyond what is currently conceivable are reason enough to do so.

Identification and characterization of additional novel OCT1 substrates will probably enable *in silico*-guided identification of common substructures, which distinguish substrates from non-substrates or substrates from mere inhibitors in future. Since molecule transport is not just binding, but a process of binding, translocation and release, distinct chemical substructures could adversely affect only single steps in this process. Identification of structural commonalities by similarity clustering might therefore be able to predict the type of interaction of a respective drug and OCT1 in future. The successful application of machine learning for the prediction of novel substrates is a first step towards the integration of this technique into molecule screening routine for OCT1 substrates. However, one does not have to be satisfied with successively expanding the model with newly found substrates or non-substrates. The next goal could be the quantitative prediction of transport by a regression model. The successful application of this will require more

data points (Göller et al. 2020). First attempts based on the existing data set were not able to make a quantitative prediction (Jensen and Dücker, unpublished data).

A non-linear model with many predictors was used in our study. This approach is good for accurate prediction, but does not allow the model to be interpreted well and could be referred to as a black box. It may also make sense to use simpler models that perform worse, but remain understandable for humans.

4.3   Stereoselective uptake of adrenergic agonists and antagonists

The investigation of the possibility of stereoselective transport has been neglected for years, though it is a well-known phenomenon in enzyme catalysis for decades (Hanson 1972). As reported in *Publication 3*, OCT1 uptake can be stereoselective. The most striking differences were found for the diastereomers fenoterol and formoterol. An interesting finding of our study was the inverted stereoselectivity for fenoterol with the highly homologous transporter OCT2. The hepatically expressed transporter OCT1 facilitates more strongly the uptake of the pharmacologically active enantiomer (*R,R*)-fenoterol, while renally expressed OCT2 showed preference for uptake of the inactive (*S,S*)-fenoterol. In the case of fenoterol, the main, but not the only, route of elimination is the liver (Dettli 1996; Dollery 1999). Ultimately, peripheral blood concentrations of fenoterol might therefore include an imbalance of both enantiomers, which is not detected under regular racemic quantification. As only (*R,R*)-fenoterol exerts the agonistic effect on the β_2-adrenoreceptor, this imbalance would be highly interesting (Beigi et al. 2006). Genetically variability in OCT1 could further mediate differing drug efficacy (Tzvetkov et al. 2018).

Significant stereospecific transport of several β-adrenoreceptor antagonists via OCT1 could not be detected in our study, neither for acebutolol nor for atenolol. This finding was in line with previous studies, in which both compounds did not show significantly different pharmacokinetics of the respective enantiomers (Mehvar und Brocks 2001; Mehvar et al. 1990; Pearson et al. 1989).

Our study showed that stereoselective transport through OCT1 can occur and this could have an impact on pharmacokinetics. Stereoselectivity should therefore always be assessed in future and should be reconsidered for all known racemic substrates of OCT1 retrospectively.

4.4   A double-Flp-In method for stable overexpression of two genes

The method developed and presented here uses two overexpression vectors, each with one gene of interest, for simultaneous transfection and subsequent directed stable integration. This approach is not the only one utilizing the fact that the Flp recombination site remains intact after the integration of a plasmid containing the exact same sequence (Ward et al. 2011). However, this is the first published protocol, which includes the validation of single integration of both vectors, which is the first step of achieving comparable gene expression. Based on its principle and

conformed by experimental experience, the Flp-In system is an overexpression system, which results in low variation of gene expression anyway (Seitz et al. 2015). Low variation of gene overexpression is one requirement for studying the effect of specific genetic variants comparatively. Other approaches, which provide overexpression of two or more genes, require thorough validation of expression strength (Fahrmayr et al. 2012). Moreover, the genetic background of cells might be altered by some techniques, as the loci for integration cannot be controlled entirely (Finn et al. 1989). Selection with several antibiotics simultaneously can be stressful for cells, leading to altered expression levels in triple-transfected cells compared to their double-transfected predecessors (Hirouchi et al. 2009). The double-Flp-In method with reading frameshifts by small insertion/deletion polymorphisms requires only one antibiotic. This can be beneficial for transfections of sensitive cell lines. In the end, the protocol of the double-Flp-In can be used like a toolbox, as validation is independent from the actual gene of interest. The results obtained and presented in *Publication 4* are crossvalidated by results from studies investigating the uptake and metabolism of proguanil to cycloguanil in human hepatocytes (Matthaei et al. 2019). Therefore, double-transfected cell lines, which arise from the double-Flp-In method, can be suitable tools, for instance, to study hepatic uptake and metabolism. By changing the employed promoters, gene expression ratios of the two integrated genes could even be adapted to *in vivo* conditions, as shown for inducible co-expression systems (Baron et al. 1995). Besides the combined uptake and metabolism, possible applications for the double-Flp-In include additive cellular uptake by two transport proteins or uptake and efflux (to mimic hepatobiliary transport) (Cui et al. 2001; Fahrmayr et al. 2012). Also, the double Flp-In could be used in future to study effects of heterozygous genotypes, as both genes of interest are expressed with equal strength. The double Flp-In might therefore be a suitable tool to in the *in vitro*-to-*in vivo* translation. In addition, protein-protein interaction studies (e.g. investigation of binding parameters of two proteins) are a broad field in which the double-Flp-In could turn out valuable in future.

4.5 Variability and Heritability of Thiamine Pharmacokinetics

Biomarkers have been identified for many enzymes and transporters. As OCT1 is highly genetically variable and plays a role in elimination of a wide range of drugs, determining its activity by the help of an endogenous biomarker seems worthwhile, even though medication adjustment has not yet been implemented in guidelines for any *in vitro* substrate of OCT1. The essential nutrient thiamine (vitamin B1) has repeatedly been suggested as an OCT1 biomarker, and OCT1 was said to alter hepatic thiamine disposition (Chen L et al. 2015; Chu et al. 2017; Liang X et al. 2018). Thiamine was shown to be a substrate of OCT1, transported with low affinity but high capacity (Chen L et al. 2014; Kato et al. 2015). Unfortunately, previous studies on thiamine as a potential biomarker for OCT1 activity were solely conducted in mice in which plasma thiamine concentrations increased upon *OCT1* knockout (Chen L et al. 2014). In contrast, in our clinical study in humans we were not able to find any differences in thiamine plasma concentrations

between the *OCT1* genotypes. This discrepancy may not be surprising, as murine Oct1 is expressed in the kidney as well, where it contributes to tubular secretion (Holle et al. 2011). Knock-out of Oct1 in mice could have lead to reduced renal clearance, thereby enhancing the effects of hepatic Oct1. This has, for example, also been shown for the OCT1 substrate fenoterol (Morse et al. 2020). Thiamine is an essential nutrient for life and as a cofactor involved in fundamental biochemical reactions, such as the α-ketoglutarate dehydrogenase complex of the citric acid cycle. So it is not surprising that there are redundant uptake processes of thiamine and thiamine pyrophosphate (Ashokkumar et al. 2006; Nabokina et al. 2015; Smithline et al. 2012; Zhang K et al. 2014). The low affinity transport of thiamine via OCT1 appears to be an interesting interaction *in vitro*, but negligible *in vivo*, at least in humans.

While the previously formulated hypothesis about OCT1 being the primary uptake transporter for thiamine in the liver, cannot be rejected completely by our investigations (Liang Y et al. 2015), results from *in vitro* studies on primary human hepatocytes showed reduced uptake upon OCT1 inhibition only at an exceptional high thiamine concentration.

Of course, other endogenous substances could still work as biomarkers for OCT1 activity. One possible candidate is isobutyrylcarnitine, which was found to correlate with a common OCT1 variant in previous genome-wide association studies (Suhre et al. 2011). Other candidates are the biogenic amines, for example serotonin, which has been shown to be translocated by OCT1 (Chen L et al. 2014; Jensen 2017; Koepsell et al. 2003). However, the influence of other transporters and enzymes must be considered here, which makes the connection increasingly complex and difficult to understand.

Ultimately, clinical studies, for example with preselected genotypes, can help to investigate further potential endogenous biomarkers. Such studies in humans are apparently necessary because rodents are not the appropriate organisms to model human OCT1 physiology (Dresser et al. 2000; Hayer et al. 1999; Zhang L. et al. 1997).

5 Outlook

While the publications which form this manuscript answered several questions on OCT1 they also lead to additional questions and interesting topics for future research.

The publication on psychostimulants showed the translocation of mescaline by OCT1 *in vitro*. Further studies should clarify the impact of *OCT1* polymorphisms on the *in vivo* uptake and elimination of mescaline, as only the minority of ingested mescaline is excreted unchanged via urine. Beyond that, also the effect of loss-of-function *OCT1* variants on mescaline pharmacokinetics as well as pharmacodynamics under the currently popular recreationally used psychoactive brew ayahuasca, which contains the MAO-A inhibitor harmine and might amplify the effects of mescaline due to reduced degradation, might be worth studying, again, in dependence on the *OCT1* genotype. Also, the fact that with mescaline only one OCT1 substrate was found amongst the 18 tested, does not mean that only a few cationic hallucinogens or psychostimulants are OCT1 substrates. The result could have turned out very differently if other substances had been selected. In this respect, testing additional psychoactive compounds could provide interesting insights into the OCT1-mediated uptake of these substances, which are widespread and usually consumed in an uncontrolled manner. Biochemically, analysis of close structural analogues of mescaline might contribute to a better understanding of what makes a good OCT1 substrate.

The database of known OCT1 substrates and non-substrates presented in this work was already able to serve as foundation for machine learning-aided identification of novel substrates. However, the current database should not be considered as final, but a continuously expanding collection of data. In future, more compounds should be investigated regarding OCT1 transport, may it be by exploration of (groups of) completely unfamiliar structures or by exploiting knowledge about known substrates and testing structurally related compounds. Also, more not so obvious compounds, such as uncharged or even negatively charged compounds should be tested. If there is a high degree of similarity between these and the previously tested cationic substrates, the importance of the charge could require reevaluation.

The database added to and curated in this work is the largest collection of commercially available drugs with their respective OCT1 transport properties and using identical methodology (Jensen et al. 2021a). An interesting next step is the evaluation of these compounds in their potency to inhibit the transport of probe drugs by OCT1. Together, the resulting database might serve as a powerful tool to distinguish transport or inhibition properties of additional compounds, or even predict so far unknown inhibitors.

While our study showed stereoselective transport by OCT1 and other solute carriers, stereoselective inhibition of OCT1 has not yet been comprehensively investigated so far. It is quite conceivable that, like the uptake of substrates, the interaction with inhibitors will also turn out differently for enantiomers. Therefore, in the search for specific inhibitors, individual

enantiomers should be tested separately so that good enantiomer inhibitors are not watered down by a poorly performing counterpart. Moreover, clinical studies, in which OCT1 showed an effect on the pharmacokinetics of a racemic drug, should be reevaluated. Enantiospecific measurements should also be included in future studies with racemates if *in vitro* studies show stereoselective transport. A subsequent determination of the enantiomers will also be useful for our *in vivo* fenoterol study that was carried out. This project has already been started.

The simultaneous transfection of two plasmids by using the double-Flp-In protocol was shown to serve as a proper technique for overexpression of two genes. Of course, numerous applications of this technique for investigating various questions are conceivable. The simultaneous overexpression of OCT1 and phase I enzymes (e.g. CYP2D6, CYP2C19) will help studying uptake and metabolism, and finding more substrates of OCT1 and CYP enzymes in a single assay. This is followed up by in an ongoing project of mine. Of course, one logical extension of double-transfection is triple transfection or transfection with even higher multiplicity. While the approach used by us may in principle be extended to multiple transfection, the requirement of multiple selection antibiotics in optimal concentrations is one hurdle we are working on. Already now, several groups have already asked for the created plasmids to study protein-protein interactions, to integrate additional reporter genes, or to overexpress additional regulatory proteins.

Finally, this thesis included a study, which rejected thiamine as a potential endogenous biomarker for OCT1 activity. Additional endogenous substances do show some correlation with OCT1 activity very well, such as isobutyrylcarnitine. The mechanisms behind OCT1 activity and isobutyrylcarnitine blood concentration have not yet been figured out, and remain as one of my ongoing projects (Jensen et al. 2021b). Metabolomics studies should help finding other potential endogenous biomarkers. By comparing accumulation of metabolites in plasma samples of OCT1-deficient individuals in comparison to OCT1-active individuals, endogenous OCT1 substrates might be found enriched in the OCT1-deficient study cohort, which serve as starting point for the future search for a suitable biomarker. This project using targeted and untargeted metabolomics has already been started.

6 References

Abramson J, Smirnova I, Kasho V, Verner G, Iwata S, Kaback HR (2003): The lactose permease of Escherichia coli: overall structure, the sugar-binding site and the alternating access model for transport. FEBS Lett 555, 96-101

Ahlin G, Karlsson J, Pedersen JM, Gustavsson L, Larsson R, Matsson P, Norinder U, Bergstrom CA, Artursson P (2008): Structural requirements for drug inhibition of the liver specific human organic cation transport protein 1. J Med Chem 51, 5932-5942

Amphoux A, Vialou V, Drescher E, Bruss M, Mannoury La Cour C, Rochat C, Millan MJ, Giros B, Bonisch H, Gautron S (2006): Differential pharmacological in vitro properties of organic cation transporters and regional distribution in rat brain. Neuropharmacology 50, 941-952

Ashokkumar B, Vaziri ND, Said HM (2006): Thiamin uptake by the human-derived renal epithelial (HEK-293) cells: cellular and molecular mechanisms. Am J Physiol Renal Physiol 291, F796-805

Baidya ATK, Ghosh K, Amin SA, Adhikari N, Nirmal J, Jha T, Gayen S (2020): In silico modelling, identification of crucial molecular fingerprints, and prediction of new possible substrates of human organic cationic transporters 1 and 2. New Journal of Chemistry 44, 4129-4143

Baron U, Freundlieb S, Gossen M, Bujard H (1995): Co-regulation of two gene activities by tetracycline via a bidirectional promoter. Nucleic Acids Res 23, 3605-3606

Becker ML, Visser LE, van Schaik RH, Hofman A, Uitterlinden AG, Stricker BH (2009): Genetic variation in the organic cation transporter 1 is associated with metformin response in patients with diabetes mellitus. Pharmacogenomics J 9, 242-247

Bednarczyk D, Ekins S, Wikel JH, Wright SH (2003): Influence of Molecular Structure on Substrate Binding to the Human Organic Cation Transporter, hOCT1. Molecular Pharmacology 63, 489-498

Beigi F, Bertucci C, Zhu W, Chakir K, Wainer IW, Xiao R-P, Abernethy DR (2006): Enantioselective separation and online affinity chromatographic characterization of R,R- and S,S-fenoterol. Chirality 18, 822-827

Boxberger KH, Hagenbuch B, Lampe JN (2014): Common drugs inhibit human organic cation transporter 1 (OCT1)-mediated neurotransmitter uptake. Drug Metab Dispos 42, 990-995

Breidert T, Spitzenberger F, Grundemann D, Schomig E (1998): Catecholamine transport by the organic cation transporter type 1 (OCT1). British journal of pharmacology 125, 218-224

Busch AE, Quester S, Ulzheimer JC, Waldegger S, Gorboulev V, Arndt P, Lang F, Koepsell H (1996): Electrogenic properties and substrate specificity of the polyspecific rat cation transporter rOCT1. J Biol Chem 271, 32599-32604

Chen EC, Khuri N, Liang X, Stecula A, Chien HC, Yee SW, Huang Y, Sali A, Giacomini KM (2017): Discovery of Competitive and Noncompetitive Ligands of the Organic Cation Transporter 1 (OCT1; SLC22A1). J Med Chem 60, 2685-2696

Chen L, Yee SW, Giacomini KM (2015): OCT1 in hepatic steatosis and thiamine disposition. Cell Cycle 14, 283-284

Chen L, Shu Y, Liang X, Chen EC, Yee SW, Zur AA, Li S, Xu L, Keshari KR, Lin MJ, et al. (2014): OCT1 is a high-capacity thiamine transporter that regulates hepatic steatosis and is a target of metformin. Proceedings of the National Academy of Sciences of the United States of America 111, 9983-9988

Christensen MM, Brasch-Andersen C, Green H, Nielsen F, Damkier P, Beck-Nielsen H, Brosen K (2011): The pharmacogenetics of metformin and its impact on plasma metformin steady-state levels and glycosylated hemoglobin A1c. Pharmacogenet Genomics 21, 837-850

Chu X, Chan GH, Evers R (2017): Identification of Endogenous Biomarkers to Predict the Propensity of Drug Candidates to Cause Hepatic or Renal Transporter-Mediated Drug-Drug Interactions. Journal of pharmaceutical sciences 106, 2357-2367

Cui Y, Konig J, Keppler D (2001): Vectorial transport by double-transfected cells expressing the human uptake transporter SLC21A8 and the apical export pump ABCC2. Mol Pharmacol 60, 934-943

Dakal TC, Kumar R, Ramotar D (2017): Structural modeling of human organic cation transporters. Comput Biol Chem 68, 153-163

Dettli L: Pharmakokinetische Daten für die Dosisanpassung. In: Sektion Klinische Pharmakologie der Schweizerischen Gesellschaft für Pharmakologie und Toxikologie (Hrsg): Grundlagen der Arzneimitteltherapie. 14. Auflage; Documed, Basel 1996, 13-21

Di Chiara G, Imperato A (1988): Drugs abused by humans preferentially increase synaptic dopamine concentrations in the mesolimbic system of freely moving rats. Proceedings of the National Academy of Sciences 85, 5274-5278

Dickens D, Owen A, Alfirevic A, Giannoudis A, Davies A, Weksler B, Romero IA, Couraud PO, Pirmohamed M (2012): Lamotrigine is a substrate for OCT1 in brain endothelial cells. Biochem Pharmacol 83, 805-814

Dixon CM, Park GR, Tarbit MH (1994): Characterization of the enzyme responsible for the metabolism of sumatriptan in human liver. Biochem Pharmacol 47, 1253-1257

Dollery C: Therapeutic drugs; 2. Auflage; Churchill Livingstone, Edinburgh 1999

Dresser MJ, Gray AT, Giacomini KM (2000): Kinetic and selectivity differences between rodent, rabbit, and human organic cation transporters (OCT1). J Pharmacol Exp Ther 292, 1146-1152

Egenberger B, Gorboulev V, Keller T, Gorbunov D, Gottlieb N, Geiger D, Mueller TD, Koepsell H (2012): A substrate binding hinge domain is critical for transport-related structural changes of organic cation transporter 1. J Biol Chem 287, 31561-31573

Fahrmayr C, König J, Auge D, Mieth M, Fromm M (2012): Identification of drugs and drug metabolites as substrates of multidrug resistance protein 2 (MRP2) using triple-transfected MDCK-OATP1B1-UGT1A1-MRP2 cells. British journal of pharmacology 165, 1836-1847

Finn GK, Kurz BW, Cheng RZ, Shmookler Reis RJ (1989): Homologous plasmid recombination is elevated in immortally transformed cells. Mol Cell Biol 9, 4009-4017

Fischer JE, Baldessarini RJ (1971): False neurotransmitters and hepatic failure. Lancet 2, 75-80

Fischer JE, Horst WD, Kopin IJ (1965): Beta-Hydroxylated Sympathomimetic Amines as False Neurotransmitters. British journal of pharmacology and chemotherapy 24, 477-484

Fowler PA, Lacey LF, Thomas M, Keene ON, Tanner RJ, Baber NS (1991): The clinical pharmacology, pharmacokinetics and metabolism of sumatriptan. European neurology 31, 291-294

Fukuda T, Chidambaran V, Mizuno T, Venkatasubramanian R, Ngamprasertwong P, Olbrecht V, Esslinger HR, Vinks AA, Sadhasivam S (2013): OCT1 genetic variants influence the pharmacokinetics of morphine in children. Pharmacogenomics 14, 1141-1151

Göller AH, Kuhnke L, Montanari F, Bonin A, Schneckener S, ter Laak A, Wichard J, Lobell M, Hillisch A (2020): Bayer's in silico ADMET platform: a journey of machine learning over the past two decades. Drug discovery today

Gorboulev V, Shatskaya N, Volk C, Koepsell H (2005): Subtype-specific affinity for corticosterone of rat organic cation transporters rOCT1 and rOCT2 depends on three amino acids within the substrate binding region. Mol Pharmacol 67, 1612-1619

Gorboulev V, Volk C, Arndt P, Akhoundova A, Koepsell H (1999): Selectivity of the polyspecific cation transporter rOCT1 is changed by mutation of aspartate 475 to glutamate. Mol Pharmacol 56, 1254-1261

Gorboulev V, Rehman S, Albert CM, Roth U, Meyer MJ, Tzvetkov MV, Mueller TD, Koepsell H (2018): Assay Conditions Influence Affinities of Rat Organic Cation Transporter 1: Analysis of Mutagenesis in the Modeled Outward-Facing Cleft by Measuring Effects of Substrates and Inhibitors on Initial Uptake. Mol Pharmacol 93, 402-415

Gorboulev V, Ulzheimer JC, Akhoundova A, Ulzheimer-Teuber I, Karbach U, Quester S, Baumann C, Lang F, Busch AE, Koepsell H (1997): Cloning and characterization of two human polyspecific organic cation transporters. DNA Cell Biol 16, 871-881

Gorbunov D, Gorboulev V, Shatskaya N, Mueller T, Bamberg E, Friedrich T, Koepsell H (2008): High-affinity cation binding to organic cation transporter 1 induces movement of helix 11 and blocks transport after mutations in a modeled interaction domain between two helices. Mol Pharmacol 73, 50-61

Grundemann D, Liebich G, Kiefer N, Koster S, Schomig E (1999): Selective substrates for non-neuronal monoamine transporters. Mol Pharmacol 56, 1-10

Gründemann D, Schechinger B, Rappold GA, Schomig E (1998): Molecular identification of the corticosterone-sensitive extraneuronal catecholamine transporter. Nature neuroscience 1, 349-351

Hanson KR (1972): Enzyme Symmetry and Enzyme Stereospecificity. Annual Review of Plant Physiology 23, 335-366

Hayer M, Bonisch H, Bruss M (1999): Molecular cloning, functional characterization and genomic organization of four alternatively spliced isoforms of the human organic cation transporter 1 (hOCT1/SLC22A1). Ann Hum Genet 63, 473-482

Hendrickx R, Johansson JG, Lohmann C, Jenvert RM, Blomgren A, Borjesson L, Gustavsson L (2013): Identification of novel substrates and structure-activity relationship of cellular uptake mediated by human organic cation transporters 1 and 2. J Med Chem 56, 7232-7242

Hirouchi M, Kusuhara H, Onuki R, Ogilvie BW, Parkinson A, Sugiyama Y (2009): Construction of triple-transfected cells [organic anion-transporting polypeptide (OATP) 1B1/multidrug resistance-associated protein (MRP) 2/MRP3 and OATP1B1/MRP2/MRP4] for analysis of the sinusoidal function of MRP3 and MRP4. Drug Metab Dispos 37, 2103-2111

Holle SK, Ciarimboli G, Edemir B, Neugebauer U, Pavenstadt H, Schlatter E (2011): Properties and regulation of organic cation transport in freshly isolated mouse proximal tubules analyzed with a fluorescence reader-based method. Pflugers Arch 462, 359-369

Hu T, Wang L, Pan X, Qi H (2016): Novel compound, organic cation transporter 3 detection agent and organic cation transporter 3 activity inhibitor, WO2015002150 A1: a patent evaluation. Expert opinion on therapeutic patents 26, 857-860

Jensen O: Effects of Genetic Polymorphisms on Uptake of Endogenous Substrates by the Human Organic Cation Transporter OCT1. Master Thesis. Göttingen 2017

Jensen O, Brockmöller J, Dücker C (2021a): Identification of Novel High-Affinity Substrates of OCT1 Using Machine Learning-Guided Virtual Screening and Experimental Validation. J Med Chem 64, 2762-2776

Jensen O, Rafehi M, Tzvetkov MV, Brockmöller J (2020a): Stereoselective cell uptake of adrenergic agonists and antagonists by organic cation transporters. Biochem Pharmacol 171, 113731

Jensen O, Matthaei J, Blome F, Schwab M, Tzvetkov MV, Brockmöller J (2020b): Variability and Heritability of Thiamine Pharmacokinetics With Focus on OCT1 Effects on Membrane Transport and Pharmacokinetics in Humans. Clin Pharmacol Ther 107, 628-638

Jensen O, Matthaei J, Klemp HG, Meyer MJ, Brockmöller J, Tzvetkov MV (2021b): Isobutyrylcarnitine as a biomarker of OCT1 activity and interspecies differences in its membrane transport. Front Pharmacol

Kapetanovic IM (2008): Computer-aided drug discovery and development (CADDD): In silico-chemico-biological approach. Chemico-biological interactions 171, 165-176

Kato K, Moriyama C, Ito N, Zhang X, Hachiuma K, Hagima N, Iwata K, Yamaguchi J, Maeda K, Ito K, et al. (2015): Involvement of organic cation transporters in the clearance and milk secretion of thiamine in mice. Pharm Res 32, 2192-2204

Keller T, Gorboulev V, Mueller TD, Dotsch V, Bernhard F, Koepsell H (2019): Rat Organic Cation Transporter 1 Contains Three Binding Sites for Substrate 1-Methyl-4-phenylpyridinium per Monomer. Mol Pharmacol 95, 169-182

Kerb R, Brinkmann U, Chatskaia N, Gorbunov D, Gorboulev V, Mornhinweg E, Keil A, Eichelbaum M, Koepsell H (2002): Identification of genetic variations of the human organic cation transporter hOCT1 and their functional consequences. Pharmacogenetics 12, 591-595

Kim HI, Raffler J, Lu W, Lee J-J, Abbey D, Saleheen D, Rabinowitz JD, Bennett MJ, Hand NJ, Brown C, et al. (2017): Fine Mapping and Functional Analysis Reveal a Role of SLC22A1 in Acylcarnitine Transport. The American Journal of Human Genetics

Koepsell H (2011): Substrate recognition and translocation by polyspecific organic cation transporters. Biol Chem 392, 95-101

Koepsell H (2015): Role of organic cation transporters in drug-drug interaction. Expert Opin Drug Metab Toxicol 11, 1619-1633

Koepsell H (2019): Multiple binding sites in organic cation transporters require sophisticated procedures to identify interactions of novel drugs. Biol Chem 400, 195-207

Koepsell H (2020): Organic Cation Transporters in Health and Disease. Pharmacol Rev 72, 253-319

Koepsell H, Keller T: Functional Properties of Organic Cation Transporter OCT1, Binding of Substrates and Inhibitors, and Presumed Transport Mechanism. Organic Cation Transporters. Springer International Publishing Switzerland 2016

Koepsell H, Schmitt BM, Gorboulev V (2003): Organic cation transporters. Reviews of physiology, biochemistry and pharmacology 150, 36-90

Kuczenski R, Segal DS (1997): Effects of methylphenidate on extracellular dopamine, serotonin, and norepinephrine: comparison with amphetamine. J Neurochem 68, 2032-2037

Leabman MK, Huang CC, DeYoung J, Carlson EJ, Taylor TR, de la Cruz M, Johns SJ, Stryke D, Kawamoto M, Urban TJ, et al. (2003): Natural variation in human membrane transporter genes reveals evolutionary and functional constraints. Proceedings of the National Academy of Sciences of the United States of America 100, 5896-5901

Liang X, Yee SW, Chien HC, Chen EC, Luo Q, Zou L, Piao M, Mifune A, Chen L, Calvert ME, et al. (2018): Organic cation transporter 1 (OCT1) modulates multiple cardiometabolic traits through effects on hepatic thiamine content. PLoS Biol 16, e2002907

Liang Y, Li S, Chen L (2015): The physiological role of drug transporters. Protein Cell 6, 334-350

Matthaei J, Seitz T, Jensen O, Tann A, Prukop T, Tadjerpisheh S, Brockmöller J, Tzvetkov MV (2019): OCT1 Deficiency Affects Hepatocellular Concentrations and Pharmacokinetics of Cycloguanil, the Active Metabolite of the Antimalarial Drug Proguanil. Clin Pharmacol Ther 105, 190-200

Matthaei J, Kuron D, Faltraco F, Knoch T, Dos Santos Pereira JN, Abu Abed M, Prukop T, Brockmöller J, Tzvetkov MV (2016): OCT1 mediates hepatic uptake of sumatriptan and loss-of-function OCT1 polymorphisms affect sumatriptan pharmacokinetics. Clin Pharmacol Ther 99, 633-641

Mehvar R, Brocks DR (2001): Stereospecific pharmacokinetics and pharmacodynamics of beta-adrenergic blockers in humans. Journal of pharmacy & pharmaceutical sciences : a publication of the Canadian Society for Pharmaceutical Sciences, Societe canadienne des sciences pharmaceutiques 4, 185-200

Mehvar R, Gross ME, Kreamer RN (1990): Pharmacokinetics of atenolol enantiomers in humans and rats. Journal of pharmaceutical sciences 79, 881-885

Meijer DK, Mol WE, Müller M, Kurz G (1990): Carrier-mediated transport in the hepatic distribution and elimination of drugs, with special reference to the category of organic cations. Journal of pharmacokinetics and biopharmaceutics 18, 35-70

Meyer-Wentrup F, Karbach U, Gorboulev V, Arndt P, Koepsell H (1998): Membrane localization of the electrogenic cation transporter rOCT1 in rat liver. Biochem Biophys Res Commun 248, 673-678

Meyer MJ: Effects of ligand structure, amino acid substitutions, and species differences on the function of organic cation transporter OCT1: utilizing polyspecificity for understanding structure-function relationships. 2020

Meyer MJ, Seitz T, Brockmöller J, Tzvetkov MV (2017): Effects of genetic polymorphisms on the OCT1 and OCT2-mediated uptake of ranitidine. PloS one 12, e0189521

Meyer MJ, Neumann VE, Friesacher HR, Zdrazil B, Brockmöller J, Tzvetkov MV (2019): Opioids as Substrates and Inhibitors of the Genetically Highly Variable Organic Cation Transporter OCT1. J Med Chem 62, 9890-9905

Minuesa G, Volk C, Molina-Arcas M, Gorboulev V, Erkizia I, Arndt P, Clotet B, Pastor-Anglada M, Koepsell H, Martinez-Picado J (2009): Transport of lamivudine [(-)-beta-L-2',3'-dideoxy-3'-thiacytidine] and high-affinity interaction of nucleoside reverse transcriptase inhibitors with human organic cation transporters 1, 2, and 3. J Pharmacol Exp Ther 329, 252-261

Moaddel R, Ravichandran S, Bighi F, Yamaguchi R, Wainer IW (2007): Pharmacophore modelling of stereoselective binding to the human organic cation transporter (hOCT1). British journal of pharmacology 151, 1305-1314

Moaddel R, Patel S, Jozwiak K, Yamaguchi R, Ho PC, Wainer IW (2005): Enantioselective binding to the human organic cation transporter-1 (hOCT1) determined using an immobilized hOCT1 liquid chromatographic stationary phase. Chirality 17, 501-506

Morrissey KM, Stocker SL, Wittwer MB, Xu L, Giacomini KM (2013): Renal Transporters in Drug Development. Annual review of pharmacology and toxicology 53, 503-529

Morse BL, Kolur A, Hudson LR, Hogan AT, Chen LH, Brackman RM, Sawada GA, Fallon JK, Smith PC, Hillgren KM (2020): Pharmacokinetics of Organic Cation Transporter 1 (OCT1) Substrates in Oct1/2 Knockout Mice and Species Difference in Hepatic OCT1-Mediated Uptake. Drug Metab Dispos 48, 93-105

Motohashi H, Sakurai Y, Saito H, Masuda S, Urakami Y, Goto M, Fukatsu A, Ogawa O, Inui K (2002): Gene expression levels and immunolocalization of organic ion transporters in the human kidney. Journal of the American Society of Nephrology : JASN 13, 866-874

Nabokina SM, Ramos MB, Valle JE, Said HM (2015): Regulation of basal promoter activity of the human thiamine pyrophosphate transporter SLC44A4 in human intestinal epithelial cells. Am J Physiol Cell Physiol 308, C750-757

Nagel G, Volk C, Friedrich T, Ulzheimer JC, Bamberg E, Koepsell H (1997): A reevaluation of substrate specificity of the rat cation transporter rOCT1. J Biol Chem 272, 31953-31956

Nielsen LM, Sverrisdottir E, Stage TB, Feddersen S, Brosen K, Christrup LL, Drewes AM, Olesen AE (2017): Lack of genetic association between OCT1, ABCB1, and UGT2B7 variants and morphine pharmacokinetics. European journal of pharmaceutical sciences : official journal of the European Federation for Pharmaceutical Sciences 99, 337-342

Nies AT, Koepsell H, Winter S, Burk O, Klein K, Kerb R, Zanger UM, Keppler D, Schwab M, Schaeffeler E (2009): Expression of organic cation transporters OCT1 (SLC22A1) and OCT3 (SLC22A3) is affected by genetic factors and cholestasis in human liver. Hepatology 50, 1227-1240

Oude Elferink RP, Meijer DK, Kuipers F, Jansen PL, Groen AK, Groothuis GM (1995): Hepatobiliary secretion of organic compounds; molecular mechanisms of membrane transport. Biochim Biophys Acta 1241, 215-268

Pearson AA, Gaffney TE, Walle T, Privitera PJ (1989): A stereoselective central hypotensive action of atenolol. J Pharmacol Exp Ther 250, 759-763

Pentikäinen PJ, Neuvonen PJ, Penttilä A (1979): Pharmacokinetics of metformin after intravenous and oral administration to man. European Journal of Clinical Pharmacology 16, 195-202

Pernicova I, Korbonits M (2014): Metformin – mode of action and clinical implications for diabetes and cancer. Nat Rev Endocrinol 10, 143-156

Popp C, Gorboulev V, Muller TD, Gorbunov D, Shatskaya N, Koepsell H (2005): Amino acids critical for substrate affinity of rat organic cation transporter 1 line the substrate binding region in a model derived from the tertiary structure of lactose permease. Mol Pharmacol 67, 1600-1611

Ritz MC, Cone EJ, Kuhar MJ (1990): Cocaine inhibition of ligand binding at dopamine, norepinephrine and serotonin transporters: A structure-activity study. Life Sciences 46, 635-645

Saadatmand AR, Tadjerpisheh S, Brockmöller J, Tzvetkov MV (2012): The prototypic pharmacogenetic drug debrisoquine is a substrate of the genetically polymorphic organic cation transporter OCT1. Biochem Pharmacol 83, 1427-1434

Sakata T, Anzai N, Shin HJ, Noshiro R, Hirata T, Yokoyama H, Kanai Y, Endou H (2004): Novel single nucleotide polymorphisms of organic cation transporter 1 (SLC22A1) affecting transport functions. Biochem Biophys Res Commun 313, 789-793

Schlessinger A, Welch MA, van Vlijmen H, Korzekwa K, Swaan PW, Matsson P (2018): Molecular Modeling of Drug-Transporter Interactions-An International Transporter Consortium Perspective. Clin Pharmacol Ther 104, 818-835

Seitz T, Stalmann R, Dalila N, Chen J, Pojar S, Dos Santos Pereira JN, Kratzner R, Brockmöller J, Tzvetkov MV (2015): Global genetic analyses reveal strong inter-ethnic variability in the loss of activity of the organic cation transporter OCT1. Genome Med 7, 56

Shikata E, Yamamoto R, Takane H, Shigemasa C, Ikeda T, Otsubo K, Ieiri I (2007): Human organic cation transporter (OCT1 and OCT2) gene polymorphisms and therapeutic effects of metformin. J Hum Genet 52, 117-122

Shu Y, Brown C, Castro RA, Shi RJ, Lin ET, Owen RP, Sheardown SA, Yue L, Burchard EG, Brett CM, et al. (2008): Effect of genetic variation in the organic cation transporter 1, OCT1, on metformin pharmacokinetics. Clin Pharmacol Ther 83, 273-280

Shu Y, Sheardown SA, Brown C, Owen RP, Zhang S, Castro RA, Ianculescu AG, Yue L, Lo JC, Burchard EG, et al. (2007): Effect of genetic variation in the organic cation transporter 1 (OCT1) on metformin action. J Clin Invest 117, 1422-1431

Shu Y, Leabman MK, Feng B, Mangravite LM, Huang CC, Stryke D, Kawamoto M, Johns SJ, DeYoung J, Carlson E, et al. (2003): Evolutionary conservation predicts function of variants of the human organic cation transporter, OCT1. Proceedings of the National Academy of Sciences of the United States of America 100, 5902-5907

Smithline HA, Donnino M, Greenblatt DJ (2012): Pharmacokinetics of high-dose oral thiamine hydrochloride in healthy subjects. BMC clinical pharmacology 12, 4

Stamer UM, Musshoff F, Stuber F, Brockmöller J, Steffens M, Tzvetkov MV (2016): Loss-of-function polymorphisms in the organic cation transporter OCT1 are associated with reduced postoperative tramadol consumption. Pain 157, 2467-2475

Stumpfe D, Bajorath J (2012): Exploring activity cliffs in medicinal chemistry. J Med Chem 55, 2932-2942

Suhre K, Shin SY, Petersen AK, Mohney RP, Meredith D, Wagele B, Altmaier E, CardioGram, Deloukas P, Erdmann J, et al. (2011): Human metabolic individuality in biomedical and pharmaceutical research. Nature 477, 54-60

Tachampa K, Takeda M, Khamdang S, Noshiro-Kofuji R, Tsuda M, Jariyawat S, Fukutomi T, Sophasan S, Anzai N, Endou H (2008): Interactions of organic anion transporters and organic cation transporters with mycotoxins. Journal of pharmacological sciences 106, 435-443

Takeda M, Khamdang S, Narikawa S, Kimura H, Kobayashi Y, Yamamoto T, Cha SH, Sekine T, Endou H (2002): Human organic anion transporters and human organic cation transporters mediate renal antiviral transport. J Pharmacol Exp Ther 300, 918-924

Tamai I, Takanaga H, Maeda H, Yabuuchi H, Sai Y, Suzuki Y, Tsuji A (1997): Intestinal brush-border membrane transport of monocarboxylic acids mediated by proton-coupled transport and anion antiport mechanisms. The Journal of pharmacy and pharmacology 49, 108-112

Tamai I, Ohashi R, Nezu J, Yabuuchi H, Oku A, Shimane M, Sai Y, Tsuji A (1998): Molecular and functional identification of sodium ion-dependent, high affinity human carnitine transporter OCTN2. J Biol Chem 273, 20378-20382

Tzvetkov MV, Dalila N, Faltraco F: Genetic Variability in Organic Cation Transporters: Pathophysiological Manifestations and Consequences for Drug Pharmacokinetics and Efficacy. In: Ciarimboli G, Gautron S, Schlatter E (Hrsg): Organic Cation Transporters: Integration of Physiology, Pathology, and Pharmacology. Springer International Publishing, Cham 2016, 93-137

Tzvetkov MV, Saadatmand AR, Lötsch J, Tegeder I, Stingl JC, Brockmöller J (2011): Genetically polymorphic OCT1: another piece in the puzzle of the variable pharmacokinetics and pharmacodynamics of the opioidergic drug tramadol. Clin Pharmacol Ther 90, 143-150

Tzvetkov MV, Saadatmand AR, Bokelmann K, Meineke I, Kaiser R, Brockmöller J (2012): Effects of OCT1 polymorphisms on the cellular uptake, plasma concentrations and efficacy of the 5-HT(3) antagonists tropisetron and ondansetron. Pharmacogenomics J 12, 22-29

Tzvetkov MV, dos Santos Pereira JN, Meineke I, Saadatmand AR, Stingl JC, Brockmöller J (2013): Morphine is a substrate of the organic cation transporter OCT1 and polymorphisms in OCT1 gene affect morphine pharmacokinetics after codeine administration. Biochem Pharmacol 86, 666-678

Tzvetkov MV, Matthaei J, Pojar S, Faltraco F, Vogler S, Prukop T, Seitz T, Brockmöller J (2018): Increased Systemic Exposure and Stronger Cardiovascular and Metabolic Adverse Reactions to Fenoterol in Individuals with Heritable OCT1 Deficiency. Clin Pharmacol Ther 103, 868-878

Tzvetkov MV, Vormfelde SV, Balen D, Meineke I, Schmidt T, Sehrt D, Sabolic I, Koepsell H, Brockmöller J (2009): The effects of genetic polymorphisms in the organic cation transporters OCT1, OCT2, and OCT3 on the renal clearance of metformin. Clin Pharmacol Ther 86, 299-306

Verhaagh S, Schweifer N, Barlow DP, Zwart R (1999): Cloning of the mouse and human solute carrier 22a3 (Slc22a3/SLC22A3) identifies a conserved cluster of three organic cation transporters on mouse chromosome 17 and human 6q26-q27. Genomics 55, 209-218

Volk C, Gorboulev V, Kotzsch A, Muller TD, Koepsell H (2009): Five amino acids in the innermost cavity of the substrate binding cleft of organic cation transporter 1 interact with extracellular and intracellular corticosterone. Mol Pharmacol 76, 275-289

Wagner DJ, Sager JE, Duan H, Isoherranen N, Wang J (2017): Interaction and Transport of Methamphetamine and its Primary Metabolites by Organic Cation and Multidrug and Toxin Extrusion Transporters. Drug Metab Dispos 45, 770-778

Wang DS, Jonker JW, Kato Y, Kusuhara H, Schinkel AH, Sugiyama Y (2002): Involvement of organic cation transporter 1 in hepatic and intestinal distribution of metformin. J Pharmacol Exp Ther 302, 510-515

Ward RJ, Alvarez-Curto E, Milligan G (2011): Using the Flp-In T-Rex system to regulate GPCR expression. Methods in molecular biology 746, 21-37

Williams JA, Hyland R, Jones BC, Smith DA, Hurst S, Goosen TC, Peterkin V, Koup JR, Ball SE (2004): Drug-drug interactions for UDP-glucuronosyltransferase substrates: a pharmacokinetic explanation for typically observed low exposure (AUCi/AUC) ratios. Drug Metab Dispos 32, 1201-1208

Wu X, Prasad PD, Leibach FH, Ganapathy V (1998): cDNA sequence, transport function, and genomic organization of human OCTN2, a new member of the organic cation transporter family. Biochem Biophys Res Commun 246, 589-595

Wu X, Huang W, Ganapathy ME, Wang H, Kekuda R, Conway SJ, Leibach FH, Ganapathy V (2000): Structure, function, and regional distribution of the organic cation transporter OCT3 in the kidney. Am J Physiol Renal Physiol 279, F449-458

Yabuuchi H, Tamai I, Nezu J, Sakamoto K, Oku A, Shimane M, Sai Y, Tsuji A (1999): Novel membrane transporter OCTN1 mediates multispecific, bidirectional, and pH-dependent transport of organic cations. J Pharmacol Exp Ther 289, 768-773

Zamek-Gliszczynski MJ, Taub ME, Chothe PP, Chu X, Giacomini KM, Kim RB, Ray AS, Stocker SL, Unadkat JD, Wittwer MB, et al. (2018): Transporters in Drug Development: 2018 ITC Recommendations for Transporters of Emerging Clinical Importance. Clin Pharmacol Ther 104, 890-899

Zhang K, Huentelman MJ, Rao F, Sun EI, Corneveaux JJ, Schork AJ, Wei Z, Waalen J, Miramontes-Gonzalez JP, Hightower CM, et al. (2014): Genetic implication of a novel thiamine transporter in human hypertension. J Am Coll Cardiol 63, 1542-1555

Zhang L, Schaner ME, Giacomini KM (1998): Functional Characterization of an Organic Cation Transporter (hOCT1) in a Transiently Transfected Human Cell Line (HeLa). Journal of Pharmacology and Experimental Therapeutics 286, 354-361

Zhang L, Strong JM, Qiu W, Lesko LJ, Huang SM (2006): Scientific perspectives on drug transporters and their role in drug interactions. Mol Pharm 3, 62-69

Zhang L, Dresser MJ, Gray AT, Yost SC, Terashita S, Giacomini KM (1997): Cloning and functional expression of a human liver organic cation transporter. Mol Pharmacol 51, 913-921

Zhu HJ, Appel DI, Grundemann D, Richelson E, Markowitz JS (2012): Evaluation of organic cation transporter 3 (SLC22A3) inhibition as a potential mechanism of antidepressant action. Pharmacol Res 65, 491-496

Zolk O (2009): Current understanding of the pharmacogenomics of metformin. Clin Pharmacol Ther 86, 595-598

7   Own Contributions

Publication 1:	Variability and Heritability of Thiamine Pharmacokinetics With Focus on OCT1 Effects on Membrane Transport and Pharmacokinetics in Humans
Authors:	Ole Jensen, Johannes Matthaei, Felix Blome, Matthias Schwab, Mladen V. Tzvetkov, and Jürgen Brockmöller
Published:	March 2020
Author contributions:	**O.J.** and J.B. wrote the manuscript. J.M., M.S., M.V.T., and J.B. designed the research. **O.J.**, J.M., and F.B. performed the research. **O.J.**, J.M., M.V.T., and J.B. analyzed the data.

Publication 2:	Stereoselective cell uptake of adrenergic agonists and antagonists by organic cation transporters
Authors:	Ole Jensen, Muhammad Rafehi, Mladen V. Tzvetkov, and Jürgen Brockmöller
Published:	27 November 2019
Author contribution:	**Ole Jensen**: Methodology, Formal analysis, Investigation, Writing - original draft, Writing - review & editing, Visualization. Muhammad Rafehi: Writing - original draft, Writing - review & editing. Mladen V. Tzvetkov: Conceptualization, Resources. Jürgen Brockmöller: Conceptualization, Resources, Writing - original draft, Writing - review & editing, Project administration, Supervision.

Publication 3:	A double-Flp-In method for stable overexpression of two genes
Authors:	Ole Jensen, Salim Ansari, Lukas Gebauer, Simon F. Müller, Kira A. A. T. Lowjaga, Joachim Geyer, Mladen V. Tzvetkov, and Jürgen Brockmöller
Published:	20 August 2020
Author contribution:	**O.J.**, J.G., M.V.T. and J.B. designed the research. **O.J.**, S.A., L.G., K.A.A.T.L. and S.F.M. performed the research and contributed to figure content. **O.J.**, L.G., S.A., S.F.M. and J.B. wrote the article. All authors edited the manuscript.

Publication 4:	Cellular Uptake of Psychostimulants — Are High- and Low-Affinity Organic Cation Transporters Drug Traffickers?
Authors:	Ole Jensen, Muhammad Rafehi, Lukas Gebauer, and Jürgen Brockmöller
Published:	20.01.2021
Author contribution:	Conceptualisation: **OJ**, MR, and JB; Funding acquisition: MR and JB; Investigation: **OJ** and LG; Methodology: **OJ** and JB; Project administration: **OJ**, MR, and JB; Supervision: JB; Visualisation: **OJ** and MR; Writing — original draft: **OJ** and MR; Writing — review and editing: MR and JB.

Publication 5:	Identification of Novel High-Affinity Substrates of OCT1 Using Machine Learning-Guided Virtual Screening and Experimental Validation
Authors:	Ole Jensen, Jürgen Brockmöller, and Christof Dücker
Published:	19.02.2021
Author contribution:	**OJ**, JB and CD conceptualized the study, CD performed the chemoinformatics analyses, **OJ** and CD developed the model, **OJ** and CD designed the experiments, **OJ** performed the wet-lab experiments, **OJ** and CD analyzed the data, **OJ**, JB and CD wrote the manuscript. All authors have given approval to the final version of the manuscript.

8 Publications and Presentations

8.1 Publications

Kotlarz D, Beier R, Murugan D, Diestelhorst J, **Jensen O**, Boztug K, Pfeifer D, Kreipe H, Pfister ED, Baumann U, et al. (2012): Loss of interleukin-10 signaling and infantile inflammatory bowel disease: implications for diagnosis and therapy. Gastroenterology 143, 347-355

Matthaei J, Seitz T, **Jensen O**, Tann A, Prukop T, Tadjerpisheh S, Brockmöller J, Tzvetkov MV (2019): OCT1 Deficiency Affects Hepatocellular Concentrations and Pharmacokinetics of Cycloguanil, the Active Metabolite of the Antimalarial Drug Proguanil. Clin Pharmacol Ther 105, 190-200

Mewes C, Buttner B, Hinz J, Alpert A, Popov AF, Ghadimi M, Beissbarth T, Tzvetkov M, **Jensen O**, Runzheimer J, et al. (2019): CTLA-4 Genetic Variants Predict Survival in Patients with Sepsis. J Clin Med 8, 70

Rafehi M, Faltraco F, Matthaei J, Prukop T, **Jensen O**, Grytzmann A, Blome FG, Berger RG, Krings U, Vormfelde SV, et al. (2019): Highly Variable Pharmacokinetics of Tyramine in Humans and Polymorphisms in OCT1, CYP2D6, and MAO-A. Front Pharmacol 10, 1297

Jensen O, Matthaei J, Blome F, Schwab M, Tzvetkov MV, Brockmöller J (2020): Variability and Heritability of Thiamine Pharmacokinetics With Focus on OCT1 Effects on Membrane Transport and Pharmacokinetics in Humans. Clin Pharmacol Ther 107, 628-638

Jensen O, Rafehi M, Tzvetkov MV, Brockmöller J (2020): Stereoselective cell uptake of adrenergic agonists and antagonists by organic cation transporters. Biochem Pharmacol 171, 113731

Jensen O, Ansari S, Gebauer L, Müller SF, Lowjaga K, Geyer J, Tzvetkov MV, Brockmöller J (2020): A double-Flp-in method for stable overexpression of two genes. Sci Rep 10, 14018

Jensen O, Rafehi M, Gebauer L, Brockmöller J (2021): Cellular Uptake of Psychostimulants — Are High- and Low-Affinity Organic Cation Transporters Drug Traffickers? Front Pharmacol 11, 609811

Jensen O, Brockmöller J, Dücker C (2021): Identification of Novel High-Affinity Substrates of OCT1 Using Machine Learning-Guided Virtual Screening and Experimental Validation. J Med Chem 64, 2762-2776

Matthaei J, Brockmöller J, Steimer W, Pischa K, Leucht S, Kullmann M, **Jensen O**, Ouethy T, Tzvetkov MV, Rafehi M (2021): Effects of genetic polymorphism in CYP2D6, CYP2C19, and the organic cation transporter OCT1 on amitriptyline pharmacokinetics in healthy volunteers and depressive disorder patients. Front Pharmacol (*accepted*)

Jensen O, Matthaei J, Klemp HG, Meyer MJ, Brockmöller J, Tzvetkov MV (2021): Isobutyrylcarnitine as a biomarker of OCT1 activity and interspecies differences in its membrane transport. Front Pharmacol (*accepted*)

8.2 Oral presentations

Transporttage 2017 in Münster *October 2017* *Münster, Germany*	"OCT1 and the pharmacokinetics of vitamin B1 in humans"
Greifswalder Transporttage *September 2018* *Greifswald, Germany*	"OCT1 as efflux transporter of acylcarnitines: Is all that glitters gold?"
2nd MAD Meeting (Methods for Analyzing Drug Transporters) *June 2019* *Rauischholzhausen, Germany*	"Double/multiple transfections using the Flp-In system"

8.3 Poster presentations

11th Transport Colloquium of the GBM study section Biomembranes *April 2018* *Rauischholzhausen, Germany*	"OCT1 as efflux transporter of acylcarnitines: Is all that glitters gold?" (awarded with poster prize)
4th German Pharm-Tox Summit *February 2019* *Stuttgart. Germany*	"Stereoselective uptake of fenoterol and atenolol by the organic cation transporter OCT1"
11th International BioMedical Transporters Conference *August 2019* *Luzern, Switzerland*	"OCT1 as an efflux transporter of acylcarnitines: Is all that glitters gold?"
5th German Pharm-Tox Summit *March 2020* *Leipzig, Germany*	"Variability and Heritability of Baseline Concentrations and High-Dose Pharmacokinetics of Thiamine (Vitamin B1)" (awarded with poster prize)